

The Impact of Nitrite on Aerobic Growth of *Paracoccus denitrificans* PD1222

Submitted for approval by

Katherine Rachel Hartop

BSc (Hons)

For the qualification of Doctor of Philosophy

University of East Anglia

School of Biological Sciences

January 2014

This copy of the thesis has been supplied on conditions that anyone who consults it is understood to recognise that its copyright rests with the author and that use of any information derived there from must be in accordance with current UK Copyright Law. In addition, any quotation or extract must include full attribution.

Acknowledgments

Utmost thanks go to my supervisors Professor David Richardson, Dr Andy Gates and Dr Tom Clarke for their continual support and boundless knowledge. I am also delighted to have been supported by the funding of the University of East Anglia for the length of my doctoral research. Thank you to the Richardson laboratory as well as those I have encountered and had the honour of collaborating with from the School of Biological Sciences. Thank you to Georgios Giannopoulos for your contribution to my research and support during the writing of this thesis. Thanks to my friends for their patience, care and editorial input. Deepest thanks to Dr Rosa María Martínez-Espinosa and Dr Gary Rowley for examining me and my research.

This work is dedicated to my parents, Keith and Gill, and my family.

Abstract

The effect of nitrite stress induced in *Paracoccus denitrificans* PD1222 was examined using additions of sodium nitrite to an aerobic bacterial culture. Nitrite generates a strong stress response in *P. denitrificans*, causing growth inhibition. This is dependent on both the concentration of nitrite present and the pH. The pH dependent effect of nitrite growth inhibition is likely a result of nitrite and free nitrous acid (FNA; $pK_a = 3.16$) and subsequent reactive nitrogen oxides, generated from the intracellular passage of FNA into *P. denitrificans*. A flavohemoglobin (*fhb*; Pd1689) and its associated NsrR family, transcriptional regulator (Pd1690), were transcribed above a ≥ 2 fold expression filter ($p \leq 0.05$) at 95% significance in qRT-PCR and a type II microarray transcriptional analysis at 12.5 mM nitrite in batch culture. Additionally, >25 fold expression of the flavohemoglobin was confirmed by qRT-PCR in continuous culture with nitrite. A deletion mutant determined *fhb* to be involved in conveying nitrite resistance at high nitrite concentrations and is linked to a stimulation of biomass generated by the presence of nitrite. The cytochrome *ba₃* oxidase was found to be associated with nitrite in transcriptional analysis, suggesting the uncoupling of the protonmotive force caused by the transport of FNA across the membrane, and subsequent dissociation in the cytoplasm were reduced by a method of counterbalance. No nitrate accumulation was seen and nitrous oxide levels were above that observed for atmospheric background levels. The microarray analysis was used to confirm that in batch growth at 12.5 mM nitrite addition, *P. denitrificans* shows an overall stress response associated with protein, DNA and lipid repair, with the addition of *fhb* detoxification and action of the cytochrome *ba₃* oxidase. It is therefore suggested that nitrite presents a pH-dependent stress response in *P. denitrificans*, likely due to the production of associated reactive nitrogen species such as NO from the internalisation of FNA and the uncoupling of the protonmotive force.

1 Introduction

Contents

1	Introduction	1
1.1	List of figures	2
1.2	The Nitrogen Cycle	3
1.2.1	Nitrogen fixation.....	4
1.2.2	Ammonia immobilisation and ammonification.....	6
1.2.3	Nitrification.....	7
1.2.4	Nitrogen assimilation	8
1.2.5	Anaerobic ammonium oxidation (anammox)	8
1.2.6	Denitrification	10
1.3	The reactive nature of nitrogen oxides	11
1.3.1	Nitric oxide and its breakdown products.....	12
1.3.2	Peroxynitrite and the generation of nitric oxide	13
1.3.3	Wastewater and the environmental impact of nitrogen oxides	14
1.3.4	Recent increases in atmospheric nitrous oxide levels	15
1.4	<i>P. denitrificans</i> as a model denitrifying microorganism.....	17
1.4.1	Nitrate reduction by the cytoplasmic nitrate reductase (NAR) in <i>P. denitrificans</i>	20
1.4.2	Nitrate reduction by the periplasmic nitrate reductase (NAP).....	22
1.4.3	Nitrate reduction in the bacterial assimilatory pathway (NAS)	26
1.4.4	The nitrite, nitric oxide and nitrous oxide reductases	27
1.5	Aims	30
1.6	References.....	31

1.1 List of figures

- Figure 1.1: Schematic illustrating the nitrogen cycle, showing the processes of nitrogen fixation. The atmosphere nitrogen (N_2) (with an oxidation state of 0) is converted to ammonium (NH_4^+ ; -3), which can be either be immobilised into the cellular structure of organisms, or oxidised via the hydroxylamine ion (NH_2OH ; -1) to nitrite (NO_2^- ; +3) and nitrate (NO_3^- ; +5) during nitrification. Ammonification or mineralisation of cellular bound organic nitrogen reintroduces nitrogen in the form of ammonia. NO_3^- can then be reduced to NO_2^- , nitric oxide (NO ; +2), nitrous oxide (N_2O ; +1) and returned to N_2 by denitrification. Additionally, anomox (anaerobic ammonium oxidation) also returns nitrogen from NH_4^+ and NO_2^- to N_2 . Heterotrophic nitrification oxidises NH_2OH to form N_2O and is a route to N_2O emissions from the nitrification pathway. Finally the three processes of respiration, dissimilation and assimilation all contribute to convert NO_3^- to NO_2^- . (Adapted from Richardson (2001) and Nature Education © 2010.) 5
- Figure 1.2. A: Haber Bosch processing for the industrialised production of nitrate fertiliser. The Haber process combines nitrogen from the air with hydrogen, derived mainly from natural gas (methane), into ammonia. The reaction is reversible and the production of ammonia is exothermic. B: Impact of manure production, fertiliser production on atmospheric N_2O production per year (sources: The European Environment Agency (EEA) and Intergovernmental Panel on Climate Change (IPCC))..... 16
- Figure 1.3: Respiratory chain for *P. denitrificans*. The movement of electrons is shown by orange arrows. Electron donors such as hydrogenases, the NADH-UQ oxidoreductase and succinate dehydrogenase provide electrons to the Ubiquinol Pool (Q-Pool) generating the formation of Ubiquinol and pumping protons into the periplasm. These electrons are then passed to the nitrate reductases and ubiquinol cytochrome *c* oxidoreductase, which in turn passes electrons to the cytochrome c_{550} / pseudoazurin and cytochrome c_{552} . Finally electrons pass to the cbb_3 and aa_3 oxidase, nitrite reductase, nitric oxide reductase, nitrous oxide reductase and cytochrome *c* peroxidase. 19
- Figure 1.4: Oxidative phosphorylation pathway featuring the NADH-UQ oxidoreductase (complex I), succinate dehydrogenase (complex II), cytochrome bc_1 complex (complex III), cytochrome aa_3 oxidase (complex IV) and ATP synthase. 21
- Figure 1.5: A schematic for metabolism of fatty acids in *P. denitrificans* and up-regulation of the periplasmic nitrate reductase (NapAB). A: β -Oxidation pathway showing metabolism of butyrate to form Acetyl Co-A. Reducing equivalents NADH and $FADH_2$ are produced by β -Oxidation and enter the Q-Pool reduce ubiquinone to ubiquinol. B: Activation of the

NapAB complex accepting electrons taken from the Q-Pool via NapC to reduce nitrate to nitrite, converting the excess ubiquinol to ubiquinone. The Q-Pool is rebalanced. 24

Figure 1.6: Enzymes available under aerobic growth conditions in *P. denitrificans*. Featuring nitrate reduction by NapABC; generation of free nitrous acid passing across the periplasmic membrane; decomposition and disproportionation of nitrogenous species in the cytoplasm; detoxification of nitric oxide (NO) by NorBC; generation of ammonia by NasC and NasBG; ammonia assimilation by GS and GOGAT. The dashed lines indicate chemical processes not mediated by enzyme catalysis and dotted lines indicate pathways present only in the absence of ammonia in media..... 25

1.2 The Nitrogen Cycle

The role of nitrogen in the biosphere is significant as it is abundant in all biological organisms. It appears in the form of amino acids and DNA, as well as chlorophyll, found specifically in photosynthetic organisms. To be used so profusely, nitrogen species are interconverted between different oxidation states by an array of processes in the nitrogen cycle represented in figure 1.1. The processes involved in cycling nitrogen in this manner require a variety of organisms interconverting nitrogen between the oxidation states. The main processes within the nitrogen cycle are nitrogen fixation, nitrification, denitrification, anammox, and ammonification (Ferguson, 1998).

A large proportion of nitrogen remains kinetically stabilised as dinitrogen (N_2) in the atmosphere, making 78% of the atmosphere composition. However this form of nitrogen is not biologically available and must be “fixed” by bacteria to become bioavailable to the primary producing organisms in the form of ammonia (NH_3). N_2 is readily soluble in fresh and salt water systems making it available to microorganisms for fixation. As NH_3 , the nitrogen can be incorporated into biomass by autotrophic organisms. In addition, a smaller contributor to N_2 fixation can occur by abiotic means through lightning or the industrial combustion of fossil fuels (Kaye and Hart, 1997).

Nitrogen follows a full cycle of transformations and can be returned to its atmospheric form by denitrifying bacteria (heterotrophs). Therefore, the bioavailability of nitrogen is dependent on how much is removed from - and subsequently returned to - the atmosphere by a varied collection of microorganisms. This has meant that it is possible to have a bioavailable nitrogen shortage in some ecosystems where the consumption is greater than

the production of bioavailable nitrogen (Kuzyakov and Xu, 2013). For example, in coastal and offshore waters of the eastern South Pacific oxygen minimum zone nitrate (NO_3^-) reduction to nitrite (NO_2^-) in denitrification and subsequent NO_2^- re-oxidation to NO_3^- has led to nitrogen loss in the water column (Lam *et al.*, 2009; Navarro-González *et al.*, 2001). Equally the intervention of human processes in the production of nitrogen oxides has led to an abundance of bioavailable nitrogen in specific ecosystems, such as NO_3^- fertilisation of agricultural soils (Vitousek *et al.*, 2013; Menge *et al.*, 2012). A significant contributor has been the industrial fixation of atmospheric nitrogen in the Haber-Bosch process. This process uses an iron catalyst and hydrogen (natural gas or petroleum supplied) under high pressure and at a temperature of 600°C to generate NH_3 . This makes it of particular importance to understand the intricate interconversions of nitrogen and the causes and consequences of any imbalance to the cycle..

1.2.1 Nitrogen fixation

Nitrogen predominantly exists in a stable state as atmospheric N_2 . Two N atoms are bonded by a triple covalent bond which requires a large amount of energy to break: $\text{N}_2 + 8\text{H}^+ + 8\text{e}^- \rightarrow 2\text{NH}_3 + \text{H}_2$. As a result N_2 is very unreactive unless specifically targeted for catalytic conversion. N_2 bonding is broken during nitrogen fixation. Sixteen molecules of ATP are needed by the prokaryotic organisms which carry out the fixation process, making the process vastly energetically expensive. These organisms can be symbiotic in nature such as *Rhizobia* and *Frankia*, which associate with a host legume organism to form nodules on its root system and can find energy by many means, including anaerobic respiration, photosynthetically and chemotrophically. By producing ammonia the organisms supply the plant with a bioavailable nitrogen source and in exchange they obtain carbohydrates from the plant which redeems the extensive energy expended by fixation. These organisms are found abundantly and in varying environments, including aerobic lakes, oceans and soils, anoxic sediments, hypersaline lakes, microbial mats as well as planktonic crustaceans and termites. They are mostly studied in plant symbiotic systems.

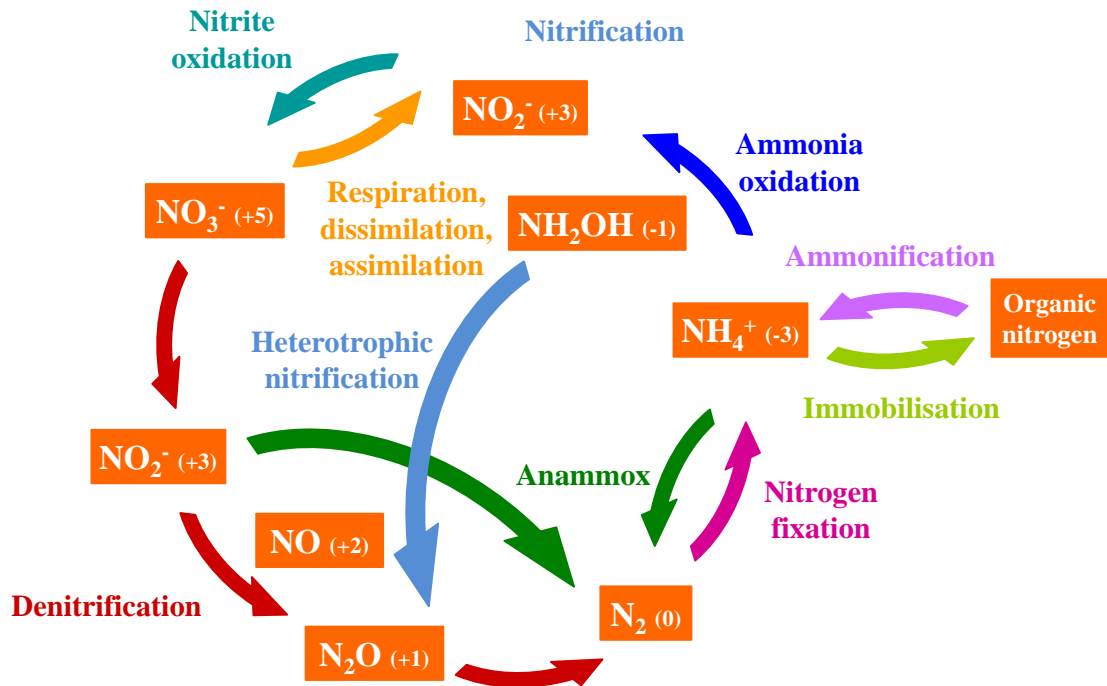


Figure 1.1: Schematic illustrating the nitrogen cycle, showing the processes of nitrogen fixation. The atmosphere nitrogen (N_2) (with an oxidation state of 0) is converted to ammonium (NH_4^+ ; -3), which can be either be immobilised into the cellular structure of organisms, or oxidised via the hydroxylamine ion (NH_2OH ; -1) to nitrite (NO_2^- ; +3) and nitrate (NO_3^- ; +5) during nitrification. Ammonification or mineralisation of cellular bound organic nitrogen reintroduces nitrogen in the form of ammonia. NO_3^- can then be reduced to NO_2^- , nitric oxide (NO ; +2), nitrous oxide (N_2O ; +1) and returned to N_2 by denitrification. Additionally, anammox (anaerobic ammonium oxidation) also returns nitrogen from NH_4^+ and NO_2^- to N_2 . Heterotrophic nitrification oxidises NH_2OH to form N_2O and is a route to N_2O emissions from the nitrification pathway. Finally the three processes of respiration, dissimilation and assimilation all contribute to convert NO_3^- to NO_2^- . (Adapted from Richardson (2001) and Nature Education © 2010.)

All nitrogen fixing organisms share a common nitrogenase enzyme which catalyses the conversion of N_2 to NH_3 . Nitrogenase activity is very oxygen sensitive and does not function when oxygen is present. Nitrogen fixing bacteria have had to adapt to allow aerobic respiration and photosynthesis while maintaining the function of a nitrogenase. For example, some photogenic bacteria act to fix nitrogen only at night and some cyanobacteria produce heterocysts to provide a low oxygen environment for the nitrogenase. Fixation results in ammonia, which can either be oxidised via the hydroxylamine ion (-1) to nitrite (NO_2^-) (+3) and nitrate (NO_3^-) (+5) during nitrification or immobilised into the cellular structure of organisms. This presents a multitude of methods by which nitrogen can be fixed to NH_3 and made biologically available for the subsequent steps in the nitrogen cycle (Vitousek *et al.*, 2013; Zehr *et al.*, 2003).

1.2.2 Ammonia immobilisation and ammonification

The biological incorporation of nitrogen is fundamental to the growth of all living organisms and so there is competition between plants and microorganisms for this resource. Immobilisation of nitrogen takes place when nitrogen is in the form of ammonia (NH_3). It is taken up by heterotrophic organisms with nitrate for incorporation into organic nitrogen, such as amino acids and nucleic acids, to produce biomass. Immobilisation is triggered in environments with a greater demand for nitrogen and therefore occurs in environments with a higher carbon to nitrogen ratio (Bengtsson *et al.*, 2003; Recous *et al.*, 1990).

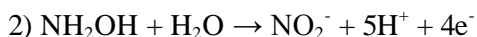
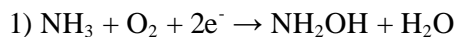
Ammonification reverses the process of immobilisation. Organic complex compounds are degraded to smaller molecules (mineralisation). This process releases the ammonia (NH_3) which has been bound into organic nitrogen-containing compounds. Organism death and excretory processes can result in nitrogen from tissues being released in the form of organic nitrogen, such as nucleic acids or amino acids. Many decomposition processes take place in the breakdown of these tissues, including prokaryotic and fungal liberation of the nitrogen in the form of NH_3 . Also, organisms can excrete excess ammonia in the form of ammonium (NH_4^+), for example in urine. In this form, nitrogen can be taken up by plants and microorganisms and returned to organic nitrogen, or oxidised in nitrification.

This release of NH_3 returns nitrogen locked into organic organism components back to the nitrogen cycle. The resultant NH_3 can be converted back to organic nitrogen

(immobilisation) and taken up by microbes and plants (assimilation) or nitrified to NO_3^- further in the nitrogen cycle (figure 1.1).

1.2.3 Nitrification

Nitrification follows the fixation of nitrogen and is the oxidation of ammonia (NH_3) to the hydroxylamine ion (NH_2OH) intermediate (1) and subsequent oxidation of the NH_2OH to nitrite (NO_2^-) (2):



The conversion of NH_3 to the intermediate ion, NH_2OH , is catalysed by an ammonia monooxygenase. The further conversion of NH_2OH to NO_2^- is catalysed by a hydroxylamine oxidoreductase. This process is exclusive to free prokaryotes, with ammonia oxidisers carrying out the conversion of NH_3 to NO_2^- . This process is not energy generous and results in slow growth of ammonia oxidisers. Aerobic ammonia oxidisers are autotrophic and fix carbon dioxide by producing organic carbon in a pathway similar to photosynthesis. This uses ammonia, not light, as the energy source. The well documented ammonia oxidisers are *Nitrosomonas*, *Nitrosospira*, and *Nitrosococcus*, representing a niche field of a small number of organisms capable of this nitrification. A recent addition has been the archaeon ammonia oxidisers, for example *Nitrosopumilus maritimus*, which has been found to outnumber the ammonia-oxidizing bacteria in many habitats and contributes significantly to nitrification. Nitrification can also be carried out by heterotrophic microorganisms. Heterotrophic nitrification describes the biochemical oxidation of NH_3 and/or organic nitrogen or NH_2OH , directly to NO_3^- , NO_2^- , N_2O or N_2 (Qiao *et al.*, 2011; Zhao *et al.*, 2010).

The NO_2^- is further oxidised to form NO_3^- : $2\text{NO}_2^- + \text{O}_2 \rightarrow 2\text{NO}_3^-$ by a distinctly separate group of nitrite oxidising prokaryotes: *Nitrobacter*, *Nitrococcus*, and *Nitrospina*, some of which share the same genera as ammonia oxidisers: *Nitrospira*. Again the energy yield for this oxidation is low and the organisms slow growing. The generation of NO_3^- marks completion of the nitrification step of the nitrogen cycle. Although ammonia oxidisers are found in many aerobic portions of environments including oceans, lakes, and soils, much study has been carried out in waste water treatment facilities where ammonia and nitrite

oxidisers remove harmful ammonia from water to be returned to the open environment (Pochana and Keller, 1999; Stark and Hart, 1997; Anthonisen *et al.*, 1976).

1.2.4 Nitrogen assimilation

Nitrogen assimilation by heterotrophic bacteria is a lesser-studied area of nitrate metabolism. Studies have been performed on *Enterobacter aerogenes* where growth conditions in minimal medium with nitrate as the sole nitrogen source were used to explore assimilatory and respiratory nitrate reduction. Nitrate reductase activity was observed to be much lower under aerobic than anaerobic conditions and nitrate reductase in aerobic growth was found to be very sensitive to sonic disintegration and other homogenisation procedures (Van'T Riet *et al.*, 1968). Other studies of the γ -proteobacterium include *Klebsiella oxytoca* (Lin and Stewart, 1998), photo-heterotroph *Rhodobacter capsulatus* (Pino *et al.*, 2006), *Bacillus subtilis* (Ogawa *et al.*, 1995). Recent studies by Gates *et al.*, and coworkers have identified and characterised a nitrate assimilatory system in *P. denitrificans* PD1222 (Luque-Almagro *et al.*, 2013; Gates *et al.*, 2011). Both cytoplasmic and periplasmic nitrate reductases are members of the molybdoenzyme family. This enzyme family all bind a molybdenum bis-molybdenum dinucleotide cofactor as the active site of NO_2^- reduction (nitrogenase however, contains a different multinuclear iron-molybdenum centre) (Arnoux *et al.*, 2003; Hille, 2002).

1.2.5 Anaerobic ammonium oxidation (anammox)

Anammox presents an alternative pathway for the oxidation of ammonia which is contrary to the traditional nitrification route and is an anaerobic process. It is a major contributing pathway alongside denitrification, to release nitrogen back to the atmosphere. Anammox was an industrially designed process for accelerated nitrogen removal in wastewater streams. The first full-scale Anammox plant started up in the Netherlands in 2002 and it has gained momentum due to its apparent increased efficiency and its reduced operational costs and CO_2 emissions.

Anammox uses NO_2^- as an oxidising agent. It is carried out by the *Planctomycetes* and was first characterised in *Brocadia anammoxidans*. The process of anammox (anaerobic

ammonium oxidation), refers to the oxidation of ammonium coupled with the reduction of nitrite under anoxic conditions, and has been predicted to be a more thermodynamically favourable process than aerobic ammonium oxidation (Broda, 1977). The anammox process oxidises ammonium by using nitrite as the electron acceptor to produce gaseous nitrogen: $\text{NH}_4^+ + \text{NO}_2^- \rightarrow \text{N}_2 + 2\text{H}_2\text{O}$. Wastewater treatment plants were again important to the understanding of the nitrogen cycle in the discovery of anammox bacteria in the facility anoxic bioreactors. Subsequently, these anammox bacteria have also been found in a variety of areas including low oxygen ocean zones, freshwater lakes and sediments (Strous *et al.*, 1999; Hu *et al.*, 2011).

Anammox is carried out by a group of planctomycete-like bacteria originally isolated from industrial ecosystems. It was discovered in a wastewater-treatment plant in The Netherlands (Mulder *et al.*, 1995). The anammox bacteria are coccoid and have a diameter of less than 1 μm . They belong to the order of *Planctomycetes* and are therefore anaerobic chemolithoautotrophic. Three genera of anammox bacteria have been discovered so far: *Brocadia*, *Kuenenia* and *Scalindua* (Schmid *et al.*, 2005). Many species have now been identified and all anammox species which have been found in marine and estuarine systems belong to the genus *Scalindua* (Schmid *et al.*, 2007). They have also been found in abundance in natural anoxic marine sediments and water columns, freshwater sediments and water columns and terrestrial ecosystems. They are also found in some special ecosystems, such as petroleum reservoirs (Kuypers *et al.*, 2005). It has been suggested that anammox attributes 50% of the marine nitrogen loss and 9–40% and 4–37% of the nitrogen loss in inland lakes and agricultural soils respectively, which is indicative of the potential for the anammox process in freshwater and terrestrial ecosystems (Jetten *et al.*, 2009).

One of the main characteristics of anammox bacteria is a membrane bound anammoxosome. This is a membrane bound compartment in the cell containing ladderane lipids (ladderanes, a structure made of rigid lipids), in which the anammox process is believed to take place. The anammoxosome membrane offers protection for the cell from the very reactive hydrazine intermediate, and limits the diffusion of protons across it. Therefore the ATPase is more efficient (van Niftrik *et al.*, 2004).

1.2.6 Denitrification

Denitrification is the process by which respiratory enzymes reduce nitrate (NO_3^-) to nitrite (NO_2^-), nitric oxide (NO), nitrous oxide (N_2O) and finally return nitrogen to its atmospheric dimeric form (Richardson, 2001). It therefore “concludes” the nitrogen cycle by returning nitrogen to a form which is no longer bioavailable. The intermediate steps also yield biologically important gases. NO is a potent cytotoxin and N_2O a significant greenhouse gas.

Denitrification uses the sequential reduction of NO_3^- to N_2 as a method of anaerobic respiration, when oxygen is unavailable to be the terminal electron acceptor and oxidising agent of the respiration chain. The complete redox reaction of denitrification is: $2\text{NO}_3^- + 10e^- + \text{H}^+ \rightarrow \text{N}_2 + 6\text{H}_2\text{O}$ and occurs in anaerobic soils, sediments, anoxic regions of lakes and oceans as well as anaerobic regions within organisms, such as in earthworm tracts (Giannopoulos *et al.*, 2011; Horn *et al.*, 2006). There is a diversity of prokaryotes carrying out denitrification and some suggestion that it occurs in some eukaryotes (Risgaard-Petersen *et al.*, 2006). Denitrifiers are predominantly facultative anaerobes and chemotrophic including *Paracoccus*, *Bacillus* and various *Pseudomonas* (Carlson and Ingraham, 1983) with some autotrophic bacteria such as *Thiobacillus denitrificans* (Vishniac and Santer, 1957) and archaea, including *Haloarchaea* (Najera-Fernandez *et al.*, 2012).

The role of denitrification is important both environmentally and economically in such areas as agriculture. This is due to the current thorough research into production of the potent greenhouse gas nitrous oxide (N_2O), which has been studied in the nutrient deficient agricultural soils of intensive farming (Sullivan *et al.*, 2013; Bouwman, 1996). Additions of nitrates applied to the soils as fertilisers is a costly area of agriculture, with much being removed after rainfall where it can be detrimental to surrounding waterways (Nixon, 1995). In wastewater treatment, denitrification is a vital component used in combination with ammonia and nitrite oxidation in the cleaning of effluent for discharge to the water systems (Zhou *et al.*, 2011). By reducing nitrates, discharged waters are less likely to cause eutrophication of surrounding waters resulting in algal blooms and removal of oxygen from the water. In this way waters can be kept near to the naturally found in the environment (Erisman *et al.*, 2013). Additionally denitrification removes nitrate from recirculated drinking water, reducing the chances of methemoglobinemia in infants (Majumdar, 2003).

Denitrification is a vital requirement for the nitrogen cycle. Denitrification provides the final step in the nitrogen cycle by returning nitrogen to its inert form at atmospheric N_2 . This

remains as the most abundant form of nitrogen, from which fixation continues the cyclic conversion of nitrogen species.

1.3 The reactive nature of nitrogen oxides

Nitrosative and oxidative stresses can be placed on microorganisms as a result of compound decomposition and disproportionation. This in turn forms cytotoxic compounds detrimental to cellular function such as nitrite (NO_2^-), nitrous acid (HNO_2) and nitric oxide (NO), in sufficient concentration and under optimal conditions to enter and affect cellular metabolism (Poole, 2005).

Nitrate is a molecule which at high levels causes toxic effects in living organisms. Human and animal consumption of nitrate can generate a reduction of nitrate in the digestive tract leading to the release of nitrite. Nitrite can be absorbed into the blood where it converts hemoglobin into methemoglobin, a substance which is incapable of transporting oxygen (Zijlstra *et al.*, 1991). This causes a poisoning effect leading to a reduction in overall health (Geraldo Neto *et al.*, 2013; Shaikat *et al.*, 2012). This does not occur in ruminants, where nitrite is converted to ammonia and incorporated into biomass of gut microorganisms therefore not accumulating to toxic levels (Holtenius, 1957). Nitrate can be introduced into the diet from plant material high in nitrate. High levels of nitrates accumulate in plant material when high levels of nitrate fertiliser are used and drought conditions exist. They are also found where a reduction in photosynthetic activity is caused by defoliation or low light conditions and certain plant species which accumulate high nitrate levels are present. Nitrate can also be introduced into the gut of humans and animals through poisoning of water supplies from agricultural soil run off, or groundwater can be contaminated from leaching of nitrate generated from fertiliser used on agricultural lands and landfill. This type of contamination leads to Blue-Baby syndrome as a result of nitrite poisoning in young children (Majumdar, 2003).

Nitrate is toxic to many microorganisms, such as *Clostridium botulinum*, which is not capable of removing nitrate or nitrite. Nitrate is used in the meat industry in this way to prevent gram-positive bacterial growth and oxidation of the meat products so the meat maintains a red colour (Christiansen *et al.*, 1973; Milkowski *et al.*, 2010). This is not effective against gram-negative bacteria such as *Escherichia coli* which has a nitrate and nitrite reductase (Poole *et al.*, 1996).

Nitrogen or oxygen-based compounds which have an unstable electron configuration or are highly chemically reactive in solution are termed as reactive nitrogen species (RNS) and reactive oxygen species (ROS). When generated in concentrations greater than can be neutralised by microorganisms, this nitrosative or oxidative stress causes cytotoxic effects such as inhibition of cellular growth, disruption of biofilm attachment, and cell death (Jiang *et al.*, 2011). RNS play vital biological roles and are continuously produced in plants as by-products of aerobic metabolism or in response to stress (Pauly *et al.*, 2006). Biological systems utilise RNS and ROS chemical action in antimicrobial defence mechanisms against bacterial pathogens (Bodenmiller and Spiro, 2006; Iovine *et al.*, 2008).

1.3.1 Nitric oxide and its breakdown products

Nitric oxide ($\bullet\text{NO}$, or NO) is a molecule containing one unpaired valence electron which occupies the orbit of the molecule singularly and not as part of an electron pair, forming a free radical. The formation of an electron pair is an energetically favourable reaction, therefore radicals typically only occur briefly during reactions as intermediate molecules and an entity that carries an unpaired electron is usually rather reactive. This reactive nature also lends NO its destructive capabilities. It is able to travel freely in biological systems through water solubility and has large reactivity in the presence of oxygen and water as a free radical; both of this leads NO to have a short life span in biological systems (Spiro, 2007).

NO addition into bacterial biofilms induces planktonic growth, which increases antimicrobial effectiveness against bacteria. This has been studied in *P. aeruginosa* as well as mixed culture wastewater treatment bioreactors (Barraud *et al.*, 2006; Webb *et al.*, 2003). *P. aeruginosa* biofilms express the nitrite reductase *nirS* and nitric oxide reductase *norBC* genes at higher levels than during planktonic growth. This suggests a requirement for controlled nitrite and nitric oxide levels to maintain biofilm formation. NO levels are regulated by quorum sensing and are highly expressed in biofilms compared to planktonic growth, which is quorum sensing dependent. This has been reaffirmed by the use of nitrite in the removal of biofilms in wastewater treatment facilities. Therefore, NO is able to facilitate the transition from biofilm to planktonic phenotype (Webb *et al.*, 2003; Barraud *et al.*, 2006).

NO is capable of directly interacting with transition metals containing protein, such as globin, cytochrome, and oxidising ferrous haem into ferric haem forms halting catalytic activity. It can also bind transition metals such as Fe, Cu, Co, and Mn. Microarrays have shown similarities between the genes upregulated in the presence of NO and genes upregulated in iron limitation growth conditions. These experiments showed upregulation of genes for iron uptake, such as ferric uptake regulator (Fur), perhaps due to the removal of iron from iron- and haem- containing proteins caused by NO damage. RNS is also detrimental to catalytic function. This commonly occurs as cysteine oxidation and tyrosine nitration, affecting protein secondary structure (Hogg *et al.*, 1992; Pacher *et al.*, 2007).

NO production could not be attributed to the effects of nitrite and proton concentration alone. Zweier *et al* (1999) described a rate law of NO formation calculated directly from the equation of free nitrous acid (FNA; HNO_2) disproportionation. This produced the following reaction scheme: NO formation occurs from the decomposition of dinitrogen trioxide: $\text{FNA} \leftrightarrow \text{nitrosonium ion (NOOH)}$, an isoform of FNA. $\text{NO}_2^- + \text{NOOH} \leftrightarrow \text{N}_2\text{O}_3 + \text{OH}^-$. which further decomposes: $\text{N}_2\text{O}_3 \rightarrow \text{NO}_2 + \text{NO}$. Additionally nitrogen dioxide can dimerise: $\text{NO}_2 \rightarrow \text{N}_2\text{O}_4 + \text{H}_2\text{O}$. Formation of NO was also pH dependent at pH 4-7 and follows a 1st order reaction which is proton concentration dependent, and at <pH 4 the formation of NO is a zero order reaction making it a proton concentration independent reaction. N_2O_3 and NOOH react readily, so therefore are considered unlikely to accumulate to levels equivalent to that of nitrite (Zweier *et al.*, 1999).

1.3.2 Peroxynitrite and the generation of nitric oxide

Reactive nitrogen species (RNS) include such nitrogen oxides as nitric oxide (NO) + superoxide (O_2^-) which can react to form peroxynitrite (ONOO^-), a membrane permeable molecule (Pacher *et al.*, 2007; Marla *et al.*, 1997; Van Dyke, 1997) able to react itself to form further reactive nitrogen species (Fukuto *et al.*, 2012). Peroxynitrite (ONOO^-) is a very reactive molecule. From it, a multitude of reactive and cytotoxic molecules can be derived. Peroxynitrite can be protonated to form ONOOH (peroxynitrous acid). This in turn is able to form nitrogen dioxide ($\bullet\text{NO}_2$) and a hydroxyl radical ($\bullet\text{OH}$). Peroxynitrite can also react with carbon dioxide (CO_2) to form nitrosoperoxycarbonate (ONOOCO_2^-), which is itself is reactive and can yield nitrogen dioxide ($\bullet\text{NO}_2$) and carbonate radical ($\text{O}=\text{C}(\text{O}\bullet)\text{O}^-$) species. (Squadrito and Pryor, 1998; Jour'dheuil *et al.*, 1999; Pacher *et al.*, 2007; Hrabarova *et al.*,

2011; Szabo *et al.*, 2007). Peroxynitrite is capable of direct cysteine oxidation and peroxynitrite derived RNS react directly with tyrosine (Pacher *et al.*, 2007). Protein denaturation occurs when the secondary and tertiary structure is disrupted. In addition to direct enzymological function, RNS are able to react with lipids, thiols, amino acid residues, DNA bases, and low-molecular weight antioxidants at a slower rate. This slow reaction rate significantly allows it to react more selectively throughout the cell (O'Donnell *et al.*, 1999).

1.3.3 Wastewater and the environmental impact of nitrogen oxides

Research into the area of nitrification, denitrification and the effects of both nitrite and derived free nitrous acid plays an important role in the understanding and physical processing of nutrient removal. Nitrogen and phosphorus removal is an important and well-studied area. Research into the area is important for wastewater treatment facilities for the safe discharge of effluent water back into waterways. It also assists in the restoration of waterways affected by eutrophication or disruption of natural water course-ways. It has additionally featured in the exploration of drainage ditches near intensive farming facilities, where accumulation from surface run off of inorganic or organic (manure from dual farming of both pastoral and arable outputs) is of particular interest.

Nutrient removal is artificially carried out in wastewater treatment plants (WWTP) and occurs naturally in areas where the natural nitrogen and phosphorus levels of water systems have been disrupted (Shuman, 2002; Nixon, 1995). Biological nitrogen removal utilises both nitrification and denitrification in a two-step process to incorporate soluble nitrogen, as nitrate in solution, into biological material in the form of biomass of heterotrophic microorganisms (Knowles, 1982; Lai *et al.*, 2004). Removal of nitrate is done in batch-fed systems or continuous systems. These systems require energy to aerate and a carbon source for denitrification, e.g. methanol or acetate (Boyle-Gotla and Elefsiniotis, 2013).

In recent research, it has been found that nitrite has an abundant cytotoxic effect on the growth of mix culture, WWTP microorganisms (Zhou *et al.*, 2011; Ye *et al.*, 2010). The nature of this effect has been received with interest as a potential method for reduction of sludge production in wastewater treatment and for the reduction of biofilm production on industrial WWTP facilities (Wang *et al.*, 2013).

1.3.4 Recent increases in atmospheric nitrous oxide levels

Nitrous oxide (N_2O) is of great importance as a greenhouse gas (GHG) and agent of ozone depletion. It has recently been identified as one of six types of GHG to be curbed under the Kyoto Protocol (Bates *et al.*, 2008). According to the IPCC's Fourth Assessment Report, N_2O has a global warming potential 298 times that of carbon dioxide (CO_2) (Forster *et al.*, 2007) and an atmospheric lifetime of approximately 114 years (IPCC-WGI, 2007). As a GHG, N_2O accounts for a small 0.03 per cent proportion of the total GHG emissions, but its radioactive potential gives rise to a vast warming potential making it a gas of significant impact (IPCC-WGIII, 2007). Considering this warming potential and expressing the impact of N_2O as Intergovernmental Panel on Climate Change approved units of CO_2 equivalents, N_2O is suggested to account for 10% of all emissions (Bates *et al.*, 2008).

Specifically it has been reported by the IPCC that overall N_2O emissions have increased by 50% since 1970, 11% of which since the year 1990 and it has been suggested to be mainly due to the increased use of fertiliser and the aggregate growth of agriculture. During this time, industrial process emissions of N_2O have fallen (IPCC-WGIII, 2007) (figure 1.2 B). A natural by-product of the increased levels of bioavailable nitrogen in agricultural soils and waterways contaminated by surface run-off has been a dramatic increase in N_2O emissions (Bates *et al.*, 2008). Fossil fuels also generated a source of both N_2O and soil nitrogen shortly after this time from motor vehicles, as deposited nitrogen and N_2O from exhaust emissions (Livesley *et al.*, 2013; Erisman *et al.*, 2013).

Anthropogenic contributions to GHG composition are proposed to comprise largely of CO_2 and methane, but with N_2O contributing a significant 7.9%. Levels of N_2O remained relatively low until the advent of the Haber-Bosch process in 1908 (figure 1.2 A). Ammonia was in large demand as a source of synthetic nitrogen fertiliser for the increasingly intensive agricultural inputs of the industrial revolution and for the manufacture of explosives during World War I and II (Thomson *et al.*, 2012). Haber-Bosch circumvents the biological nitrogen cycle as an industrial scale chemical nitrogen fixation method of reducing atmospheric nitrogen to form ammonia. Additional contributions come from animal waste in soils and waterways, increased human population and wastewater treatment plants (Kimochi *et al.*, 1998; Davidson, 2009).

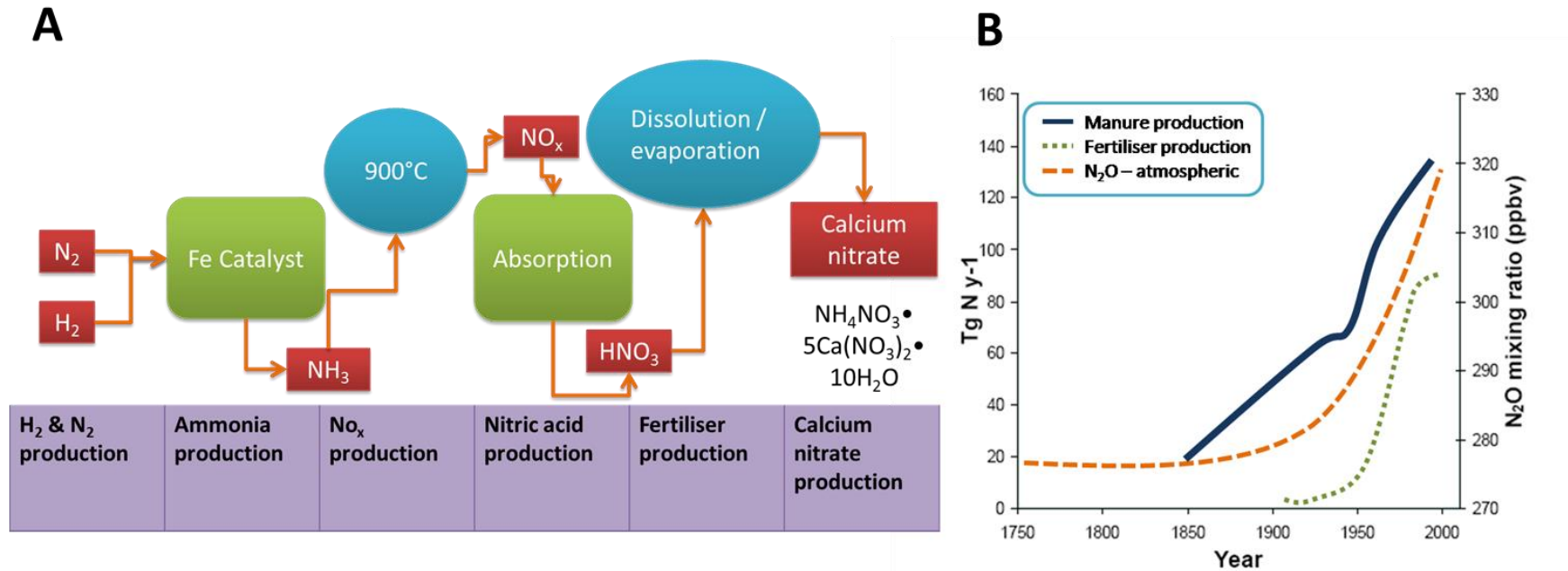


Figure 1.2. A: Haber Bosch processing for the industrialised production of nitrate fertiliser. The Haber process combines nitrogen from the air with hydrogen, derived mainly from natural gas (methane), into ammonia. The reaction is reversible and the production of ammonia is exothermic. B: Impact of manure production, fertiliser production on atmospheric N_2O production per year (sources: The European Environment Agency (EEA) and Intergovernmental Panel on Climate Change (IPCC)).

Identified over 200 years ago as a nontoxic, non-flammable, colourless gas (Keys, 1941), N₂O has subsequently had a multitude of purposes due to its useful anaesthetic and analgesic properties. Euphoric effects experienced upon inhalation gave N₂O the common name of ‘laughing gas’ and gave rise to its use as a recreational drug in Britain from 1799 (Lynn *et al.*, 1972; Whalley and Brooks, 2009). It was first used as an anaesthetic in dental operations by Horace Wells in 1844 and was in general use for dentistry in 1863 (Sneader, 2005). It has also found a use as an oxidising agent in motor car racing engines and rocketry (Kramlich and Linak, 1994; Yoo *et al.*, 2012). The largest proportion of N₂O emissions come directly from biological processes as part of the nitrogen cycle as nitrification and denitrification pathways are utilised by fungus and bacteria for respiration (Oenema *et al.*, 2005). These processes account for over two-thirds of the N₂O emissions. Therefore the exploration of N₂O production routes in microorganisms is of great importance, especially in the developing fields of agriculture and wastewater management (Kimochi *et al.*, 1998).

1.4 *P. denitrificans* as a model denitrifying microorganism

This gram-negative, facultative anaerobe displays an energy metabolism similar to the mitochondrion of eukaryotes with an electron-transfer-linked phosphorylation chain (Otten *et al.*, 1999). A complex and adaptive system, it may be a product of the natural environment *P. denitrificans* inhabits, as Van Spanning suggests: “*survival of unicellular organisms is defined by the adaptability of the cell’s metabolism to available carbon and free-energy sources in its natural surrounding environment*” (Van Spanning *et al.*, 1995). *P. denitrificans* bears close evolutionary characteristics to the eukaryotic mitochondria which lead to a model for oxidative phosphorylation studies in the late 80s (van Verseveld and Bosma, 1987). This homology can be seen in the complexes of I, II and IV which are the NADH-UQ oxidoreductase, cytochrome *bc*₁ complex and cytochrome *aa*₃ oxidase. Differences arise in the number of subunits, which are less in the prokaryotic analogs of the mitochondrial respiratory complexes. An adaption unique to *P. denitrificans* is the addition of two further oxidases, homologous to the *aa*₃ oxidase. These are the *cbb*₃-type cytochrome *c* oxidase and the *ba*₃-type quinol oxidase. Both contain a haem-copper binuclear centre and are capable of acting as proton pumps. The *ba*₃ oxidase directly oxidises ubiquinol, not cytochrome *c* as is the case with the *aa*₃ oxidase and this causes a shunted respiratory chain. The *cbb*₃ oxidase performs the same reaction *aa*₃ oxidase, requiring the cytochrome *c* oxidase, but shows little homology to the *aa*₃ oxidase. It bears homology instead to the nitric

oxide reductases and leads to a suggestion of cross overs between aerobic and anaerobic respiration at an evolutionary level (Pitcher and Watmough, 2004).

P. denitrificans was originally isolated from a dyke in Holland and can be found in soil, sewage and sludge. These are largely water-logged, but fluctuating environments in which microbes experience and adapt to aerobicity and anaerobicity, pH change and interaction with other microbial metabolites and breakdown products. *P. denitrificans* can therefore be suggested as an example agricultural soil bacterium and provide insight into the metabolic alterations a fluctuating soil environment can expose such bacteria to. The evolutionary heritage of *P. denitrificans* is of the *Rhodobacterales* order of the α -proteobacteria which contains many waterborne bacteria. *P. denitrificans* has been utilised for its nitrate removing abilities in the treatment of waste. *P. denitrificans* was paired with *Nitrosomonas europaea*, which can reduce ammonia to nitrite, inside a bioreactor vessel. *P. denitrificans* therefore presents itself as a representative model organism which can inform both the agricultural soil bacterial and wastewater industrial studies.

P. denitrificans displays an adaptive ability to utilise a vast array of alternative compounds for electron donation for respiration and expresses a branched electron transfer network, capable of utilising the many electron donors and acceptors available to it (Otten *et al.*, 1999; Van Spanning *et al.*, 1995). The variety of oxidisable substrates and terminal electron acceptors found in bacteria is due to the variety of environments in which bacteria and archaea have colonised. By expressing the appropriate terminal oxidase, respiration can occur under differing oxygen levels in aerobic growth whether allowing respiration to continue despite anoxia or in near pure oxygen atmosphere. *P. denitrificans* can express primary dehydrogenases which are adapted to act efficiently under differing oxygen tensions.

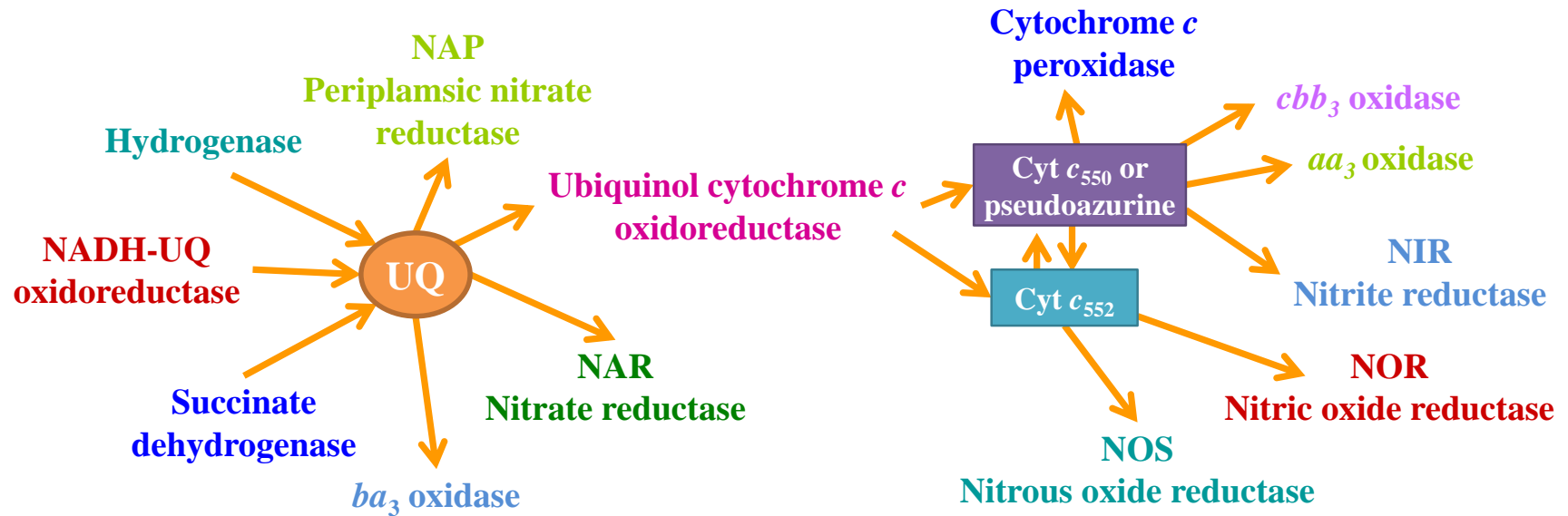


Figure 1.3: Respiratory chain for *P. denitrificans*. The movement of electrons is shown by orange arrows. Electron donors such as hydrogenases, the NADH-UQ oxidoreductase and succinate dehydrogenase provide electrons to the Ubiquinol Pool (Q-Pool) generating the formation of Ubiquinol and pumping protons into the periplasm. These electrons are then passed to the nitrate reductases and ubiquinol cytochrome *c* oxidoreductase, which in turn passes electrons to the cytochrome c_{550} / pseudoazurine and cytochrome c_{552} . Finally electrons pass to the cbb_3 and aa_3 oxidase, nitrite reductase, nitric oxide reductase, nitrous oxide reductase and cytochrome *c* peroxidase.

In the same way, bacteria are able to upregulate enzymatic systems to continue respiration in anaerobic growth conditions. These use alternate terminal electron acceptors, replacing the use of oxygen entirely. These can be nitrogen oxides, metalloids oxyanions, transition metals and organic sulphoxides (Ellington *et al.*, 2002; Ellington *et al.*, 2003). These terminal electron acceptors generate less energy per molecule metabolised, but allow bacteria to colonise areas which are entirely anaerobic by adaptation of respiration and control of electron flux (Arnoux *et al.*, 2003; Richardson *et al.*, 1998; Richardson, 2000; Baker *et al.*, 1998). Nitrogen oxides and oxyanion reduction are used for the termination of the membrane associated respiratory electron transport pathway in bacteria (Zumft, 1997). *P. denitrificans* is capable of reducing nitrate to nitrite by three nitrate reductases: the cytoplasmic nitrate reductase (NAR), periplasmic nitrate reductase (NAP) and the bacterial assimilatory nitrate reductase (NAS).

1.4.1 Nitrate reduction by the cytoplasmic nitrate reductase (NAR) in *P. denitrificans*

P. denitrificans contains three distinct nitrate reductases (Richardson, 2000; Richardson, 2001). The membrane bound nitrate reductase found on the cytoplasmic side of the bacterial membrane in *P. denitrificans* is NarGHI. NarG contains Mn and acts to directly bind and reduce nitrate to nitrite. NarH binds three [4Fe-4S] and one [3Fe-4S] for the transfer of electrons from NarI to NarG. NarI is the quinol dehydrogenase membrane bound domain of the NarGHI complex and contains two haem groups (Jormakka *et al.*, 2004) (figure 1.4). Aerobic nitrate reduction has been attributed to the periplasmic nitrate reductase (NAP) and only with growth on a reduced carbon source (Sears *et al.*, 1997). Due to the cytoplasmic active site of the nitrate reductase enzyme, a nitrogen oxyanion transporter protein (NarK) imports nitrate from the periplasmic side of the bacterial membrane and returns nitrite back across the membrane to the periplasmic side (Goddard *et al.*, 2008; Richardson *et al.*, 2001).

1.4.2 Nitrate reduction by the periplasmic nitrate reductase (NAP)

Finally, the periplasmic nitrate reductase is the third nitrate reductase found in *P. denitrificans*. NapA and NapB are the soluble component of NapABC, found on the periplasmic side of the inner bacterial membrane, resulting in NAP being first isolated as the heterodimer NapAB. NapA contains four structural domains of 91kDa total size. Its active site features a Mn cofactor and [4Fe-4S] cluster anchored by a 4 cysteine motif at the N-terminal to carry out the nitrate reduction to nitrite. Electrons for the reduction of nitrate are passed through two *c*-type cytochromes both *bis*-His ligated which are found in the 17kDa NapB from the integral membrane bound tetrahaem quinol dehydrogenase (NapC) (Berks *et al.*, 1995; Roldán *et al.*, 1998).

NapAB has been described in monomeric form expressed in *Rhodobacter sphaeroides* (Sabaty *et al.*, 1999) which has provided significant advances in the identification and localisation of the cofactors associated with function of the periplasmic nitrate reductase (Arnoux *et al.*, 2003). Nap acts when *P. denitrificans* cells are grown on a highly reduced carbon source. The large numbers of electrons provided by the reduced carbon source shifts the equilibrium of the ubiquinol/ubiquinone pool in favour of ubiquinol (figure 1.4), resulting in NapABC being proposed as an electron sink in cellular redox balancing for the dissipation of excessive reduction potential across the cellular membrane. It is described as an initiator of aerobic denitrification and scavenger of nitrate (Arnoux *et al.*, 2003; Richardson, 2001) (figure 1.6). The periplasmic nitrate reductase found in *P. denitrificans* is different to that found in *Rhodobacter sphaeroides*, in which both aerobic and anaerobic denitrification is initiated by the periplasmic nitrate reductase (Sabaty *et al.*, 1999; Jormakka *et al.*, 2004).

NapAB is up-regulated in the presence of a highly reduced carbon source is due to the metabolism of those reduced carbon sources inside the cell via the β -oxidation which feeds into the citric acid cycle (figure 1.5). The β -oxidation converts butyrate (4C) into acetyl-CoA (2C) which enters the citric acid cycle and occurs across the membrane and cytoplasm of the bacterial cells. This conversion generates 1 NADH and 1 FADH₂ (by electron transfer flavoprotein) (Watmough and Frerman, 2010).

This process activates butyrate by addition of a thioester bond followed with dehydrogenation by acyl-coA-dehydrogenase requiring FAD⁺ to form a trans- Δ^2 -enoyl-CoA.

This molecule is hydrated to form L-3-hydroxyacyl CoA and oxidised by NAD^+ converting the hydroxyl group into a keto group and forming a β -ketoacyl CoA. The final step is thiolysis of the β -ketoacyl CoA, forming two acetyl-CoA molecules.

These two acetyl- CoA molecules enter the citric acid cycle and turn it twice (once for each molecule) yielding a further 1 FADH_2 and 3 NADH per round. Therefore for each butyrate molecule 10 NADH and FADH_2 molecules are generated. These feed directly into the ubiquinol / quinone pool in the Q-Cycle, disrupting membrane potential and generating ubiquinol. Inhibition of the oxidation of ubiquinol to ubiquinone may limit the catalytic action of the cytochrome bc_1 complex. Catalysis by the cytochrome bc_1 complex reduces one molecule of ubiquinone to allow oxidation of ubiquinol to occur. If this action is prevented ubiquinol oxidation does not occur. A deficit of ubiquinol in the membrane caused by β -oxidation of butyrate may prevent ubiquinone reduction preventing the ubiquinol oxidation (Kurihara *et al.*, 1992; Müller *et al.*, 2010; Kunau *et al.*, 1995). NapC removes electrons from the Q-Pool, by oxidising ubiquinol to ubiquinone, and passes them to the NapAB complex where the electrons are used for the reduction of NO_3^- to NO_2^- .

When compared to growth on a non-reduced carbon source, such as succinate, less ubiquinol equivalents are generated. Succinate enters the tricarboxylic acid (TCA) cycle in the form of succinyl-CoA, which can be oxidised by the citric acid cycle to malate. This generates just 4 ubiquinol equivalents, being 2.5 times less than that molecule per molecule of butyrate. NapAB is up-regulated when ubiquinol levels exceed that of ~25%. By reducing nitrate, NapC oxidises ubiquinol to ubiquinone and restores the balance of oxidised membrane electron carrier for respiration to continue (Jepson *et al.*, 2007).

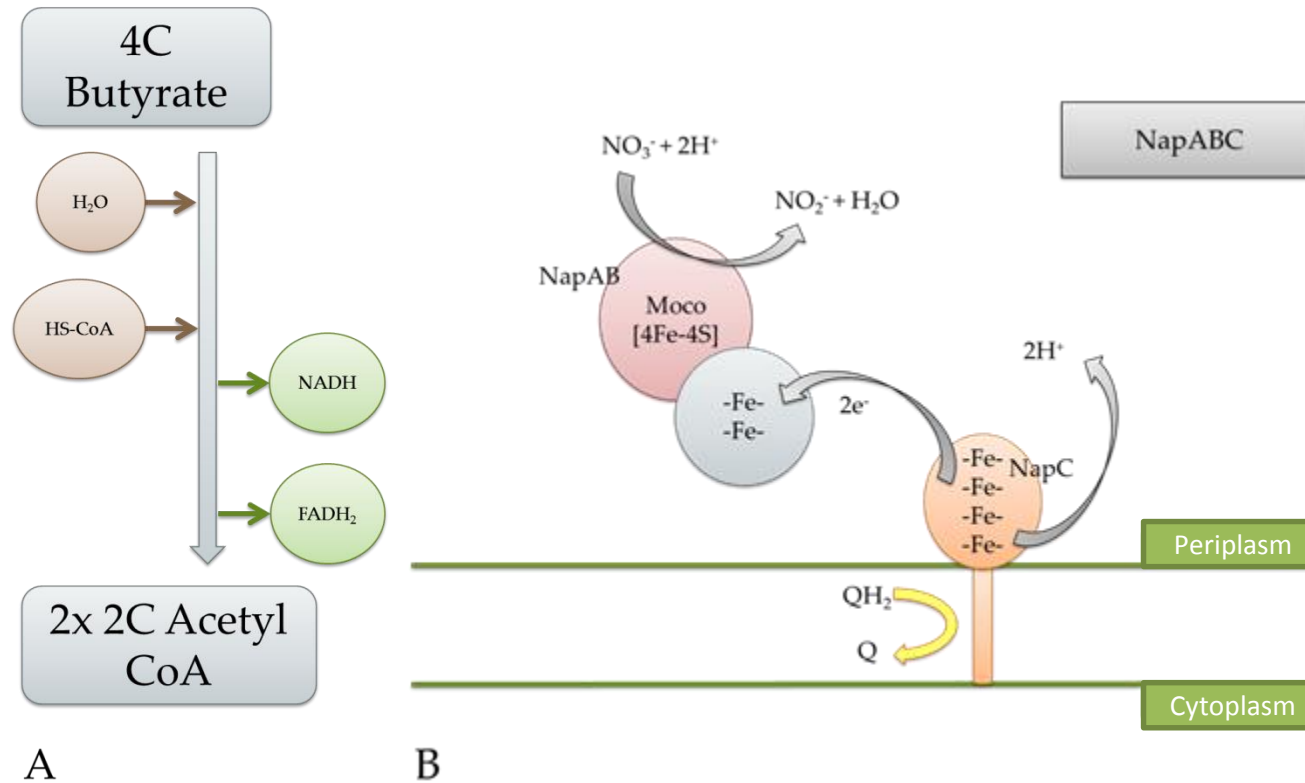


Figure 1.5: A schematic for metabolism of fatty acids in *P. denitrificans* and up-regulation of the periplasmic nitrate reductase (NapAB). **A:** β -Oxidation pathway showing metabolism of butyrate to form Acetyl Co-A. Reducing equivalents NADH and FADH₂ are produced by β -Oxidation and enter the Q-Pool reduce ubiquinone to ubiquinol. **B:** Activation of the NapAB complex accepting electrons taken from the Q-Pool via NapC to reduce nitrate to nitrite, converting the excess ubiquinol to ubiquinone. The Q-Pool is rebalanced.

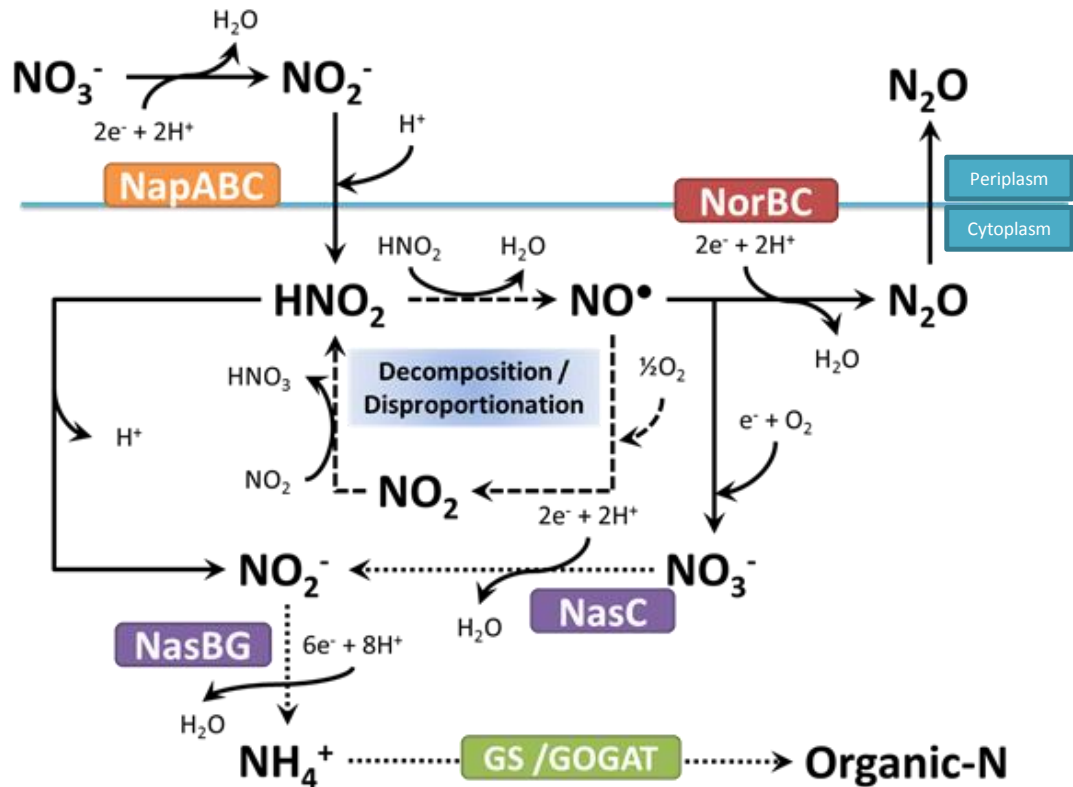


Figure 1.6: Enzymes available under aerobic growth conditions in *P. denitrificans*. Featuring nitrate reduction by NapABC; generation of free nitrous acid passing across the periplasmic membrane; decomposition and disproportionation of nitrogenous species in the cytoplasm; detoxification of nitric oxide (NO) by NorBC; generation of ammonia by NasC and NasBG; ammonia assimilation by GS and GOGAT. The dashed lines indicate chemical processes not mediated by enzyme catalysis and dotted lines indicate pathways present only in the absence of ammonia in media.

1.4.3 Nitrate reduction in the bacterial assimilatory pathway (NAS)

The assimilation of nitrate requires two electron reduction of nitrate to form nitrite and is carried out by the molybdoenzymes which are cytoplasmic proteins. These have a distinctly different structure and function to the of the NAP and NAR nitrate reductases. All three however, bind a Mo-*bis*-molybdopterin guanine dinucleotide cofactor (MO-*bis*-MGD) and one or more [4Fe-4S] clusters.

Without ammonium available for incorporation into biomass, *P. denitrificans* expresses the NAS to produce ammonium from nitrate and or nitrite. The *nasTSABGHC* gene cluster (Pd4455 – 4449) encodes each component of the assimilatory system. NasC works in conjunction with assimilatory enzyme NasBG to perform the eight electron reduction of NO_3^- to ammonium (NH_4^+) (figure 1.6). Electrons are passed from the FAD-containing NasB subunit through the Fe-S cluster within NasG and finally NasC which catalyses the reduction of nitrate to nitrite. NasC contains an [4Fe-4S] cluster and MGD as the active site of NO_3^- reduction. Electrons are supplied by a NADH oxidising domain present in NasB NasH and NasA are required for the active transport of nitrate and nitrite into the cytoplasm where catalysis can take place (Wu and Stewart, 1998; Gates *et al.*, 2011).

The NAS system is also prevalent in other microorganisms, such as the archaeon *Haloferax mediterraneii* and cyanobacteria such as *Azotobacter vinelandii*. In these organisms NAS is a ferredoxin or flavodoxin-dependent enzyme (Martínez-Espinosa *et al.*, 2001; Gutierrez *et al.*, 1995). *A. vinelandii* contains a monomeric 105 kDa nitrate reductase Haloarchaeon *H. mediterraneii* in comparison, contains a dimeric 105 and 50 kDa nitrate reductase. Both receive electrons solely from flavodoxin. Cyanobacterial nitrate reductase is an 80 kDa monomer and can receive electrons from both flavodoxin and ferredoxin. The NADH dependent enzyme is found in heterotrophic bacteria such as *Klebsiella*, *Bacillus* and *Rhodobacter*. *Klebsiella* contains a 92 kDa catalytic subunit (NasA) and a smaller 43 kDa electron transfer subunit. The NAS system has been well studied in *Klebsiella* resulting in the development of an electron flow schematic: $\text{NADH} \rightarrow \text{FAD} \rightarrow [2\text{Fe-2S}] \rightarrow [4\text{Fe-2S}] \rightarrow \text{MGD} \rightarrow \text{NO}_3^-$.

The larger subunit, NasA, binds the MGD, a [4Fe-2S] cluster at the N-terminal and a [2Fe-2S] at the C-terminal, which is a unique extension not found in other bacterial NAS systems such as *Bacillus*. The smaller subunit is the FAD / NADH oxidoreductase and mediates the

electron transfer to NasA. In *Bacillus*, this smaller subunit contains two putative [2Fe-2S] centres additional to the FAD (Lin *et al.*, 1993).

The assimilation of ammonium is carried out by the glutamine synthase (GS) pathway and by NADPH-dependent glutamine: 2-oxoglutarate amidotransferase (GOGAT), the glutamate synthase. Both systems are of interest due to their tolerance of the presence of ammonia; high levels of ammonia lead to the suppression of the GS and GOGAT assimilatory pathways (Tempest *et al.*, 1970). Under more alkaline conditions, ammonium can diffuse freely across the membrane, but in more neutral to acidic conditions, transport is largely undertaken by ammonium transporters (AMT). GS is widely found in both prokaryotic and eukaryotic cells and catalyses an ATP dependent amidation of glutamate and forms a glutamine molecule. GOGAT then catalyses the reductive transfer of an amide group from the glutamine to 2-oxoglutarate, forming two glutamate molecules. This allows the incorporation of ammonium into 2-oxoglutarate and produces glutamate with ATP consumption. Glutamates play a large role in proton pathways such as the cytochrome *bc*₁ complex, which has been shown to have a crucial glutamate facilitating proton transfer through a rotational mechanism (Crofts *et al.*, 2006). Another example is the ATP synthase which has a conserved glutamate in the ion binding site of the *c*-ring (Meier *et al.*, 2005). Direct incorporation of ammonium into 2-oxoglutarate is also carried out by the glutamate dehydrogenase (GDH), but this is less effective at lower ammonium concentrations and so is considered a more minor alternative for the incorporation of ammonium (Kremeckova *et al.*, 1992; Muro-Pastor *et al.*, 2005).

1.4.4 The nitrite, nitric oxide and nitrous oxide reductases

Following nitrate reduction, the anaerobic respiratory sequential reduction continues with nitrite reduction. Nitrite is further reduced in a one electron reduction reaction to form nitric oxide by the nitrite reductase (NIR) in *P. denitrificans*: $\text{NO}_2^- + 2\text{H}^+ + \text{e}^- \rightarrow \text{NO} + \text{H}_2\text{O}$. The NIR found in bacterial metabolism is found in three forms. The iron based cytochrome *cd*₁ (*cd*₁NIR) and a copper containing nitrite reductase (CuNIR) are respiratory NIR. The multihaem cytochrome NIR catalyses nitrite to form ammonia: $\text{NO}_2^- + 8\text{H}^+ + 6\text{e}^- \rightarrow \text{NH}_4^+ + 2\text{H}_2\text{O}$ and is found to be involved in nitrite assimilation or detoxification. The CuNIR are found in many different bacteria for example *Pseudomonas*, *Bordetella*, *Alcaligenes*, and *Achromobacter*. All CuNIR contain at least one type 1 Cu centre, which is similar to azurin

in their bonding structure: the type 1 Cu is bonded to thiolate sulphur from cysteine, two imidazole nitrogens from different histidine residues, and an axial methionine ligand sulphur atom. This induces a distorted tetrahedral molecular geometry. *P. denitrificans* contains a cd_1 NIR which acts as a tetrahaem dimer containing two *c*-type and two d_1 -type haems and is found in the bacterial periplasm. The specialised d_1 haem is located at the active site bound in an 8-bladed β -propeller, where nitrite is bound and reduced (Gordon *et al.*, 2003; Pearson *et al.*, 2003)

Nitric oxide (NO) is reduced by *P. denitrificans* in the respiratory denitrification process using the nitric oxide reductase (NOR). NO is reduced by NorB and NorC with an electron donor: $2\text{NO} + 2e^- + 2\text{H}^+ \rightarrow \text{N}_2\text{O} + \text{H}_2\text{O}$. NOR from *P. denitrificans* also catalyses the reduction of O_2 to H_2O as a side reaction (Zumft, 1997). NOR can be found in many microorganisms, including fungi, where NOR is a member of the P450 family of proteins. The fungus *Fusarium oxysporum* provided the first 3D structure of NOR (Park *et al.*, 1997). In fungi it is a soluble 46 kDa protein containing a haem active site, and receives electrons from NADH (Shiro *et al.*, 1995). This differs to the bacterial NOR which are membrane proteins which receive electrons from cytochrome *c*, pseudoazurin or quinone/semi-quinone (Butland *et al.*, 2001). The *c*- and *q*-type NORs are very similar in the catalytic site. The *c*NOR is typically a soil bacteria NOR and is expressed during low oxygen conditions when NO is present. NOR activation has been seen at NO concentrations of 5-50 nM in *Pseudomonas stutzeri* (Zumft, 2005). *P. denitrificans* contains a *c*NOR, acts as a dimer and consists of two subunits with catalytic capability (NorC and NorB). NorC is 17 kDa and a membrane-bound cytochrome *c* and is suggested to be the site electrons enter from cytochrome *c*. NorC is predicted to have one single trans-membrane helix that anchors the more globular haem *c* containing portion and faces it to the periplasm (Hendriks *et al.*, 1998). The larger NorB subunit of 54 kDa binds a haem *b*, b_3 and a non-haem iron. The b_3 and a non-haem iron are suggested to form the active site of NOR (Grönberg *et al.*, 1999; Berks *et al.*, 1995).

The structure of NorB has been extensively studied in *P. stutzeri* which shows high sequence similarity to the *P. denitrificans* NorB. This allows some insight into the cofactor coordination in NorB. It is suggested that there is histidine coordination of cofactors: haem *b* His53 (in helix II) and His336 (helix X), for haem b_3 His334 (helix X) and for the FeB His194 (helix VI) and His245 and His246 (helix VII) (Girsch and De Vries, 1997). A *cis*-mechanism has been suggested as the entrance of NO to the active site for catalysis, binding

two NO molecules to one cofactor known as the *cis-b₃* mechanism and the *trans*-mechanism in which binding of one NO molecule to each cofactor occurs (Zumft, 2005; Kapetanaki *et al.*, 2008). The *trans*-mechanism suggests a sequential binding of the NO molecules and has been proposed from steady-state kinetic experiments and rapid-freeze quench EPR experiments with the fully-reduced NOR (Girsch and De Vries, 1997). The *cis*-FeB mechanism fits the very low redox potential of haem *b₃*, which should make the three-electron reduced enzyme prevalent during turnover (Grönberg *et al.*, 1999; Grönberg *et al.*, 2004). However theoretical calculations and experimental results demonstrate that NO binds to haem *b₃*, which has prevented a sure decision on the mechanisms of NOR action (Blomberg *et al.*, 2006; Hendriks *et al.*, 2002)

Nitrous oxide produced is finally reduced to di-nitrogen by the nitrous oxide reductase NOS: $\text{N}_2\text{O} + 2\text{e}^- + 2\text{H}^+ \rightarrow \text{N}_2 + \text{H}_2\text{O}$. Studies of *Pseudomonas nautical* and *P. denitrificans* have brought to light the structural composition of NOS in recent work. NOS is a copper containing periplasmic homodimer of 65 kDa. It includes a copper containing subunit which binds a dinuclear CuA electron entry site with structural similarities to the *aa₃* oxidase, and a tetra-nuclear Cu_z catalytic centre. Therefore each monomer is made of a CuA domain containing a cupredoxin fold and a Cu_z domain with a seven bladed β -sheet propeller. This organisation allows the inner electron transfer from CuA of one monomer to Cu_z of a second monomer. The electrons utilised in the reduction are received either from cytochrome *c₅₅₀* or pseudoazurin via the cytochrome *bc₁* complex. Catalysis occurs in the Cu_z tetra-nuclear copper cluster (Brown *et al.*, 2000). This process is highly copper dependent, requiring 12 copper ions for reduction to take place. It is therefore susceptible to copper depletion which can prevent nitrous oxide reduction and cause accumulation. NOS is sensitive to and repressed by the presence of oxygen (Sullivan *et al.*, 2013). Environmentally speaking the regulation of NOs is important in the level of N₂O generated by microbial activity. The Cu_z centre has been characterised as a new type of metal cluster containing four copper ion ligands supported by seven histidine residues, two hydroxide molecules and a bridging sulphide (Rasmussen *et al.*, 2000). Catalysis is suggested to be carried out by the binding of N₂O to the Cu_z centre via a single copper ion, with remaining copper acting as an electron reservoir. Also suggested is a mechanism using the inorganic sulphide as an N₂O binding site in which the oxygen atom can form sulphoxide before being protonated and released with the N₂ (Brown *et al.*, 2000).

1.5 Aims

Denitrifying bacteria such as *P. denitrificans* reduce nitrate sequentially via nitrite, nitric oxide and nitrous oxide to dinitrogen. These reductive reactions are an alternative to oxygen respiration, coupled to the generation of a protonmotive force and therefore to cell maintenance and growth under anoxic conditions.

Under anoxic conditions, denitrifying bacteria express respiratory enzymes that can serve to reductively destroy extra cytoplasmic NO_2^- and NO, which is generated in the periplasm from NO_3^- reduction. These are the nitrite reductase (*nir*) and the nitric oxide reductase (*nor*). In *P. denitrificans* *nir* and *nor* gene expression is co regulated by the same transcriptional regulator NnrR (an FNR-like activator protein which is suggested to be an NO sensor). This ensures that the production and consumption of reactive nitrogen species are tightly coupled. However, expression of the *nir* and *nos* systems is repressed by oxygen and activity of the enzymes themselves is inhibited by oxygen. Denitrifying bacteria colonise many environments at the oxic-anoxic interface, generating energy from the nitrite and nitrate denitrification substrates that arise from the aerobic nitrification process. This leads to the interaction of these microorganisms and NO_2^- .

In this study, the characterisation of the specific microbial interaction and parameters associated with nitrosative stress and the denitrifying organism *P. denitrificans* is explored. This has been carried out using the bacterial cell culturing, metabolic analysis and transcription characterisation of nitrosative stress induced by specifically sodium nitrite. By exposing *P. denitrificans* to the NO_2^- ion in an aerobic environment, this work will replicate the interaction of the NO_2^- and *P. denitrificans* and can inform the research area.

The role of the NO_2^- ion in nitrosative stress can inform the interaction of microorganisms within a soil and wastewater environment. This work will contribute to the understanding of microorganisms and nitrogenous interaction, by characterising the transcriptional and metabolic features and metabolic characteristics of the response seen in *P. denitrificans*.

The accessibility of the microarray technique to characterise transcriptional regulation in *P. denitrificans* whole genome offers a novel exploration of nitrosative stress and detoxifications of nitrogenous oxides. It complements phenotypic observation and metabolic profiling of *P. denitrificans* under nitrosative stress. Nitrosative stress has intrinsic links to the oxidative cycling of nitrogen globally and an important role to play more specifically in the denitrification processes both anaerobically and aerobically. The metabolic impact of

nitrite and the detoxification of associated cytotoxic nitrogenous oxides can offer profound insights into possible aerobic routes to nitrous oxide emissions, linked to the natural and agricultural soils environment. This manuscript offers a postulate metabolic model for the aerobic denitrification nitrate and nitrite. Here, focus is on the *in vitro* techniques that have identified one mechanism of nitrosative stress and the microbiological response at a metabolic and transcriptional level within *P. denitrificans*.

The initial observations made by this study focus on the high-throughput screening of growth conditions conducive to the production of nitrite stress. Traditionally, the batch culture technique has been used for the study of many aspects of microbial physiology, metabolism, expression of genes and interaction with compounds. The main advantages of batch culture include reproducibility and control of the system, with relatively standard laboratory equipment. In continuous growth, the planktonic culture within a fermenter vessel is fed with a nutrient media limited by a nutrient component within the media ingredients, at a determined dilution rate. This preserves bacterial population in the exponential or log phase of growth and maintains a steady state of continuous growth which, in theory, could be maintained for any required length of time (with the assumption of no contamination or mutation of the organism genome as a response to the growth conditions) (Pelczar *et al.*, 1986). For continuous growth to be maintained, the bacteria, products of growth, media components, and waste products are kept at a constant level (Monod, 1950).

1.6 References

- ANTHONISEN, A. C., LOEHR, R. C., PRAKASAM, T. B. S. & SRINATH, E. G. 1976. Inhibition of nitrification by ammonia and nitrous acid. *Journal of the Water Pollution Control Federation*, 48, 835-852.
- ARNOUX, P., SABATY, M., ALRIC, J., FRANGIONI, B., GUIGLIARELLI, B., ADRIANO, J. M. & PIGNOL, D. 2003. Structural and redox plasticity in the heterodimeric periplasmic nitrate reductase. *Nature Structural Biology*, 10, 928-934.
- BAKER, S. C., FERGUSON, S. J., LUDWIG, B., PAGE, M. D., RICHTER, O. M. & VAN SPANNING, R. J. 1998. Molecular genetics of the genus *Paracoccus*: metabolically versatile bacteria with bioenergetic flexibility. *Microbiology and Molecular Biology Reviews*, 62, 1046-78.

- BARRAUD, N., HASSETT, D. J., HWANG, S. H., RICE, S. A., KJELLEBERG, S. & WEBB, J. S. 2006. Involvement of nitric oxide in biofilm dispersal of *Pseudomonas aeruginosa*. *Journal of Bacteriology*, 188, 7344-7353.
- BATES, B., KUNDZEWICZ, Z., WU, S. & PALUTIKOF, J. 2008. Climate change and water. *Technical Paper of the Intergovernmental Panel on Climate Change*, Geneva, Switzerland: IPCC.
- BENGTSSON, G., BENGTSON, P. & MÅNSSON, K. F. 2003. Gross nitrogen mineralization-, immobilization-, and nitrification rates as a function of soil C/N ratio and microbial activity. *Soil Biology and Biochemistry*, 35, 143-154.
- BERKS, B. C., FERGUSON, S. J., MOIR, J. W. B. & RICHARDSON, D. J. 1995. Enzymes and associated electron transport systems that catalyse the respiratory reduction of nitrogen oxides and oxyanions. *Biochimica et Biophysica Acta - Bioenergetics*, 1232, 97-173.
- BLOMBERG, L. M., BLOMBERG, M. R. A. & SIEGBAHN, P. E. M. 2006. Reduction of nitric oxide in bacterial nitric oxide reductase—a theoretical model study. *Biochimica et Biophysica Acta - Bioenergetics*, 1757, 240-252.
- BODENMILLER, D. M. & SPIRO, S. 2006. The *yjeB* (*nsrR*) gene of *Escherichia coli* encodes a nitric oxide-sensitive transcriptional regulator. *Journal of Bacteriology*, 188, 874-881.
- BOUWMAN, A. F. 1996. Direct emission of nitrous oxide from agricultural soils. *Nutrient Cycling in Agroecosystems*, 46, 53-70.
- BOYLE-GOTLA, A. & ELEFSINIOTIS, P. 2013. Biological nitrogen removal of ammonia-rich centrate in batch systems. *Journal of Environmental Science and Health*, 48, 331-7.
- BRODA, E. 1977. Two kinds of lithotrophs missing in nature. *Zeitschrift für Allgemeine Mikrobiologie*, 17, 491-493.
- BROWN, K., DJINOVIC-CARUGO, K., HALTIA, T., CABRITO, I., SARASTE, M., MOURA, J. J. G., MOURA, I., TEGONI, M. & CABBILLAU, C. 2000. Revisiting the catalytic CuZ cluster of nitrous oxide (N₂O) reductase: Evidence of a bridging inorganic sulfur. *Journal of Biological Chemistry*, 275, 41133-41136.
- BUTLAND, G., SPIRO, S., WATMOUGH, N. J. & RICHARDSON, D. J. 2001. Two conserved glutamates in the bacterial nitric oxide reductase are essential for activity but not assembly of the enzyme. *Journal of Bacteriology*, 183, 189-199.

- CARLSON, C. A. & INGRAHAM, J. L. 1983. Comparison of denitrification by *Pseudomonas stutzeri*, *Pseudomonas aeruginosa*, and *Paracoccus denitrificans*. *Applied and Environmental Microbiology*, 45, 1247-1253.
- CHRISTIANSEN, L. N., JOHNSTON, R. W., KAUTTER, D. A., HOWARD, J. W. & AUNAN, W. J. 1973. Effect of nitrite and nitrate on toxin production by *Clostridium botulinum* and on nitrosamine formation in perishable canned comminuted cured meat. *Applied Microbiology*, 25, 357-62.
- CROFTS, A. R., LHEE, S., CROFTS, S. B., CHENG, J. & ROSE, S. 2006. Proton pumping in the bc1 complex: A new gating mechanism that prevents short circuits. *Biochimica et Biophysica Acta (BBA) - Bioenergetics*, 1757, 1019-1034.
- DAVIDSON, E. A. 2009. The contribution of manure and fertilizer nitrogen to atmospheric nitrous oxide since 1860. *Nature Geoscience*, 2, 659-662.
- ELLINGTON, M. J. K., BHAKOO, K. K., SAWERS, G., RICHARDSON, D. J. & FERGUSON, S. J. 2002. Hierarchy of carbon source selection in *Paracoccus pantotrophus*: Strict correlation between reduction state of the carbon substrate and aerobic expression of the *nap* operon. *Journal of Bacteriology*, 184, 4767-4774.
- ELLINGTON, M. J. K., SAWERS, G., SEARS, H. J., SPIRO, S., RICHARDSON, D. J. & FERGUSON, S. J. 2003. Characterization of the expression and activity of the periplasmic nitrate reductase of *Paracoccus pantotrophus* in chemostat cultures. *Microbiology*, 149, 1533-1540.
- ERISMAN, J. W., GALLOWAY, J. N., SEITZINGER, S., BLEEKER, A., DISE, N. B., PETRESCU, A. M., LEACH, A. M. & DE VRIES, W. 2013. Consequences of human modification of the global nitrogen cycle. *Philosophical Transactions of the Royal Society B: Biological Sciences*, 368, 20130116.
- FERGUSON, S. J. 1998. Nitrogen cycle enzymology. *Current Opinion in Chemical Biology*, 2, 182-193.
- FORSTER, P., RAMASWAMY, V., ARTAXO, P., BERNTSEN, T., BETTS, R., FAHEY, D. W., HAYWOOD, J., LEAN, J., LOWE, D. C., MYHRE, G., NGANGA, J., PRINN, R., RAGA, G., SCHULZ, M. & VAN DORLAND, R. 2007. Changes in Atmospheric Constituents and in Radiative Forcing. *Climate Change 2007: The Physical Science Basis. Contribution of Working Group I to the Fourth Assessment Report of the Intergovernmental Panel on Climate Change [Solomon, S., D. Qin, M. Manning, Z. Chen, M. Marquis, K.B. Averyt, M. Tignor and H.L. Miller (eds.)]. Cambridge University Press, Cambridge, United Kingdom and New York, NY, USA.*

- FUKUTO, J. M., CARRINGTON, S. J., TANTILLO, D. J., HARRISON, J. G., IGNARRO, L. J., FREEMAN, B. A., CHEN, A. & WINK, D. A. 2012. Small molecule signaling agents: The integrated chemistry and biochemistry of nitrogen oxides, oxides of carbon, dioxygen, hydrogen sulfide, and their derived species. *Chemical Research in Toxicology*, 25, 769-793.
- GATES, A. J., LUQUE-ALMAGRO, V. M., GODDARD, A. D., FERGUSON, S. J., ROLDÁN, M. D. & RICHARDSON, D. J. 2011. A composite biochemical system for bacterial nitrate and nitrite assimilation as exemplified by *Paracoccus denitrificans*. *Biochemical Journal*, 435, 743-753.
- GERALDO NETO, S. A., LIMA, J. M., CAMARA, A. C., GADELHA, I. C., OLINDA, R. G., BATISTA, J. S. & SOTO-BLANCO, B. 2013. Spontaneous and experimental poisoning by *Marsdenia megalantha* Goyder & Morillo in ruminants and a pig. *Toxicon*, 63, 116-9.
- GIANNOPOULOS, G., VAN GROENIGEN, J. W. & PULLEMAN, M. M. 2011. Earthworm-induced N₂O emissions in a sandy soil with surface-applied crop residues. *Pedobiologia*, 54, Supplement, S103-S111.
- GIRSCH, P. & DE VRIES, S. 1997. Purification and initial kinetic and spectroscopic characterization of NO reductase from *Paracoccus denitrificans*. *Biochimica et Biophysica Acta - Bioenergetics*, 1318, 202-216.
- GODDARD, A. D., MOIR, J. W., RICHARDSON, D. J. & FERGUSON, S. J. 2008. Interdependence of two NarK domains in a fused nitrate/nitrite transporter. *Molecular Microbiology*, 70, 667-681.
- GORDON, E. H., SJOGREN, T., LOFQVIST, M., RICHTER, C. D., ALLEN, J. W., HIGHAM, C. W., HAJDU, J., FULOP, V. & FERGUSON, S. J. 2003. Structure and kinetic properties of *Paracoccus pantotrophus* cytochrome cd1 nitrite reductase with the d1 heme active site ligand tyrosine 25 replaced by serine. *J Biol Chem*, 278, 11773-81.
- GRÖNBERG, K. L. C., ROLDÁN, M. D., PRIOR, L., BUTLAND, G., CHEESMAN, M. R., RICHARDSON, D. J., SPIRO, S., THOMSON, A. J. & WATMOUGH, N. J. 1999. A low-redox potential heme in the dinuclear center of bacterial nitric oxide reductase: Implications for the evolution of energy-conserving heme- copper oxidases. *Biochemistry*, 38, 13780-13786.
- GRÖNBERG, K. L. C., WATMOUGH, N. J., THOMSON, A. J., RICHARDSON, D. J. & FIELD, S. J. 2004. Redox-dependent Open and Closed Forms of the Active Site of

- the Bacterial Respiratory Nitric-oxide Reductase Revealed by Cyanide Binding Studies. *Journal of Biological Chemistry*, 279, 17120-17125.
- GUTIERREZ, J.-C., RAMOS, F., ORTNER, L. & TORTOLERO, M. 1995. nasST, two genes involved in the induction of the assimilatory nitrite—nitrate reductase operon (nasAB) of *Azotobacter vinelandii*. *Molecular Microbiology*, 18, 579-591.
- HENDRIKS, J., WARNE, A., GOHLKE, U., HALTIA, T., LUDOVICI, C., LÜBBEN, M. & SARASTE, M. 1998. The active site of the bacterial nitric oxide reductase is a dinuclear iron center. *Biochemistry*, 37, 13102-13109.
- HENDRIKS, J. H. M., JASAITIS, A., SARASTE, M. & VERKHOVSKY, M. I. 2002. Proton and electron pathways in the bacterial nitric oxide reductase. *Biochemistry*, 41, 2331-2340.
- HILLE, R. 2002. Molybdenum and tungsten in biology. *Trends in Biochemical Sciences*, 27, 360-367.
- HOGG, N., DARLEY-USMAR, V. M., WILSON, M. T. & MONCADA, S. 1992. Production of hydroxyl radicals from the simultaneous generation of superoxide and nitric oxide. *Biochemical Journal*, 281 (Pt 2), 419-24.
- HOLTENIUS, P. 1957. Nitrite poisoning in sheep, with special reference to the detoxification of nitrite in the rumen. *Acta Agriculturae Scandinavica*, 7, 113-163.
- HORN, M. A., DRAKE, H. L. & SCHRAMM, A. 2006. Nitrous oxide reductase genes (*nosZ*) of denitrifying microbial populations in soil and the earthworm gut are phylogenetically similar. *Applied and Environmental Microbiology*, 72, 1019-26.
- HRABAROVA, E., JURANEK, I. & SOLTES, L. 2011. Pro-oxidative effect of peroxynitrite regarding biological systems: A special focus on high-molar-mass hyaluronan degradation. *General Physiology and Biophysics*, 30, 223-228.
- HU, B. L., SHEN, L. D., XU, X. Y. & ZHENG, P. 2011. Anaerobic ammonium oxidation (anammox) in different natural ecosystems. *Biochem Soc Trans*, 39, 1811-6.
- IOVINE, N. M., PURSNANI, S., VOLDMAN, A., WASSERMAN, G., BLASER, M. J. & WEINRAUCH, Y. 2008. Reactive nitrogen species contribute to innate host defense against *Campylobacter jejuni*. *Infection and Immunity*, 76, 986-993.
- IPCC-WGI 2007. Working group I: the physical science basis. In *IPCC Fourth Assessment Report (AR4): Climate change 2007*, (eds. S. Solomon, D. Qin, M. Manning, Z. Chen, M. Marquis, K. B. Averyt, M. Tignor, h. L. Miler).

- IPCC-WGIII 2007. Working group III: Mitigation of Climate Change. *In IPCC Fourth Assessment Report (AR4): Climate change 2007*, (eds. S. Solomon, D. Qin, M. Manning, Z. Chen, M. Marquis, K. B. Averyt, M. Tignor, h. L. Miler).
- JEPSON, B. J. N., MOHAN, S., CLARKE, T. A., GATES, A. J., COLE, J. A., BUTLER, C. S., BUTT, J. N., HEMMINGS, A. M. & RICHARDSON, D. J. 2007. Spectropotentiometric and structural analysis of the periplasmic nitrate reductase from *Escherichia coli*. *Journal of Biological Chemistry*, 282, 6425-6437.
- JETTEN, M. S. M., NIFTRIK, L. V., STROUS, M., KARTAL, B., KELTJENS, J. T. & OP DEN CAMP, H. J. M. 2009. Biochemistry and molecular biology of anammox bacteria biochemistry and molecular biology of anammox bacteria M.S.M. Jetten et al. *Critical Reviews in Biochemistry and Molecular Biology*, 44, 65-84.
- JIANG, G., GUTIERREZ, O. & YUAN, Z. 2011. The strong biocidal effect of free nitrous acid on anaerobic sewer biofilms. *Water Research*, 45, 3735-3743.
- JORMAKKA, M., RICHARDSON, D., BYRNE, B. & IWATA, S. 2004. Architecture of NarGH reveals a structural classification of Mo-bisMGD enzymes. *Structure*, 12, 95-104.
- JOURD'HEUIL, D., MIRANDA, K. M., KIM, S. M., ESPEY, M. G., VODOVOTZ, Y., LAROUX, S., MAI, C. T., MILES, A. M., GRISHAM, M. B. & WINK, D. A. 1999. The oxidative and nitrosative chemistry of the nitric oxide/superoxide reaction in the presence of bicarbonate. *Archives of Biochemistry and Biophysics*, 365, 92-100.
- KAPETANAKI, S. M., FIELD, S. J., HUGHES, R. J. L., WATMOUGH, N. J., LIEBL, U. & VOS, M. H. 2008. Ultrafast ligand binding dynamics in the active site of native bacterial nitric oxide reductase. *Biochimica et Biophysica Acta - Bioenergetics*, 1777, 919-924.
- KAYE, J. P. & HART, S. C. 1997. Competition for nitrogen between plants and soil microorganisms. *Trends in Ecology and Evolution*, 12, 139-143.
- KEYS, T. E. 1941. The development of anesthesia. *Anesthesiology*, 2, 552-574.
- KIMOCHI, Y., INAMORI, Y., MIZUOCHI, M., XU, K. Q. & MATSUMURA, M. 1998. Nitrogen removal and N₂O emission in a full-scale domestic wastewater treatment plant with intermittent aeration. *Journal of Fermentation and Bioengineering*, 86, 202-206.
- KNOWLES, R. 1982. Denitrification. *Microbiological Reviews*, 46-70, 43-70.

- KRAMLICH, J. C. & LINAK, W. P. 1994. Nitrous oxide behavior in the atmosphere, and in combustion and industrial systems. *Progress in Energy and Combustion Science*, 20, 149-202.
- KREMECKOVA, H., SVRCULA, B. & MIKES, V. 1992. Purification and some properties of glutamate dehydrogenase and glutamine synthetase from *Paracoccus denitrificans*. *Journal of General Microbiology*, 138, 1587-1591.
- KUNAU, W. H., DOMMES, V. & SCHULZ, H. 1995. β -oxidation of fatty acids in mitochondria, peroxisomes, and bacteria: A century of continued progress. *Progress in Lipid Research*, 34, 267-342.
- KURIHARA, T., UEDA, M., OKADA, H., KAMASAWA, N., NAITO, N., OSUMI, M. & TANAKA, A. 1992. Beta-oxidation of butyrate, the short-chain-length fatty acid, occurs in peroxisomes in the yeast *Candida tropicalis*. *Journal of Biochemistry*, 111, 783-787.
- KUYPERS, M. M. M., LAVIK, G., WOEBKEN, D., SCHMID, M., FUCHS, B. M., AMANN, R., JØRGENSEN, B. B. & JETTEN, M. S. M. 2005. Massive nitrogen loss from the Benguela upwelling system through anaerobic ammonium oxidation. *Proceedings of the National Academy of Sciences of the United States of America*, 102, 6478-6483.
- KUZYAKOV, Y. & XU, X. 2013. Competition between roots and microorganisms for nitrogen: mechanisms and ecological relevance.
- LAI, E., SENKPIEL, S., SOLLEY, D. & KELLER, J. 2004. Nitrogen removal of high strength wastewater via nitrification/denitrification using a sequencing batch reactor.
- LAM, P., LAVIK, G., JENSEN, M. M., VAN DE VOSSENBERG, J., SCHMID, M., WOEBKEN, D., GUTIÉRREZ, D., AMANN, R., JETTEN, M. S. M. & KUYPERS, M. M. M. 2009. Revising the nitrogen cycle in the Peruvian oxygen minimum zone. *Proceedings of the National Academy of Sciences*, 106, 4752-4757.
- LIN, J. T., GOLDMAN, B. S. & STEWART, V. 1993. Structures of genes *nasA* and *nasB*, encoding assimilatory nitrate and nitrite reductases in *Klebsiella pneumoniae* M5a1. *Journal of Bacteriology*, 175, 2370-2378.
- LIN, J. T. & STEWART, V. 1998. Nitrate assimilation by bacteria.
- LIVESLEY, S. J., IDCZAK, D. & FEST, B. J. 2013. Differences in carbon density and soil $\text{CH}_4/\text{N}_2\text{O}$ flux among remnant and agro-ecosystems established since European settlement in the Mornington Peninsula, Australia. *Science of the Total Environment*, 465, 17-25.

- LUQUE-ALMAGRO, V. M., LYALL, V. J., FERGUSON, S. J., ROLDÁN, M. D., RICHARDSON, D. J. & GATES, A. J. 2013. Nitrogen oxyanion-dependent dissociation of a two-component complex that regulates bacterial nitrate assimilation. *Journal of Biological Chemistry*, 288, 29692-29702.
- LYNN, E. J., WALTER, R. G., HARRIS, L. A., DENDY, R. & JAMES, M. 1972. Nitrous oxide: It's a gas. *Journal of Psychoactive Drugs*, 5, 1-7.
- MAJUMDAR, D. 2003. The Blue Baby Syndrome. *Resonance*, 8, 20-30.
- MARLA, S. S., LEE, J. & GROVES, J. T. 1997. Peroxynitrite rapidly permeates phospholipid membranes. *Proceedings of the National Academy of Sciences of the United States of America*, 94, 14243-14248.
- MARTÍNEZ-ESPINOSA, R. M., MARHUENDA-EGEA, F. C. & BONETE, M. A. J. 2001. Assimilatory nitrate reductase from the haloarchaeon *Haloferax mediterranei*: purification and characterisation. *FEMS Microbiology Letters*, 204, 381-385.
- MEIER, T., POLZER, P., DIEDERICHS, K., WELTE, W. & DIMROTH, P. 2005. Structure of the rotor ring of F-type Na⁺-ATPase from *Ilyobacter tartaricus*. *Science*, 308, 659-662.
- MENGE, D. N. L., HEDIN, L. O. & PACALA, S. W. 2012. Nitrogen and phosphorus limitation over long-term ecosystem development in terrestrial ecosystems. *PLoS ONE*, 7, e42045.
- MILKOWSKI, A., GARG, H. K., COUGHLIN, J. R. & BRYAN, N. S. 2010. Nutritional epidemiology in the context of nitric oxide biology: A risk-benefit evaluation for dietary nitrite and nitrate. *Nitric Oxide*, 22, 110-119.
- MONOD, J. 1950. La technique de culture continue, theorie et applications. *Annales de l'Institut Pasteur*, 79, 390-410.
- MULDER, A., VAN DE GRAAF, A. A., ROBERTSON, L. A. & KUENEN, J. G. 1995. Anaerobic ammonium oxidation discovered in a denitrifying fluidized bed reactor. *FEMS Microbiology Ecology*, 16, 177-184.
- MÜLLER, N., WORM, P., SCHINK, B., STAMS, A. J. M. & PLUGGE, C. M. 2010. Syntrophic butyrate and propionate oxidation processes: From genomes to reaction mechanisms. *Environmental Microbiology*, 2, 489-499.
- MURO-PASTOR, M. I., REYES, J. & FLORENCIO, F. 2005. Ammonium assimilation in cyanobacteria. *Photosynthesis Research*, 83, 135-150.

- NAJERA-FERNANDEZ, C., ZAFRILLA, B., BONETE, M. J. & MARTINEZ-ESPINOSA, R. M. 2012. Role of the denitrifying *Haloarchaea* in the treatment of nitrite-brines. *International Microbiology*, 15, 111-9.
- NAVARRO-GONZÁLEZ, R., MCKAY, C. P. & MVONDO, D. N. 2001. A possible nitrogen crisis for Archaeal life due to reduced nitrogen fixation by lightning. *Nature*, 412, 61-64.
- NIXON, S. W. 1995. Coastal marine eutrophication: a definition, social causes, and future concerns. *ccpo.odu.edu*, Ophelia.
- O'DONNELL, V. B., EISERICH, J. P., CHUMLEY, P. H., JABLONSKY, M. J., KRISHNA, N. R., KIRK, M., BARNES, S., DARLEY-USMAR, V. M. & FREEMAN, B. A. 1999. Nitration of unsaturated fatty acids by nitric oxide-derived reactive nitrogen species peroxynitrite, nitrous acid, nitrogen dioxide, and nitronium ion. *Chemical Research in Toxicology*, 12, 83-92.
- OENEMA, O., WRAGE, N., VELTHOF, G., GROENIGEN, J. W., DOLFING, J. & KUIKMAN, P. 2005. Trends in global nitrous oxide emissions from animal production systems. *Nutrient Cycling in Agroecosystems*, 72, 51-65.
- OGAWA, K. I., AKAGAWA, E., YAMANE, K., SUN, Z. W., LACELLE, M., ZUBER, P. & NAKANO, M. M. 1995. The *nasB* operon and *nasA* gene are required for nitrate/nitrite assimilation in *Bacillus subtilis*. *Journal of Bacteriology*, 177, 1409-1413.
- OTTEN, M. F., REIJNDERS, W. N. M., BEDAUX, J. J. M., WESTERHOFF, H. V., KRAB, K. & VAN SPANNING, R. J. M. 1999. The reduction state of the Q-pool regulates the electron flux through the branched respiratory network of *Paracoccus denitrificans*. *European Journal of Biochemistry*, 261, 767-774.
- PACHER, P., BECKMAN, J. S. & LIAUDET, L. 2007. Nitric oxide and peroxynitrite in health and disease. *Physiological Reviews*, 87, 315-424.
- PARK, S. Y., SHIMIZU, H., ADACHI, S. I., NAKAGAWA, A., TANAKA, I., NAKAHARA, K., SHOUN, H., OBAYASHI, E., NAKAMURA, H., LIZUKA, T. & SHIRO, Y. 1997. Crystal structure of nitric oxide reductase from denitrifying fungus *Fusarium oxysporum*. *Nature Structural Biology*, 4, 827-832.
- PAULY, N., PUCCIARIELLO, C., MANDON, K., INNOCENTI, G., JAMET, A., BAUDOIN, E., HÉROUART, D., FRENDO, P. & PUPPO, A. 2006. Reactive oxygen and nitrogen species and glutathione: Key players in the legume-*Rhizobium* symbiosis. *Journal of Experimental Botany*, 57, 1769-1776.

- PEARSON, I. V., PAGE, M. D., VAN SPANNING, R. J. M. & FERGUSON, S. J. 2003. A Mutant of *Paracoccus denitrificans* with Disrupted Genes Coding for Cytochrome c 550 and Pseudoazurin Establishes These Two Proteins as the In Vivo Electron Donors to Cytochrome cd 1 Nitrite Reductase. *Journal of Bacteriology*, 185, 6308-6315.
- PELCZAR, M. J., CHAN, E. C. S. & KRIEG, N. R. 1986. *Microbiology*, McGraw-Hill.
- PINO, C., OLMO-MIRA, F., CABELLO, P., MARTÍNEZ-LUQUE, M., CASTILLO, F., ROLDÁN, M. D. & MORENO-VIVIÁN, C. 2006. The assimilatory nitrate reduction system of the phototrophic bacterium *Rhodobacter capsulatus* EIF1. *Biochemical Society Transactions*, 34, 127-129.
- PITCHER, R. S. & WATMOUGH, N. J. 2004. The bacterial cytochrome cbb3 oxidases. *Biochimica et Biophysica Acta (BBA) - Bioenergetics*, 1655, 388-399.
- POCHANA, K. & KELLER, J. 1999. Study of factors affecting simultaneous nitrification and denitrification (SND). *Water Science and Technology*, 39, 61-68.
- POOLE, R. K. 2005. Nitric oxide and nitrosative stress tolerance in bacteria. *Biochemical Society Transactions*, 33, 176-180.
- POOLE, R. K., ANJUM, M. F., MEMBRILLO-HERNANDEZ, J., KIM, S. O., HUGHES, M. N. & STEWART, V. 1996. Nitric oxide, nitrite, and Fnr regulation of *hmp* (flavo-hemoglobin) gene expression in *Escherichia coli* K-12. *Journal of Bacteriology*, 178, 5487-92.
- QIAO, N., WANG, G., YANG, X. H., YIN, X., GAO, B. & YU, D. Y. 2011. Microbial fuel cells with the performance of wastewater denitrification based on heterotrophic nitrification-aerobic denitrifier bacteria. *Fresenius Environmental Bulletin*, 20, 2610-2615.
- RASMUSSEN, T., BERKS, B. C., SANDERS-LOEHR, J., DOOLEY, D. M., ZUMFT, W. G. & THOMSON, A. J. 2000. The Catalytic Center in Nitrous Oxide Reductase, Cu₂Z, Is a Copper-Sulfide Cluster†. *Biochemistry*, 39, 12753-12756.
- RECOUS, S., MARY, B. & FAURIE, G. 1990. Microbial immobilization of ammonium and nitrate in cultivated soils. *Soil Biology and Biochemistry*, 22, 913-922.
- RICHARDSON, D. J. 2000. Bacterial respiration: A flexible process for a changing environment. *Microbiology*, 146, 551-571.
- RICHARDSON, D. J. 2001. Introduction: Nitrate reduction and the nitrogen cycle. *Cellular and Molecular Life Sciences*, 58, 163-164.

- RICHARDSON, D. J., BERKS, B. C., RUSSELL, D. A., SPIRO, S. & TAYLOR, C. J. 2001. Functional, biochemical and genetic diversity of prokaryotic nitrate reductases. *Cellular and Molecular Life Sciences*, 58, 165-178.
- RICHARDSON, D. J., WEHRFRITZ, J. M., KEECH, A., CROSSMAN, L. C., ROLDAN, M. D., SEARS, H. J., BUTLER, C. S., REILLY, A., MOIR, J. W. B., BERKS, B. C., FERGUSON, S. J., THOMSON, A. J. & SPIRO, S. 1998. The diversity of redox proteins involved in bacterial heterotrophic nitrification and aerobic denitrification. *Biochemical Society Transactions*, 26, 401-408.
- RISGAARD-PETERSEN, N., LANGEZAAL, A. M., INGVARSDEN, S., SCHMID, M. C., JETTEN, M. S. M., OP DEN CAMP, H. J. M., DERKSEN, J. W. M., PIÑA-OCHOA, E., ERIKSSON, S. P., NIELSEN, L. P., REVSBECH, N. P., CEDHAGEN, T. & VAN DER ZWAAN, G. J. 2006. Evidence for complete denitrification in a benthic foraminifer. *Nature*, 443, 93-96.
- ROLDÁN, M. D., SEARS, H. J., CHEESMAN, M. R., FERGUSON, S. J., THOMSON, A. J., BERKS, B. C. & RICHARDSON, D. J. 1998. Spectroscopic characterization of a novel multiheme *c*-type cytochrome widely implicated in bacterial electron transport. *Journal of Biological Chemistry*, 273, 28785-28790.
- SABATY, M., SCHWINTNER, C., CAHORS, S., RICHAUD, P. & VERMÉGLIO, A. 1999. Nitrite and nitrous oxide reductase regulation by nitrogen oxides in *Rhodobacter sphaeroides* f. sp. *denitrificans* IL106. *Journal of Bacteriology*, 181, 6028-6032.
- SCHMID, M. C., MAAS, B., DAPENA, A., VAN DE PAS-SCHOONEN, K., VAN DE VOSSENBERG, J., KARTAL, B., VAN NIFTRIK, L., SCHMIDT, I., CIRPUS, I., KUENEN, J. G., WAGNER, M., SINNINGHE DAMSTE, J. S., KUYPERS, M., REVSBECH, N. P., MENDEZ, R., JETTEN, M. S. & STROUS, M. 2005. Biomarkers for in situ detection of anaerobic ammonium-oxidizing (anammox) bacteria. *Appl Environ Microbiol*, 71, 1677-84.
- SCHMID, M. C., RISGAARD-PETERSEN, N., VAN DE VOSSENBERG, J., KUYPERS, M. M. M., LAVIK, G., PETERSEN, J., HULTH, S., THAMDRUP, B., CANFIELD, D., DALSGAARD, T., RYSGAARD, S., SEJR, M. K., STROUS, M., OP DEN CAMP, H. J. M. & JETTEN, M. S. M. 2007. Anaerobic ammonium-oxidizing bacteria in marine environments: widespread occurrence but low diversity. *Environmental Microbiology*, 9, 1476-1484.

- SEARS, H. J., SPIRO, S. & RICHARDSON, D. J. 1997. Effect of carbon substrate and aeration on nitrate reduction and expression of the periplasmic and membrane-bound nitrate reductases in carbon-limited continuous cultures of *Paracoccus denitrificans* PD1222. *Microbiology*, 143, 3767-3774.
- SHAIKAT, A. H., HASSAN, M. M., AZIZUL ISLAM, S. K. M., ALI KHAN, S., HOQUE, M. A., ISLAM, M. N. & HOSSAIN, M. B. 2012. Non-protein nitrogen compound poisoning in cattle. *Zoology*, 31, 65-68.
- SHIRO, Y., FUJII, M., IIZUKA, T., ADACHI, S. I., TSUKAMOTO, K., NAKAHARA, K. & SHOUN, H. 1995. Spectroscopic and kinetic studies on reaction of cytochrome P450_{nor} with nitric oxide: Implication for its nitric oxide reduction mechanism. *Journal of Biological Chemistry*, 270, 1617-1623.
- SHUMAN, L. M. 2002. Phosphorus and nitrate nitrogen in runoff following fertilizer application to turfgrass. *Journal of Environmental Quality*, 31, 1710-1715.
- SNEADER, W. 2005. Drug Discovery –A History. John Wiley and Sons, Retrieved 2012-08-29.
- SQUADRITO, G. L. & PRYOR, W. A. 1998. Oxidative chemistry of nitric oxide: The roles of superoxide, peroxyxynitrite, and carbon dioxide. *Free Radical Biology and Medicine*, 25, 392-403.
- STARK, J. M. & HART, S. C. 1997. High rates of nitrification and nitrate turnover in undisturbed coniferous forests. *Nature*, 385, 61-64.
- STROUS, M., KUENEN, J. G. & JETTEN, M. S. 1999. Key physiology of anaerobic ammonium oxidation. *Applied and Environmental Microbiology*, 65, 3248-50.
- SULLIVAN, M. J., GATES, A. J., APPIA-AYME, C., ROWLEY, G. & RICHARDSON, D. J. 2013. Copper control of bacterial nitrous oxide emission and its impact on vitamin B12-dependent metabolism. *Proceedings of the National Academy of Sciences*.
- SZABO, C., ISCHIROPOULOS, H. & RADI, R. 2007. Peroxyxynitrite: biochemistry, pathophysiology and development of therapeutics.
- TEMPEST, D. W., MEERS, J. L. & BROWN, C. M. 1970. Synthesis of glutamate in *Aerobacter aerogenes* by a hitherto unknown route. *Biochemical Journal*, 117, 405-407.
- THOMSON, A. J., GIANNOPOULOS, G., PRETTY, J., BAGGS, E. M. & RICHARDSON, D. J. 2012. Biological sources and sinks of nitrous oxide and strategies to mitigate emissions. *Philosophical Transactions of the Royal Society B: Biological Sciences*, 367, 1157-1168.

- VAN'T RIET, J., STOUTHAMER, A. H. & PLANTA, R. J. 1968. Regulation of nitrate assimilation and nitrate respiration in *Aerobacter aerogenes*. *Journal of Bacteriology*, 96, 1455-1464.
- VAN DYKE, K. 1997. The possible role of peroxynitrite in Alzheimer's disease: a simple hypothesis that could be tested more thoroughly. *Medical Hypotheses*, 48, 375-80.
- VAN NIFTRIK, L. A., FUERST, J. A., DAMSTÉ, J. S. S., KUENEN, J. G., JETTEN, M. S. M. & STROUS, M. 2004. The anammoxosome: an intracytoplasmic compartment in anammox bacteria. *FEMS Microbiology Letters*, 233, 7-13.
- VAN SPANNING, R. J. M., DE BOER, A. P. N., REIJNDERS, W. N. M., DE GIER, J. W. L., DELORME, C. O., STOUTHAMER, A. H., WESTERHOFF, H. V., HARMS, N. & VAN DER OOST, J. 1995. Regulation of oxidative phosphorylation: The flexible respiratory network of *Paracoccus denitrificans*. *Journal of Bioenergetics and Biomembranes*, 27, 499-512.
- VAN VERSEVELD, H. W. & BOSMA, G. 1987. The respiratory chain and energy conservation in the mitochondrion-like bacterium *Paracoccus denitrificans*. *Microbiological Sciences*, 4, 329-333.
- VISHNIAC, W. & SANTER, M. 1957. The *Thiobacilli*. *Bacteriological reviews*, 21, 195-213.
- VITOUSEK, P. M., MENGE, D. N. L., REED, S. C. & CLEVELAND, C. C. 2013. Biological nitrogen fixation: Rates, patterns and ecological controls in terrestrial ecosystems. *Philosophical Transactions of the Royal Society B: Biological Sciences*, 368.
- WANG, Q., YE, L., JIANG, G. & YUAN, Z. 2013. A free nitrous acid (FNA)-based technology for reducing sludge production. *Water Research*, 47, 3663-3672.
- WATMOUGH, N. J. & FRERMAN, F. E. 2010. The electron transfer flavoprotein: Ubiquinone oxidoreductases. *Biochimica et Biophysica Acta - Bioenergetics*, 1797, 1910-1916.
- WEBB, J. S., THOMPSON, L. S., JAMES, S., CHARLTON, T., TOLKER-NIELSEN, T., KOCH, B., GIVSKOV, M. & KJELLEBERG, S. 2003. Cell death in *Pseudomonas aeruginosa* biofilm development. *Journal of Bacteriology*, 185, 4585-4592.
- WHALLEY, M. G. & BROOKS, G. B. 2009. Enhancement of suggestibility and imaginative ability with nitrous oxide. *Psychopharmacology*, 203, 745-752.

- WU, Q. & STEWART, V. 1998. NasFED proteins mediate assimilatory nitrate and nitrite transport in *Klebsiella oxytoca (pneumoniae)* M5a1. *Journal of Bacteriology*, 180, 1311-1322.
- YE, L., PIJUAN, M. & YUAN, Z. 2010. The effect of free nitrous acid on the anabolic and catabolic processes of glycogen accumulating organisms. *Water Research*, 44, 2901-2909.
- YOO, D.-H., NITTA, Y., IKAME, M., HAYASHI, M., FUJITA, H. & LIM, J.-K. Exhaust characteristics of Nitrous oxide from marine engine. OCEANS, 2012 - Yeosu, 21-24 May 2012 2012. 1-7.
- ZEHR, J. P., JENKINS, B. D., SHORT, S. M. & STEWARD, G. F. 2003. Nitrogenase gene diversity and microbial community structure: a cross-system comparison. *Environmental Microbiology*, 5, 539-54.
- ZHAO, B., HE, Y. L. & ZHANG, X. F. 2010. Nitrogen removal capability through simultaneous heterotrophic nitrification and aerobic denitrification by *Bacillus* sp. LY. *Environmental Technology*, 31, 409-416.
- ZHOU, Y., OEHMEN, A., LIM, M., VADIVELU, V. & NG, W. J. 2011. The role of nitrite and free nitrous acid (FNA) in wastewater treatment plants. *Water Research*, 45, 4672-4682.
- ZIJLSTRA, W. G., BUURSMA, A. & MEEUWSEN-VAN DER ROEST, W. P. 1991. Absorption spectra of human fetal and adult oxyhemoglobin, de-oxyhemoglobin, carboxyhemoglobin, and methemoglobin. *Clin Chem*, 37, 1633-8.
- ZUMFT, W. G. 1997. Cell biology and molecular basis of denitrification? *Microbiology and Molecular Biology Reviews*, 61, 533-616.
- ZUMFT, W. G. 2005. Nitric oxide reductases of prokaryotes with emphasis on the respiratory, heme-copper oxidase type. *Journal of Inorganic Biochemistry*, 99, 194-215.
- ZWEIER, J. L., SAMOUILOV, A. & KUPPUSAMY, P. 1999. Non-enzymatic nitric oxide synthesis in biological systems. *Biochimica et Biophysica Acta - Bioenergetics*, 1411, 250-262.

2 Materials and Methods

Contents

2	Materials and Methods	45
2.1	List of figures	47
2.2	List of tables	47
2.3	Bacterial strains and storage.....	49
2.3.1	Growth media and growth technique for <i>P. denitrificans</i> and <i>E. coli</i>	49
2.3.2	Minimal salts media for aerobic growth experiments with <i>P. denitrificans</i> ..	50
2.4	Growth techniques	52
2.4.1	Aerobic plate reader batch culture technique.....	52
2.4.2	Calculation of the plate reader pathlength for conversion of optical density values to a standard 1 cm pathlength	53
2.4.3	Aerobic shaking flask batch culture	53
2.4.4	Aerobic continuous culture of <i>P. denitrificans</i>	55
2.4.5	Use of aseptic technique to minimise contamination of the growth cultures	57
2.4.6	Calculation of apparent growth rate.....	58
2.4.7	Measurement of growth using optical density	59
2.5	RNA transcriptional analysis by quantitative RT-PCR.....	61
2.5.1	RNA extraction from whole cells	61
2.5.2	Removal of DNA contamination from RNA samples by Ambion® TURBO™ DNase.....	62
2.5.3	RNA degradation analysis with gel electrophoresis	62
2.5.4	Quantitative real-time reverse transcription PCR.....	63
2.6	Type II microarray analysis	64
2.6.1	Preparation and quantification of RNA and genomic DNA	64
2.6.2	Drying of RNA samples	64

2.6.3	Reverse Transcription of RNA samples	65
2.6.4	Bonding of fluorescent dye to genomic DNA sample	66
2.6.5	Cleaning of RNA and DNA samples	66
2.6.6	Hybridisation of complementary DNA and genomic DNA to slides	67
2.6.7	Preparation of Aligent slides and gasket	67
2.6.8	Slide preparation and scanning	68
2.7	Molecular biology techniques	69
2.7.1	Oligonucleotide design and PCR amplifications	69
2.7.2	Polymerase Chain Reaction	73
2.7.3	Agarose gel electrophoresis	74
2.7.4	Gel extraction of DNA from agarose gels	75
2.7.5	Plasmid DNA extraction	75
2.7.6	Plasmid dephosphorylation	76
2.8	Mutation studies with <i>E. coli</i>	77
2.8.1	PCR amplification of the flavohemoglobin flanking regions for insertion into the pK18 <i>mobsacB</i> plasmid	77
2.8.2	Construction of the pKH002 suicide plasmid from pK18 <i>mobsacB</i>	78
2.8.3	Conjugal transfer of pKH002 to <i>P. denitrificans</i> and deletion of the flavohemoglobin gene	81
2.8.4	Flavohemoglobin complementation with vector reinsertion into <i>P. denitrificans</i>	82
2.8.5	Recombinant plasmid formation	84
2.9	Bioinformatics analysis	86
2.9.1	Gene identification	86
2.9.2	DNA sequencing	87
2.10	Metabolic analytical methods	87
2.10.1	Calculation of free nitrous acid concentration	87
2.10.2	High pressure liquid chromatography (HPLC) analysis of nitrate and nitrite	89

2.10.3	Gas chromatography of nitrous oxide	90
2.11	References.....	91

2.1 List of figures

Figure 2.1: The Beer-Lambert law: $A = \epsilon lc$, for the calculation of methylene blue extinction coefficient (ϵ) at 600 nm using, known concentrations of methylene blue (c) and absorbance values experimentally obtained (A_{600nm}) with a 1 cm pathlength (l). Calculation of plate reader pathlength (lx) using A values taken from the plate reader using a 100 μ L volume in a well..... 54

Figure 2.2: Semi log plot for the growth of *P. denitrificans* in minimal salts media at pH 7.5. The gradient of the linear portion of the growth curve has been used to measure a line of best fit (red line). The gradient of this line is used as $\mu_{app} h^{-1}$. The gradient is shown in the table insert. This table shows the output associated with the gradient calculated by OriginPro. ... 60

Figure 2.3: pK18*mobsacB* plasmid showing the multicloning site containing *Pst*I, *Xba*I and *Xma*I restriction sites, the lac Z alpha, neomycin phosphotransferase conveying kanamycin resistance, levansucrase (*sacB*) and pMB1 replication origin site..... 79

Figure 2.4: The pOT2 vector with features. Gentamycin resistance (orange), open reading frames (blue), green fluorescence protein (GFP) (green) and primer and terminator sequences (purple). The *Xba*I restriction cut site for insertion of the flavohemoglobin (*fhb*) is shown at 202 bp (black)..... 83

2.2 List of tables

Table 2.1: Minimal salts growth media and Vishniac's trace elements. Growth media was autoclave sterilised prior to use. Trace elements solution was prepared separately in stock solution and filter sterilised before addition to media post-autoclaving. Carbon and nitrate sources were filter sterilised and added as required. Additional compounds are listed and annotated according to use as carbon and nitrogen sources..... 51

.Table 2.2: The apparent growth values ($\mu_{app} h^{-1}$) for growth curves of *P. denitrificans* growth in minimal salts media pH 7.5. Each growth curve has been plotted as a semi log. The μ_{app} is calculated by taking a gradient of the linear portion of the semi log lot. μ_{app} has been measured on three biologically independent replicates: A, B and C. The three μ_{app}

values have then been averaged manually: D. A separate μ_{app} value has been derived using a semi log plot of the average of the three biologically independent growth curves: E. 59

Table 2.3: SensiFAST SYBR No-ROX Kit reaction mix composition for standard 20 μ l final reaction mix volume for qRT-PCR..... 63

Table 2.4: Real-time PCR conditions suitable for the SensiFAST SYBR No-ROX Kit with amplicons up to 200bp 64

Table 2.5: Agilent Technologies AffinityScript™ reaction mix for single sample. Reaction mix made to number of samples (n) +1..... 65

Table 2.6: Bonding of fluorescent marker to gDNA using Klenow enzyme for use in type II microarray analysis for single sample. Reaction mix made to number of samples (n) +1.... 66

Table 2.7: Type II microarray hybridisation buffer mixture for single sample. Reaction mix made per slide (four array blocks per slide). Using morpholine-4-ethanesulfonic acid (MES) hydrate (pH 6.5)..... 67

Table 2.8: Array slide wash buffers 1: 6XSSPE, 0.005% N-lauryl sarcosine and 2: 0.06X SSPE, 0.18% polyethylene glycol 200. 68

Table 2.9: Oligonucleotides used throughout *some manual manipulation was required when added restriction sites 70

Table 2.10: MyTaq Mix reaction mix composition for standard 50 μ l final reaction mix volumes for PCR 73

Table 2.11: PCR conditions suitable for the MyTaq Mix 73

Table 2.12: MyFi™ reaction mix composition for standard 20 μ l final reaction mix volume for PCR..... 74

Table 2.13: PCR conditions suitable for the MyFi™ Mix 74

Table 2.14: rAPid Alkaline Phosphatase reagents for the dephosphorylation of plasmid DNA..... 76

Table 2.15: Oligonucleotide primers used for PCR amplification of 5' and 3' flanking regions up and downstream of *fhb* for cloning into pK18*mobsacB* and for confirmation of *fhb* deletion in *P. denitrificans*. Restriction sites and additional bases are shown in capital text. 77

Table 2.16: Oligonucleotides used for PCR amplification of *fhb* for complementation *in trans*. Restriction sites and additional bases are shown in capitals and gene sequence in lowercase. 82

Table 2.17: Ligation reaction mix volumes 85

Table 2.18: Plasmids used in mutant and complementation 86

2.3 Bacterial strains and storage

Paracoccus denitrificans strain PD1222 is used throughout the study as a model α -proteobacterium and denitrifier. *P. denitrificans* has a sequenced genome and well characterised denitrification and assimilatory pathways. This presents a versatile model organism for study. Mutational studies were carried out using *Escherichia Coli* JM101 (Yanisch-Perron *et al.*, 1985) (section 2.6). *Escherichia Coli* was used as a competent cell line for plasmid replication in mutational studies. Additionally an *Escherichia Coli* helper strain containing pRK2013 was also used for the conjugation of a plasmid to *P. denitrificans*.

2.3.1 Growth media and growth technique for *P. denitrificans* and *E. coli*

Growth of *P. denitrificans* and *E. coli* was initiated from glycerol stocks stored in the Centre for Microbiological and Structural Biochemistry (CMSB) at -80°C with 25% (v/v) glycerol (Fisher Scientific UK G/0600/17) as a cryoprotectant. *E. coli* JM101 was grown on agar plates made up of high-salt nutrient Luria-Bertani (LB) broth with 1.5% agar (ForMedium™ AGA02). Selection of single, pure culture *P. denitrificans* colonies was also carried out on agar plates with high-salt nutrient Luria-Bertani (LB) broth with 1.5% agar and antibiotic selection was used with the addition of $100\ \mu\text{g}\cdot\text{ml}^{-1}$ rifampicin (LB^{rif}). High-salt LB agar was prepared using 10 g tryptone, 5 g yeast extract, 10 g NaCl (supplied as combined powder LMM0102 by ForMedium™) per litre reverse osmosis (RO) water. Media powder was dissolved with a magnetic stirrer with stirring bar and distributed into 250 mL conical flasks as 100 mL aliquots. The flasks were sealed with an air-permeable bung and tin-foil to maintain sterility. Flasks were autoclave sterilised (LTE Scientific Ltd.) for 20 min at 121°C . For construction of LB^{rif} agar plates, prepared LB agar is microwave melted (by manufacturer's instructions) and allowed to cool to approximately 60°C (hand-hot temperature) before addition of rifampicin antibiotic (Melford Laboratories Ltd. R0146) at $100\ \mu\text{g}\cdot\text{ml}^{-1}$. While still liquid, approximately 25 mL agar was poured into each standard petri dish using aseptic technique in a class II safety cabinet (Walker Safety Cabinets Ltd.) and allowed to solidify for approximately 15 min.

Plates were streaked from bacterial stocks using a heat sterilised inoculation loop and aseptic technique. *P. denitrificans* plates were left for growth in an incubator (Heraeus®) at 30°C

until colonies reached a size of approximately 2-3 mm diameter and were suitable for picking (approximately 1.5 - 2 days). *E. coli* plates were left for growth in an incubator (Heraeus®) at 37°C overnight (~18 h) until colonies reached a size of approximately 1-2 mm diameter and were suitable for picking. All plates were stored at 4°C for mid-term storage of between 2-4 weeks at which time new streaked plates were prepared as agar became drier. Single colonies were picked using autoclaved flat wood pick (Portia) or a heat sterilised inoculation loop, placed into vials containing 5 mL LB^{rif} overnight and incubated at 30°C and 200 rpm shaking in a controlled temperature room. Lower volume high-salt LB liquid media was prepared in the same manner as for agar and distributed into 20 mL glass vials as 5 mL aliquots sealed with a screw cap to maintain sterility. The LB^{rif} starter culture was used for inoculation into minimal salts media growth conditions for batch culture and continuous culture growth experiments. For long-term strain storage, all bacteria strains were grown in LB media with appropriate antibiotic selection, from a single colony to late exponential / early stationary phase. They were then pelleted and resuspended in fresh media with antibiotic for long term storage at -80°C with 25% (v/v) glycerol cryoprotectant.

2.3.2 Minimal salts media for aerobic growth experiments with *P. denitrificans*

All *P. denitrificans* experimental growth conditions used a minimal salts media recipe supplemented with trace elements, carbon and nitrogen sources. A 1% inoculum from a 5 mL LB^{Rif} overnight growth was used to inoculate 5 mL minimal media grown overnight at 30°C and 200 rpm before inoculation into experimental conditions. All growth carried out in minimal salts media used the recipe: Na₂HPO₄ 29 mM, KH₂PO₄ 11 mM, MgSO₄ 0.4 mM, (Robertson and Kuenen, 1983) with additional Vishniac's trace elements (adjusted to pH 6.6) solution 2 mL L⁻¹ (Vishniac and Santer, 1957) and NH₄Cl 10 mM. This media base was made up in large quantity, approximately 5 L batches, which were then separated into required volumes for autoclaving. Vishniac's trace elements and the filter sterilised addition of carbon and nitrogen were added to the autoclaved base media to make the concentration required. Nitrogenous compound additions were made with the following: ammonium chloride (NH₄Cl) 10 mM, with sodium nitrate (NaNO₃) and sodium nitrite (NaNO₂) various concentrations as stated under the experimental growth conditions specified. Carbon source sodium succinate (C₄H₄Na₂O₄) provided at 30 mM for batch growth conditions. Media pH

was determined using a pH probe (Mettler-Toledo International) and adjusted as required using NaOH 10 M and H₂SO₄ 10 M. Standard growth conditions were aerobic, pH 7.5, in minimal salts media with NH₄Cl 10 mM nitrogen source (table 2.1). Aerobic growth was carried out by two methods. Firstly, in 250 mL conical flasks containing 50 mL volume at 30°C and shaken at 200 rpm, allowing sampling of liquid and gas phase (section 2.4.3) for further metabolic assaying techniques and RNA extraction. Secondly in 96 well plates, using the FLUOstar Omega Multi-mode microplate reader containing 100 µL per well and orbital shaking 400 rpm (section 2.4.1) for high throughput screening of multiple growth conditions.

Table 2.1: Minimal salts growth media and Vishniac's trace elements. Growth media was autoclave sterilised prior to use. Trace elements solution was prepared separately in stock solution and filter sterilised before addition to media post-autoclaving. Carbon and nitrate sources were filter sterilised and added as required. Additional compounds are listed and annotated according to use as carbon and nitrogen sources.

Compound Name	Compound		Concentration	RFM
	Formula	Mass (g L ⁻¹)	(mM)	(g.mol ⁻¹)
Disodium Hydrogen Phosphate (DSP) *	Na ₂ HPO ₄	4.1	29	141.96
Potassium Phosphate Monobasic *	KH ₂ PO ₄	1.5	11	136.09
Magnesium Sulphate *	MgSO ₄	0.098	0.8	120.37
Ammonium Chloride	NH ₄ Cl	0.53	10	53.49
Sodium Nitrate ²	NaNO ₃	1.7	20	84.99
Disodium Succinate ³	Na ₂ C ₄ H ₄ O ₄	1.18	10	118.09
Sodium Butyrate ³	NaC ₄ H ₇ O ₂	0.88	10	88.11
Trace metal solution (Vishniac's solution) ⁴	-	2 mL L ⁻¹	-	-
Rifampicin (3-(4-Methylpiperazinyl)iminomethyl) rifamycin SV)	Rif ^R	50 mg L ⁻¹	-	-

⁴**Trace Element solution (adjusted to pH 6.6)**

Ethylenediamine	tetra-	$C_{10}H_{16}N_2O_8$	48.39	166	292.24
ferrooxidans		(EDTA)			
Zinc Sulphate		$ZnSO_4$	2.2	14	161.47
Manganese(II) chloride		$MnCl_2$	4.95	25	196.75
Iron(II) Sulphate		$FeSO_4$	5.14	34	151.91
Ammonium Heptamolybdate		$(NH_4)_6Mo_7O_{27}$	1.09	0.9	1211.81
Copper(II) Sulphate		$CuSO_4$	1.59	10	159.61
Cobalt(II) chloride		$CoCl_2$	1.6	6.72	129.84
Calcium chloride		$CaCl_2$	5.5	37.4	110.98

*Added to all minimal media¹ Nitrogen source² Nitrate source³ (Vishniac and Santer, 1957)⁴

2.4 Growth techniques

2.4.1 Aerobic plate reader batch culture technique

Growth curves were carried out with the FLUOstar Omega Multi-mode microplate reader which allows high throughput screen of multiple growth conditions and was used to establish growth phenotype. This was to ensure aerobicity of growth and direct comparison of both growth techniques. Plate reader absorbance data was corrected to 1 cm pathlength. Basic growth media components were made up to recipe in a large volume as per table 2.1. Media was transferred to conical flasks in 200 mL aliquots, to which succinate and Vishniac's trace elements solution were added. Filter sterilised stock nitrite was transferred to universal tubes to generate a final concentration in solution. To these tubes 10 mL of minimal media and 1% inoculum were added, thoroughly mixed by inversion. This used for three technical replicates. An aliquot of 100 μ L was placed in each individual well of the 96 well plate.

2.4.2 Calculation of the plate reader pathlength for conversion of optical density values to a standard 1 cm pathlength

Determination of plate reader pathlength was carried out by calculating the concentration specific extinction coefficient for known concentrations of methylene blue (Arp and Burris, 1981) using absorbance values taken from 1 cm spectrophotometer as shown in figure 2.1. The Beer-Lambert law, $A = \epsilon lc$, rearranged to $\epsilon = A / lc$, was used to calculate the extinction coefficient (ϵ). The method was repeated using the plate reader, and a rearrangement of the Beer-Lambert law, $l = A / \epsilon c$, was used to determine the pathlength of the plate reader well. The average pathlength generated by this method for the plate reader was 0.192 cm.

2.4.3 Aerobic shaking flask batch culture

Plate reader experiments were upscaled to shaking flask growing conditions. Media volume was increased to 50 mL, held in a 250 mL conical flask and shaken at 200 rpm to aerate the culture. Conical flasks were sealed using a gas permeable foam bung and aluminium foil lightly pressed around the edge. Flasks were sampled directly for media sampling of selected growth conditions for metabolic and transcriptional analysis, and headspace sampling for gas analysis. Method was adapted from (Henzler and Schedel, 1991). The biological replicates were taken from three separate colonies grown on LB^{Rif} agar and grown on in LB^{Rif} liquid culture overnight. The overnight cultures were used to inoculate minimal salts media without nitrite addition and were also grown overnight to allow adaption to the minimal salts media. Each overnight culture was then used to inoculate two flasks at 1% by volume. This provided each biologically independent cell line to be exposed to experimental conditions.

Growth was monitored spectrophotometrically using an Eppendorf® Biophotometer at 600 nm. Gas samples as well as liquid samples were required. To reduce disruption to the gas headspace of the shaking flask set up, two sets of flasks were used for each growth condition; one for liquid sampling and one for gas sampling only. Optical density samples and supernatant samples were extracted directly, using aseptic technique, from the first set of flask.

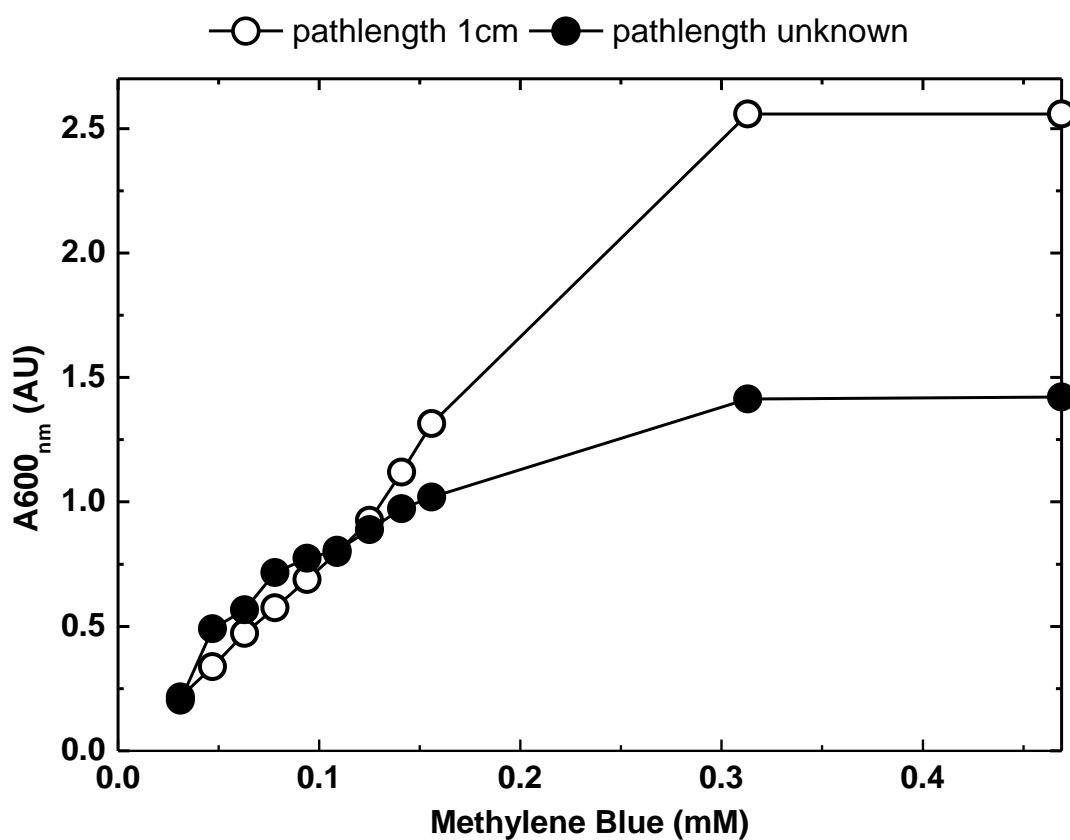


Figure 2.1: The Beer-Lambert law: $A = \epsilon lc$, for the calculation of methylene blue extinction coefficient (ϵ) at 600 nm using, known concentrations of methylene blue (c) and absorbance values experimentally obtained (A_{600nm}) with a 1 cm pathlength (l). Calculation of plate reader pathlength (lx) using A values taken from the plate reader using a 100 μ L volume in a well.

Cells were pelleted from the sample, and the remaining supernatant was kept at -20°C for nitrite and nitrate separation using High Pressure Liquid Chromatography (HPLC) in a Dionex IP900. The second sets of flasks were kept with foam bung in place. Gas samples were taken from these flasks by means of foil removal and the application of a heat sterilised needle for the direct sampling of headspace within the flask. The OD_{600nm} at the start inoculation (T₀) and final 18 h point (T₁₈) were taken and assayed for nitrite, nitrate and nitrous oxide levels. Flasks from the same biological replicate were compared directly. Levels of nitrate, nitrite and nitrous oxide were matched for each biological replicate. Growth curves are shown as semi-log plots for accurate representation and comparison of exponential growth. Growth rates were taken from these as apparent maximum growth rate (μ_{app}) from the gradient of exponential growth phase.

2.4.4 Aerobic continuous culture of *P. denitrificans*

The continuous culture of *P. denitrificans* was carried out using 2.5 L bio-reactors (BioFlo 310, New Brunswick Scientific) (Heijnen and Romein, 1995; Kovárová-Kovar and Egli, 1998). Of this total volume, 1.5 L contained media. This media is saturated with air using atmospheric air pumped through stainless steel piping ending at the base of the vessel. The piping is perforated at the base of the vessel to allow pressurised air to be expelled through perforations and bubble air through the media, maintaining the levels of air in the vessel as a standard saturation. Spinning impellers allow full distribution and mixing of the vessel liquid. These were kept rotating at 400 rpm. The level of dissolved oxygen was maintained at 100% (air saturation). The remaining 1 L volume within the vessel head space contains atmospheric air which is bubbled through the liquid media. The vessel was set up with water for calibration and both probe and computer systems checks. At this point, calibration of the pH probe was carried out. The bioreactor was then filled with media (without nitrite or Vishniac's solution) and aseptically sealed. The vessel tubes were sealed using clamps, cotton and foil. The air condenser remained open using a 0.2 μ m filter for air expansion during the autoclave cycle. The autoclave cycle did not use forced cooling as this would shatter the glass vessel.

The pH value was kept constant automatically using the inbuilt software, as was aeration (dissolved oxygen) and media addition for maintenance of steady state growth. The pH, dissolved oxygen (DO), temperature, acid, base and media addition were constantly

monitored and recorded using the Biocommand programme. Data acquisition was automatic via the multipoint control unit (MCU) reactor process controller (RPC) to BioCommand software at 30 min intervals. The pH was monitored with an InGold pH electrode (Mettler Toledo) and adjusted automatically with the addition of 1.0 M NaOH and 0.1 M H₂SO₄ using a dead-band of 0.05pH units. The dead-band prevents fluctuations in pH by preventing pH adjustment ± 0.05 units of the required pH value. The pH electrode was calibrated with calibration solutions supplied by Fisher Scientific at pH 4 and pH 9.2. The pH of the media was maintained at 7.5 automatically using computer control. An increase or decrease in solution pH activates one of two peristaltic pumps designated “acid” and “base”. A solution of 1 M sulphuric acid is attached via tubing to the “acid” pump and solution of 0.1 M sodium hydroxide attached via tubing to the “base” pump. Peristaltic pumping of correct acidic or basic solution delivers drop wise additions and adjustment of pH. When solution pH reaches $7.5 \pm$, the acid or base pumps cease pumping, which stops the flow of acid or base solution into the chemostat. The dead band of 0.05 is to prevent excessive fluctuation of pH during adjustment by addition of acid or base caused by an “over-” or “under-shoot” of the required pH value.

Temperature was monitored with a resistance temperature sensor (RTD). The temperature is controlled with an intergraded water jacket containing circulated water from the temperature controlled tank of the main control unit. Agitation was also monitored and controlled by an MCU controlled motor attached to shaft and two submerged Rushton-type impellers.

Dissolved oxygen was monitored with an inline, InPro polarographic electrode (Mettler Toledo) which was previously calibrated in air saturated (100%) or nitrogen saturated (0%) medium. Air and gas mixture supply were controlled by the MCU through specific electromechanical gas valves. The values generated by the DO probe and recorded using the Biocommand program represent a percentage saturation based on the parameters set during calibration; zeroed to nitrogen saturation of media represented as 0% and spanning to oxygen saturation of media represented as 100%. This 100% represents 21% oxygen in the atmospheric air passed through the media at 5 L min^{-1} . The saturation point of media at 30°C is 0.25 mM oxygen, calculated according to Henry's law which states that the solubility of a gas in a liquid is given by: $c = P_g / K_H$ (Harvey and Smith, 2007). Percentage readings were converted to mM of dissolved O₂ using the solubility formula:

$$c = P_g / K_{30}$$

$$c = (0.21 / 845.16)$$

$$c = 2.48 \text{ M or } \mathbf{0.248 \text{ mM}}$$

P_g is the partial fraction of O_2 at one atmosphere in water, and is calculated as 0.21 (21% of the atmosphere is oxygen) \times 1 atmosphere = 0.21 atm. K_{30} is the constant at 30°C and is calculated using the following adaption:

$$K_H = K_T^\ominus \cdot \exp [C \cdot (1/T - 1/T^\ominus)]$$

$$K_{30} = K_T^\ominus \times \exp [1700 \times (1/298 - 1/303)]$$

$$1700 \times (1/298 - 1/303) = 0.094$$

$$e^{0.094} = \mathbf{845.16 \text{ atm M}^{-1}}$$

Solubility is affected by the intermolecular forces generated by the solvent and solute. These are in turn affected themselves by temperature and pressure. Solvent composition also influences these forces. However the composition of minimal salts media is similar to that of water and has been treated as such (Murray and Riley, 1969; Andersen, 1980; Barton, 1975; Wilhelm *et al.*, 1977; Battino and Clever, 1966). C is derived as a constant in Kelvins specific to the gas species oxygen. It takes into account the change in solubility dependent on temperature. Largely, gas solubility decreases with increasing temperature and therefore the partial pressure of the gas concentration in solution will also increase. The C constant is generated using $C = -\Delta_{\text{solv}}H / R = d [\ln K_H (T)] / d (1/T)$ with $\Delta_{\text{solv}}H$ is the enthalpy of solution and R the gas constant. The C value for oxygen is 1700 (Sander, 1999). Therefore, all DO % values are divided by $(100 / 0.248) = 403.226$, for conversion of % DO into mM DO. Gas flow was shut off during gas sampling time for 20 min. This time period was selected because initial tests showed that the culture remained aerobic and the gas metabolite accumulated without flushing out

2.4.5 Use of aseptic technique to minimise contamination of the growth cultures

Culture handling, inoculation and sampling was carried out using aseptic technique to minimise contamination of the *P. denitrificans* culture with additional bacterial and fungal

strains. Preparation of working space required 80% ethanol solution for wiping down of bench area and equipment to sterilise the working environment. Windows and doors remained closed in proximity and for the duration of work with cultures to minimise disruption of air currents. Apparatus and materials were prepared and kept within reach prior to work with cultures. Sterile equipment was kept from contact with non-sterile surfaces.

Media preparation, with addition of Vishniac solution and nitrite was carried out under a Bunsen flame. Opening of vessels was kept to a minimum and took place under a Bunsen flame where currents of air are drawn upwards. When opening culture vessels, the neck was heated in the Bunsen flame and held at near horizontal or 90° angle to draw air currents up and away from the vessel. Agar plates were also handled under the Bunsen flame and plate lids were kept on where possible to reduce exposure of the agar to contaminated air. All equipment in contact with *P. denitrificans* was sterilised prior and after exposure.

2.4.6 Calculation of apparent growth rate

The rate of exponential growth was measured using the OriginPro 8.5 and 9.0 (OriginLab) from a semi log plot of OD_{600nm} measurements. An example of the semi log plot is shown in figure 2.2. The semi log plot linearizes the exponential growth phase and from this a line of best fit can be drawn and is shown in red on figure 2.2. The gradient of this line and associated error was used as an apparent value of exponential growth and for comparison of growth phenotypes. Tests were carried out to ascertain the reproducibility of the technique across biological replicates and averaged mean lines. It was found that the μ_{app} value obtained for an averaged growth curve was within the error of the biological replicates, averaged as shown in figure 2.2.

Table 2.2: The apparent growth values ($\mu_{app} h^{-1}$) for growth curves of *P. denitrificans* growth in minimal salts media pH 7.5. Each growth curve has been plotted as a semi log. The μ_{app} is calculated by taking a gradient of the linear portion of the semi log lot. μ_{app} has been measured on three biologically independent replicates: A, B and C. The three μ_{app} values have then been averaged manually: D. A separate μ_{app} value has been derived using a semi log plot of the average of the three biologically independent growth curves: E.

Growth curve	$\mu_{app} h^{-1}$	$\pm SE$
A	0.320	
B	0.312	
C	0.315	
D (manual)	0.316	0.004
E (OriginPro)	0.316	0.010

$\pm SE = \text{standard error } n=3$

2.4.7 Measurement of growth using optical density

Growth of *P. denitrificans* was measured spectrophotometrically (Eppendorf® Biophotometer) using 880 μL sample 1 cm pathlength cuvettes (Sarstedt, DE). Optical density was measured at 600 nm. These values measure the light change through a turbid solution and do not offer any insight to the change of morphology or state of the organism. In this work, OD readings are used as the reproducible, high through-put method of growth phenotyping. Conversion of OD measurements to an estimated biomass value used a dry weight measurement for *P. denitrificans*. Conversion of OD to biomass is shown as follows: $\text{Biomass } g.L^{-1} = OD_{600nm} \times 0.518 g.L^{-1}$

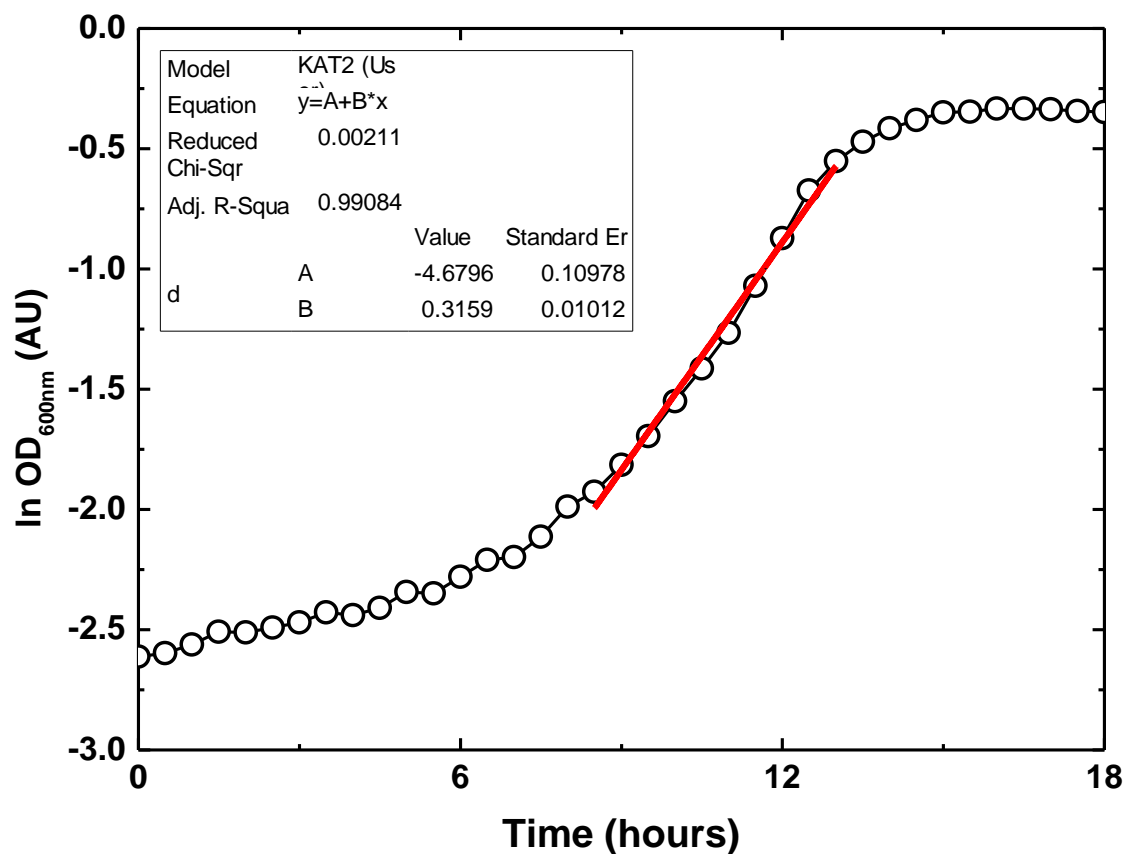


Figure 2.2: Semi log plot for the growth of *P. denitrificans* in minimal salts media at pH 7.5. The gradient of the linear portion of the growth curve has been used to measure a line of best fit (red line). The gradient of this line is used as $\mu_{app} h^{-1}$. The gradient is shown in the table insert. This table shows the output associated with the gradient calculated by OriginPro.

2.5 RNA transcriptional analysis by quantitative RT-PCR

2.5.1 RNA extraction from whole cells

RNA extraction was carried out on comparable conditions and in biologically differing triplicates. The growth conditions for *P. denitrificans* were minimal salt medium pH 7.5 with NH_4Cl 10 mM grown aerobically at 30°C 200rpm. Test growth conditions used an addition of NaNO_2 to induce stress response. Growth conditions were grown to an $\text{OD}_{600\text{nm}}$ of between 0.45-0.52 for the extraction of RNA. Surfaces and equipment were treated using RNaseZAP® from Ambion or autoclaved to reduce damage by RNase activity prior to any handling of RNA samples. Pipette tips were TipOne® RNase-free filter tips from StarLab®.

Whole cell samples were immediately put on ice using addition of 2:5 ratio phenol 5% - ethanol 96% (Sigma): bacteria culture (v/v) and 1 h incubation on ice for the stabilisation of RNA. Cells were then pelleted at 5000 x rcf (g) 10 min 4°C using a Beckman Coulter Allegra® 25R Bench-top Centrifuge and supernatant discarded leaving ~1 mL Residual supernatant for the resuspension and transfer of cells into RNase free 1.5 mL centrifuge tubes. These tubes were centrifuged at 13k rpm for 2 min using a Sigma 3K30C-Kubota centrifuge and the remaining supernatant was removed by micropipette. Pelleted cells were immediately frozen in liquid nitrogen prior to RNA extraction. RNA extraction and purification was carried out using the SV Total RNA Isolation System from Promega® Z3100 for both qRT-PCR and microarray analysis.

Quantification of RNA yield was obtained spectrophotometrically in a Thermo Scientific NanoDrop 2000™ Spectrophotometer at 260 nm. A 1 µl sample was taken and purity estimated spectrophotometry using the relative absorbance ratios: A_{260}/A_{280} and A_{260}/A_{230} . A_{260}/A_{280} reflects the purity of the RNA sample and samples of ~2.0 were carried on to further analysis. A_{260}/A_{230} reflects largely residual impurities largely residual of phenol extraction, a value of >1.7 was expected to ensure purity of RNA.

2.5.2 Removal of DNA contamination from RNA samples by Ambion® TURBO™ DNase

DNA contamination was removed using Ambion® TURBO™ DNase. RNA degradation was checked by RNA electrophoresis using the BIO-RAD® Experion™ RNA StdSens Analysis Kit and DNA contamination checked by PCR using genomic *P. denitrificans* DNA and MyTaq polymerase (section 2.7.1). The NanoDrop 2000™ Spectrophotometer was selected as a cuvette free spectrophotometer design to accurately quantify micro-volumes of sample. Following RNA extraction, samples were found to have varying levels of DNA contamination. This was eliminated with a further DNase step, prior to determining quality and final concentration of RNA. Ambion® TURBO™ DNase was used by the manufacturer's supplied instructions to cleave double-stranded DNA non-specifically and leave 5' phosphorylated oligodeoxynucleotides.

2.5.3 RNA degradation analysis with gel electrophoresis

RNA samples extracted from growth of *P. denitrificans* were examined before use in transcriptional analysis techniques. Validation and reproduction of transcriptional analysis is reliant both on the quality of RNA extracted and level of contamination by phenol and DNA. The BIO-RAD® Experion™ RNA StdSens Analysis Kit is an accurate tool for RNA micro-volumes of sample, and was used to determine RNA integrity by visually representing the quantity of high quality RNA. These appear as sharp peaks of fluorescence representing 23S and 16S RNA in an electropherogram and are converted to distinct bands on an automated electrophoresis gel. Calculation of size, concentration and percentage of total sample is also automatic. RNA samples were examined using the Experion Automated Electrophoresis System (BIO-RAD®) by manufacturer's instruction. Each RNA sample was examined using the Experion RNA StdSens Analysis kit (BIO-RAD®) reagents and 1 µl of sample loaded on to an Experion RNA StdSens chip.

2.5.4 Quantitative real-time reverse transcription PCR

Quantitative real-time reverse transcription PCR (qRT-PCR) was used to quantify mRNA for gene expression profiling and qualification of type II microarray analysis. This was carried out on the BIO-RAD® C1000 Thermal Cycler and CFX96 Real-time PCR detection system. The cycles used were a 2 min 95°C initial denaturation; 40 × 5 sec 95°C denaturation and 15 sec 60°C primer annealing/elongation cycling procedure. The total reaction volume was 20 µL comprised of: 10 µL 2× SensiFAST™ SYBR® Green Master Mix (Bioline reagents Ltd), 0.4 µM of forward and reverse primers as stated, 1 µL of cDNA at 500 ng µL⁻¹ and 8.2 µL Sigma RNase free molecular reagent water (Sigma, BP28191) (table 2.3 and table 2.4).

Fluorescence was recorded during annealing and elongation for each cycle, and a melting curve was generated at the end of each PCR reaction by gradually increasing the temperature from 60 to 95°C (table 2.4). The fluorescence was also recorded and primer specificity was confirmed from this by a single peak at the melting temperature of the PCR product. Each of the three biological replicates was processed in three technical triplicates to ensure statistical accuracy. The use of a fixed fluorescence threshold for derivation of C(t) values allowed direct comparison during analysis of expression values and allowed a relative expression ratio (R) to be derived.

Table 2.3: SensiFAST SYBR No-ROX Kit reaction mix composition for standard 20 µl final reaction mix volume for qRT-PCR

Reagent	Volume x1 (Total vol. 20 µl)	Final concentration
2x SensiFAST SYBR No-ROX Mix	10	1X
Forward primer	0.4	400 nM
Reverse primer	0.4	400 nM
Template cDNA	1	500 ng
Water RNase free	8.2	-

Table 2.4: Real-time PCR conditions suitable for the SensiFAST SYBR No-ROX Kit with amplicons up to 200bp

Step	N°. cycles	Temperature (°C)	Time (sec)	Purpose
1	1	95	120	Polymerase activation
2	40	95	5	Denaturation
		60	15	Annealing/extension

2.6 Type II microarray analysis

2.6.1 Preparation and quantification of RNA and genomic DNA

Preparation of mRNA was carried out as specified in the above section. RNA was checked for DNA contamination and degradation using the steps shown in sections 2.5.2 and 2.5.3. Good RNA yields were considered to be above 200-300 ng μ L⁻¹ of RNA. Genomic DNA was extracted using the QIAamp[®] DNA Mini Kit from QIAGEN[®] following manufacturer's instructions. A 9 mL overnight *P. denitrificans* culture grown in LB broth was pelleted and resuspended in RNaseA containing buffer. These cells were lysed and DNA extracted, then cleaned and stored in RNA-free water at -20°C. The gDNA was diluted to approximately 200 ng/ μ L in 100 μ L H₂O. Concentration of gDNA was determined with the NanoDrop 2000[™] Spectrophotometer concentration taking at least 3 readings.

2.6.2 Drying of RNA samples

A concentration of 10 μ g of RNA is required for microarray analysis. For this, samples of RNA extracted from biological samples were dried down to a concentration of 10 μ g. The aliquot of RNA was removed and placed into an ice-cold 1.5 mL RNA-free microtube which was kept on ice at all times to maintain temperature. The volume required of RNA (V_{RNA}) (μ L) was calculated as follows, using the concentration of RNA extracted and stored (ng. μ L⁻¹): $V_{\text{RNA}} = 10000 / [\text{RNA}]$.

The gDNA samples were also prepared at one per microarray slide. From the gDNA 180 ng/ μL^{-1} stock, 2 μg of gDNA was removed and brought to a total volume of 21 μL . This total volume was calculated as follows: $V_{\text{gDNA}} = 2000 / 180.9 = 11.1 \mu\text{L}$. RNA-Free H_2O was added to this at $21 - 11.1 = 9.9 \mu\text{L}$. RNA samples were then vacuum-dried for approximately 10 min at 35°C , until a volume of 7.74 μL was reached. This acted to concentrate the RNA samples. Tin foil is used to cover the samples to prevent UV degradation.

2.6.3 Reverse Transcription of RNA samples

RNA was reverse transcribed (RT) using Agilent Technologies AffinityScript™ to cDNA using 1.66 μL of stock 3 $\mu\text{g}/\mu\text{L}$ random primers (hexamers). This adds a working concentration of 5 μg random primers and brings the total volume of the RNA to 9.4 μL . The RNA samples are incubated at 70°C for 5 min, and then chilled on ice for 10 min.

Samples were then spun for 4 seconds and RT reaction mix (table 2.5) was added at 4.6 μL per sample. During this step, 2 μL Cy5-dCTP Blue (Amersham) was incorporated for fluorescent labelling. To this 4 μL of Reverse Transcriptase Affinity Script Mix (kept on ice) is added, mixed by flicking, and spun down briefly. Samples are covered with foil and left at RT in a dark cupboard for 10 min, then mixed and stored on ice. Dyes are very light-sensitive so were kept covered and on ice at all times when not in use. The RNA samples were incubated at 42°C overnight, covered in foil.

Table 2.5: Agilent Technologies AffinityScript™ reaction mix for single sample. Reaction mix made to number of samples (n) +1.

Component	μL
10x RT Buffer AffinityScript	2
0.1 M DDT	2
50x dNTP's	0.6

2.6.4 Bonding of fluorescent dye to genomic DNA sample

Cy3-dCTP Red labelled chromosomal DNA of 2 mg was combined with labelled cDNA 1/5 (v/v) with a Gibco Bioprime DNA labelling system. The gDNA is added with 20 μL of 2.5x Random Primer Reaction Buffer, then boiled for 5 min at 100°C and chilled on ice for 5 min. Samples were spun for 4 seconds and the dNTPs and Cy3 Red DNA dye added, mixed by flicking the tube and spun down for 4 seconds before adding the Klenow enzyme (Bioprime Invitrogen Kit). The DNA samples were incubated at 37°C overnight (table 2.6).

Table 2.6: Bonding of fluorescent marker to gDNA using Klenow enzyme for use in type II microarray analysis for single sample. Reaction mix made to number of samples (n) +1.

Component	μL
10x dNTP's	5
CY3 Red DNA dye	3
Klenow enzyme	1

2.6.5 Cleaning of RNA and DNA samples

Samples are kept covered with foil and handled in a dark area of the room when labelled with dyes to reduce degradation of the dye. Samples are removed from incubation and spun down for 4 seconds. The cDNA (reverse transcribed RNA) samples were hydrolysed using 15 μL of 0.1 M NaOH and incubation at 70°C for 10 min. This was neutralised with 15 μL of 0.1 M HCl and pipette mixed, making a total volume of 50 μL . The QIAGEN® QIAquick® PCR Purification Kit to clean-purify DNA and RNA (now cDNA) samples from excessive dye and enzymes using 5x volumes of PB Buffer: 50 μL of gDNA / cDNA sample = 250 μL of PB Buffer for each sample. This is mixed well, but gently, by pipetting. A QIAquick® spin column is used for each sample, placed in a 2 mL tube to which the sample is added and spun down for 30 seconds. An additional wash of 0.75 mL of PE buffer is added followed by a 30 seconds spin and the sample dried with an additional 1 min spin. Fresh RNA-free tubes are used to collect the cleaned samples, eluted with 2 x 50 μL RNA-free H₂O washes. Samples are kept covered with foil and on ice.

2.6.6 Hybridisation of complementary DNA and genomic DNA to slides

The gDNA and cDNA samples are dried to 30 μL by vacuum drying while covered, at 35°C. The volume of gDNA is measured by pipette and 1/5 of gDNA volume is added to each cDNA sample, and then mixed by pipette. RNA-free H_2O is added to bring the samples to a final volume of 43 μL . Samples are denatured at 94°C for 2 min and centrifuged for 2 min then left to cool to room temperature for 1 min. Samples are hybridised on an Agilent custom made *P. denitrificans* oligonucleotide array, in a 90 μL volume per array, with hybridisation buffer as shown in table 2.7. To each sample, 75 μL of Hybridization Buffer is added and mixed gently by pipetting.

Table 2.7: Type II microarray hybridisation buffer mixture for single sample. Reaction mix made per slide (four array blocks per slide). Using morpholine-4-ethanesulfonic acid (MES) hydrate (pH 6.5)

Component	μL
12x MES	45
5M Sodium Chloride	108
Formamide	108
0.5 M EDTA	22.5
10% Triton X-100	54

2.6.7 Preparation of Aligent slides and gasket

The slide was prepared by placing the cover slide on the metal base of the gasket, with the label facing up. The entire 90 μL volume of probe was loaded onto the centre of the gasket area, with care taken to avoid bubbles. The DNA array slide was then placed on the cover slide with the Aligent label facing down and was held on top of the gasket slide using a stainless steel hybridisation chamber base, placed over the array slide, and thumb screwed tightly to hold both slides together. The metal gasket was promptly secured on the rotor. The arrays were hybridised at 55°C for 60 h in a darkened hybridisation oven at 8 rpm.

2.6.8 Slide preparation and scanning

After removal from the hybridisation chamber, the array slide was washed with buffer 1 (6XSSPE, 0.005% N-lauryl sarcosine) for 5 min under agitation and for 5 min with buffer 2 (0.06X SSPE, 0.18% polyethylene glycol 200) (table 2.8) before being dried in an ArrayIt® Microarray High-Speed Centrifuge for 30 seconds. Forceps were used to remove the slide from the gasket and carefully open (separate) the DNA array slide before placing it into a glass container, containing buffer 1 and then a second containing buffer 2. A stirrer and metal stirring bar were used to mix the buffers. Each wash lasted 5 min.

Table 2.8: Array slide wash buffers 1: 6XSSPE, 0.005% N-lauryl sarcosine and 2: 0.06X SSPE, 0.18% polyethylene glycol 200.

	Component	mL
Buffer 1	20x SSPE Buffer	150
	Analytical H ₂ O	350
	20% N-Lauroylsarcosine	0.125
Buffer 2	20x SSPE Buffer	0.75
	Analytical H ₂ O	248
	PEG 200	0.45

Microarray slides were scanned with a GenePix 4000A scanner. The fluorescence intensity was imaged with Genepix Pro 7.0 Software. Both were Axon Instruments. The block area is manually selected. Saturation tolerance was typically set at 0.05 or 5%. Wavelengths are set at 635 and 532 for green / red laser beam. Feature size was set at 50 μm and obvious blemishes and spots with a reference signal lower than background fluorescence and two standard deviations of the background were removed by filtering so as not to be present in analysis. Fluorescence intensity of each dot was quantified by subtraction of background fluorescence and by red/green (Cy5/Cy3) ratio. Intensity values were normalised with the Batch Anti-Banana Algorithm in R (BABAR) algorithm and software package (Alston *et al.*, 2010). Fluorescence values were quality control checked using Agilent Gene Spring 7.3 software and statistically analysed using rank product analysis (Breitling and Herzyk, 2005).

Genes were filtered with a ≥ 2 fold expression filter ($p \leq 0.1$) and exported into Microsoft Excel.

2.7 Molecular biology techniques

2.7.1 Oligonucleotide design and PCR amplifications

Oligonucleotides were ordered through Eurofins MWG® Operon with sequence analysis after primer design was carried out. Oligonucleotides were designed using Artemis: Genome Browser and Annotation Tool from the Sanger Institute (Rutherford *et al.*, 2000). Oligonucleotides were selected, where possible, with a GC content of $< 60\%$, with a melting temperature (T_m) of approximately 60°C and a length of between 18-20 base pairs (bp). Sequence fragments were selected using Primer 3 software (Rozen and Skaletsky, 1999) with parameters set as approximately 100 bp in length, GC content of $< 60\%$, with an annealing temperature of approximately 60°C , or manually, selecting for similar parameters checked using free software such as Promega BioMath Calculators T_m Calculations for Oligos. Oligonucleotides used in this study are listed in table 2.9.

Initial specificity of oligonucleotides was determined by polymerase chain reaction (PCR) using genomic *P. denitrificans* DNA and MyTaq polymerase (table 2.10 and table 2.11). Visualisation of the PCR products was carried out on 0.8% w/v agarose gels containing 0.025% (v/v) ethidium bromide (EtBr) in 1x Tris-acetate-EDTA (TAE) buffer containing 45 mM Tris-borate, 1 mM EDTA, pH 8.0. Artificial restriction enzyme sites were added in accordance with New England Biolabs to the 5' end of shoulder primer sequences with an additional two bases (AT) at the far 5' end. Amplified PCR products were purified, using the High Pure PCR Product Purification Kit by Roche Applied Science, by manufacturer specification and final quantification carried out using a NanoDrop 2000™ Spectrophotometer.

Table 2.9: Oligonucleotides used throughout *some manual manipulation was required when added restriction sites

Oligonucleotide name	Sequence listed 5'-3' (manual additions in bold)*	Usage
fhb_5fln_F2	AGCCCGGG GAGAATTACGGCTATTATCTG	Insertion to pMT220 5' flank <i>fhb</i> mutant forward
fhb_5flnR1	AGTCTAGAC GATATCAAGACCATGAG	Insertion to pMT220 5' flank <i>fhb</i> mutant reverse
fhb3fln_F1	AGTCTAGAC CAAGCGCAACTATTCGAT	Insertion to pMT220 3' flank <i>fhb</i> mutant forward
fhb3fln_R1	AGCTGCAGC GATCAGGTAGAGCATGACC	Insertion to pMT220 3' flank <i>fhb</i> mutant reverse
fhbcompF1	AGTCTAGAC GTTCACCAGATCGTTGATG	Insertion to pOT2 plasmid complementation of <i>fhb</i> mutant forward
fhbcompR1	AGTCTAGAC GACATGGACGATCCG	Insertion to pOT2 plasmid complementation of <i>fhb</i> mutant reverse
fhbqPCR2F	TGGATCCAGGTGAACAACAA	qRT-PCR detection of <i>fhb</i> gene forward
fhbqPCR2R	GTTTGCATAAGCCAGGATCG	qRT-PCR detection of <i>fhb</i> gene reverse
napA1F	TGGATCCAGGTGAACAACAA	qRT-PCR detection of <i>napA</i> gene forward
napA1R	GTCCGAGACGACGATGAAAT	qRT-PCR detection of <i>napA</i> gene reverse
nasBGqPCR2F	CCTATAAATGGGTGGCCAAG	qRT-PCR detection of <i>nasBG</i> gene forward
nasBGqPCR2R	CGATAGACCGACTGGCTGAT	qRT-PCR detection of <i>nasBG</i> gene reverse
nirS1F	AATTCGGCATGAAGGAGATG	qRT-PCR detection of <i>nirS</i> gene forward
nirS1R	TCCAGATCCCAGTCGTTTTTC	qRT-PCR detection of <i>nirS</i> gene reverse
norB1F	TATGTCAGCCCGAACTTCCT	qRT-PCR detection of <i>norB</i> gene forward

norB1R	TTCGGGCAGGATGTAATAGG	qRT-PCR detection of <i>norB</i> gene reverse
nosZ1F	ACAACCTGGACCGAAGAGGTG	qRT-PCR detection of <i>nosZ</i> gene forward
nosZ1R	CCTTGACGGTAAAGCTCTCG	qRT-PCR detection of <i>nosZ</i> gene reverse
narG1F	GCGAGGAGGTCTGCTACAAC	qRT-PCR detection of <i>narG</i> gene forward
narG1R	ATCCATTCGTGGTCCTGGTA	qRT-PCR detection of <i>narG</i> gene reverse
1690qPCR3F	GACGCGCTATAACCGATTACG	qRT-PCR microarray <i>fhb</i> BadM reg. confirmation forward
1690qPCR3R	CGTTCACCAGATCGTTGATG	qRT-PCR microarray <i>fhb</i> BadM reg. confirmation reverse
1129qPCR3F	CGCGCTGATCCTCTATGC	qRT-PCR microarray Von Willebrand confirmation forward
1129qPCR3R	CGAGATCAGCACGAGATCC	qRT-PCR microarray Von Willebrand confirmation reverse
5108qPCR2F	ATCTGCTGGACCCCTATCG	qRT-PCR microarray <i>ba₃</i> confirmation forward
5108qPCR2R	ACAGCCATTTCCAGTCCATC	qRT-PCR microarray <i>ba₃</i> confirmation reverse
3429qPCR3F	CTGATCTTCTACGTCATCC	qRT-PCR microarray DctM subunit confirmation forward
3429qPCR3R	AACCAGACCTTGTCGTAG	qRT-PCR microarray DctM subunit confirmation reverse
1629qPCR2F	GCGACAGTGACAAGGTTGG	qRT-PCR microarray sigma-24 confirmation forward
1629qPCR2R	CCCAGAAGCGCAGAAAGAC	qRT-PCR microarray sigma-24 confirmation reverse

3605qPCR1F	AGCTAGAGCGGGTGACATTC	qRT-PCR microarray Acid stress ¹ confirmation forward
3605qPCR1R	GGACCCCAGAACTTGAAGG	qRT-PCR microarray Acid stress ¹ confirmation reverse
GAPDH1F	GCTGAAGGGCATCCTAGGCTATA	qRT-PCR housekeeping gene <i>gapdh</i> forward
GAPDH1R	ACTCGTTGTCATACCAGGTCAGG	qRT-PCR housekeeping gene <i>gapdh</i> reverse
POLB	CATGTCGTGGGTCAGCATAC	qRT-PCR housekeeping gene <i>polB</i> forward
POLB	CTCGCGACCATGCATATAGA	qRT-PCR housekeeping gene <i>polB</i> reverse

¹ highest fold change in microarray dataset

2.7.2 Polymerase Chain Reaction

Polymerase Chain Reaction (PCR) was used to amplify DNA fragments or plasmid to check primer function, DNA contamination in RNA samples and to amplify desired oligonucleotides for insertion in plasmids and transformation. PCR was carried out on a Techne TC-512 Thermal Cycler. Taq DNA polymerase (Bioline) was used according to the manufacturer's instructions and supplied reagents.

Table 2.10: MyTaq Mix reaction mix composition for standard 50 µl final reaction mix volumes for PCR

Reagent	Volume x1 (Total vol. 50 µl)
5x MyTaq Reaction Buffer	10
Template	1
Forward primer	0.4
Reverse primer	0.4
Water RNase free	8.2

Table 2.11: PCR conditions suitable for the MyTaq Mix

Step	Nº. cycles	Temperature (°C)	Time (sec)	Purpose
1		95	15	Melt
2	35	60	5	Annealing
3		72	30	Extension
4	-	10	-	Final hold

DNA fragments for recombination were amplified with the more sensitive and specific MyFi™ DNA polymerase (

table 2.12 and table 2.13) and subsequently cleaned using gel extraction and a PCR product purification kit.

Table 2.12: MyFi™ reaction mix composition for standard 20 µl final reaction mix volume for PCR

Reagent	Volume x1 (Total vol. 50 µl)
2x MyFi Mix	25
Template	1
Forward primer	1
Reverse primer	1
Water RNase free	22

Table 2.13: PCR conditions suitable for the MyFi™ Mix

Step	N° cycles	Temperature (°C)	Time (sec)	Purpose
1	1	95	180	Initial denaturation
2		95	60	Denaturation
3	35	58	15	Annealing
4		72	45	Extension
5	-	10	-	Final hold

2.7.3 Agarose gel electrophoresis

The agarose gels were prepared using 1.2 g agarose (0.8%) in 150 mL of premade 1x Tris-Acetate-EDTA buffer (TAE). This was melted in a microwave before cooling to hand touch temperature. TAE was made from a 50x stock (ForMedium™). To visualise RNA and DNA molecules 5 µL of the fluorescent nucleic acid tag ethidium bromide (C₂₁H₂₀BrN₃) was added. This solution was poured into a mould containing a well comb and allowed to cool and solidify under a gas extraction hood (approximately 20 min). The agarose gel was loaded into the gel box (electrophoresis unit) which was filled with 1xTAE to cover the gel. A molecular weight ladder (HYPERLADDER™ 1 kb from Bioline reagents Ltd) was loaded to determine band sizes. Loading buffer is added to each sample before loading into the gel wells. Gels were typically run at an electrical field of 100 volts to run an electrical field and

move the negatively charged DNA toward a positive electrode through the gel matrix. Gels were then imaged with a BIO-RAD® UV imager and Quantity One® imaging software.

2.7.4 Gel extraction of DNA from agarose gels

DNA fragments were run on agarose gels to purify the fragments from contamination. DNA fragment extraction from agarose gel slices was carried out using the QIAGEN QIAquick Gel Extraction kit. An agarose gel was run until a clear band at the correct size was observed. Single bands were cut from the gel using UV illumination. A clean scalpel was used to cut away any gel not containing DNA. Most agarose gel was removed whilst minimising loss of DNA. The gel fragment was placed into a pre-weighed 1.5 mL centrifugation tube. To this tube, three volumes (w/v) of QG buffer were added to the gel fragment and the tube was incubated for 10 min at 50°C with intermediate vortex mixing to ensure gel was dissolved. The provided column was washed with 750 µL PE buffer and centrifuged at 13k rpm for 1 min and the eluate discarded. The column was centrifuged again at 13k rpm for 1 min before transferal to a clean 1.5 mL centrifugation tube. The DNA was eluted with 50 µL RNase-free H₂O which was allowed to sit for 1 min before centrifugation at 13k rpm for 1 min. DNA was stored at -20°C. PCR product purification was carried out using the Roche Applied Science High Pure PCR Product Purification Kit as detailed by manufacturer binding. The DNA binds to a high pure filter glass fibre fleece matrix in chemotropic salt. This allows contaminants to be removed by using a wash buffer, centrifugally removed from filter into a collection tube and discarded. Clean DNA is eluted into RNase free water by centrifugation into a fresh 1.5 mL centrifuge tube.

2.7.5 Plasmid DNA extraction

Plasmid extraction was carried out using the QIAGEN® Diaper Spin Maniple Kits by manufacturer's instructions. For the mini kit preparation used 5 mL overnight culture spun at 6000 rpm for 10 min. Cells were lysed and the DNA extracted into a clean 1.5 mL centrifugation tube. Elution of the plasmid DNA from the spin column was with 50 µL of RNA-free H₂O. The spin columns containing the H₂O and the DNA were left for 2 min and

spun for 1 min at 13 k rpm. The eluent containing the plasmid DNA was checked for DNA concentration using a NanoDrop 2000™ Spectrophotometer and stored at -20°C.

Midi kit preparation used 100 mL overnight culture which was split into two 50 mL centrifugation tubes and spun for 15 min at 6k rpm. The precipitated plasmid DNA was distributed equally between clean 1.5 mL centrifugation tubes. These were spun for 30 min at 13 k rpm. The precipitated plasmid pellets were combined in one 1.5 mL tube. The tube was spun again for 15 min at 13 k rpm and residual isopropanol removed. The pellet was washed with 70:30 ethanol:H₂O and spun for 10 min. Supernatant was removed by pipettor and the pellet was left to air-dry for 10 min before being re-hydrated with 70 µL of RNA-free H₂O, checked for DNA concentration using a NanoDrop 2000™ Spectrophotometer, and stored at -20°C.

2.7.6 Plasmid dephosphorylation

Plasmids undergoing ligation had 5' phosphatase dephosphorylation to prevent self-ligation and ensure ligation to insert DNA was likely to occur. This was carried out using the rAPid Alkaline Phosphatase from Roche® in the proportions shown in table 2.14. This was held for 30 min at 37°C. The enzyme was heat killed at 75°C for 15 min. Quantification by NanoDrop 2000™ Spectrophotometer was carried out post-dephosphorylation.

Table 2.14: rAPid Alkaline Phosphatase reagents for the dephosphorylation of plasmid DNA.

Reagent	Volume (µl)
Plasmid DNA	20
10x rAPid Alkaline Phosphatase Buffer	2
rAPid Alkaline Phosphatase	1

2.8 Mutation studies with *E. coli*

2.8.1 PCR amplification of the flavohemoglobin flanking regions for insertion into the pK18*mobsacB* plasmid

A flavohemoglobin (*fhb*) mutant was constructed using a double allelic exchange to remove *fhb* from the genome of *P. denitrificans*. This was carried out with polymerase chain reaction (PCR) amplification and purification of two deoxyribonucleic acid (DNA) fragments to span the 5' and 3' flanking regions of the *fhb* gene in *P. denitrificans*. One upstream and one downstream of *fhb* were selected using Artemis Genome browser (Sanger Institute, Cambridge UK). These 5' and 3' regions were designed in such a way that excision and deletion of the *fhb* gene would occur when the 5' and 3' regions were exchanged with their chromosomal counterparts. Oligonucleotide primers of ~20 bp were selected with melting temperatures (T_M) values of ~ 60°C (table 2.15) using the web-based Primer³ Plus from Wageningen Bioinformatics Webportal (Rozen and Skaletsky, 2000) as detailed in the methods.

Table 2.15: Oligonucleotide primers used for PCR amplification of 5' and 3' flanking regions up and downstream of *fhb* for cloning into pK18*mobsacB* and for confirmation of *fhb* deletion in *P. denitrificans*. Restriction sites and additional bases are shown in capital text.

	Forward primer	Reverse primer
3' flank	AGTCTAGAccaagcgcaactattcgat	AGCTGCAGcgatcaggtagagcatgacc
5' flank	AGCCCGGGagaattacggetattatctg	AGTCTAGacgatatcaagaccatgag
Δfhb check	gcatcctgattgcatgtttctg	ccattcctcggatgatcagcc

To these primers were added restriction sites to enable restriction digestion and insertion into the plasmid pK18*mobsacB*. These restriction sites were *Pst*I, *Xba*I and *Xma*I. The restriction site on end position of the flanking region is shown diagrammatically in figure 2.3. This yielded two fragments of sizes 771 and 868 bp for 5' and 3' regions respectively. Selection of fragments used two designed primer oligonucleotides 5' forward primer: *fhb_5fln_F2*, 5' reverse primer: *fhb_5flnR1*, 3' forward primer: *fhb_3fln_F1* and 3' reverse primer:

fhb_3fln_R1 as shown in table 2.9. Restriction sites for *Xma*I, *Xba*I and *Pst*I recombinant endonucleases were added to the DNA fragments prior to amplification for insertion into vector. DNA fragments were amplified from *P. denitrificans* genomic DNA using MyFi™ DNA polymerase (Bioline) (section 2.7.2). Fragments were gel extracted on 0.8% w/v agarose gels with 0.025% (v/v) ethidium bromide (EtBr) in 1x Tris-acetate-EDTA (TAE) buffer containing 45 mM Tris-borate, 1 mM EDTA, pH 8.0 and purified using the Roche High pure PCR product purification kit (section 2.7.1). Restriction sites 5'-*Xma*I, *Xba*I and *Pst*I -3' were added to the DNA fragment prior to amplification for insertion into plasmid pK18*mobsacB* (Schafer *et al.*, 1994) (table 2.18). The recombinant DNA was transformed into competent *Escherichia coli* JM101, screening with the IPTG and X-gal blue-white selection. Triparental mating used *E. coli* DH5 α (pRK2013) as helper (Figurski and Helinski, 1979). The pK18*mobsacB* plasmid contains a neomycin phosphotransferase gene conveying kanamycin resistance (NPT II) and levansucrase (*sacB*). The *sacB* gene encodes a levan sucrose, which catalyses sucrose hydrolysis and levan extension. In *P. denitrificans*, the products of this reaction are toxic, and the cells are sucrose sensitive. This provides an additional selection tool for transformation of the pK18*mobsacB* plasmid.

2.8.2 Construction of the pKH002 suicide plasmid from pK18*mobsacB*

The two flanking regions were inserted into the pK18*mobsacB* plasmid as shown diagrammatically, creating plasmid pKH002 for conjugation into *P. denitrificans*. PCR products were purified for quantification and quantified by Nanodrop yielding 277.9 and 128.7 ng.ml⁻¹ for the 3' and 5' flanking regions respectively. The 3' fragment and the pK18*mobsacB* vector were digested using *Xba*I and *Pst*I to generate sticky ends for ligation of the 3' fragment into pK18*mobsacB*. Following digestion, pK18*mobsacB* was treated with alkaline phosphatase to remove 5' and 3' phosphate groups. This aids the generation of recombinant plasmids since dephosphorylation prevents vector re-ligation and ensures only the insert (which is un-treated) will ligate into the digested plasmid. These preparatory steps are described in the methods. The digested plasmid and inserts were analysed by DNA gel electrophoresis to check the plasmid had been cut and fragment sizes were correct, before gel extraction of the PCR product. This yielded 40.4 ng.ml⁻¹ of digested plasmid and 26.5 ng.ml⁻¹ of the digested 3' flanking region.

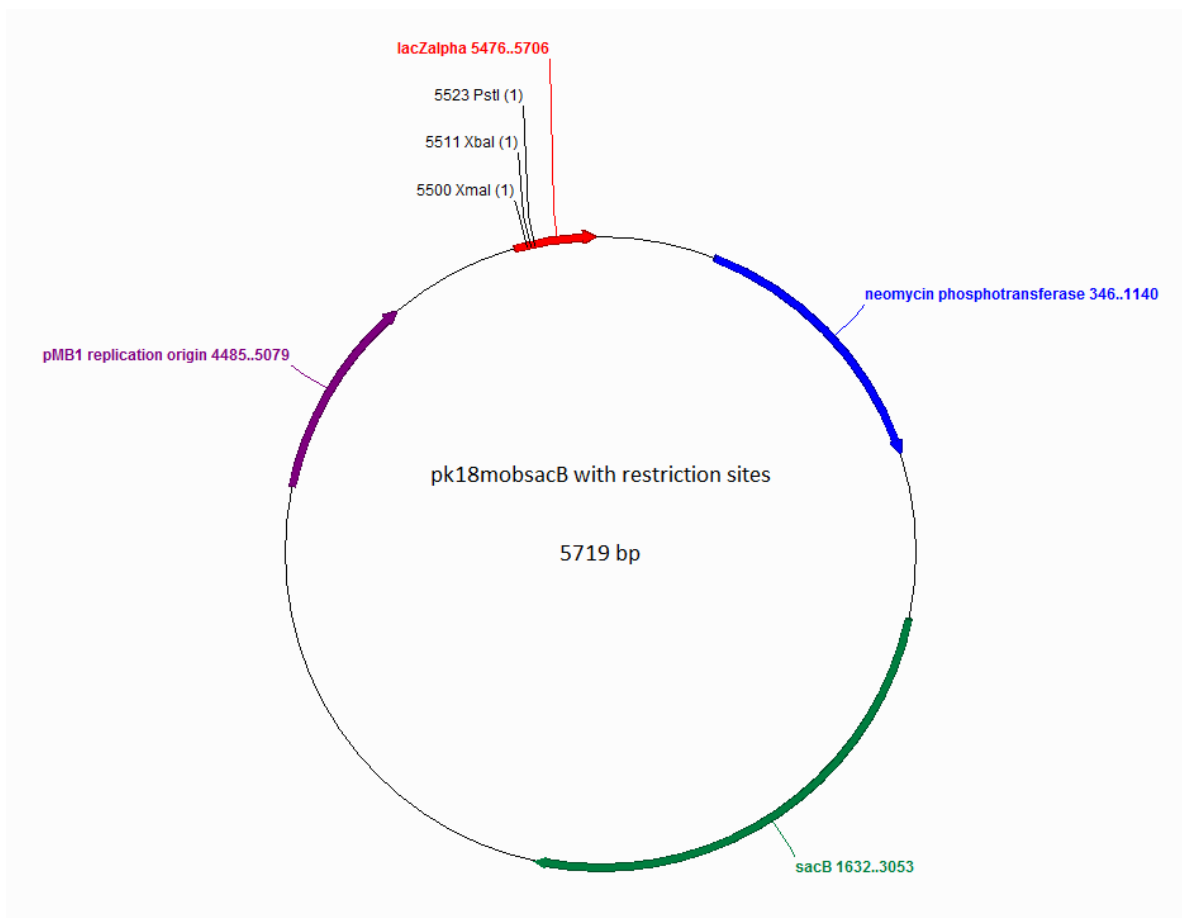


Figure 2.3: pK18mobsacB plasmid showing the multicloning site containing *PstI*, *XbaI* and *XmaI* restriction sites, the lac Z alpha, neomycin phosphotransferase conveying kanamycin resistance, levansucrase (*sacB*) and pMB1 replication origin site.

Regions were checked for the presence of *Pst*I, *Xba*I and *Xma*I sites and the TAG within the TCTAGA *Xba*I site was allocated in-frame creating a premature stop codon. Template for PCR reactions used genomic DNA isolated from *P. denitrificans*. The 5' and 3' regions of *fhb* were amplified to produce DNA products 771 and 868 bp in size for the 5' and 3' regions, respectively, confirmed using a 0.8% ethidium bromide agarose gel. A 5 μ L sample of the PCR products was run on the gel and a single product of correct size was observed. The two flanking regions were inserted into the pK18*mob*sacB plasmid, producing plasmid pKH002 for conjugation into *P. denitrificans*.

Ligation used a 1:3 molar ratio of pK18*mob*sacB vector to 3' fragment insert with the T4 DNA ligase. The number of nanograms and length of each DNA molecule is used to approximate a molar mass and therefore a molar concentration. This is then used to generate a ratio of 1 mole of vector to 3 moles of insert. This is calculated using the size of insert, per size of vector, multiplied by the concentration of vector and finally multiplied by 3: ((bp of insert/bp vector). ng. μ L⁻¹ vector. 3). This provides the volume, in μ L, of insert to combine with plasmid 1 μ L of vector. This used the 3' flanking fragment and additionally with a water efficiency control. Each ligation reaction transformed into competent *E. coli* JM101 cells with a control for transforming using uncut plasmid and digested plasmid. The transformations were selected by plating on solid LB agar containing kanamycin. Single-colony transformants that grew were a mixture of white and blue colonies, indicating that the ligations and transformations had worked. The corresponding recombinant plasmids were isolated by mini preparation and their inserts were checked by restriction digest using *Xba*I and *Pst*I followed by DNA gel electrophoresis. This yielded one plasmid which contained a fragment the same size as the 3' fragment. This plasmid was termed pKH001.

The pKH001 plasmid containing the 3' insert fragment and the gel-extracted and purified 5' flanking fragment were digested using *Xma*I and *Xba*I which produced 13 ng.ml⁻¹ of 5' flanking region and 48.2 ng.ml⁻¹ of plasmid for ligation. The plasmid dephosphorylated for ligation and subsequent transformation. For the 5' flank insertion a kanamycin resistance screen was used. A transformation screen used the same controls and again yielded several colonies as potential candidates showing kanamycin resistance. Kanamycin resistance is transferred to the *P. denitrificans* while the plasmid is in the genome.

2.8.3 Conjugal transfer of pKH002 to *P. denitrificans* and deletion of the flavohemoglobin gene

The pKH002 plasmid was inserted into *P. denitrificans* using triparental mating using *E. coli* containing the conjugal transfer plasmid pRK2013. A mixture of *E. coli* JM101 containing pKH002, *E. coli* containing pRK2013 and *P. denitrificans* were combined and centrifuged to pellet the cells. This cell-pellet mixture was resuspended in 200 μ L of LB media and gently transferred to a cellulose acetate 0.2 μ m filter placed on a LB agar plate with no antibiotics. This allows for the bacteria to access the nutrients in the solid medium, but they can be easily harvested for subsequent selections. After growth at 30°C for 2 days, the cell mixture was harvested by resuspension in 50% glycerol. This resuspension was then serially-diluted from 10^0 to 10^{-4} , and 100 μ L of each dilution was pKH002. These plates were incubated for 3 days at 30°C until colonies of *P. denitrificans* were visible. These Kan^R transconjugants were picked and purified with re-streaking on to LB Rif Kan plates.

To select for a double cross over event and induce the deletion of the chromosomal *fhb* gene by allelic exchange, a second selection was carried out. Kan^R transconjugants were grown in LB medium, in the absence of antibiotics until stationary phase. These stationary phase cells were serially diluted and 100 μ L of the 10^0 – 10^{-6} dilutions were plated on to LB media containing 20% sucrose (w/v). In addition, the 10^{-6} dilutions were also plated on to media without sucrose as an extra control, and all plates were incubated for 4 days at 30°C.

A sucrose screen was used to detect the loss of the pKH002-derived DNA encoding the Kan^R marker. The colonies were picked with sterile toothpicks to LB plates containing Rif, and subsequently to plates containing Rif and Kan. Those that had lost the Kan^R marker were then screened by PCR to further characterise the deletion. These were inoculated to LB media and grown to stationary phase prior to extraction of genomic DNA. These DNA isolations were then used as templates to amplify the region surrounding *fhb*, using primers that flanked the site of the deletion called “ Δ *fhb* check” and shown in table 2.15. These primers were selected to amplify a region 1154 bp in size in the WT *P. denitrificans* genome which contains the *fhb* genomic DNA isolated from the WT and mutant *P. denitrificans* genome were analysed by DNA gel electrophoresis.

2.8.4 Flavohemoglobin complementation with vector reinsertion into *P. denitrificans*

Complementation was carried out *in trans* by reinsertion of the *fhb* into *P. denitrificans* using the wide host-range pOT2 vector (Spaink *et al.*, 1987) shown in figure 2.4. Primers were designed to amplify *fhb* plus 264 bp of DNA upstream to include any native *cis*-acting elements. As for the mutant generation, oligonucleotide primers of ~20 bp were selected with T_M values of ~60°C, shown in table 2.16 using Primer³ Plus (Rozen and Skaletsky, 2000) as detailed in the methods. *Xba*I restriction sites were added to these oligonucleotides to enable restriction digestion of the plasmid pOT2 at the *Xba*I site and insertion of the amplified PCR product.

Table 2.16: Oligonucleotides used for PCR amplification of *fhb* for complementation *in trans*. Restriction sites and additional bases are shown in capitals and gene sequence in lowercase.

Forward primer	Reverse primer
AGTCTAGAcggtcaccagatcggtgatg	TCTAGAgacgacatggacgatccg

Genomic DNA isolated from *P. denitrificans* was used as a template for PCR reactions and the complementary fragment containing *fhb* was amplified to the DNA product of 1499 bp. This was confirmed by running a 5 µL sample on a 0.8% ethidium bromide agarose gel. The fragment was cleaned by gel extraction. The pOT2 plasmid was dephosphorylated with alkaline phosphatase to remove 5' and 3' phosphate groups. This ensured un-treated insert ligation into the digested plasmid and prevented pOT2 re-ligation. PCR products were cleaned and ligated using a 1:3 molar ratio of pOT2 to fragment insert with the T4 DNA ligase and transformed into competent *E. coli* JM101 cells. Transformations were selected by plating on solid LB agar with a gentamycin screen.

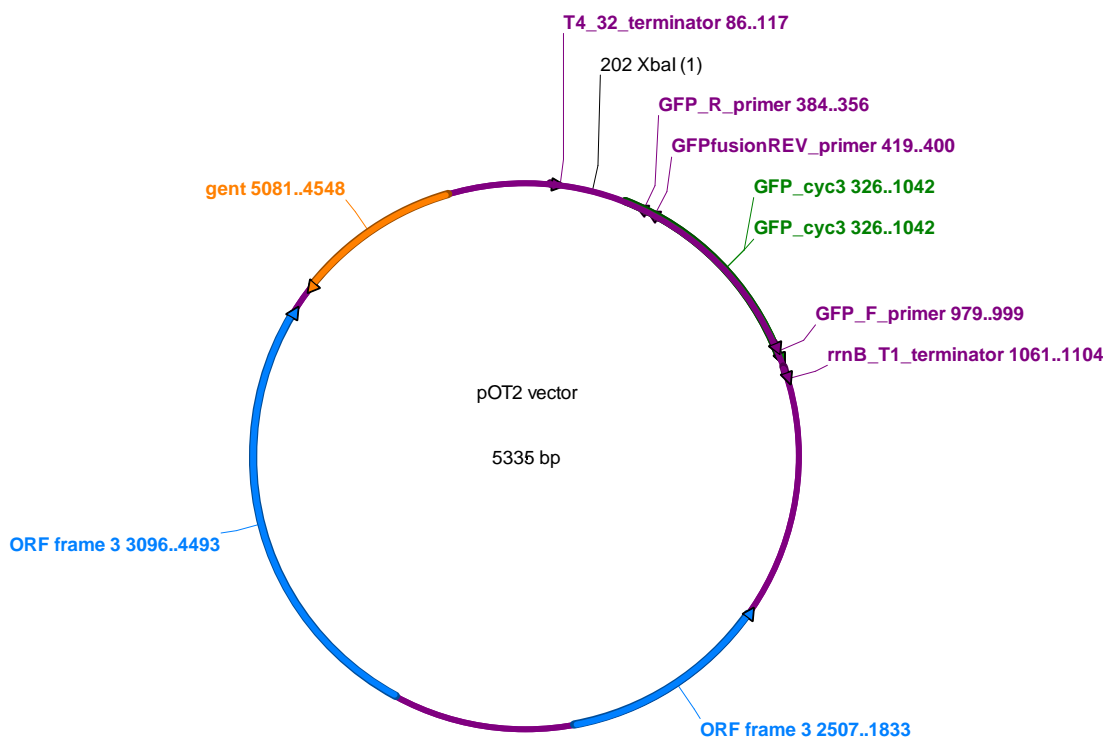


Figure 2.4: The pOT2 vector with features. Gentamycin resistance (orange), open reading frames (blue), green fluorescence protein (GFP) (green) and primer and terminator sequences (purple). The *Xba*I restriction cut site for insertion of the flavohemoglobin (*fhb*) is shown at 202 bp (black).

The colonies produced underwent colony PCR to identify candidates containing the *fhb* fragment and select them for plasmid mini preparation. These were then restriction digested with *Xba*I for confirmation of *fhb* gene, and the resulting plasmid was entered into the *P. denitrificans* genome using triparental mating. Colonies were screened with gentamycin confirming pOT2 plasmid presence and midi prepped for *Xba*I restriction digestion. This plasmid was labelled pKH003. Conjugation of the pKH003 into *P. denitrificans* used triparental mating. The transfer mixture of *E. coli* JM101 containing pKH003, *E. coli* containing the conjugal transfer plasmid pRK2013 and *P. denitrificans* was centrifuged to pellet the cells. When resuspended in 200 μ L of LB media, the mixture was gently transferred to a cellulose acetate 0.2 μ m filter placed on a LB agar plate devoid of antibiotic. After growth at 30°C for 2 days, the cell mixture was harvested by resuspension in 50% glycerol. This resuspension was then serially-diluted from 10^0 to 10^{-4} , and 100 μ L of each dilution was plated on to LB agar containing gentamycin. These plates were incubated for 3 days at 30°C until colonies of *P. denitrificans* were visible. These Gent^R transconjugants were then picked and purified by re-streaking on to new plates of LB Rif Gent plates to confirm growth of *P. denitrificans*.

2.8.5 Recombinant plasmid formation

Restriction enzyme digests were carried out using restriction enzymes and associated buffers (supplementary information) provided by Roche Applied Science and New England Biolabs by manufacturer instruction. Digestion was carried out for 3 h at 37°C followed by heat kill at 75°C for 15 min. Plasmid fragments were dephosphorylated to prevent spontaneous annealing, using the alkaline phosphatase rAPID treatment for 30 min at 37°C followed by heat kill at 75°C for 15 min. PCR products were ligated with a specified vector cut at the same restriction enzyme sites in the same manner, using the Rapid DNA Ligation Kit both by Roche Applied Science using T4 DNA Ligase. They were incubated at 4°C for 16 h followed by inactivation at 75°C for 15 min to form recombinant plasmids (table 2.17). Ligation control is carried out using no insert and increased water addition. Insert volume addition is calculated using the following formula:

A: ligation calculation for concentration of insert required, B: calculation for volume of insert for ligation

$$\text{A: insert required (ng)} = \frac{\text{vector concentration (ng)} \times \text{insert size (kb)}}{\text{vector size (kb)}} \times 3$$

$$\text{B: volume insert (}\mu\text{l)} = \frac{\text{insert required (ng)}}{\text{insert stock (ng)}}$$

Table 2.17: Ligation reaction mix volumes

Reagent	Volume (μ l)
10x ligation buffer	1
T4 DNA ligase	1
Plasmid	1
Insert	(as calculated)
RNase free water	(7-insert volume)

Competent *Escherichia coli* JM101 were prepared from a single colony grown on LB agar shaking, incubated overnight at 37°C 200 rpm in 5 mL LB media. This was used to inoculate 100 mL LB grown to ~0.4 OD_{600nm} before pelleting in two 50 mL conical bottom centrifuge tubes (Corning®) at 6k rpm for 10 min at 4°C. Cell pellets were immediately transferred to ice and the supernatant discarded. Cell pellets were resuspended and combined in 15 mL 0.1 M calcium chloride (CaCl₂), which was kept on ice for 30 min. Then cells were pelleted by centrifugation and immediately put on ice. The supernatant was discarded and pellet resuspended in 2 mL 0.1 M CaCl₂ and incubated on ice for >2 h, or overnight at 4°C.

Competent *E. coli* were transformed with plasmid DNA or ligated plasmid DNA using 200 μ l of cells. Cells are added to plasmid DNA in 1.5 mL centrifuge tubes and incubated on ice for 30 min. Cells are heat shocked at 42°C for 3 min and transferred immediately to ice for 1 min. LB media is added at 500 μ l to each tube and incubated at 37°C for 1 h. After growth at 37°C, cells are pelleted by centrifugation at 13k rpm for 1 min and 100 μ l supernatant retained. The pellet is resuspended, and the transformation mix is plated out and spread onto screening plates containing appropriate antibiotic or appropriate screening technique.

Control transformations carried out in each instance are 200 µl competent cells with 1: 1 µl plasmid and 2: 1 µl restriction digested plasmid.

Table 2.18: Plasmids used in mutant and complementation

Name	Function	Characteristics	Reference
pK18 <i>mobsacB</i>	Creation of <i>fhb</i> mutant	mobilisable multi-purpose cloning vector with kanamycin resistance and conveying sucrose intolerance	(Schafer <i>et al.</i> , 1994)
pOT2 (AJ310442)	Creation of <i>fhb</i> mutant complement	A pBBR replicon with gentamicin resistance	(Allaway <i>et al.</i> , 2001)

2.9 Bioinformatics analysis

2.9.1 Gene identification

Gene sequences were located on the National Center for Biotechnology Information <http://www.ncbi.nlm.nih.gov/> NCBI (Benson *et al.*, 2009; Sayers *et al.*, 2009) and UniProt (<http://www.uniprot.org>). The translated protein sequences were BLAST analysed against NCBI data base. Sequence similarity was determined by bit maximum scoring with percentage identity also taken into consideration. Multiple alignments were carried out using downloaded FASTA sequences imported to Jalview (Waterhouse *et al.*, 2009) and aligned using the Clustral Omega alignment tool (Sievers *et al.*, 2011; Goujon *et al.*, 2010) colouring by percentage identity to the primary sequence. Characterisation of conserved domains was taken from the NCBI protein database and UniProt. Exploration of *E. coli* used the addition of EcoCyc (www.biocyc.org) (Keseler *et al.*, 2011). Protein function was estimated using BLAST analysis and characterisation of aligned sequence function to postulate the function of the gene. Bioinformatic analysis is used in the result chapters and explained in the context of the method, with further detail.

2.9.2 DNA sequencing

DNA sequencing confirmation of the flavohemoglobin mutation was carried out by Genome Enterprise Ltd., (John Innes Centre, UK) by Baptism 3730 capillary sequencing. Returned sequences were compared against designed sequences using the National Center for Biotechnology Information <http://www.ncbi.nlm.nih.gov/> NCBI) (Benson *et al.*, 2009; Sayers *et al.*, 2009).

2.10 Metabolic analytical methods

2.10.1 Calculation of free nitrous acid concentration

FNA itself cannot be assayed for directly. Instead nitrite is directly assayed and the known pH and temperature of solution is used to estimate the concentration of FNA in solution and in these defined conditions. Therefore the quantities of FNA shown are calculated using the pK_a value of the equilibrium for NO_2^- / FNA, along with pH of solution and concentration of NO_2^- . The conjugate base NO_2^- sits in equilibrium with its weak acid counterpart FNA: $\text{NO}_2^- + \text{H}^+ \leftrightarrow \text{HNO}_2$. This is carried out using a formula derived from the Henderson-Hasselbalch equation (De Levie, 2003). The Henderson-Hasselbalch equation itself is derived from the acid dissociation constant and is used to measure dissociation and quantify acidity of a solution in standard conditions. It is used frequently as a logarithmic measure (pK_a) due to the large magnitudes spanned by the acid dissociation constant.

The Henderson-Hasselbalch equation is shown here in two equivalent forms (A and B) with nitrite (NO_2^-) and free nitrous acid (FNA) incorporated as weak acid and conjugate base

$$\text{A: } \text{pH} = \text{p}K_a + \log_{10} ([\text{NO}_2^-] / [\text{FNA}])$$

$$\text{B: } \text{pH} = \text{p}K_a - \log_{10} ([\text{FNA}] / [\text{NO}_2^-])$$

These parameters must be incorporated using this formula in order to determine the concentration of FNA for a known NO_2^- concentration. The nitrite equilibrium equation has pK_a value of 3.16 (Goddard *et al.*, 2008; da Silva *et al.*, 2006). Shown below are, A: acid dissociation constant according to the law of dissociation; B: logarithmic measure of the acid constant; C: pH equation

$$A: K_a = ([H^+][NO_2^-] / [FNA])$$

$$B: pK_a = -\log_{10} K_a$$

$$C: pH = -\log [H^+]$$

The formula for determination of free nitrous acid (FNA) from known nitrite (NO_2^-) concentration and solution pH as derived from the Henderson-Hasselbalch equation is:

$$[FNA] = [NO_2^-] / 10^{(pH-pK_a)}$$

Description for generation of the Henderson-Hasselbalch equation from the acid dissociation equation. Taking log on both sides of the acid dissociation constant:

$$\log_{10} K_a = \log_{10} ([A^-][H^+] / [HA])$$

Substitution of species (A^-) and protonated (HA) for nitrite (NO_2^-) and free nitrous acid (FNA) respectively from nitrite equilibrium equation:

$$\log_{10} K_a = \log_{10} ([H^+][NO_2^-] / [FNA])$$

Splitting logged terms for removal of H^+ from numerator position allowing NO_2^- and FNA to form a ratio and substitution of $\log_{10}[H^+]$ in subsequent steps:

$$\log_{10} K_a = \log_{10}[H^+] + \log_{10} ([NO_2^-] / [FNA])$$

As $-\log_{10} [H^+] = pH$ using the pH equation

$$-\log_{10} [H^+] = pH$$

Multiplication of each side of the pH equation by -1

$$\log_{10} [H^+] = -pH$$

Substitution of pH equation; $\log_{10} [H^+]$:

$$\log_{10} K_a = -pH + \log_{10} ([NO_2^-] / [FNA])$$

Using the logarithmic acid dissociation constant $-\log_{10} K_a = pK_a$, multiplication of each side of the logarithmic acid dissociation constant equation by $\log_{10} K_a = -pK_a$

Substitution of logarithmic acid dissociation constant $\log_{10} K_a$:

$$pK_a = \text{pH} + \log_{10} ([\text{NO}_2^-] / [\text{FNA}])$$

Removal of subtraction by rearrangement which provides the Henderson-Hasselbalch equation

$$\text{pH} = pK_a + \log_{10} ([\text{NO}_2^-] / [\text{FNA}])$$

From the Henderson-Hasselbalch equation, the FNA formula can be derived. This is carried out in the following steps:

Subtraction of pK_a term

$$\text{pH} - pK_a = \log_{10} ([\text{NO}_2^-] / [\text{FNA}])$$

Removal of logarithm by rising to power of 10

$$10^{(\text{pH} - pK_a)} = ([\text{NO}_2^-] / [\text{FNA}])$$

Rearrangement of terms for FNA formula

$$[\text{FNA}] \cdot 10^{(\text{pH} - pK_a)} = [\text{NO}_2^-]$$

$$[\text{FNA}] = [\text{NO}_2^-] / 10^{(\text{pH} - pK_a)}$$

2.10.2 High pressure liquid chromatography (HPLC) analysis of nitrate and nitrite

Quantitative analysis of extracellular nitrate and nitrite was carried out using the Dionex® ICS-900 HPLC system, fitted with DS5 conductivity detection, with samples run at room temperature. A 2 mm x 250 mm IonPac® AS22 analytical carbonate eluent anion-exchange column was used for separation and suppressed conductivity detection of nitrate and nitrite compounds. Samples were loaded by a Dionex® AS40 automated sampler and detection was carried out using a suppressed conductivity using an anion self-regenerating suppressor. Prior to injection into the column, samples were diluted 1:10 into analytical reagent grade water (Fisher) and filtered through a sterile syringe filter pore size 0.2 µm (Minisart® from Sartorius Stedim UK Ltd.) into vials. They were capped and fitted into a Dionex® AS40 automated sampler. Sample sequence began with samples containing analytical grade water, followed by known nitrate and nitrite standards from stock solution freshly made, followed

by growth curve samples containing unknown amounts of nitrate and nitrite. Carbonate eluent, consisting of 4.5 mM sodium carbonate (Na_2CO_3) and 1.4 mM sodium bicarbonate (NaHCO_3) was used to carry the sample through the system with regeneration being carried out using 10 mM sulphuric acid (H_2SO_4).

After separation of anions through the column, a conductivity detector was used for detection. Cation exchange occurred through an ion-specific membrane. Retention time for both nitrate and nitrite was ~7.5 and 4.7 min respectively. Identification of the anions was by retention time. Serial dilutions of freshly made standard nitrate and nitrite stocks were used to derive a calibration curve of known concentrations. The peak area for each known concentration was used to determine the unknown concentrations of nitrate and nitrite from experimental samples.

2.10.3 Gas chromatography of nitrous oxide

Nitrous oxide detection was carried out using a Perkin Elmer Clarus® 500 gas chromatographer (isotope ^{63}Ni , activity 15m Ci) with an electron capture detector (ECD) and Elite-PLOT Q (DVB Plot Column, 30 m, 0.53 mm ID using the carrier gas: nitrogen, make-up gas: 95% argon/5% methane). This was run with an auxiliary gas flow of 58 psi, carrier gas flow 60 psi ~197 mL/min; make up gas flow of 30 mL, with a 20ml/min split. Oven temperature was set at a constant 90°C and ECD at a constant 350°C. The chromatographer was set up and allowed equilibration before use. Gas samples were separated through the column at 90°C and detected and the ^{63}Ni electron capture detector (ECD) was heated constantly at 350°C. Nitrous oxide produced a retention time of 5.2 min, which was used for identification of the gas. Gas cylinders used were BOC 95% argon/5% methane and zero nitrogen 200 bar compressed gas.

Gas samples were extracted from experimental conditions using a gas tight Hamilton syringe and injected to fill a gas tight vial (Labco Exetainer®) for storage before analysis. Large samples were taken in 12ml vials while smaller shaking flask experiments used 3 mL vials. Gas samples were taken in a 0.5 mL gas tight Hamilton, allowed to equilibrate to atmospheric pressure and injected immediately into the GC for detection. Calibration gases are Scientific and Technical Gases Ltd. (STG) 0.4, 5, 100 and 1000 ppm nitrous oxide in nitrogen 12 Bar 20 Da Bar compressed gas were used for quantification of nitrous oxide

levels. Initial atmospheric samples were used for detection of atmospheric levels of nitrous oxide. These were taken from the atmosphere over the course of the experiment and averaged before subtraction. Atmospheric levels were, on average, assayed to be 0.3 ± 0.05 ppm. Standards were then used to generate a calibration curve. The peak area for each known concentration was used to determine the unknown concentrations of nitrous oxide from the experimental samples.

2.11 References

- ALLAWAY, D., SCHOFIELD, N. A., LEONARD, M. E., GILARDONI, L., FINAN, T. M. & POOLE, P. S. 2001. Use of differential fluorescence induction and optical trapping to isolate environmentally induced genes. *Environmental Microbiology*, 3, 397-406.
- ALSTON, M. J., SEERS, J., HINTON, J. C. D. & LUCCHINI, S. 2010. BABAR: An R package to simplify the normalisation of common reference design microarray-based transcriptomic datasets. *BMC Bioinformatics*, 11.
- ANDERSEN, H. C. 1980. Molecular dynamics simulations at constant pressure and/or temperature. *Journal of Chemical Physics*, 72, 2384-2393.
- ARP, D. J. & BURRIS, R. H. 1981. Kinetic mechanism of the hydrogen-oxidizing hydrogenase from soybean nodule bacteroids. *Biochemistry*, 20, 2234-40.
- BARTON, A. F. M. 1975. Solubility parameters. *Chemical Reviews*, 75, 731-753.
- BATTINO, R. & CLEVER, H. L. 1966. The solubility of gases in liquids. *Chemical Reviews*, 66, 395-463.
- BENSON, D. A., KARSCH-MIZRACHI, I., LIPMAN, D. J., OSTELL, J. & SAYERS, E. W. 2009. GenBank. *Nucleic Acids Research*, 37, D26-31.
- BREITLING, R. & HERZYK, P. 2005. Rank-based methods as a non-parametric alternative of the *t*-statistic for the analysis of biological microarray data. *Journal of Bioinformatics and Computational Biology*, 3, 1171-1189.
- DA SILVA, G., KENNEDY, E. M. & DLUGOGORSKI, B. Z. 2006. Ab Initio Procedure for Aqueous-Phase pKa Calculation: The Acidity of Nitrous Acid. *The Journal of Physical Chemistry*, 110, 11371-11376.
- DE LEVIE, R. 2003. The Henderson-Hasselbalch equation: Its history and limitations. *Journal of Chemical Education*, 80, 146.

- FIGURSKI, D. H. & HELINSKI, D. R. 1979. Replication of an origin-containing derivative of plasmid RK2 dependent on a plasmid function provided in trans. *Proceedings of the National Academy of Sciences*, 76, 1648-1652.
- GODDARD, A. D., MOIR, J. W., RICHARDSON, D. J. & FERGUSON, S. J. 2008. Interdependence of two NarK domains in a fused nitrate/nitrite transporter. *Molecular Microbiology*, 70, 667-681.
- GOUJON, M., MCWILLIAM, H., LI, W., VALENTIN, F., SQUIZZATO, S., PAERN, J. & LOPEZ, R. 2010. A new bioinformatics analysis tools framework at EMBL-EBI. *Nucleic Acids Research*, 38, W695-9.
- HARVEY, A. H. & SMITH, F. L. 2007. Avoid common pitfalls when using Henry's Law. *Chemical Engineering Progress*, 103, 33 - 39.
- HEIJNEN, J. J. & ROMEIN, B. 1995. Derivation of kinetic equations for growth on single substrates based on general properties of a simple metabolic network. *Biotechnology Progress*, 11, 712-716.
- HENZLER, H. J. & SCHEDEL, M. 1991. Suitability of the shaking flask for oxygen supply to microbiological cultures. *Bioprocess Engineering*, 7, 123-131.
- KESELER, I. M., COLLADO-VIDES, J., SANTOS-ZAVALETA, A., PERALTA-GIL, M., GAMA-CASTRO, S., MUNIZ-RASCADO, L., BONAVIDES-MARTINEZ, C., PALEY, S., KRUMMENACKER, M., ALTMAN, T., KAIPA, P., SPAULDING, A., PACHECO, J., LATENDRESSE, M., FULCHER, C., SARKER, M., SHEARER, A. G., MACKIE, A., PAULSEN, I., GUNSALUS, R. P. & KARP, P. D. 2011. EcoCyc: a comprehensive database of *Escherichia coli* biology. *Nucleic Acids Research*, 39, D583-90.
- KOVÁROVÁ-KOVAR, K. & EGLI, T. 1998. Growth kinetics of suspended microbial cells: From single-substrate- controlled growth to mixed-substrate kinetics. *Microbiology and Molecular Biology Reviews*, 62, 646-666.
- MURRAY, C. N. & RILEY, J. P. 1969. The solubility of gases in distilled water and sea water—II. Oxygen. *Deep Sea Research and Oceanographic Abstracts*, 16, 311-320.
- ROBERTSON, L. A. & KUENEN, J. G. 1983. *Thiosphaera pantotropha* gen. nov. sp. nov., a facultatively anaerobic, facultatively autotrophic sulphur bacterium. *Journal of General Microbiology*, 2847-2855.
- ROZEN, S. & SKALETSKY, H. 1999. Primer3 on the WWW for General Users and for Biologist Programmers.

- ROZEN, S. & SKALETSKY, H. 2000. Primer3 on the WWW for general users and for biologist programmers. *Methods in Molecular Biology*, 132, 365-86.
- RUTHERFORD, K., PARKHILL, J., CROOK, J., HORSNELL, T., RICE, P., RAJANDREAM, M. A. & BARRELL, B. 2000. Artemis: Sequence visualization and annotation. *Bioinformatics*, 16, 944-5.
- SANDER, R. 1999. *Compilation of Henry's Law constants for inorganic and organic species of potential importance in environmental chemistry* [Online]. Rolf Sander. Available: <http://www.henrys-law.org>.
- SAYERS, E. W., BARRETT, T., BENSON, D. A., BRYANT, S. H., CANESE, K., CHETVERNIN, V., CHURCH, D. M., DICUCCIO, M., EDGAR, R., FEDERHEN, S., FEOLO, M., GEER, L. Y., HELMBERG, W., KAPUSTIN, Y., LANDSMAN, D., LIPMAN, D. J., MADDEN, T. L., MAGLOTT, D. R., MILLER, V., MIZRACHI, I., OSTELL, J., PRUITT, K. D., SCHULER, G. D., SEQUEIRA, E., SHERRY, S. T., SHUMWAY, M., SIROTKIN, K., SOUVOROV, A., STARCHENKO, G., TATUSOVA, T. A., WAGNER, L., YASCHENKO, E. & YE, J. 2009. Database resources of the National Center for Biotechnology Information. *Nucleic Acids Research*, 37, D5-15.
- SCHAFER, A., TAUCH, A., JAGER, W., KALINOWSKI, J., THIERBACH, G. & PUHLER, A. 1994. Small mobilizable multi-purpose cloning vectors derived from the Escherichia coli plasmids pK18 and pK19: selection of defined deletions in the chromosome of Corynebacterium glutamicum. *Gene*, 145, 69-73.
- SIEVERS, F., WILM, A., DINEEN, D., GIBSON, T. J., KARPLUS, K., LI, W., LOPEZ, R., MCWILLIAM, H., REMMERT, M., SODING, J., THOMPSON, J. D. & HIGGINS, D. G. 2011. Fast, scalable generation of high-quality protein multiple sequence alignments using Clustal Omega. *Molecular Systems Biology*, 7, 539.
- SPAINK, H. P., OKKER, R. J. H., WIJFFELMAN, C. A., PEES, E. & LUGTENBERG, B. J. J. 1987. Promoters in the nodulation region of the *Rhizobium leguminosarum* Sym plasmid pRL1J1. *Plant Molecular Biology*, 9, 27-39.
- VISHNIAC, W. & SANTER, M. 1957. The *Thiobacilli*. *Bacteriological reviews*, 21, 195-213.
- WATERHOUSE, A. M., PROCTER, J. B., MARTIN, D. M., CLAMP, M. & BARTON, G. J. 2009. Jalview Version 2--a multiple sequence alignment editor and analysis workbench. *Bioinformatics*, 25, 1189-91.

WILHELM, E., BATTINO, R. & WILCOCK, R. J. 1977. Low-pressure solubility of gases in liquid water. *Chemical Reviews*, 77, 219-262.

YANISCH-PERRON, C., VIEIRA, J. & MESSING, J. 1985. Improved M13 phage cloning vectors and host strains: nucleotide sequences of the M13mp18 and pUC19 vectors. *Gene*, 33, 103-19.

3 The effect of extracellular pH and nitrite on batch culture growth kinetics of *P. denitrificans*

Contents

3	The effect of extracellular pH and nitrite on batch culture growth kinetics of <i>P. denitrificans</i>	95
3.1	List of figures	96
3.2	List of tables	98
3.3	Introduction	98
3.3.1	The effect of pH on microbial growth.....	99
3.3.2	The pH dependent formation of free nitrous acid (FNA).....	99
3.3.3	The biological impacts of nitrite and free nitrous acid.....	103
3.4	Results	104
3.4.1	Growth of <i>P. denitrificans</i> over a pH range of 6.0 – 8.5.....	104
3.4.2	Effect on growth of <i>P. denitrificans</i> at nitrite concentrations between 0 and 10 mM	108
3.4.3	Growth of <i>P. denitrificans</i> at nitrite concentrations above 10 mM	111
3.4.4	Growth kinetics of <i>P. denitrificans</i> in the presence of nitrite and over a pH range of 7.0 – 8.5.....	118
3.5	Discussion	121
3.5.1	The influence of pH and effect of nitrite on the growth of <i>P. denitrificans</i> .	121
3.5.2	The role of free nitrous acid in nitrite toxicity	122
3.5.3	Dual stimulatory and inhibitory role of nitrite	124
3.6	References.....	127

3.1 List of figures

- Figure 3.1: The pH dependence of nitrite and FNA concentration showing the percentage of nitrite (solid line) and free nitrous acid (FNA) (dashed line) present at a range of pH values. This is calculated using the FNA equation derived from the Henderson-Hasselbalch equation to show the effect of pH on the protonation of nitrite and generation of FNA. A: pH range 0 – 9. B: higher resolution at physiological pH range between pH 7.0 and 8.5.....102
- Figure 3.2: The effect of pH on the growth of *P. denitrificans*. Minimal salts media, supplemented with ammonium chloride, 10 mM, sodium succinate, 30 mM and Vishniac trace element solution. Measured by optical density at 600 nm (OD_{600nm}) adjusted to a pathlength of 1 cm against time (h). Cells were grown aerobically in 100 μ l total volume with shaking at 400 rpm. OD_{600nm} was measured every 0.5 h, 1 h values shown. Error bars denote standard error $n = \geq 3$. The pH values are shown in the key at the top of the figure. 106
- Figure 3.3: Maximum optical density produced (Y_{max}) and apparent growth rate constant (μ_{app}) for the effect of media pH on the growth of *P. denitrificans*. Minimal salts media, supplemented with ammonium chloride, 10 mM, sodium succinate, 30 mM and Vishniac trace element solution. Measured by optical density at 600 nm (OD_{600nm}) adjusted to a pathlength of 1 cm against time (h). Cells were grown in 100 μ l total volume with shaking at 400 rpm. Error bars denote standard error $n = \geq 3$. Y_{max} (open circle) and μ_{app} (closed circle) are shown in the key at the top of the figure.....107
- Figure 3.4: Stimulation of growth of *P. denitrificans* in minimal salts media, supplemented with ammonium chloride, 10 mM, sodium succinate, 30 mM and Vishniac trace element solution. Measured by optical density at 600 nm (OD_{600nm}) adjusted to a pathlength of 1 cm against time (h). OD_{600nm} was measured every 0.5 h, 1 h values shown. Cells were grown in 100 μ l total volume with shaking at 400 rpm. Sodium nitrite concentration addition is shown in the key at the top of the figure. Error bars denote standard error $n = \geq 3$110
- Figure 3.5: Growth of *P. denitrificans* in minimal salts media, pH 7.0, supplemented with ammonium chloride, 10 mM, sodium succinate, 30 mM and Vishniac trace element solution, with various sodium nitrite concentrations (mM) as shown in the key at the top of the figure. Measured by optical density at 600 nm (OD_{600nm}) adjusted to a pathlength of 1 cm against time (h). Cells were grown in 100 μ l total volume with shaking at 400 rpm. OD_{600nm} was measured every 0.5 h, 1 h values shown. Error bars denote standard error $n = \geq 3$112
- Figure 3.6: Growth of *P. denitrificans* in minimal salts media, pH 7.5, supplemented with ammonium chloride, 10 mM, sodium succinate, 30 mM and Vishniac trace element solution, with various sodium nitrite concentrations (mM) as shown in the key above the figure.

Measured by optical density at 600 nm (OD_{600nm}) adjusted to a pathlength of 1 cm against time (h). Cells were grown in 100 μ l total volume with shaking at 400 rpm. OD_{600nm} was measured every 0.5 h, 1 h values shown. Error bars denote standard error $n = \geq 3$ 113

Figure 3.7: Growth of *P. denitrificans* in minimal salts media, pH 8.0, supplemented with ammonium chloride, 10 mM, sodium succinate, 30 mM and Vishniac trace element solution, with various sodium nitrite concentrations (mM) as shown in the key above the figure. Measured by optical density at 600 nm (OD_{600nm}) adjusted to a pathlength of 1 cm against time (h). Cells were grown in 100 μ l total volume with shaking at 400 rpm. OD_{600nm} was measured every 0.5 h, 1 h values shown. Error bars denote standard error $n = \geq 3$ 114

Figure 3.8: Growth of *P. denitrificans* in minimal salts media, pH 8.5, supplemented with ammonium chloride, 10 mM, sodium succinate, 30 mM and Vishniac trace element solution, with various sodium nitrite concentrations (mM) as shown in the key above the figure. Measured by optical density at 600 nm (OD_{600nm}) adjusted to a pathlength of 1 cm against time (h). Cells were grown in 100 μ l total volume with shaking at 400 rpm. OD_{600nm} was measured every 0.5 h, 1 h values shown. Error bars denote standard error $n = \geq 3$ 116

Figure 3.9: Summarised growth of *P. denitrificans* in minimal salts media, pH 7.0, 7.5, 8.0 and 8.5, supplemented with ammonium chloride, 10 mM, sodium succinate, 30 mM and Vishniac trace element solution, with various sodium nitrite concentrations (mM) as shown in the key above the figure. Measured by optical density at 600 nm (OD_{600nm}) adjusted to a pathlength of 1 cm against time (h). Cells were grown in 100 μ l total volume with shaking at 400 rpm. OD_{600nm} was measured every 0.5 h, 1 h values shown. Error bars denote standard error $n = \geq 3$ 117

Figure 3.10: Summarised maximum optical density produced (Y_{max} AU) over the pH range 7.0 – 8.5 as shown in the key above the figure for the growth of *P. denitrificans* in minimal salts media, pH 7.0, 7.5, 8.0 and 8.5, supplemented with ammonium chloride, 10 mM, sodium succinate, 30 mM and Vishniac trace element solution. Measured by optical density at 600 nm (OD_{600nm}) adjusted to a pathlength of 1 cm against time (h). Error bars denote standard error $n = \geq 3$ 119

Figure 3.11: Summarised apparent growth constant (μ_{app}) over a pH range of 7.0 – 8.5 as shown in the key above the figure for the growth of *P. denitrificans* in minimal salts media, pH 7.0, 7.5, 8.0 and 8.5, supplemented with ammonium chloride, 10 mM, sodium succinate, 30 mM and Vishniac trace element solution. Measured by optical density at 600 nm (OD_{600nm}) adjusted to a pathlength of 1 cm against time (h). Error bars denote standard error $n = \geq 3$ 120

Figure 3.12: Summary of pH dependent and independent effects linked to the growth of *P. denitrificans* and the effects of nitrite.126

3.2 List of tables

Table 3.1: List of nitrate and nitrite with conjugate acids nitric acid and FNA, showing chemical formula, structure, molecular weight and pK_a value.....101

Table 3.2: Stimulation of growth shown by Y_{max} (AU) for growth of *P. denitrificans* under standard growth conditions at various sodium nitrite concentrations: minimal salts media, supplemented with ammonium chloride, 10 mM; sodium succinate, 30 mM; Vishniac trace element solution.108

3.3 Introduction

Environmental stresses on microbial soil communities are diverse and frequent. These stresses can include the fluctuation in oxygen levels, the bioavailability of nutrients and the fluctuation in pH. Stress induction can also come in the form of toxic by-products from metabolic processes or toxic compounds from neighbouring microorganism defence mechanisms. It is evolutionary pressure which positively selects microorganisms capable of surviving fluctuations in the surrounding environment and therefore bacteria have evolved coping strategies in order to maintain successful growth in a changeable environment.

A common hazard for *P. denitrificans* are by-products of denitrification. The most toxic of the denitrification pathway compounds are nitrite (NO_2^-) and nitric oxide (NO). These compounds are metabolised promptly within the *P. denitrificans* cell to prevent intracellular accumulation and associated cellular damage. Nitrite is a known toxin which undergoes nitrosylation with amines and amides form nitrosamines (Rostkowska *et al.*, 1998; Drabløs *et al.*, 2004). NO can alter the oxidation state of metal ion cofactors such as ferrous iron, affecting ATP generation and active transport (Rowe *et al.*, 1979). Although the toxic nature of nitrite has been documented, little is known about the method in which nitrite is detrimental to growth of bacteria and where this cytotoxicity is focused to bring about detrimental to cellular function.

3.3.1 The effect of pH on microbial growth

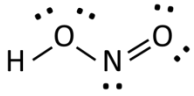
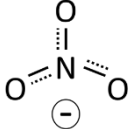
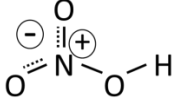
Environmental pH plays an important role in diversity within microbial communities. The environmental pressure of pH has led to microorganism specialisation to occupy uniquely inhospitable niches within the environment and it influences species distribution in mixed communities. It is sometimes possible to predict a naturally occurring bacterial community composition on the basis of the surrounding pH. This observation appears directly linked to the often narrow pH optimum, which is specific to each individual bacterial species (Rosso *et al.* (1995); Lauber *et al.*, 2009). A range of 1.5 pH unit change within the immediate soil environment of an established bacterial community reduces bacterial activity by 50%, leading to competition from more tolerant species and a community composition change (Bååth and Anderson, 2003; Fernández-Calviño and Bååth, 2010). This effect is due to the large range of cellular processes which are directly affected by pH. Protein activity can be reduced by change in pH, leading to loss of biological activity and preventing the function of normally cellular processes. Additionally, pH affects ionisation and therefore the binding and interaction of molecular processes including rendering key nutrients biologically unavailable or insoluble. Although pH is a well-studied parameter in science, it impacts on many cellular processes and can activate less harmful molecules into toxins.

3.3.2 The pH dependent formation of free nitrous acid (FNA)

FNA (HNO_2) is formed by the protonation of the nitrite anion which carries a negative charge allowing the addition of one proton as shown table 3.1. The single protonation for this conjugate acid-base relationship is described by the following equilibrium: $\text{NO}_2^- + \text{H}^+ \leftrightarrow \text{HNO}_2$ ($pK_a = 3.16$) (Goddard *et al.*, 2008; da Silva *et al.*, 2006). This reaction yields a weak, but reactive acid. This equilibrium can be seen in the Henderson-Hasselbalch derived dissociation curve in figure 3.1 which shows low levels of FNA being formed at average physiological pH level (6 – 8). This differs from nitrate which has a pK_a of -1.3 (table 3.1) (Moir and Wood, 2001). The concentration of FNA in solution is determined by known pH and nitrite concentration. Total concentration of FNA is dependent on solution pH causing a shift in the equilibrium of nitrite and FNA in favour of FNA. Using the pK_a value of FNA with the Henderson-Hasselbalch equation the concentration of FNA can be determined. FNA and nitrite concentration as defined by the Henderson-Hasselbalch equation are shown

normalised to 100% (figure 3.1). To determine these values, the Henderson-Hasselbalch equation was used to derive a FNA equation. FNA can be spontaneously formed on the Earth's surface such as soils, vegetation and urbanised areas such as buildings where water is present. This has been documented both on mobile and stationary surfaces (Pitts Jr *et al.*, 1978; Finlayson-Pitts *et al.*, 2003). This has led to large amounts of interest in the area of atmospheric chemistry as a source of OH[·] in urban atmospheres (Lammel and Cape, 1996), in the formation of carcinogenic nitrosamines and biofilm clearance (Wei *et al.*, 2014; Jiang *et al.*, 2011).

Table 3.1: List of nitrate and nitrite with conjugate acids nitric acid and FNA, showing chemical formula, structure, molecular weight and pK_a value.

Base	Base structure	Molecular weight g mol^{-1}	Acid	Acid structure	Molecular weight g mol^{-1}	pK_a value
Nitrite (NO_2^-)		46.01	FNA (HNO_2)		47.01	3.25 (Goddard <i>et al.</i> , 2008)
Nitrate (NO_3^-)		62.01	Nitric acid (HNO_3)		63.01	-1.3 (Moir and Wood, 2001)

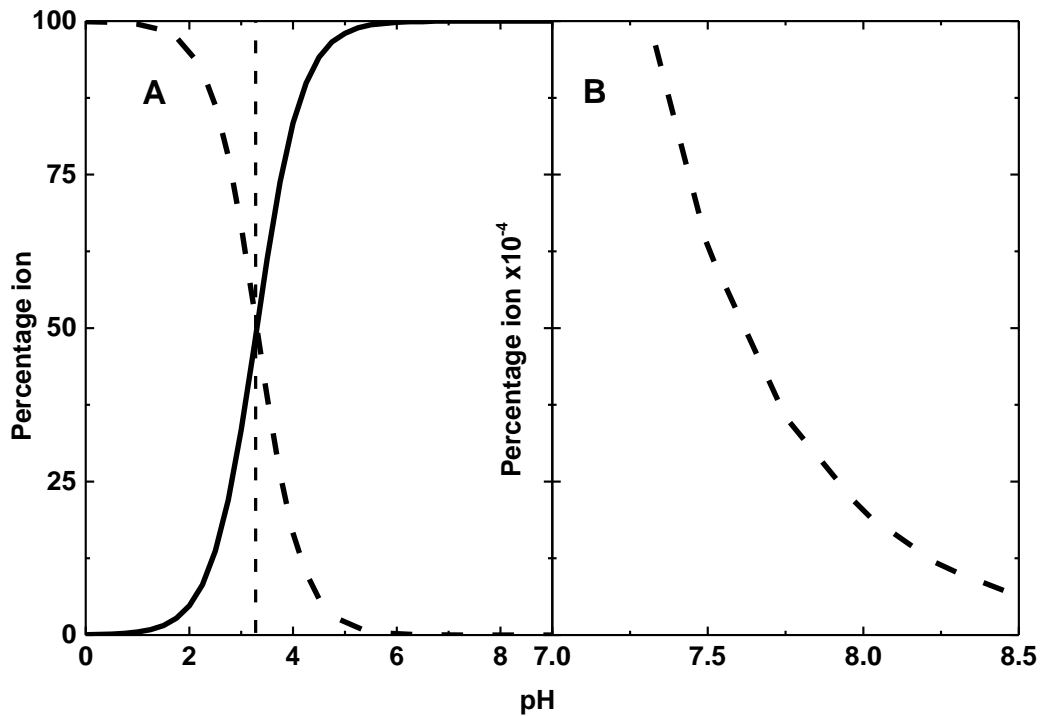


Figure 3.1: The pH dependence of nitrite and FNA concentration showing the percentage of nitrite (solid line) and free nitrous acid (FNA) (dashed line) present at a range of pH values. This is calculated using the FNA equation derived from the Henderson-Hasselbalch equation to show the effect of pH on the protonation of nitrite and generation of FNA. A: pH range 0 – 9. B: higher resolution at physiological pH range between pH 7.0 and 8.5.

3.3.3 The biological impacts of nitrite and free nitrous acid

It has been found in recent studies that accumulation of nitrite can inhibit the metabolism of several groups of bacteria in studies investigating the nitrogen removal in wastewater treatment plants (WWTP). This process utilises ammonia oxidation to nitrite and further nitrite reduction to dinitrogen to remove harmful levels in wastewater effluents (Anthonisen *et al.*, 1976; Vadivelu *et al.*, 2006b). This has also been seen in denitrifiers (Almeida *et al.*, 1995) and polyphosphate accumulators (Zhou *et al.*, 2008; Fux *et al.*, 2003). However this nitrite inhibition has been attributed to the protonated conjugate acid of nitrite: free nitrous acid (FNA) (Yarbrough *et al.*, 1980). Extensive work by Ye *et al.* (2010) has suggested that this is a likely case for many observed nitrite linked growth inhibition. It was observed that both catabolic and anabolic processes were affected, in this case, in the consumption of PHA, glycogen production and the growth observed for the mixed culture of enriched PAO and GAO bacteria comprising largely of *Competibacter*. It was found that complete inhibition of growth occurred at an FNA concentration of 7×10^{-3} mg-HNO₂L⁻¹ and 50% inhibition occurred at 1.5×10^{-3} mg-HNO₂L⁻¹ (Yang, 1985).

The mechanism by which nitrite and its counterpart, FNA, is reported to act as a cytotoxic agent is postulated to be one, or all of, the following. It has been suggested the FNA crosses the cell wall to interact directly with cellular components and thus interfere with the protein and metabolic function of the organism (Rowe *et al.*, 1979; Yang *et al.*, 1985). Additionally FNA has been suggested to act as an uncoupler, as was suggested by Sijbesma (1996). This suggests FNA acts to circumvent the ATP synthesis route, as has been reported in *P. denitrificans*. A short-circuit is formed by FNA transporting protons across the inner membrane and back into the cell and increasing the permeability of the cytoplasmic membrane (Meijer *et al.*, 1979). Inhibition directly of electron carriers, exclusive of an uncoupling effect has also been a suggested inhibitory mechanism attributed to nitrite and FNA in *P. denitrificans* and two *Pseudomonas* strains (Rake and Eagon, 1980; Rowe *et al.*, 1979; Williams *et al.*, 1978). Due to the formation of FNA resulting from a protonation reaction, pH is a determining factor in its formation. Inhibitory effects seen with nitrite are often unclear when pH is not a controlled factor in experimental procedure as was examined by Zhou *et al.* (2007). It was therefore suggested that this provided further evidence toward FNA as the predominant cytotoxic over that of nitrite alone. In this study with *Accumulibacter*, a PAO, experimentation focused on the maintenance of pH and observation of FNA as the sole inhibitor. Here, 0.02 mg HNO₂-NL⁻¹ was the concentration at which

inhibition of phosphate uptake was total (Zhou *et al.*, 2007) which was corroborated by Jiang (2011) who saw a 75% decrease of biofilm after exposure to 0.2 – 0.3 mg HNO₂-N L⁻¹.

3.4 Results

3.4.1 Growth of *P. denitrificans* over a pH range of 6.0 – 8.5

In order to investigate the effect of pH change on the sensitivity of *P. denitrificans* to nitrite, batch cultures were used to grow *P. denitrificans* under different pH values and nitrite concentrations. Aerobic growth of *P. denitrificans* was screened across a range of pH units using a plate reader (see methods). The pH range investigated was: 6.0, 6.5, 7.0, 7.5, 8.0, 8.5 and 9.0. Minimal salts media was prepared and pH adjusted as described in the methods, prior to use in the plate reader. The growth of *P. denitrificans* was monitored at 600 nm for change in optical density. This measurement shows the change in light scatter caused by bacteria cells and is used as an arbitrary unit of growth. It does not reflect the morphology of the cells being monitored. The curves produced are shown in figure 3.2. These show distinct growth characteristics which are specific to each media pH. The growth of *P. denitrificans* is characterised using optical density reading taken at 600 nm with a pathlength of 1 cm (OD_{600nm} AU). The highest value of OD_{600nm} achieved during growth is defined as Y_{max} (AU) and is used for comparison of the maximum optical density achieved at each growth condition examined. Quantification of growth curve kinetics for each pH unit was carried out and compared directly. Maximum optical density (Y_{max}) shown in OD_{600nm} AU has been taken directly from the growth curve data. Exponential growth was quantified using the linear gradient taken from a semi log plot of the growth curve data, as described in the methods. The growth kinetics for the pH range 6.0 – 9.0 is shown graphically in figure 3.3. The growth kinetics data are tabulated in the appendix.

Increasing the pH from 8.0 to 8.5 presented a unique characteristic; a steep exponential growth resulting in a peak of growth, which exceeded that of the more acidic pH 8.0. At pH 7.0, exponential growth is reduced, with a final Y_{max} similar to that of the pH 7.5 – 8.5 range. The most alkaline pH unit of 9.0 shows reduction of growth. This is observed by an extension of lag phase, reduction in the exponential growth phase and reduction in the final Y_{max}. The largest reduction in growth characteristics can be seen at the acidic pH units 6.0 and 6.5. Lag phase of growth extends towards the extremity pH values pH 6.5 and 9.0. At

pH 6.5, growth is severely attenuated; lag is extended, with Y_{\max} and μ_{app} vastly reduced. Growth is entirely inhibited at pH 6.0 (figure 3.2). The largest Y_{\max} of 3.68 ± 0.05 is generated at pH 7.5. At pH ≤ 6.5 growth is severely impaired. The fastest rate of cellular division is observed at pH 8.0 with an apparent growth constant (μ_{app}) of $0.51 \pm 0.01 \text{ h}^{-1}$. The maximum optical density (Y_{\max}), $3.7 \pm 0.1 \text{ AU}$, is generated at pH 7.5. The values for Y_{\max} and μ_{app} at pH 7.5 have been taken as a baseline for comparison.

When pH is more acidic, there is a distinct change in the observed Y_{\max} . At pH 7.0, Y_{\max} was similar to that of pH 7.5 ($Y_{\max} 3.4 \pm 0.1 \text{ AU}$) and an additionally similar exponential growth phase of μ_{app} of $0.40 \pm 0.01 \text{ h}^{-1}$. Both were lower than that measured at pH 7.5, at ~90% of that achieved at pH 7.5 (percentage deviation from pH 7.5 is shown in the appendix. At pH 6.5, Y_{\max} was significantly reduced to that achieved at pH 7.5. At pH 6.5 the Y_{\max} is reduced to less than 1 % of that at pH 7.5. However, the μ_{app} reduces to a lesser extent and remains at $0.29 \pm 0.02 \text{ h}^{-1}$, 65% of the μ_{app} measured at pH 7.5. The final, most acidic pH examined was 6.0, at which growth was inhibited (figure 3.3).

In more alkali media, growth also reduced from the optimum of pH 7.5, exponential growth increased at pH 8.0 and 8.5, before substantially decreasing in the more alkaline pH 9.0 media. At pH 8.0 and 8.5, Y_{\max} maintained a high value with 82% of Y_{\max} under standard growth conditions achieving $3.0 \pm 0.06 \text{ AU}$. The apparent exponential growth curve at pH 8.0 shows a μ_{app} $0.51 \pm 0.01 \text{ h}^{-1}$, higher than that of pH 7.5. The media of pH 8.5 achieved an Y_{\max} of $3.2 \pm 0.002 \text{ AU}$ and μ_{app} $0.48 \pm 0.01 \text{ h}^{-1}$, which is 87% and 109% of standard pH 7.5 growth conditions respectively. Finally at pH 9.0, Y_{\max} and μ_{app} dropped by 60% of that at pH 7.5; $2.2 \pm 0.1 \text{ AU}$ and $0.27 \pm 0.02 \text{ h}^{-1}$, respectively, but maintained an observable level of growth. From these data presented in figure 3.3, it is clear that *P. denitrificans* growth is relatively stable between a pH range of 7.0 – 8.5 in minimal salts media. This pH range was then selected for further examination. These pH values were chosen to reduce the pH growth effect in the determination of nitrite effect.

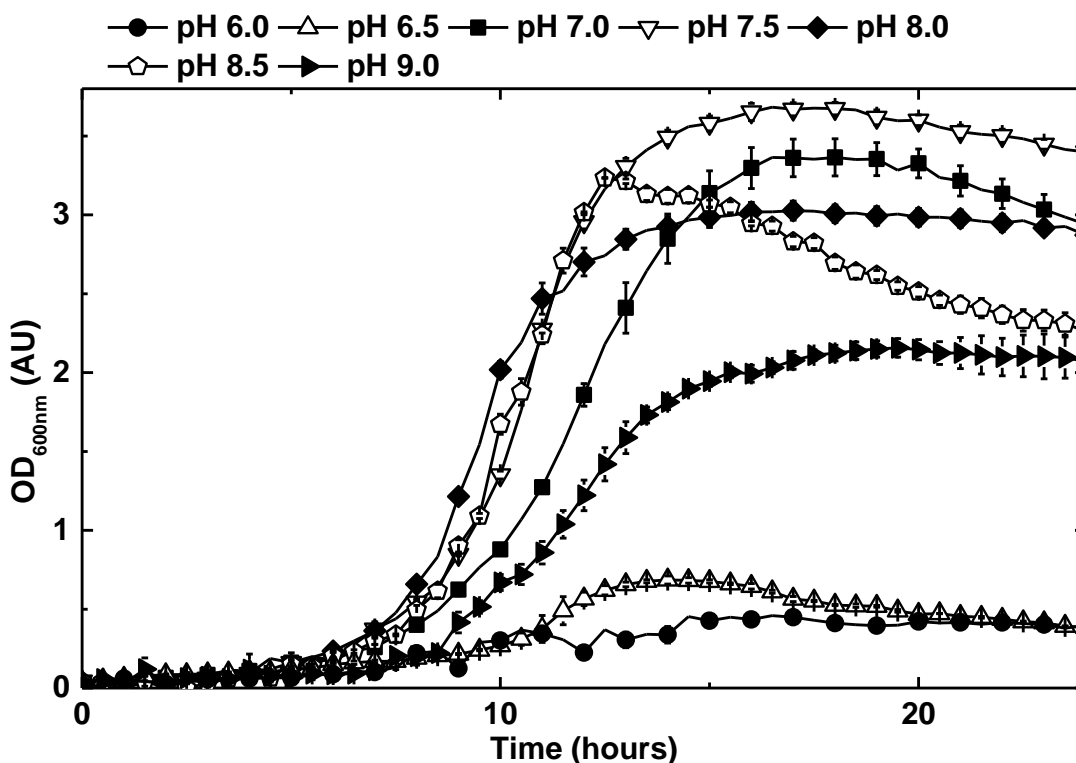


Figure 3.2: The effect of pH on the growth of *P. denitrificans*. Minimal salts media, supplemented with ammonium chloride, 10 mM, sodium succinate, 30 mM and Vishniac trace element solution. Measured by optical density at 600 nm (OD_{600nm}) adjusted to a pathlength of 1 cm against time (h). Cells were grown aerobically in 100 μ l total volume with shaking at 400 rpm. OD_{600nm} was measured every 0.5 h, 1 h values shown. Error bars denote standard error $n = \geq 3$. The pH values are shown in the key at the top of the figure.

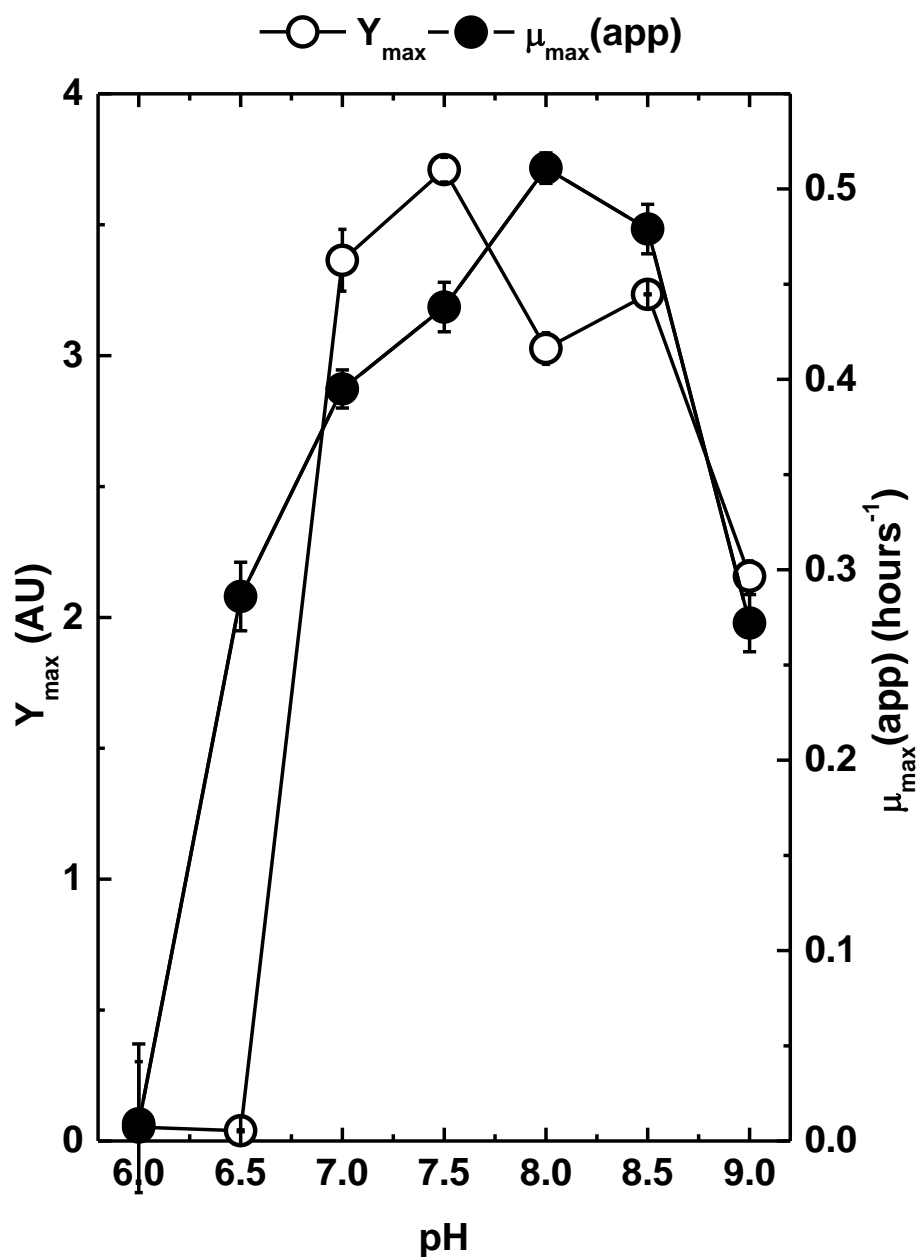


Figure 3.3: Maximum optical density produced (Y_{\max}) and apparent growth rate constant (μ_{app}) for the effect of media pH on the growth of *P. denitrificans*. Minimal salts media, supplemented with ammonium chloride, 10 mM, sodium succinate, 30 mM and Vishniac trace element solution. Measured by optical density at 600 nm ($OD_{600\text{nm}}$) adjusted to a pathlength of 1 cm against time (h). Cells were grown in 100 μl total volume with shaking at 400 rpm. Error bars denote standard error $n \geq 3$. Y_{\max} (open circle) and μ_{app} (closed circle) are shown in the key at the top of the figure.

3.4.2 Effect on growth of *P. denitrificans* at nitrite concentrations between 0 and 10 mM

The effect of nitrite concentration on the growth of *P. denitrificans* was investigated using identical minimal salts media brought to pH as detailed in methods 2.1. Filter sterilised stock sodium nitrite solution was added to the sterilised media at final concentrations of 2, 5 and 10 mM. Growth of *P. denitrificans* at these nitrite concentrations were directly compared to that without nitrite addition using the plate reader technique (methods 2.2). Addition of nitrite has the effect of increasing growth of *P. denitrificans* at the selected range of media pH units 7.0 – 8.5 investigated (figure 3.4). Kinetic parameters were taken from these growth curves and are summarised in table 3.2.

Table 3.2: Stimulation of growth shown by Y_{\max} (AU) for growth of *P. denitrificans* under standard growth conditions at various sodium nitrite concentrations: minimal salts media, supplemented with ammonium chloride, 10 mM; sodium succinate, 30 mM; Vishniac trace element solution.

pH	Y_{\max}^* (AU) with nitrite addition			
	0 mM	2 mM	5 mM	10 mM
7.0	3.364	3.655	3.819	3.992
7.5	3.683	4.870	5.418	5.357
8.0	3.027	3.859	4.269	4.361
8.5	3.234	3.689	3.689	3.559

Y_{\max} (AU) = Maximum optical density produced * Y_{\max} stated as OD_{600nm} corrected to 1 cm pathlength

At pH 7.0, each addition of nitrite creates a consistent, stepwise increase in maximum optical density generated (Y_{\max}) by approximately 0.2 AU. This increases from 3.4 ± 0.1 AU without nitrite present, to 4.0 ± 0.2 AU at the maximum addition of 10 mM nitrite. At pH 7.5 a different growth phenotype is observed. At 2 mM Y_{\max} increases by 1.2 AU from 3.7 ± 0.1 AU to an Y_{\max} of 4.9 ± 0.1 AU, whereas 5 and 10 mM nitrite produce similarly high Y_{\max} of 5.4 ± 0.08 and 5.4 ± 0.2 AU respectively (figure 3.4). The increased Y_{\max} at pH 7.5 is the largest of the four pH values examined and the largest Y_{\max} value generated is 1.1 AU higher than that of the second largest Y_{\max} produced at pH 8.0 (4.4 ± 0.1 AU). This is seen for the Y_{\max} values observed for *P. denitrificans* growth at pH 8.0. When 2 mM nitrite was added to the media, the Y_{\max} increased by 0.9 AU to 3.9 ± 0.06 , compared to growth without nitrite. Subsequently, when 5 mM nitrite was added, there was a further increase of 0.4 AU to an Y_{\max} of 4.3 ± 0.3 AU. No further increase in Y_{\max} was observed at the addition of 10 mM nitrite. Increase in biomass was also seen at pH 8.5, the overall growth reaches a maximum at 2 and 5 mM with Y_{\max} values of 3.7 ± 0.01 and ± 0.1 AU respectively, 0.5 AU greater than pH 8.5 nitrite free media. The Y_{\max} value remained at 3.6 ± 0.1 AU with the addition of 10 mM nitrite. Calculated Y_{\max} values are listed in the appendix. At 2 – 10 mM of nitrite, there is an increase in the growth of *P. denitrificans*, the extent at which progresses at higher nitrite concentrations is explored in media supplemented in the pH range 7.0 – 8.5.

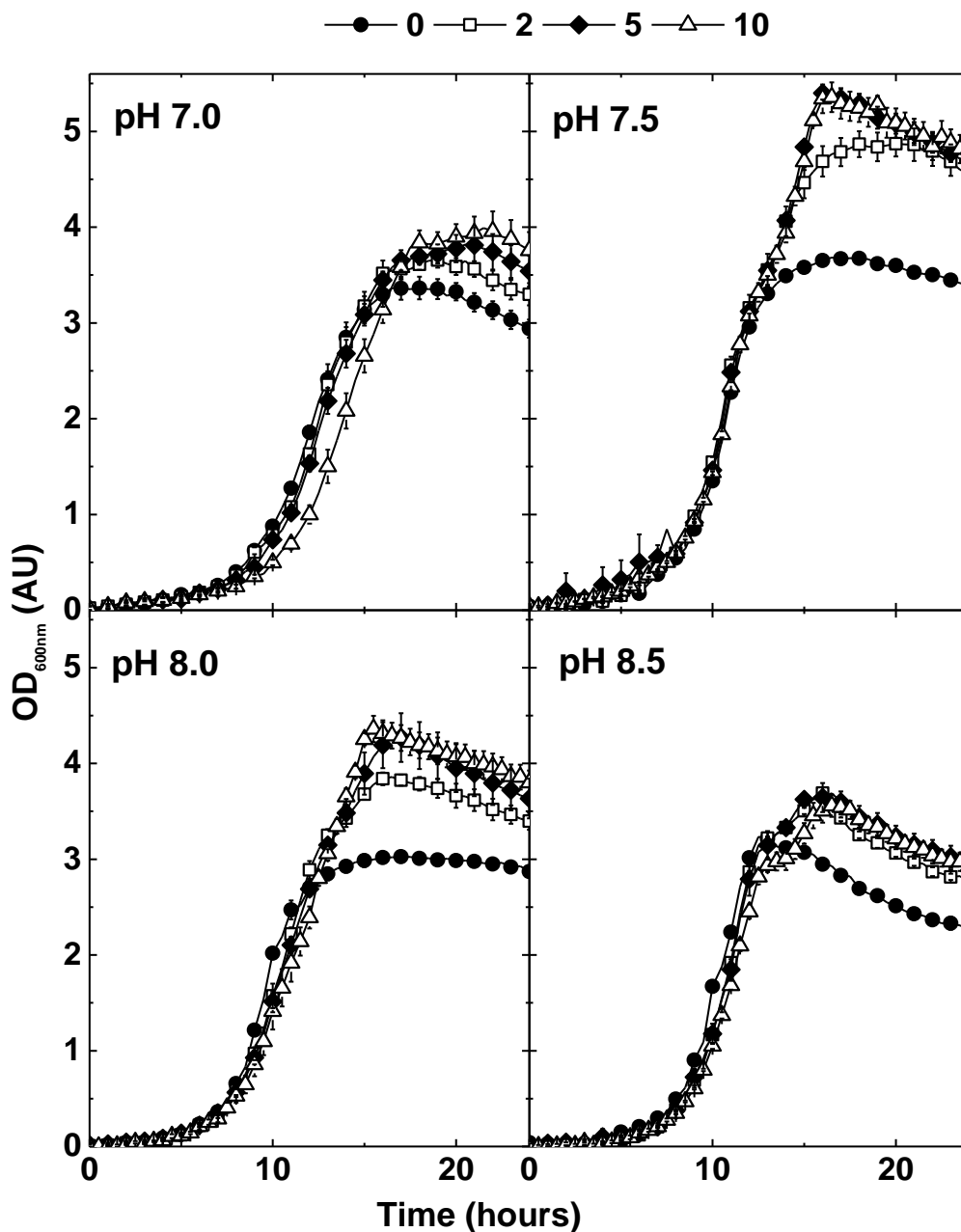


Figure 3.4: Stimulation of growth of *P. denitrificans* in minimal salts media, supplemented with ammonium chloride, 10 mM, sodium succinate, 30 mM and Vishniac trace element solution. Measured by optical density at 600 nm (OD_{600nm}) adjusted to a pathlength of 1 cm against time (h). OD_{600nm} was measured every 0.5 h, 1 h values shown. Cells were grown in 100 μ l total volume with shaking at 400 rpm. Sodium nitrite concentration addition is shown in the key at the top of the figure. Error bars denote standard error $n = \geq 3$.

3.4.3 Growth of *P. denitrificans* at nitrite concentrations above 10 mM

The effect of sodium nitrite on the growth of *P. denitrificans* was investigated at levels of nitrite above 10 mM across the pH range of 7.0 to 8.5. At pH 7.0, the growth of *P. denitrificans* is increased at nitrite concentrations which are between 0 and 10 mM nitrite (figure 3.4). At pH 7.0 with 12 mM nitrite, growth increases to a maximum Y_{\max} measured at pH 7.0 of 4.5 ± 0.003 AU (figure 3.5). The growth of *P. denitrificans* at 20 mM nitrite is reduced but remains at a higher Y_{\max} than that of growth at pH 7.0 without nitrite present. At 25 mM nitrite, growth inhibition is apparent. This can be seen by a greater lag phase extension and reduction in Y_{\max} which is lower than that of the growth of *P. denitrificans* without nitrite present. No growth is observed at 30 mM nitrite media.

A different growth pattern for *P. denitrificans* is observed at growth in media at pH 7.5 (figure 3.6). Growth is observed at higher concentrations than that of pH 7.0 and reaches a higher maximum optical density (Y_{\max}). Lag phase extension is not at an equivalent nitrite concentration to that observed at pH 7.0. The initial increase in Y_{\max} has a maximum of 5.4 ± 0.2 AU at 10 mM nitrite. High Y_{\max} values and a lag phase of compact duration are observed up to a nitrite concentration of 30 mM. However, at nitrite concentrations >30 mM, the lag phase increases substantially and Y_{\max} decreases. As nitrite concentration increases from 40 mM nitrite, there is a continued increase in the lag phase of growth and decrease in Y_{\max} . Notably, this ceases at 55 mM nitrite, where growth is no longer observed. At pH 7.5 *P. denitrificans* is capable of growth at 52.5 mM, which is higher than that of pH 7.0.

Growth of *P. denitrificans* in media at pH 8.0 is shown in figure 3.7. Growth occurs up to 105 mM nitrite, at which point growth is inhibited. Growth of *P. denitrificans* is possible at a higher nitrite concentration in pH 8.0 media, than that of pH 7.5 and pH 7.0. Increase in the growth of *P. denitrificans* is apparent and occurs at concentrations >80 mM nitrite addition. This is less than that observed at pH 7.5 and reaches a maximum Y_{\max} of 4.9 ± 0.1 AU 20 mM nitrite. However, growth at the nitrite concentrations 0 mM and 20 mM show lag phase which is similar as growth increases. At concentrations >20 mM, lag phase steadily increases while Y_{\max} decreases. This decrease remains above that of *P. denitrificans* growth at pH 8.0 without nitrite until 70 mM nitrite. Growth steady decreases and lag phase extends until growth inhibition is achieved at 110 mM for pH 8.0.

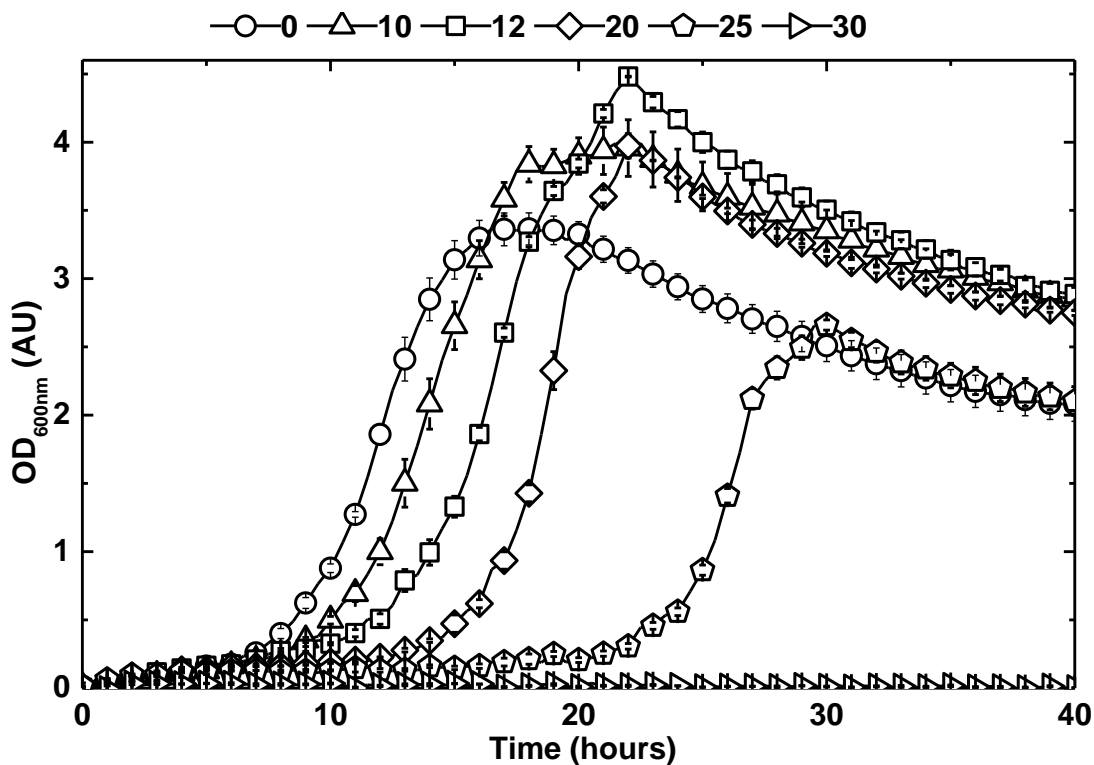


Figure 3.5: Growth of *P. denitrificans* in minimal salts media, pH 7.0, supplemented with ammonium chloride, 10 mM, sodium succinate, 30 mM and Vishniac trace element solution, with various sodium nitrite concentrations (mM) as shown in the key at the top of the figure. Measured by optical density at 600 nm (OD_{600nm}) adjusted to a pathlength of 1 cm against time (h). Cells were grown in 100 μ l total volume with shaking at 400 rpm. OD_{600nm} was measured every 0.5 h, 1 h values shown. Error bars denote standard error $n = \geq 3$.

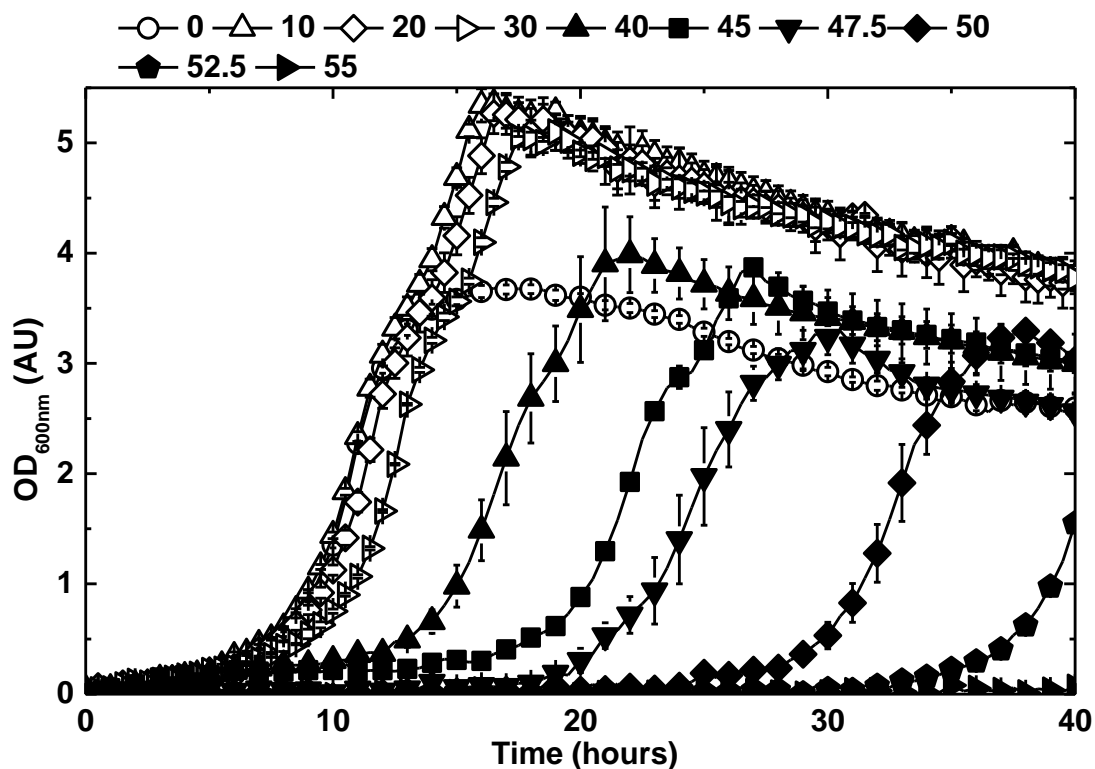


Figure 3.6: Growth of *P. denitrificans* in minimal salts media, pH 7.5, supplemented with ammonium chloride, 10 mM, sodium succinate, 30 mM and Vishniac trace element solution, with various sodium nitrite concentrations (mM) as shown in the key above the figure. Measured by optical density at 600 nm (OD_{600nm}) adjusted to a pathlength of 1 cm against time (h). Cells were grown in 100 μ l total volume with shaking at 400 rpm. OD_{600nm} was measured every 0.5 h, 1 h values shown. Error bars denote standard error $n = \geq 3$.

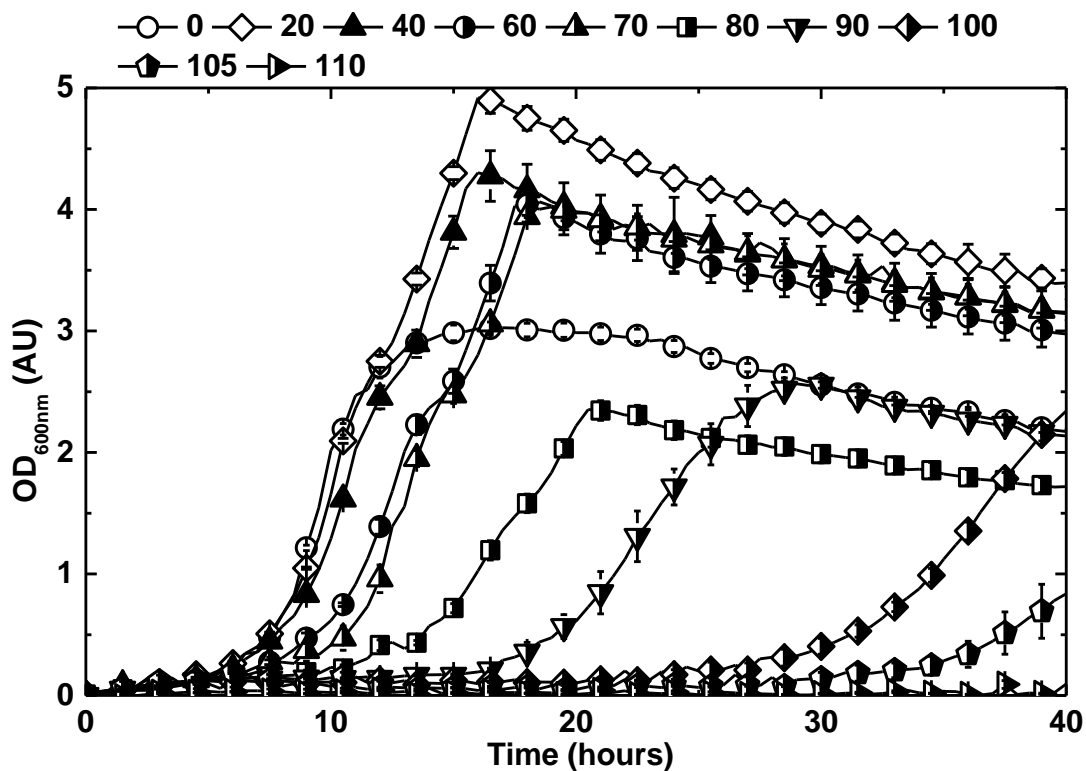


Figure 3.7: Growth of *P. denitrificans* in minimal salts media, pH 8.0, supplemented with ammonium chloride, 10 mM, sodium succinate, 30 mM and Vishniac trace element solution, with various sodium nitrite concentrations (mM) as shown in the key above the figure. Measured by optical density at 600 nm (OD_{600nm}) adjusted to a pathlength of 1 cm against time (h). Cells were grown in 100 μ l total volume with shaking at 400 rpm. OD_{600nm} was measured every 0.5 h, 1 h values shown. Error bars denote standard error $n = \geq 3$.

At the most alkaline pH 8.5, growth and Y_{\max} is less than that observed at pH 7.0, 7.5 and 8.0. The growth of *P. denitrificans* results in an Y_{\max} of 3.7 ± 0.08 . The growth remains in excess of that observed at pH 8.5 without nitrite addition for concentrations <110 mM. Over this range of nitrite concentration, lag continually extends and growth decreases. At concentrations of nitrite <100 mM, lag phase extension increases and growth decreases to a lesser extent. At pH 8.5, growth is less than that of more acid pH values 7.0 – 8.0 and the presence of nitrite does not inhibit the growth of *P. denitrificans* until the concentration of 145 mM nitrite (figure 3.8).

The three fold effect on the growth of *P. denitrificans* is summarised in figure 3.9. This figure highlights the three distinct aspects of growth characteristics in the presence of nitrite at the pH range of 7.0 – 8.5. Firstly, it is observed that nitrite has a direct impact on the growth of *P. denitrificans*; initially causing a stimulation of growth characterised by an increase in growth and the maximum yield of growth (Y_{\max}). The nitrite level reaches a concentration at which it is no longer exhibiting a stimulatory effect and appears to inhibit the growth of *P. denitrificans*. This culminates in a concentration at which nitrite inhibits growth entirely. Secondly, this nitrite effect is pH dependent. Nitrite toxicity is reduced by the increase in alkalinity of the growth media. This leads to a higher nitrite concentration requirement for inhibition of growth at a higher pH value. Finally, there is pH dependence for the growth of *P. denitrificans*. Growth maintains its highest growth and highest Y_{\max} at pH 7.5. High levels of growth are also achieved at pH 8.0. Growth is noticeably reduced at the acidic pH 7.0 and is least effective at the most alkaline pH 8.5. This provides an additional pH dependent effect to be considered. To examine the multiple aspects of the pH and nitrite effects, kinetic data was extracted and directly compared.

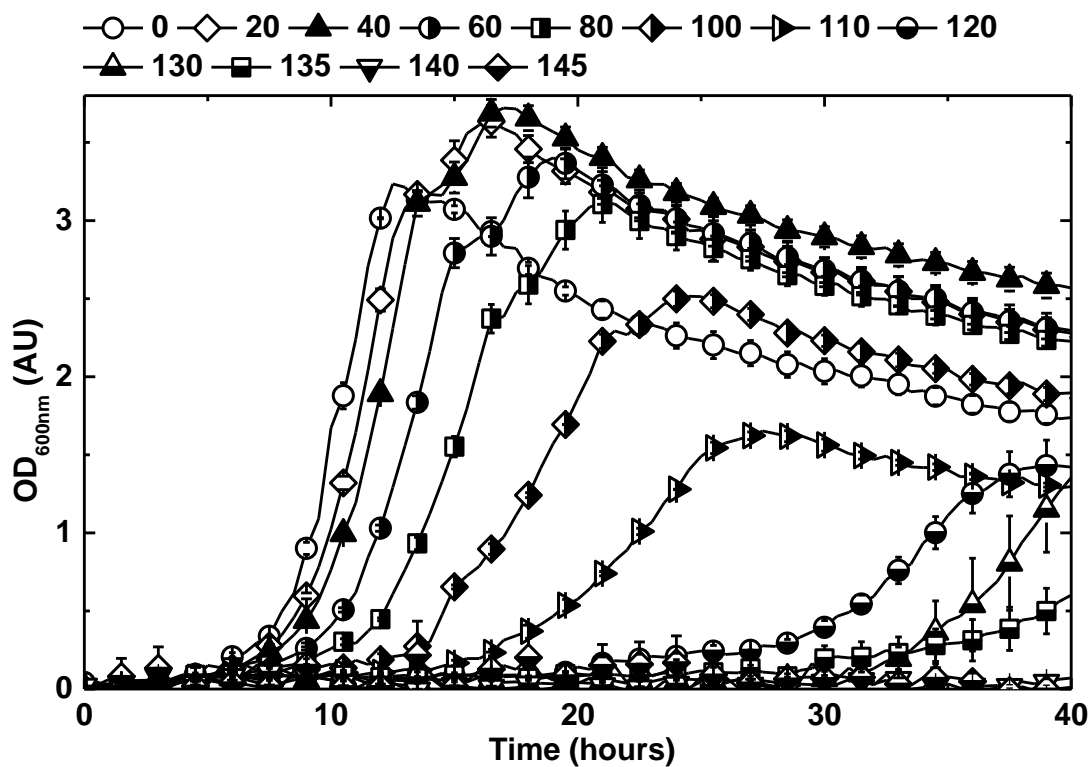


Figure 3.8: Growth of *P. denitrificans* in minimal salts media, pH 8.5, supplemented with ammonium chloride, 10 mM, sodium succinate, 30 mM and Vishniac trace element solution, with various sodium nitrite concentrations (mM) as shown in the key above the figure. Measured by optical density at 600 nm (OD_{600nm}) adjusted to a pathlength of 1 cm against time (h). Cells were grown in 100 μ l total volume with shaking at 400 rpm. OD_{600nm} was measured every 0.5 h, 1 h values shown. Error bars denote standard error $n = \geq 3$.

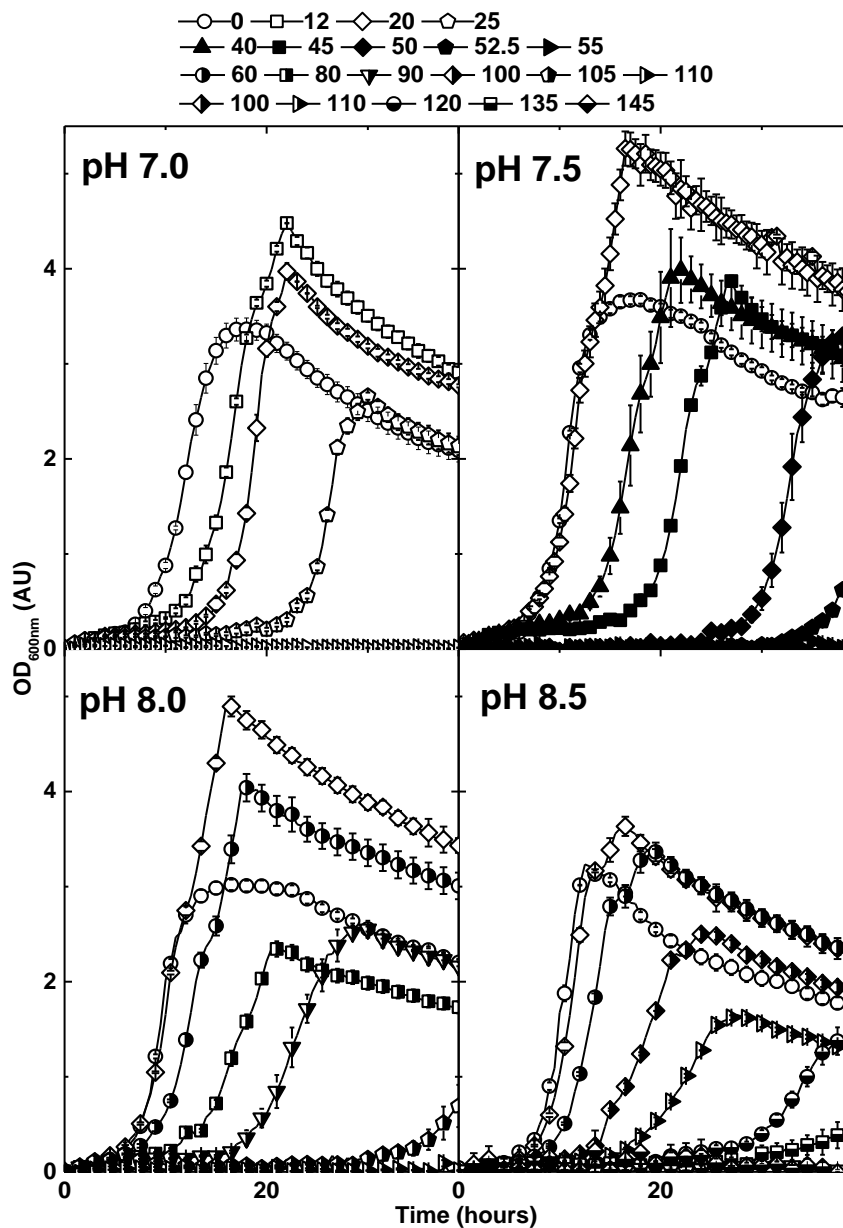


Figure 3.9: Summarised growth of *P. denitrificans* in minimal salts media, pH 7.0, 7.5, 8.0 and 8.5, supplemented with ammonium chloride, 10 mM, sodium succinate, 30 mM and Vishniac trace element solution, with various sodium nitrite concentrations (mM) as shown in the key above the figure. Measured by optical density at 600 nm (OD_{600nm}) adjusted to a pathlength of 1 cm against time (h). Cells were grown in 100 μ l total volume with shaking at 400 rpm. OD_{600nm} was measured every 0.5 h, 1 h values shown. Error bars denote standard error $n = \geq 3$.

3.4.4 Growth kinetics of *P. denitrificans* in the presence of nitrite and over a pH range of 7.0 – 8.5

From the growth curves obtained in the results, the maximum growth yield (Y_{\max} AU) was extracted to quantify the yield of growth under each growth conditions. To examine the growth rate, a gradient of linearized growth was taken from a semi log plot to provide the apparent maximum specific growth rate (μ_{app} h^{-1}) as described in methods. Values are presented in the appendix. In figure 3.10 the nitrite effect on growth can be clearly observed. At each pH value, there is an initial increase in Y_{\max} as growth is stimulated, this gradually descends and culminates in a distinctly sharp zero point at which nitrite concentration becomes inhibitory to growth. The pH dependence of the nitrite effect can be clearly observed. The cut off increases from 30 to 55, 110 and finally 140 mM for pH 7.0, 7.5, 8.0 and 8.5 respectively. This shows that the inhibitory nitrite concentration initially doubles with each 0.5 pH unit increase. This reduces to a 30% increase in nitrite concentration between pH 8.0 and 8.5. The initial stimulation of growth seen in the Y_{\max} of *P. denitrificans* in the presence of nitrite is not reflected in the apparent maximum specific growth rate (μ_{app} h^{-1}), which is derived from the same growth curve data figure 3.11 At pH 7.0 without nitrite present, the μ_{app} is 0.40 ± 0.01 h^{-1} . At 2 mM and 5 mM nitrite μ_{app} remains stable with 0.37 ± 0.06 0.36 ± 0.06 h^{-1} . A reduction trend is also seen at pH 7.5 – 8.5. The nitrite specific effect previously observed causes a general downwards trend in μ_{app} . This shows a reduction in the rate of exponential growth phase for *P. denitrificans* as a function of nitrite concentration increase and culminates in the complete inhibition of growth at the same, pH dependent concentrations of nitrite for as that observed for Y_{\max} .

It is also noted that the μ_{app} values suggest unique pH dependence to that observed for the Y_{\max} values. There is twofold pH dependence; firstly the trend of a higher Y_{\max} at pH 7.5, which decreases in both raised and lowered pH, and secondly a trend of higher μ_{app} at pH 8.5, which decreases with lowered pH. The highest μ_{app} values are generated at pH 8.5, the most alkaline pH examined. Growth at pH 8.5 reaches an μ_{app} value of 0.51 ± 0.02 h^{-1} at 2 mM nitrite addition and this rate of growth is maintained until a concentration of 30 mM nitrite. As nitrite concentration increases from this point there is the observed continued reduction in μ_{app} . At pH 8.0, μ_{app} is highest without nitrite present at 0.51 ± 0.008 h^{-1} , similar to that seen at pH 8.5. At pH 7.5, this reduces, with the maximum μ_{app} achieved at this pH occurring with 2 mM nitrite present and reaching 0.46 ± 0.008 h^{-1} . This reduces further at pH 7.0. Maximum μ_{app} occurs without nitrite present 0.40 ± 0.01 h^{-1} .

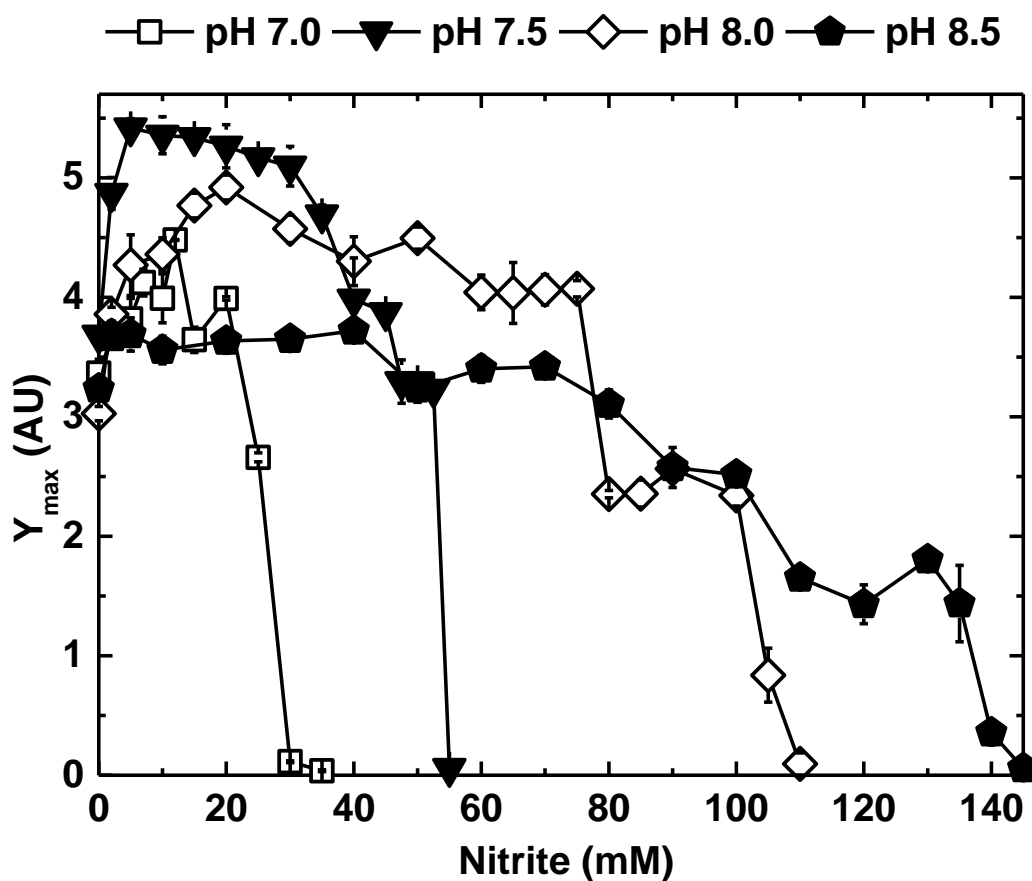


Figure 3.10: Summarised maximum optical density produced (Y_{\max} AU) over the pH range 7.0 – 8.5 as shown in the key above the figure for the growth of *P. denitrificans* in minimal salts media, pH 7.0, 7.5, 8.0 and 8.5, supplemented with ammonium chloride, 10 mM, sodium succinate, 30 mM and Vishniac trace element solution. Measured by optical density at 600 nm ($OD_{600\text{nm}}$) adjusted to a pathlength of 1 cm against time (h). Error bars denote standard error $n = \geq 3$.

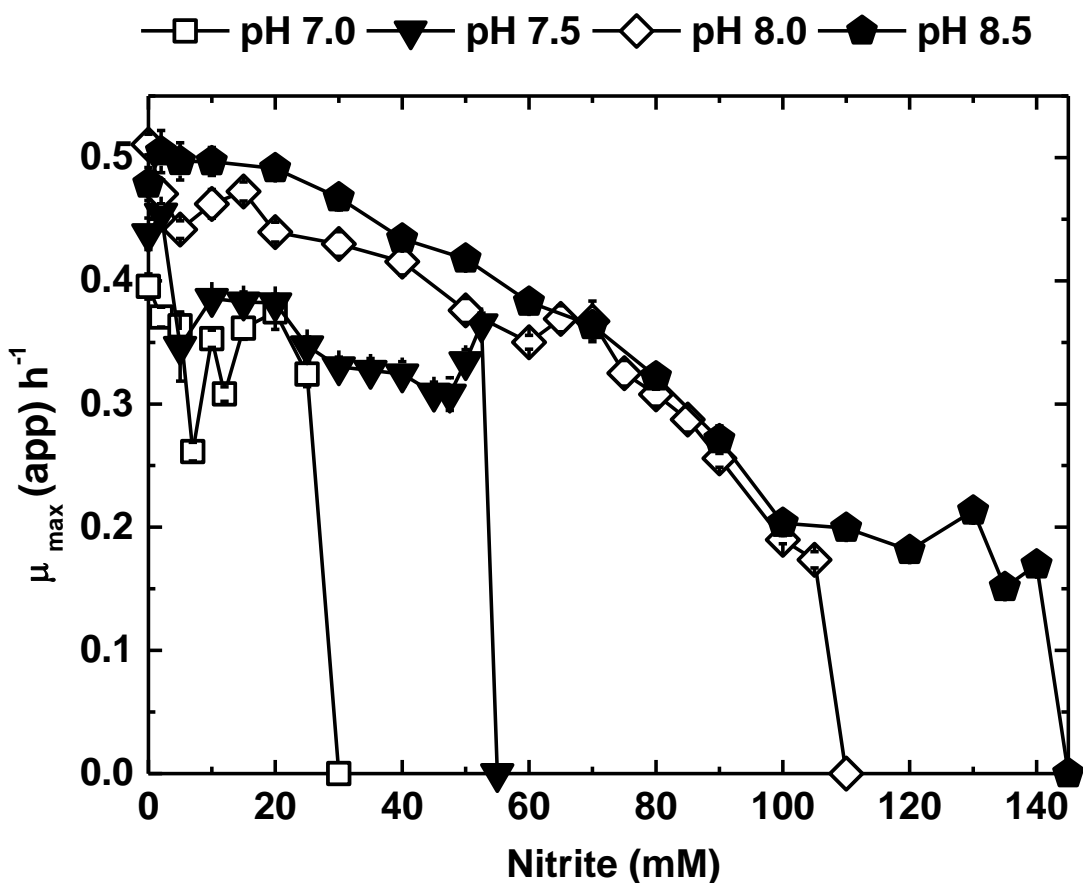


Figure 3.11: Summarised apparent growth constant (μ_{app}) over a pH range of 7.0 – 8.5 as shown in the key above the figure for the growth of *P. denitrificans* in minimal salts media, pH 7.0, 7.5, 8.0 and 8.5, supplemented with ammonium chloride, 10 mM, sodium succinate, 30 mM and Vishniac trace element solution. Measured by optical density at 600 nm (OD_{600nm}) adjusted to a pathlength of 1 cm against time (h). Error bars denote standard error $n = \geq 3$.

It is apparent that there is increasing inhibition of *P. denitrificans* growth linked to high concentrations of sodium nitrite present in media. In addition, a two-fold pH-specific effect is also observed. Firstly, the growth phenotype of *P. denitrificans* in the absence or with nitrite addition is pH dependent and, secondly, high pH causes an increase in the nitrite concentration required for inhibition of growth. In figure 3.10 and figure 3.11 it can be seen that pH and nitrite have a close relationship between pH and nitrite has a defining role on the effect of nitrite. Nitrite can be protonated to form free nitrous acid (FNA). One way to investigate this is to calculate the proportion of FNA present at the known concentrations of nitrite and pH of media solution.

3.5 Discussion

3.5.1 The influence of pH and effect of nitrite on the growth of *P. denitrificans*

The extracellular proton concentration or pH value has an impact on the growth of *P. denitrificans* and on the inhibitory growth effects of nitrite. Initially revealing a pH optimal for *P. denitrificans* and further exhibiting a vast role in the effect of nitrite. Initially, it is apparent that there are pH optima for the growth of *P. denitrificans*. This optimisation between pH 7.5, in which growth is at the maximal value (Y_{\max}) and pH 8.0, which shows a higher doubling rate as seen by the μ_{app} value, as detailed in figure 3.3. The pH 7.0 – 8.5 provided the pH range for exploration of nitrite effect and reduced the pH growth effect seen at acidic pH 6.5 and alkaline pH 9.0. A suggested pH range of optimal growth would be pH 7.5 – 8.0, with pH 7.5 being optimal in these conditions for growth and pH 8.0 generating a more efficient exponential growth rate.

Growth of *P. denitrificans* is pH dependent with an optimum of growth being the optimum pH for growth was observed to be pH 7.5 and secondly pH 8.0. Media more acid or more alkali saw a reduction in the Y_{\max} achieved by *P. denitrificans*. Acidic media had a more detrimental effect on growth reduction that that of alkali media, suggesting *P. denitrificans* is more tolerant to conditions which tend to alkalinity than acidity. A 0.5 pH unit increase (0.31 M H^+ difference) in acidity from optimum pH 7.5 to pH 7.0 shows a slightly reduced apparent exponential growth rate. This alludes to a reduction in cell division in an acidified environment, with a reduced use of media nutrients to achieve final Y_{\max} at stationary phase

of growth. The ability for an organism to survive in extreme acidity depends upon its evolved survival mechanism to maintain homeostasis within the cytoplasmic environment. An example of an acid-tolerant bacterium is *Helicobacter pylori*, a pathogen capable of existence in the human stomach track can tolerate a pH of 1.0 (0.1 M H⁺) for a limited period of time by maintaining urease activity within the cytoplasm to generate export of ammonium ions, providing a buffering zone to counter balance the acidity of the external environment (Stingl *et al.*, 2002). It is apparent that *P. denitrificans* tends to grow optimally in the pH range of 7.5 – 8.0. Other bacteria that specialise in environments which tend to alkalinity, such as areas in which alkaline minerals are generated by black smokers, do so by maintaining a neutral cytoplasmic pH level. Maintaining this homeostasis requires the net import of positively charged ions through ion specific Na⁺ (K⁺ or Ca⁺) / H⁺ electrogenic antiporters (Lee *et al.*, 2013). This exchanges a large inflow of H⁺ for a relatively lower outflow of Na⁺ leading to an acidification of internal cellular environment. The antiporters of *P. denitrificans* and its method of alkaline tolerance are not well documented.

3.5.2 The role of free nitrous acid in nitrite toxicity

The observed toxic effect shown at each pH value used in the experiment shows that the concentration at which nitrite causes a toxic effect and inhibits growth relates to the pH of the external environment. Inhibition of growth occurs at 30 mM sodium nitrite at pH 7.0, 55 mM sodium nitrite at pH 7.5, 110 mM sodium nitrite at pH 8.0 and 145 mM sodium nitrite at pH 8.5. It has been widely shown that nitrite toxicity is closely modulated by pH (Van Verseveld *et al.*, 1977; Rake and Eagon, 1980). The pH dependence of nitrite toxicity of aerobic growth of the denitrifying bacterium *P. denitrificans* suggests protonation of nitrite to form free nitrous acid (FNA) as a likely route of nitrite import. This transport of protons associated with FNA has been suggested to act as an uncoupler in previous work (Zhou *et al.*, 2011; Wang *et al.*, 2013). The influx of protons generated by the diffusion of FNA has been suggested to uncouple respiration by reducing the membrane potential thus uncoupling and “short circuiting” the oxidative phosphorylation respiration pathway of *P. denitrificans*, which would be of considerable hindrance to the bacterium in the aerobic conditions explored here.

Once protonated, nitrite can diffuse freely as a small nonpolar molecule. Once inside the cell FNA can undertake a variety of chemical reactions and generate reactive nitrogenous species

as a product. FNA is able to decompose forming reactive molecules such as nitric oxide (NO); a cytotoxic nitrogen species. The nonpolar FNA diffuses across the bacterial cell membrane following a gradient of high to low concentration. Here, decomposition of FNA to NO and other cytotoxic reactive nitrogen species (RNS) occurs and in combination with other reactive oxygen species (ROS) from aerobic growth conditions is linked to inhibition of growth in microorganisms, disruption of biofilm attachment and cell death. This research has led to the recent exploration of nitrite as an antimicrobial agent and disrupter biofilms (Jiang *et al.*, 2011; Webb *et al.*, 2003) and increased interest in the nature of nitrite and its protonated form, free nitrous acid. The biocidal effect of FNA has been observed with regards to wastewater treatment where levels of FNA inhibiting these mixed microorganism communities growth both anaerobically and aerobically (Vadivelu *et al.*, 2006b; Vadivelu *et al.*, 2006a; Vadivelu *et al.*, 2007). Other potential reactive species generated inside the cytoplasm of bacterial cells may include nitrogen dioxide (NO₂), peroxyxynitrite (ONOO⁻), hydroxide ion (OH⁻) and hydrogen peroxide (H₂O₂) (Wiseman and Halliwell, 1996; Marnett, 2000). FNA has also been documented to sit in equilibrium with nitrite and the nitrosonium ion which is represented as NOOH and associated intermediates which are isoforms of FNA. Nitrite and FNA also sits in equilibrium with dinitrogen trioxide; $FNA \leftrightarrow H^+ + NO_2^-$, $FNA \leftrightarrow NOOH$, $NO_2^- + FNA \leftrightarrow N_2O_3$ (Lammel and Cape, 1996; Vadivelu *et al.*, 2006b; Park and Lee, 1988).

One molecule likely accountable for inhibition of *P. denitrificans* growth is nitric oxide (NO) generated in the cytoplasmic space once internalised in the form of FNA, via a decomposition reaction from nitrogen dioxide (NO₂); $N_2O_3 \rightarrow NO_2 + NO$. Additional reactions generate additional nitrogenous molecules including the dimerization of NO₂ to form dinitrogen tetroxide (N₂O₄), dinitrogen trioxide (N₂O₃), S-nitrosothiols and subsequently a return to formation of nitrite and nitrate and generation of oxygen derivatives, such as peroxyxynitrite ONOO⁻. Nitric oxide and its effect on cellular function has been well characterised in mammalian cells. Its production is largely associated with a host immune response from host macrophage cells causing expression of an inducible NO synthase and generating NO (Paulsen *et al.*, 2002; Gill *et al.*, 2005; Tunbridge *et al.*, 2006). But in addition, NO is a cytotoxic at concentrations lower than 100 nM and is capable of inactivating [4Fe-4S] containing hydratases (Li *et al.*, 2008).

The observed pH effect was further examined by investigation of potential pH dependent nitrogenous species production, namely the protonation of nitrite to form the charge free

compound free nitrous acid (FNA). The concentration of this compound cannot be measured directly. Determining the amount of probable FNA present in solution at a known pH and with a known concentration of nitrite, can be predicted using an adaption of the Henderson-Hasselbalch equation. The Henderson-Hasselbalch describes pH as a measure of the acid dissociation constant (pK_a). The Henderson-Hasselbalch equation is a rearranged form of the acid dissociation constant according to the law of dissociation: $K_a = ([H^+] [NO_2^-] / [FNA])$ to form $pH = pK_a + \log_{10} ([NO_2^-] / [FNA])$. (This requires the substitution of the logarithmic measure of the acid constant: $pK_a = -\log_{10} K_a$ and the pH equation: $pH = -\log [H^+]$.) The derivation of the Henderson-Hasselbalch equation is detailed in the methods. From the Henderson-Hasselbalch equation, a rearrangement allows an estimation of FNA levels when nitrite concentration and pH are known:

$$pH - pK_a = \log_{10} ([NO_2^-] / [FNA])$$

$$10^{(pH-pK_a)} = ([NO_2^-] / [FNA])$$

$$[FNA] \cdot 10^{(pH-pK_a)} = [NO_2^-]$$

$$[FNA] = [NO_2^-] / 10^{(pH-pK_a)}$$

The pK_a for FNA / nitrite was determined experimentally by da Silva (2006) using UV/visible absorbance spectra of both the nitrite and nitrous ion generated by stopped-flow spectrophotometry. This value was confirmed by theoretical calculation of the aqueous free energy of FNA / nitrite. This equation was used to estimate the levels of FNA which may be present in equilibrium with the nitrite additions and are shown in the appendix. The possible calculated concentration of FNA, inhibitory to the growth of *P. denitrificans* was determined was $2.8 \pm 0.45 \mu\text{M}$ ($n = 26$). This value was derived from the average calculated FNA concentrations at the inhibitory nitrite concentration and the starting media pH.

3.5.3 Dual stimulatory and inhibitory role of nitrite

Nitrite appears to produce two opposing effects of the growth of *P. denitrificans*: at low concentration nitrite stimulates the growth as measured by $OD_{600\text{nm}}$ at all pH values, while not affecting the lag or exponential rate of growth. This effect may be due to the direct uptake of extracellular nitrite or by an increase respiration and ATP synthesis. Nitrite uptake is possible by two routes: firstly by the assimilatory pathway in which nitrite is actively

imported into the cell, converted to ammonia and incorporated into cellular material such as protein and DNA (NAS) (Sears *et al.*, 1997). Secondly by partial anaerobicity at levels of high cell density leading to denitrification during the late exponential stage of growth (Richardson, 2000).

In order exhibit a stimulatory effect on the growth of *P. denitrificans*, it is likely that nitrite must be internalised. Nitrite exists as both free nitrite and free nitrous acid (FNA), the protonated form of nitrite. FNA can diffuse across the phospholipid bilayer and dissociate to nitrite and a proton in the cytoplasm (Goddard *et al.*, 2008). This may provide a passive transport method to internalisation of nitrite which is explored in the next section. NasH and NarK2 the nitrate/H⁺ importer and nitrate / nitrite antiporter respectively are postulated to be involved in the import of nitrite in collaboration with NasA. Once in the cytoplasm, nitrite could undergo conversion to ammonium by NasB using electrons from NADH: $\text{NO}_2^- + 8\text{H}^+ + 6\text{e}^- \rightarrow \text{NH}_4^+ + 2\text{H}_2\text{O}$ (Gates *et al.*, 2011). Ammonium is incorporated in cellular material such as DNA and amino acids via the glutamine synthase (GS) and glutamate synthase (GOGAT) and further secondary transfer reactions (Kremeckova *et al.*, 1992; Ogawa *et al.*, 1995). This incorporation into cellular material is in the form of nitrogenous compounds by assimilation, or by the anaerobic respiration of nitrite to dinitrogen could explain the increased Y_{max} seen at these low levels of nitrite.

It has been observed that 1.0 mM nitrite is an optimum concentration of nitrite to support active transport of carbohydrates and amino acids, while concentrations higher than this inhibited active transport in *Pseudomonas aeruginosa* (Rowe *et al.*, 1979; Williams *et al.*, 1978). The increased growth seen in *P. denitrificans* may therefore contribute to the uptake of sodium succinate uptake in and increase metabolism at <10 mM nitrite levels. Hormesis is a known phenomenon in which low doses of a toxic compound can have a reversed effect to the inhibitory or toxic effects that would be expected. It has been used to describe an unusually favourable reaction to low doses of toxin or stress. This occurrence has been documented in *Mycobacterium tuberculosis* (Brugmann and Firmani, 2005) in response to nitrite and nitric oxide dosing (Ristow and Zarse, 2010) and has been suggested as an important evolutionarily adaptive strategy in dose-response relationships (Calabrese and Baldwin, 2001).

1	Alkaline pH		growth
	Optima pH 7.5 / 8.0		growth
	Acidic pH		growth
2	Low nitrite		biomass
3	High nitrite		growth

Figure 3.12: Summary of pH dependent and independent effects linked to the growth of *P. denitrificans* and the effects of nitrite.

It is now known that nitrite has a direct inhibitory effect on the growth of denitrifying bacteria (Van Verseveld *et al.*, 1977; Rake and Eagon, 1980). Studies have been carried out in *P. denitrificans* exploring the effect of nitrite on oxidase activity (Kucera *et al.*, 1986). Many studies have been performed on the organism under aerobic growth conditions *P. aeruginosa* and have found direct inhibition of active transport, respiration and oxidative phosphorylation by nitrite, which was linked to a direct interaction with the terminal oxidase as being the key component in this biocidal effect (Rowe *et al.*, 1979; Yang, 1985). This inhibition has been attributed to the oxidation of electron carriers containing ferrous iron. *P. aeruginosa* shares the respiratory ability of *P. denitrificans* to use both oxygen and nitrogenous oxides as a terminal electron acceptor for respiration. It was also seen that nitrite at >10 mM levels prevented the formation of ATP and generated a rapid depletion of intracellular ATP levels in *P. aeruginosa* (Rowe *et al.*, 1979).

It has been seen in this work that at low levels of nitrite, nitrite acts as a stimulatory compound for the growth of *P. denitrificans*. There is a point at which this stimulatory effect becomes inhibitory at higher nitrite concentrations. The point at which growth stimulation occurs shows no distinct pH dependence and may be due to the a stimulated uptake of active transport of carbohydrate and amino acids, or by the direct transport of nitrite into the cell body where it can then be incorporated directly into cellular material. At high levels of nitrite, pH dependence becomes more apparent. The inhibitory effect of nitrite is likely due to a number of factors largely due to the interaction of ferrous proteins and the nitrite compound causing prevention of oxidase function, ineffective ATP production and limited oxygen uptake. Both the pH and nitrite effects have led to a complex network of factors effecting growth, which are summarised in figure 3.12.

To further explore the possible internalisation of FNA and subsequent generation of nitrogenous species, transcriptional analysis was carried out to investigate the presence of detoxifying genes under nitrite induced stress using bioinformatic analysis and Real-Time Quantitative Reverse Transcription PCR.

3.6 References

- ALMEIDA, J. S., REIS, M. A. M. & CARRONDO, M. J. T. 1995. Competition between nitrate and nitrite reduction in denitrification by *Pseudomonas fluorescens*. *Biotechnology and Bioengineering*, 46, 476-484.

- ANTHONISEN, A. C., LOEHR, R. C., PRAKASAM, T. B. S. & SRINATH, E. G. 1976. Inhibition of nitrification by ammonia and nitrous acid. *Journal of the Water Pollution Control Federation*, 48, 835-852.
- BÅÅTH, E. & ANDERSON, T. H. 2003. Comparison of soil fungal/bacterial ratios in a pH gradient using physiological and PLFA-based techniques. *Soil Biology and Biochemistry*, 35, 955-963.
- BRUGMANN, W. B. & FIRMANI, M. A. 2005. Low concentrations of nitric oxide exert a hormetic effect on *Mycobacterium tuberculosis* in vitro. *Journal of Clinical Microbiology*, 43, 4844-6.
- CALABRESE, E. J. & BALDWIN, L. A. 2001. The frequency of U-shaped dose responses in the toxicological literature. *Toxicological Sciences*, 62, 330-8.
- DA SILVA, G., KENNEDY, E. M. & DLUGOGORSKI, B. Z. 2006. Ab Initio Procedure for Aqueous-Phase pKa Calculation: The Acidity of Nitrous Acid. *The Journal of Physical Chemistry*, 110, 11371-11376.
- DRABLØS, F., FEYZI, E., AAS, P. A., VAAGBØ, C. B., KAVLI, B., BRATLIE, M. S., PEÑA-DIAZ, J., OTTERLEI, M., SLUPPHAUG, G. & KROKAN, H. E. 2004. Alkylation damage in DNA and RNA - Repair mechanisms and medical significance. *DNA Repair*, 3, 1389-1407.
- FERNÁNDEZ-CALVIÑO, D. & BÅÅTH, E. 2010. Growth response of the bacterial community to pH in soils differing in pH. *FEMS Microbiology Ecology*, 73, 149-156.
- FINLAYSON-PITTS, B. J., WINGEN, L. M., SUMNER, A. L., SYOMIN, D. & RAMAZAN, K. A. 2003. The heterogeneous hydrolysis of NO₂ in laboratory systems and in outdoor and indoor atmospheres: An integrated mechanism. *Physical Chemistry Chemical Physics*, 5, 223-242.
- FUX, C., LANGE, K., FAESSLER, A., HUBER, P., GRUENIGER, B. & SIEGRIST, H. 2003. Nitrogen removal from digester supernatant via nitrite-SBR or SHARON? *Water Science and Technology*, 48, 9-18.
- GATES, A. J., LUQUE-ALMAGRO, V. M., GODDARD, A. D., FERGUSON, S. J., ROLDÁN, M. D. & RICHARDSON, D. J. 2011. A composite biochemical system for bacterial nitrate and nitrite assimilation as exemplified by *Paracoccus denitrificans*. *Biochemical Journal*, 435, 743-753.
- GILL, S. R., FOUTS, D. E., ARCHER, G. L., MONGODIN, E. F., DEBOY, R. T., RAVEL, J., PAULSEN, I. T., KOLONAY, J. F., BRINKAC, L., BEANAN, M., DODSON,

- R. J., DAUGHERTY, S. C., MADUPU, R., ANGIUOLI, S. V., DURKIN, A. S., HAFT, D. H., VAMATHEVAN, J., KHOURI, H., UTTERBACK, T., LEE, C., DIMITROV, G., JIANG, L., QIN, H., WEIDMAN, J., TRAN, K., KANG, K., HANCE, I. R., NELSON, K. E. & FRASER, C. M. 2005. Insights on evolution of virulence and resistance from the complete genome analysis of an early methicillin-resistant *Staphylococcus aureus* strain and a biofilm-producing methicillin-resistant *Staphylococcus epidermidis* strain. *Journal of Bacteriology*, 187, 2426-38.
- GODDARD, A. D., MOIR, J. W., RICHARDSON, D. J. & FERGUSON, S. J. 2008. Interdependence of two NarK domains in a fused nitrate/nitrite transporter. *Molecular Microbiology*, 70, 667-681.
- JIANG, G., GUTIERREZ, O. & YUAN, Z. 2011. The strong biocidal effect of free nitrous acid on anaerobic sewer biofilms. *Water Research*, 45, 3735-3743.
- KREMECKOVA, H., SVRCULA, B. & MIKES, V. 1992. Purification and some properties of glutamate dehydrogenase and glutamine synthetase from *Paracoccus denitrificans*. *Journal of General Microbiology*, 138, 1587-1591.
- KUCERA, I., KOZÁK, L. & DADÁK, V. 1986. The inhibitory effect of nitrite on the oxidase activity of cells of *Paracoccus denitrificans*. *FEBS Letters*, 205, 333-336.
- LAMMEL, G. & CAPE, J. N. 1996. Nitrous acid and nitrite in the atmosphere. *Chemical Society Reviews*, 25, 361-369.
- LAUBER, C. L., HAMADY, M., KNIGHT, R. & FIERER, N. 2009. Pyrosequencing-based assessment of soil pH as a predictor of soil bacterial community structure at the continental scale. *Applied and Environmental Microbiology*, 75, 5111-5120.
- LEE, C., KANG, H. J., VON BALLMOOS, C., NEWSTEAD, S., UZDAVINYS, P., DOTSON, D. L., IWATA, S., BECKSTEIN, O., CAMERON, A. D. & DREW, D. 2013. A two-domain elevator mechanism for sodium/proton antiport. *Nature*, 501, 573-7.
- LI, B. R., ANDERSON, J. L. R., MOWAT, C. G., MILES, C. S., REID, G. A. & CHAPMAN, S. K. 2008. *Rhodobacter sphaeroides* haem protein: A novel cytochrome with nitric oxide dioxygenase activity. *Biochemical Society Transactions*, 36, 992-995.
- MARNETT, L. J. 2000. Oxyradicals and DNA damage. *Carcinogenesis*, 21, 361-370.
- MEIJER, E. M., VAN DER ZWAAN, J. W. & STOUTHAMER, A. H. 1979. Location of the proton-consuming site in nitrite reduction and stoichiometries for proton

- pumping in anaerobically grown *Paracoccus denitrificans*. *FEMS Microbiology Letters*, 5, 369-372.
- MOIR, J. W. B. & WOOD, N. J. 2001. Nitrate and nitrite transport in bacteria. *Cellular and Molecular Life Sciences*, 58, 215-224.
- OGAWA, K. I., AKAGAWA, E., YAMANE, K., SUN, Z. W., LACELLE, M., ZUBER, P. & NAKANO, M. M. 1995. The *nasB* operon and *nasA* gene are required for nitrate/nitrite assimilation in *Bacillus subtilis*. *Journal of Bacteriology*, 177, 1409-1413.
- PARK, J. Y. & LEE, Y. N. 1988. Solubility and decomposition kinetics of nitrous acid in aqueous solution. *Journal of Physical Chemistry*, 92, 6294-6302.
- PAULSEN, I. T., SESHADRI, R., NELSON, K. E., EISEN, J. A., HEIDELBERG, J. F., READ, T. D., DODSON, R. J., UMayAM, L., BRINKAC, L. M., BEANAN, M. J., DAUGHERTY, S. C., DEBOY, R. T., DURKIN, A. S., KOLONAY, J. F., MADUPU, R., NELSON, W. C., AYODEJI, B., KRAUL, M., SHETTY, J., MALEK, J., VAN AKEN, S. E., RIEDMULLER, S., TETTELIN, H., GILL, S. R., WHITE, O., SALZBERG, S. L., HOOVER, D. L., LINDLER, L. E., HALLING, S. M., BOYLE, S. M. & FRASER, C. M. 2002. The *Brucella suis* genome reveals fundamental similarities between animal and plant pathogens and symbionts. *Proceedings of the National Academy of Sciences*, 99, 13148-53.
- PITTS JR, J. N., GROSJEAN, D., VAN CAUWENBERGHE, K., SCHMID, J. P. & FITZ, D. R. 1978. Photooxidation of aliphatic amines under simulated atmospheric conditions: formation of nitrosamines, nitramines, amides, and photochemical oxidant. *Environmental Science and Technology*, 12, 946-953.
- RAKE, J. B. & EAGON, R. G. 1980. Inhibition, but not uncoupling, of respiratory energy coupling of three bacterial species by nitrite. *Journal of Bacteriology*, 144, 975-982.
- RICHARDSON, D. J. 2000. Bacterial respiration: A flexible process for a changing environment. *Microbiology*, 146, 551-571.
- RISTOW, M. & ZARSE, K. 2010. How increased oxidative stress promotes longevity and metabolic health: The concept of mitochondrial hormesis (mitohormesis). *Experimental Gerontology*, 45, 410-418.
- ROSSO, L., LOBRY, J. R., BAJARD, S. & FLANDROIS, J. P. 1995. Convenient model to describe the combined effects of temperature and pH on microbial growth. *Applied and Environmental Microbiology*, 61, 610-616.

- ROSTKOWSKA, K., ZWIERZ, K., RÓZAŃSKI, A., MONIUSZKO-JAKONIUK, J. & ROSZCZENKO, A. 1998. Formation and metabolism of *N*-nitrosamines. *Polish Journal of Environmental Studies*, 7, 321-325.
- ROWE, J. J., YARBROUGH, J. M., RAKE, J. B. & EAGON, R. G. 1979. Nitrite inhibition of aerobic bacteria. *Current Microbiology*, 2, 51-54.
- SEARS, H. J., LITTLE, P. J., RICHARDSON, D. J., BERKS, B. C., SPIRO, S. & FERGUSON, S. J. 1997. Identification of an assimilatory nitrate reductase in mutants of *Paracoccus denitrificans* GB17 deficient in nitrate respiration. *Archives of Microbiology*, 167, 61-66.
- SIJBESMA, W. F., ALMEIDA, J. S., REIS, M. A. & SANTOS, H. 1996. Uncoupling effect of nitrite during denitrification by *Pseudomonas fluorescens*: An in vivo (31)P-NMR study. *Biotechnology and Bioengineering*, 52, 176-82.
- STINGL, K., ALTENDORF, K. & BAKKER, E. P. 2002. Acid survival of *Helicobacter pylori*: How does urease activity trigger cytoplasmic pH homeostasis? *Trends in Microbiology*, 10, 70-4.
- TUNBRIDGE, A. J., STEVANIN, T. M., LEE, M., MARRIOTT, H. M., MOIR, J. W., READ, R. C. & DOCKRELL, D. H. 2006. Inhibition of macrophage apoptosis by *Neisseria meningitidis* requires nitric oxide detoxification mechanisms. *Infection and Immunity*, 74, 729-33.
- VADIVELU, V. M., KELLER, J. & YUAN, Z. 2006a. Effect of free ammonia and free nitrous acid concentration on the anabolic and catabolic processes of an enriched *Nitrosomonas* culture. *Biotechnology and Bioengineering*, 95, 830-839.
- VADIVELU, V. M., KELLER, J. & YUAN, Z. 2007. Free ammonia and free nitrous acid inhibition on the anabolic and catabolic processes of *Nitrosomonas* and *Nitrobacter*.
- VADIVELU, V. M., YUAN, Z., FUX, C. & KELLER, J. 2006b. The inhibitory effects of free nitrous acid on the energy generation and growth processes of an enriched *Nitrobacter* culture. *Environmental Science and Technology*, 40, 4442-4448.
- VAN VERSEVELD, H. W., MEIJER, E. M. & STOUTHAMER, A. H. 1977. Energy conservation during nitrate respiration in *Paracoccus denitrificans*. *Archives of Microbiology*, 112, 17-23.
- WANG, Q., YE, L., JIANG, G. & YUAN, Z. 2013. A free nitrous acid (FNA)-based technology for reducing sludge production. *Water Research*, 47, 3663-3672.

- WEBB, J. S., THOMPSON, L. S., JAMES, S., CHARLTON, T., TOLKER-NIELSEN, T., KOCH, B., GIVSKOV, M. & KJELLEBERG, S. 2003. Cell death in *Pseudomonas aeruginosa* biofilm development. *Journal of Bacteriology*, 185, 4585-4592.
- WEI, D., XUE, X., YAN, L., SUN, M., ZHANG, G., SHI, L. & DU, B. 2014. Effect of influent ammonium concentration on the shift of full nitrification to partial nitrification in a sequencing batch reactor at ambient temperature. *Chemical Engineering Journal*, 235, 19-26.
- WILLIAMS, D. R., ROWE, J. J., ROMERO, P. & EAGON, R. G. 1978. Denitrifying *Pseudomonas aeruginosa*: Some parameters of growth and active transport. *Applied and Environmental Microbiology*, 36, 257-263.
- WISEMAN, H. & HALLIWELL, B. 1996. Damage to DNA by reactive oxygen and nitrogen species: Role in inflammatory disease and progression to cancer. *Biochemical Journal*, 313, 17-29.
- YANG, D., OYAIZU, Y., OYAIZU, H., OLSEN, G. J. & WOESE, C. R. 1985. Mitochondrial origins. *Proceedings of the National Academy of Sciences*, 82, 4443-4447.
- YANG, T. 1985. Mechanism of nitrite inhibition of cellular respiration in *Pseudomonas aeruginosa*. *Current Microbiology*, 12, 35-40.
- YARBROUGH, J. M., RAKE, J. B. & EAGON, R. G. 1980. Bacterial inhibitory effects of nitrite: Inhibition of active transport, but not of group translocation, and of intracellular enzymes. *Applied and Environmental Microbiology*, 39, 831-834.
- YE, L., PIJUAN, M. & YUAN, Z. 2010. The effect of free nitrous acid on the anabolic and catabolic processes of glycogen accumulating organisms. *Water Research*, 44, 2901-2909.
- ZHOU, Y., OEHMEN, A., LIM, M., VADIVELU, V. & NG, W. J. 2011. The role of nitrite and free nitrous acid (FNA) in wastewater treatment plants. *Water Research*, 45, 4672-4682.
- ZHOU, Y., PIJUAN, M. & YUAN, Z. 2007. Free nitrous acid inhibition on anoxic phosphorus uptake and denitrification by poly-phosphate accumulating organisms. *Biotechnology and Bioengineering*, 98, 903-912.
- ZHOU, Y., PIJUAN, M., ZENG, R. J. & YUAN, Z. 2008. Free nitrous acid inhibition on nitrous oxide reduction by a denitrifying-enhanced biological phosphorus removal sludge. *Environmental Science and Technology*, 42, 8260-8265.

4 The role of flavohemoglobin in *P. denitrificans* under nitrite induced stress

Contents

4	The role of flavohemoglobin in <i>P. denitrificans</i> under nitrite induced stress	133
4.1	List of figures	134
4.2	List of tables	136
4.3	Introduction	137
4.3.1	Stress tolerance in <i>P. denitrificans</i>	137
4.3.2	Aerobic nitric oxide detoxifications by flavohemoglobin and flavorubredoxin 138	
4.3.3	Anaerobic nitric oxide detoxification by the nitric oxide reductase and nitrite reductase 140	
4.4	Results	141
4.4.1	Comparison of plate reader and shake flask technique	141
4.4.2	Identification and transcriptional analysis of the novel flavohemoglobin in <i>P. denitrificans</i> PD1222	144
4.4.3	Transcription of the flavohemoglobin in <i>P. denitrificans</i> during batch growth in the presence of nitrite	147
4.4.4	Flavohemoglobin mutation study in <i>P. denitrificans</i> using SacB-mediated allelic exchange	150
4.4.5	Conjugal transfer of pKH002 to <i>P. denitrificans</i> and deletion of the flavohemoglobin gene	156
4.4.6	Growth phenotype of the <i>P. denitrificans</i> flavohemoglobin deletion mutant 162	
4.4.7	The flavohemoglobin complementation using vector reinsertion into <i>P. denitrificans</i>	165
4.5	Discussion	166

4.5.1	Comparison of the batch culture growth in 250 ml flasks and 0.1 µl plate well	166
4.5.2	The role of <i>P. denitrificans</i> flavohemoglobin in nitrite tolerance	167
4.5.3	Bioinformatic characterisation of a transcriptional regulator in association with the flavohemoglobin in <i>P. denitrificans</i>	170
4.6	References.....	171

4.1 List of figures

Figure 4.1: Comparative growth curves of <i>P. denitrificans</i> grown in minimal salt media, pH 7.5 A: without nitrite addition, and B: with 12.5 mM nitrite addition to growth media. The two methods of bacterial growth which are compared in this figure are the plate reader (PR) batch culture technique (open symbol), and shaking flask (SF) batch culture technique (closed symbol). Biomass production shown in OD _{600nm} 1 cm pathlength corrected. Plate reader data was taken at half hourly intervals, shown at one hour intervals for clarity. Standard error bars denote n = 3.....	143
Figure 4.2: Alignment of the <i>Salmonella typhimurium</i> Hmp and <i>P. denitrificans</i> Fhb Pd1689 using NCBI:BLAST analysis. Multiple sequence alignment using EMBL-EBI:Clustral Omega and presented using JalView alignment tool. Blue indicates conserved residues....	145
Figure 4.3: NCBI:BLAST analysis with EMBL-EBI:Clustral Omega multiple protein alignment presented in JalView of the flavohemoglobin Pd1689 to the <i>P. denitrificans</i> genome. Alignment was shown to Pd2831, Pd1179, Pd1188, Pd2831, Pd4896 and Pd4806 in the FAD binding / oxidoreductase domain. Blue indicates conserved residues.....	146
Figure 4.4: Alignment of the <i>E. coli</i> NorW to <i>P. denitrificans</i> genome using NCBI:BLAST analysis. NorW is aligned to the top five candidates. Multiple protein alignment using EMBL-EBI:Clustral Omega presented in JalView, colouring by percentage identity.	148
Figure 4.5: Experion virtual RNA gel showing samples of RNA from the growth of <i>P. denitrificans</i> using the shaking flask technique in minimal salts media, pH 7.5, supplemented with ammonium chloride, 10 mM, sodium succinate, 30 mM and Vishniac trace element solution, with sodium nitrite additions as stated. Ladder (bp): 1, 13; standard (no nitrite) 2 (563.3 ng.µl ⁻¹), 3 (193.6ng.µl ⁻¹) 14 (277.4ng.µl ⁻¹); 10 mM nitrite: 15 (307.0 ng.µl ⁻¹), 16 (310.0 ng.µl ⁻¹), 17 (304.9ng.µl ⁻¹); 12.5 mM nitrite 4 (541.6 ng.µl ⁻¹), 5 (212.6 ng.µl ⁻¹), 6	

(186.5 ng.µl⁻¹); 15 mM nitrite: 7 (164.1 ng.µl⁻¹), 8 (578.2 ng.µl⁻¹), 9 (249.4 ng.µl⁻¹); 17.5 mM nitrite 10 (275.5 ng.µl⁻¹), 11 (278.5ng.µl⁻¹), 12 (286.7 ng.µl⁻¹).149

Figure 4.6: Normalised expression of the flavohemoglobin (*fhb*) (Pd1689) in *P. denitrificans* in the presence of nitrite. Expression normalised to the glyceraldehyde 3-phosphate dehydrogenase (GAPDH) housekeeping gene. Error bars denote standard error n = 3.151

Figure 4.7: The 3' and 5' flanking regions with restriction sites (A) either site of the flavohemoglobin gene from *P. denitrificans*. The flanking regions are amplified with corresponding sticky ends by addition of restriction sites to primers. These restriction sites are used for insertion into the pK18*mobsacB* plasmid (B).153

Figure 4.8: Insertion of the 3' and 5' flanking regions into the pK18*mobsacB* plasmid. A: insertion of 3' flanking region into pK18*mobsacB* plasmid. B: insertion of 5' flanking region to plasmid containing ligated 3' flanking region. PCR amplification of flanking regions. Followed by restriction digestion with complementary restriction enzymes of both the plasmid and insert. This is followed by ligation of insert to plasmid.154

Figure 4.9: The pK18*mobsacB* plasmid showing the inserted 3' and 5' flanking fragments and restriction cut sites: *Xma*I, *Xba*I and *Pst*I. Also shown is the levan sucrose *sacB* (1421 bp) and neomycin phosphotransferase gene conveying kanamycin resistance NPT II (794 bp) and disruption of the *lacZ-α*.157

Figure 4.10: Single and double cross over of the pKH002 plasmid in *P. denitrificans* yielding two colonies devoid the kanamycin resistance and sucrose induced levan toxin. A: primary cross over inserting plasmid into the *P. denitrificans* genome and conveying kanamycin resistance to the organism. B: Plasmid in *P. denitrificans* genome. The secondary cross over removes plasmid and flavohemoglobin gene from the *P. denitrificans* genome. C: Cross overs complete, levan sucrose *sacB* and neomycin phosphotransferase gene NPT II are removed from the *P. denitrificans* genome, losing kanamycin resistance. The subsequent *P. denitrificans* genome lacking *fhb* is termed PDKH001.158

Figure 4.11: Genomic DNA extracted from wild type (WT) *P. denitrificans* and mutant *P. denitrificans* showing deletion of ~500 bp region at the site of the flavohemoglobin gene (*fhb*). 1: DNA ladder, 2 & 3 two colonies of *P. denitrificans* genomic DNA (gDNA) of approximately 600 bp, 4 & 5 WT *P. denitrificans* gDNA of approximately 1.1 kb. There is a ~500 bp loss of DNA in the mutant *P. denitrificans* genome.160

Figure 4.12: Sequencing of the flavohemoglobin mutation. Sequencing data is (grey) against the *P. denitrificans* genome (red). A: 5' to 3' sequence read and B: 3' to 5' sequence read of

genomic DNA from *P. denitrificans* using *fhb* primers showing missing portion of the *fhb* gene.....161

Figure 4.13: A: Growth of FHB deletion mutant, error bars denote standard error n = 3 and B: Growth of WT *P. denitrificans*, error bars denote standard error n = ≥ 3 . Minimal salts media, pH 7.5, supplemented with ammonium chloride, 10 mM, sodium succinate, 30 mM and Vishniac trace element solution, with various sodium nitrite concentrations (mM) as shown in the key above the figure. Measured by optical density at 600 nm (OD_{600nm}) adjusted to a pathlength of 1 cm against time (h). Cells were grown in 100 μ l total volume with shaking at 400 rpm. OD_{600nm} was measured every 0.5 h, 1 h values shown.....163

Figure 4.14: Summarised apparent growth constant (μ_{app}) and maximum biomass produced (Y_{max} AU) at various calculated nitrite (mM) concentrations for the growth of *P. denitrificans* and the Δfhb mutant. Growth in minimal salts media, pH 7.5, supplemented with ammonium chloride, 10 mM, sodium succinate, 30 mM and Vishniac trace element solution. Measured by optical density at 600 nm (OD_{600nm}) adjusted to a pathlength of 1 cm against time (h). Error bars denote standard error n = ≥ 3164

Figure 4.15: Restriction digests of screened colonies containing pOT2 with the flavohemoglobin insert. L: 1 kb ladder, 1 – 13: colonies selected from gentamicin screening plates after transformation of the flavohemoglobin fragment and pOT2 plasmid, analysed by plasmid mini preparation and digestion with *Xba*I.....168

Figure 4.16: Growth of *P. denitrificans* wild type (WT), FHB deletion mutant and FHB complement strain (as shown in key at the top of the figure). Grown in minimal salts media, pH 7.5, supplemented with ammonium chloride, 10 mM, sodium succinate, 30 mM and Vishniac trace element solution, with 50 mM sodium nitrite. Measured by optical density at 600 nm (OD_{600nm}) adjusted to a pathlength of 1 cm against time (h). Cells were grown in 100 μ l total volume with shaking at 400 rpm. OD_{600nm} was measured every 0.5 h, 1 h values shown. Error bars denote standard error n = 3.....169

4.2 List of tables

Table 4.1: The apparent exponential growth rates (μ_{app}) and maximum optical density (Y_{max} (AU)) for both the shaking flask and plate reader batch growth conditions for growth without nitrite (-nitrite) and with 12.5 mM nitrite (+nitrite).....142

4.3 Introduction

In chapter 3, an interaction of pH and nitrite stress which generates a unique growth phenotype in *P. denitrificans* was discussed. It was observed that pH affects the growth of *P. denitrificans*, and established that the optimal pH range for growth of *P. denitrificans* is pH 7.5 – 8.0. Addition of nitrite to the aerobic culture of *P. denitrificans* caused stimulation of growth at levels of nitrite <10 mM. This stimulation occurs at the maximum biomass achieved measured as optimal density (Y_{\max}) and does not affect the exponential rate of *P. denitrificans* growth (μ_{app}). At concentrations of nitrite >10 mM, nitrite has a detrimental effect on the growth seen in Y_{\max} and μ_{app} as well as extension of the lag phase of growth. It has therefore been suggested that nitrite has a cytotoxic effect on the cellular components and metabolism of the *P. denitrificans* cells. The concentration at which nitrite becomes toxic is pH dependent in nature. It is suggested that the nitrite enters the cell and forms reactive nitrogen species (RNS), which would generate a stress response within *P. denitrificans*. This stress response includes the nitrite reductase, nitric oxide reductase as well as a flavohemoglobin (Fhb) and flavohemoglobin-associated regulatory protein.

4.3.1 Stress tolerance in *P. denitrificans*

It has been observed that at higher nitrite concentrations, growth of *P. denitrificans* is inhibited. This inhibitory concentration of nitrite is pH dependent, and this introduces free nitrous acid (FNA) as a potential candidate for the intracellular movement of nitrite. The diffusion of nitrite as FNA may be one route for the internalisation of nitrite and subsequent production of intracellular cytotoxins such as nitric oxide (NO) and peroxynitrite. RNS are known to interact and damage protein function by acting on residues and DNA (Daiber *et al.*, 2013; Van Dyke, 1997; Pacher *et al.*, 2007). Reactive nitrogen species such as NO require removal by detoxification proteins to prevent extensive cellular damage (Andrews *et al.*, 1992; Hutchings *et al.*, 2002). Such a mechanism in nitrite stressed *P. denitrificans* would be evident in the increased transcription of a detoxification protein gene in the presence of nitrite. It is known that *P. denitrificans* already employs nitric oxide (NO) detoxification proteins in anoxic conditions, however little is known about the aerobic mechanism of NO defence. Broadly, NO removal can be carried out in bacteria by the nitric oxide reductase (NorBC) (Field *et al.*, 2008), the flavohemoglobin (HmpA) (Stevanin *et al.*, 2002), the flavorubredoxin (NorVW) (Gardner *et al.*, 2002) or the multihaem nitrite

reductase (NrfA) (Poock *et al.*, 2002). Our bioinformatics analysis suggest that the latter two are not found in *P. denitrificans*, while expression of *norBC* only occurs under anoxic growth conditions (De Boer *et al.*, 1996)

Under anoxic conditions, denitrifying bacteria express respiratory enzymes that can serve to reductively remove extra cytoplasmic nitrite as well as NO that is generated in the periplasm as a product of nitrate reduction. These are the nitrite reductase (Nir) and the nitric oxide reductase (Nor). Indeed, in *P. denitrificans* *nir* and *nor* gene expression is co-regulated by the same transcriptional regulator NnrR (an FNR-like activator protein which is suggested to be an NO sensor). It is suggested that NnrR senses NO and coordinates expression of the *nir* and *nor* genes to begin transcription of the nitrite and nitric oxide reductases. This ensures production and consumption of RNS are tightly coupled. However, expression of the *nir* and *nor* systems is repressed by oxygen and activity of the enzymes themselves is inhibited by oxygen (Tucker *et al.*, 2010).

4.3.2 Aerobic nitric oxide detoxifications by flavohemoglobin and flavorubredoxin

Flavohemoglobins are part of a broader family of bacterial haemoglobins (Poole and Hughes, 2000) classified into three groups of functionality; small single-domain (Tarricone *et al.*, 1997; Wakabayashi *et al.*, 1986), truncated globins (Pesce *et al.*, 2000) and finally flavohemoglobins. The first gene of a soluble flavohemoglobin found in many bacteria, including many pathogenic bacteria such as *Escherichia coli* and *Salmonella enterica* serovar *Typhimurium*, is the cytoplasmic HmpA (Mason *et al.*, 2009; Mills *et al.*, 2008). HmpA resembles a ferredoxin reductase at the C-terminal end and can be described as a nitric oxide dioxygenase (Mills *et al.*, 2005) or denitrosylase (Laver *et al.*, 2010; Stevanin *et al.*, 2002). It is a single polypeptide with a C-terminal NADH binding site for electron transfer to a haem located in the globin domain of the protein. A haemb is located at the N-terminus (Vasudevan *et al.*, 1991). HmpA is regulated by the NsrR transcriptional regulator. NsrR is a member of the Rrf2 family of transcription repressors and acts in response to the binding of NO to the [2Fe-2S] cluster (Browning *et al.*, 2010). It is also associated with the global response to NO with ~60 suspected target genes in *E. coli* NO detoxification and a generalised stress response (Tucker *et al.*, 2010). In aerobic conditions the flavohemoglobin catalyses the conversion of NO to nitrate: $2\text{NO} + 2\text{O}_2 + \text{NAD(P)H} \rightarrow 2\text{NO}_3^- + \text{NAD(P)}^+ +$

H⁺ (Stevanin *et al.*, 2002; Hausladen *et al.*, 1998; Gardner *et al.*, 2000; Gardner *et al.*, 1998). In anoxic conditions the lack of oxygen alters this reactive mechanism to form nitrous oxide (N₂O) (Hausladen *et al.*, 1998; Kim *et al.*, 1999). The mechanism of nitric oxide dioxygenase action has been suggested to occur through a series of redox reactions within the iron centres of the protein (Gardner *et al.*, 1998). Initial FAD reduction NAD(P)H + FAD + H⁺ → NAD(P)⁺ + FADH₂, primary iron reduction FADH₂ + Fe³⁺ → Fe²⁺ + FADH + H⁺, secondary iron reduction FADH + Fe³⁺ → FAD + Fe²⁺ + H⁺, O₂ binding Fe²⁺ + O₂ → Fe³⁺(O₂⁻), and finally NO dioxygenation Fe³⁺(O₂⁻) + NO → Fe³⁺ + NO₃⁻.

The 479 aa flavorubredoxin (NorVW) has been characterised in *Escherichia coli*, where it acts as a nitric oxide reductase, producing nitrous oxide (N₂O) as a product of NO reduction. The mode of action for NorV requires NADH and its reductive partner NorW, although others have been speculated about but not identified. NorV binds 3 irons and one FMN per monomer, which has led to a suggested reaction mechanism of NO binding to a di-iron centre, with electrons donated by the reductase at a rubredoxin FMN centre and the di-iron centre (Hutchings *et al.*, 2002). Mutational studies of the flavorubredoxin *norVW* by Gardner (2002) suggest the NorVW function as a single transcriptional unit. However, NorV shows a key role in the metabolism of NO and NorW an ancillary role. The function of NorVW is regulated by NorR. NorR is suggested to act in response to NO through a mononuclear non-haem iron centre and regulate the activation of a σ⁵⁴ directed transcription of NorV (Tucker *et al.*, 2010). It has been suggested that the nitric oxide reductase function of NorVW is required in anoxic conditions. However, expression of the complex is activated in both anoxic and aerobic growth conditions (Gardner *et al.*, 2002).

NorVW and HmpA catalyse reaction mechanisms which would be possible in the aerobic conditions of treatment explored in this work, with ample availability of oxygen. These examples have been selected for comparison to the *P. denitrificans* genome to suggest potential gene candidates showing homology to the known flavohemoglobin of nitric oxide dioxygenase function, Hmp and the known flavorubredoxin of *E. coli*, NorVW.

4.3.3 Anaerobic nitric oxide detoxification by the nitric oxide reductase and nitrite reductase

Nitric oxide reductase (NorBC) is a characterised enzyme in the denitrification pathway. It catalyses anoxic nitric oxide reduction to nitrous oxide (N₂O) the potent greenhouse gas and ozone depletion agent: $2\text{NO} + 2\text{e}^- + 2\text{H}^+ \rightarrow \text{N}_2\text{O} + \text{H}_2\text{O}$. Nor can be found in *P. denitrificans* as well as many pathogenic bacteria such *Staphylococcus aureus* (Gill *et al.*, 2005) and *Neisseria meningitides* (Tunbridge *et al.*, 2006). A single component qNor is found in many non-denitrifying pathogenic bacteria (Busch *et al.*, 2002). Its frequency in pathogenic bacteria suggests an escape mechanism to circumvent host defence by detoxification of NO, which has been seen by qNor in *Neisseria gonorrhoeae* (Householder *et al.*, 2000). *N. gonorrhoeae* also contains an active nitrite reductase, suggesting qNor may be needed to protect against endogenously produced NO (Busch *et al.*, 2002). NorBC is a membrane protein isolated as a two-subunit complex with four redox centres including a NorB high-spin haem_b (haem_{b3}) coupled magnetically to a nearby non-haem iron (FeB) and an additional low-spin haem that receives electrons from a low-spin haem_c, from periplasmic electron donors, such as cytochrome *c*₅₅₀ or pseudoazurin (Thorndycroft *et al.*, 2007). NorBC derives its substrate protons from the periplasm (Bell *et al.*, 1992) and can couple energy conservation and electron transfer from NADH dehydrogenase and the *bc*₁ complex with NO reduction by NOR via periplasmic electron carriers such as cupredoxin or a *c*-type cytochrome (De Boer *et al.*, 1996). *P. denitrificans* contains a cNor protein with accompanying accessory genes for NorD, NorE, NorF, and NorQ/NirQ proteins, found in most cNor containing bacteria. These accessory genes affect the activity, assembly and stability of NorBC in *P. denitrificans*. In α -proteobacteria *Rhodobacter sphaeroides* 2.4.1, it has been suggested that the function of NOR is to use environmental NO for the generation of energy, rather than as a protection mechanism to the toxicity of NO (Kwiatkowski *et al.*, 1997).

The nitrite reductase (NrfA) functions as a membrane bound NO detoxifier which generates ammonia as the NO reactive product of detoxification, which is carried out in the periplasm. It is 478 aa in size and has been investigated in *Salmonella enterica*. It was first fully characterised in *Escherichia coli* by Darwin (1993) as a tetrahaem *c*-type cytochrome (belonging to the cytochrome *c*-552 family) and terminal reductase of the formate-dependent pathway of nitrite reduction to ammonia. NrfA contains four haems and two calcium atoms per monomer. NrfA catalyses the reduction of nitrite and is also believed to catalyse the

reduction of NO (Mills *et al.*, 2008; Browning *et al.*, 2010). Expression of NrfA promoter is tightly coupled to anaerobicity and is activated by the regulatory protein fumarate and nitrate reductase regulator (FNR). Repression is controlled by the binding of NarL or NarP. Both of these act as transcription activators and are triggered by the presence of nitrite and nitrate (Browning *et al.*, 2002). FNR is a small RNA which is expressed exclusively within bacteria under anaerobic growth conditions and acts as an oxygen sensor. It features in the negative regulation of genes associated primarily with aerobic function, such as those involved in oxidative stress of anaerobic respiration (Boysen *et al.*, 2010). Its expression is repressed by oxygen and fully induced by an absence of oxygen and the presence of nitrite. Partial induction is seen in the absence of oxygen and nitrite, suggesting that oxygen is the primary repressor of NrfA expression (Darwin *et al.*, 1993). NrfA has been shown to be regulated by the NsrR transcriptional repressor.

These proteins have only been characterised as functionally active in anoxic conditions and they are suppressed by the presence of oxygen. *P. denitrificans* is therefore less likely to have genes encoding proteins with homology to NorBC or NrfA, which are involved in the detoxification of NO under the conditions tested in this work. To explore the reactive mechanism of *P. denitrificans* under nitrosative stress bioinformatic mining of the *P. denitrificans* genome was undertaken to find candidates of NO detoxification. This bioinformatic method identified a flavohemoglobin that could be active under aerobic growth conditions in *P. denitrificans*. The activity of this gene was investigated in *P. denitrificans* using transcriptional analysis and the function of this gene at a cellular level was tested using a deletion mutant.

4.4 Results

4.4.1 Comparison of plate reader and shake flask technique

For transcriptional analysis a large volume of *P. denitrificans* cells is needed for RNA extraction. The shaking flask technique was employed to batch culture *P. denitrificans* aerobically at a volume of 50 ml, as described in the methods to gain a larger volume of cells to be harvested. The experimental design used 250 ml conical flasks holding a total of 50 ml minimal salts media. This was supplemented with trace elements and 10 mM ammonium chloride, with 20 mM sodium succinate as the carbon source - the same media composition

used in the plate reader batch culture. Aerobicity of the shaking flask was maintained by using a low volume within the flasks to maximise surface to air ratio, and by agitation of the flasks at 200 rpm. Flasks were kept aseptic with a foam bung and foil as detailed in the methods (Henzler and Schedel, 1991). A comparison of *P. denitrificans* batch growth using the shaking flask (SF) technique and the plate reader (PR) technique can be seen in figure 4.1. Both growth curves made using the different growth techniques are similar in growth characteristics. An apparent feature is an extension of lag phase seen in the plate reader technique. The apparent exponential growth rates (μ_{app}) and maximum optical density (Y_{max} (AU)) for both the SF and PR batch growth techniques are shown in table 4.1. A table of the total kinetic parameters of the growth curves from batch SF and PR culture is shown in the appendix. Without nitrite present, μ_{app} were identical at $0.44 \pm 0.01 \text{ h}^{-1}$. The μ_{app} values were also identical for SF and PR with the addition of 12.5 mM sodium nitrite: $0.35 \pm 0.01 \text{ h}^{-1}$ (figure 4.1). RNA extraction occurs at mid exponential growth which is approximately 0.45 AU. The μ_{app} PR batch growth is replicated in SF batch growth conditions. This establishes the SF method for the culture of *P. denitrificans* cells in a volume suitable for RNA extraction and subsequent transcriptional analysis.

Table 4.1: The apparent exponential growth rates (μ_{app}) and maximum optical density (Y_{max} (AU)) for both the shaking flask and plate reader batch growth conditions, for growth without nitrite (-nitrite) and with 12.5 mM nitrite (+nitrite).

Batch growth					
Nitrite*	method	μ_{app}	$\pm SE$	Y_{max}	$\pm SE$
+	PR	0.35	0.01	3.37	0.02
	SF	0.35	0.01	3.88	0.17
-	PR	0.44	0.01	3.68	0.05
	SF	0.44	0.01	3.68	0.05

PR = plate reader and SF = shaking flask

* amount of nitrite present in growth condition: +nitrite = 12.5 mM sodium nitrite addition and -nitrite = no nitrite present

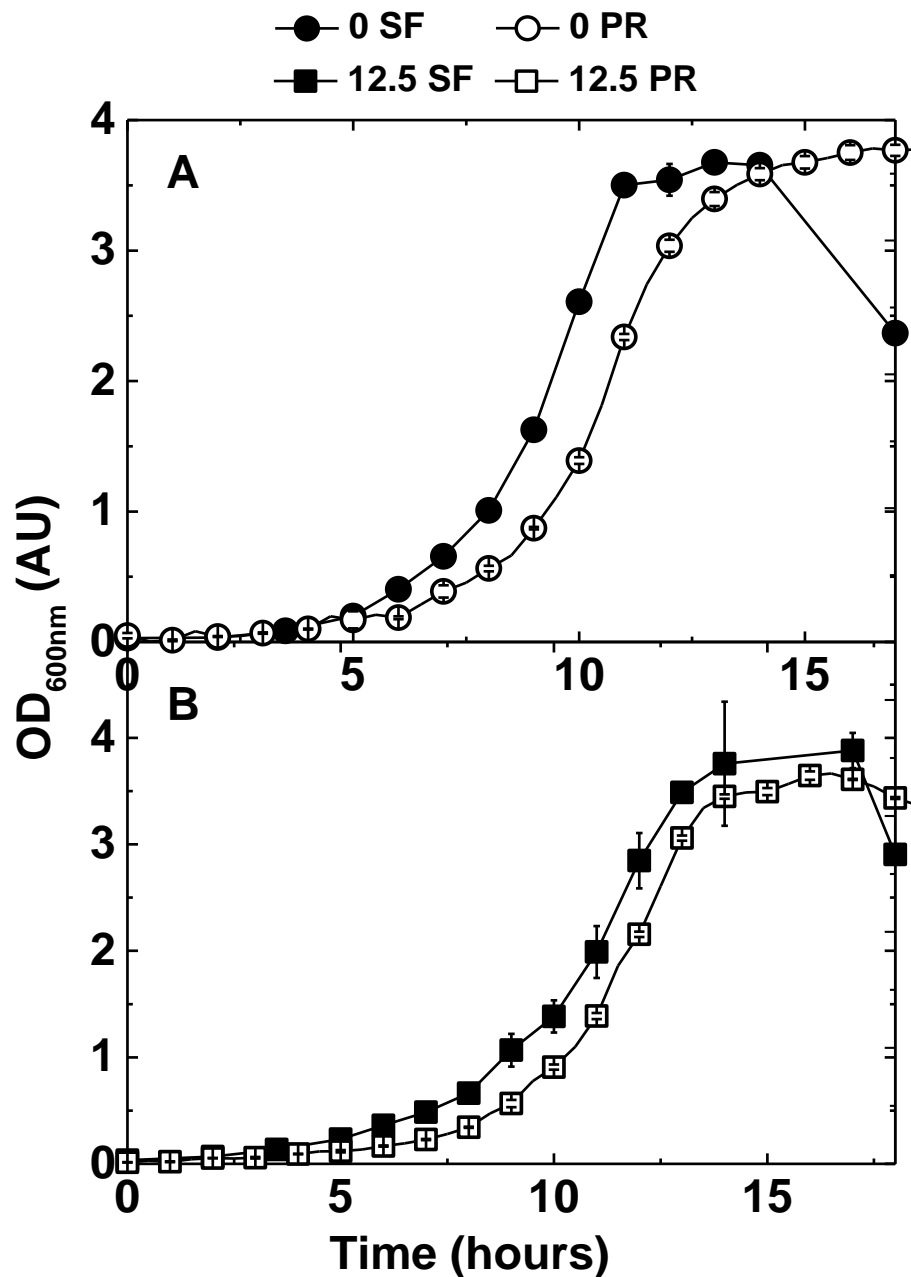


Figure 4.1: Comparative growth curves of *P. denitrificans* grown in minimal salt media, pH 7.5 A: without nitrite addition, and B: with 12.5 mM nitrite addition to growth media. The two methods of bacterial growth which are compared in this figure are the plate reader (PR) batch culture technique (open symbol), and shaking flask (SF) batch culture technique (closed symbol). Biomass production shown in OD_{600nm} 1 cm pathlength corrected. Plate reader data was taken at half hourly intervals, shown at one hour intervals for clarity. Standard error bars denote n = 3.

4.4.2 Identification and transcriptional analysis of the novel flavohemoglobin in *P. denitrificans* PD1222

The growth phenotype of *P. denitrificans* explored in chapter 3 showed that *P. denitrificans* grown in the presence of nitrite expresses a stressed growth phenotype. This suggests a stress response by *P. denitrificans*. This is likely to be due to internalisation of nitrite and mediated by a detoxification protein which is transcribed in the presence of nitrite. To further explore the suggested stress response, the genome of *P. denitrificans* was explored for gene candidates that showed potential function as NO detoxification protein. To identify a candidate involved in NO detoxification, the *Salmonella typhimurium* (strain LT2 / SGSC1412 / ATCC 700720) Hmp flavohemoprotein (accession: P26353) was aligned to the *P. denitrificans* genome shown in figure 4.2. This was carried out using the NCBI:BLAST online alignment tool (National Center for Biotechnology Information: Basic Local Alignment Search Tool).

The BLAST alignment of *S. typhimurium* Hmp against the *P. denitrificans* genome generated one result with high sequence homology to Hmp as a pairwise sequence alignment. Pd1689 (Pden_1689, accession: YP_915482, gene ID: 4580097) showed 43% protein sequence homology to Hmp in the alignment. The regions of similarity are shown in blue in figure 4.1. Pd1689 is annotated on the NCBI database as a nitric oxide dioxygenase (YP_915482), and globin (ABL69786) with a dihydropteridine reductase contig annotation (WP_011747984). Exploration of the conserved domain within Pd1689 reveals a flavoheme-like FAD/NAD binding site, a bifunctional nitric oxide dioxygenase/dihydropteridine reductase 2, and a hemoglobin domain within a 402 amino acid protein, which identifies the protein as a flavohemoglobin (Fhb). BLAST analysis of this Fhb against the *P. denitrificans* genome reveals that *P. denitrificans* has five postulated proteins sharing 24 - 33% identity to Fhb. These genes are Pd1179, Pd1188, Pd2831, Pd4896 and Pd4806. These five protein sequences are shown aligned to Fhb in figure 4.3. Alignment to the Fhb was found in the flavoheme (FNR-like) superfamily with 80-200_{max} scores for the aligned genes Pd2831, Pd1179, Pd1188, Pd2831, and 50-80 alignment score for Pd4896 (Marchler-Bauer *et al.*, 2011). Pd2831, Pd4896, Pd1188 and Pd2831 are annotated as ferredoxin with a flavodoxin reductase and Hmp conserved region (Lacelle *et al.*, 1996; Vasudevan *et al.*, 1991; Ermler *et al.*, 1995). Pd1179 is broadly annotated as an oxidoreductase.

```

Hmp      1 MLD AQT IATVKATI FLLVETGPKLTAHFYDRMFTHNPELKEIFNMSNQRNGD-QREALFN AIAAYASNIENLPALLPAVEKIAQKHTSFQIKPEQYNI VVG99
Fhb      1 PLS AQTIALVKATVPAIEAHGLDIVREMYARMF-QNPEIRDLFNQSHQDGAEAQPRALTGAILAYANNIDNVTALVPAVERIAQKHVGLQILPEHYPHVA99

Hmp     100 THLLATLDEM F-NPG-QEVLDAWGKAYGVLANVFIHREAEIYHENASKDGGWEGTRPFRIVAKTTPRSALITSEFEFEPVDGGTVAEYRFGQYLG VWLKPEG197
Fhb     100 EALLGAIRAVLGDAAATDEVLEAWGEAYWFLANIL IARERRIYDEQQA SEGGWNGWR AFRIDEVIRE SSTIASFVLR PVDGGP VMAHKPGOYLTFWLEIPG199

Hmp     198 FAHOEIROYSLTRKFDGKGYRIAVKREDGGQVSNWLHHAASVGDGVHLAAPAGDFFMNVAADTFVSLISAGVGOTPMLAMLDTLAKEOHTAQVNWFHAAE297
Fhb     200 HAPAK-RNYSISAAFNGRTYRISVKREPQGLASGWLHEQAP-GAVLKIAAPAGEFFLAERPERPVVLLSGGVGLTPMVAMLEALVQSGAQVPVHYIHGTH297

Hmp     298 NGDVHAFADENVSELGRTLPRFTAHTWYREPTESDRAQRLFDS EGLMDLSKLEAAISDPAMQFYL CGPVGFMQFAAKQLVSLGVN NENIHYECFGPHKVL 396
Fhb     298 DRDTHAMRAHVRA LAEGQPQIRVTD FHQTPLADEVAGRDYDHAGLI TEEWLLANTPAGEADYYICGPRPFLRAAVAA LSLAGVPSDR IHYEFGPADEL 396
    
```

Figure 4.2: Alignment of the *Salmonella typhimurium* Hmp and *P. denitrificans* Fhb Pd1689 using NCBI:BLAST analysis. Multiple sequence alignment using EMBL-EBI:Clustal Omega presented using JalView alignment tool. Blue indicates conserved residues.

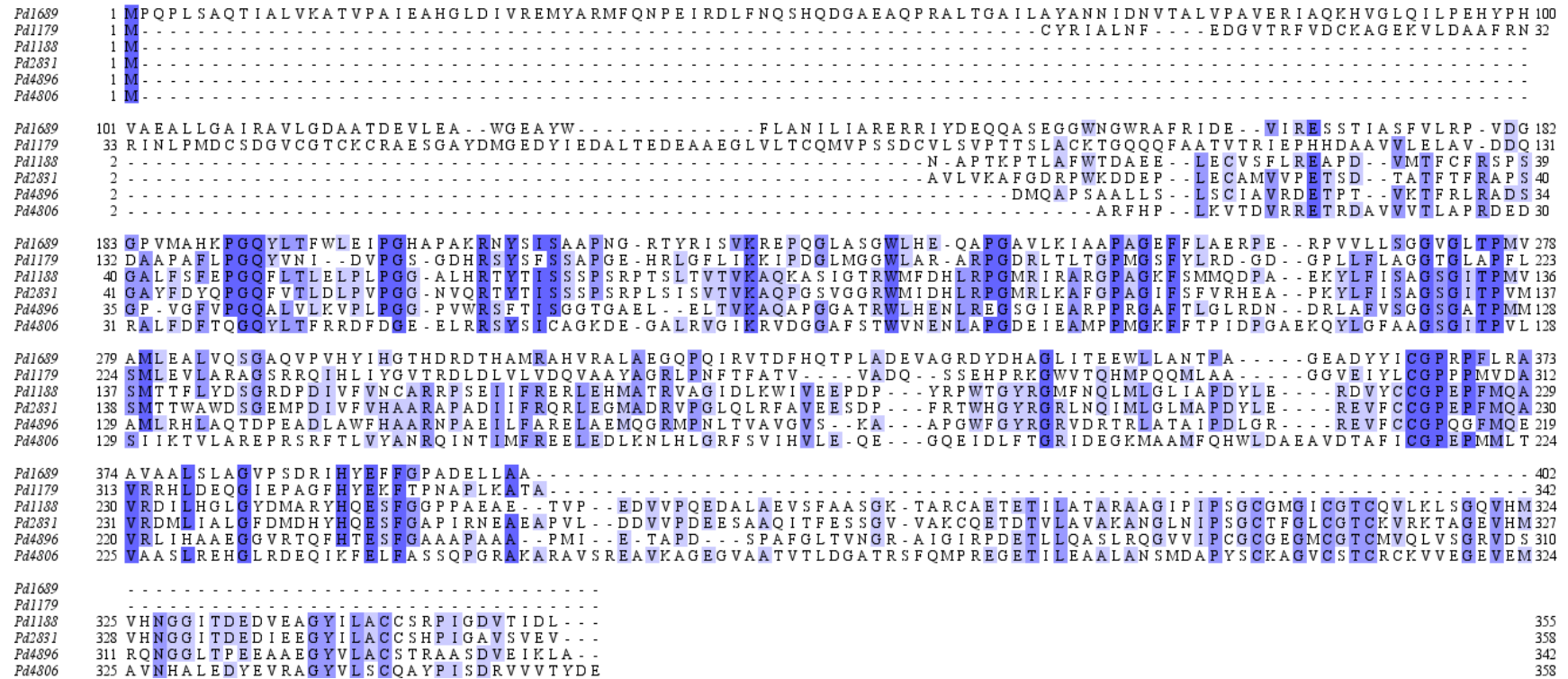


Figure 4.3: NCBI:BLAST analysis with EMBL-EBI:Clustal Omega multiple protein alignment, presented in JalView of the flavohemoglobin Pd1689 to the *P. denitrificans* genome. Alignment was shown to Pd2831, Pd1179, Pd1188, Pd2831, Pd4896 and Pd4806 in the FAD binding / oxidoreductase domain. Blue indicates conserved residues.

To determine if an additional nitric oxide reductase is present in the genome of *P. denitrificans* and not yet identified, the NorBC complex was BLAST analysed against the *P. denitrificans* genome. Analysis by BLAST alignment of Pd2483, the nitric oxide reductase subunit B (NorB) and Pd2484 subunit C (NorC) found the *P. denitrificans* genome offered no additional candidates which aligned to NorBC. The flavorubredoxin (NorVW) was also aligned to the genome of *P. denitrificans* to identify potential flavorubredoxin candidates in figure 4.4. NorV did not show any candidates with sequence similarity. The NorW component showed several candidates. The nitrite reductase (Nir) showed 128 bit_{max} score with 29% identity to NorW. Pd2324 and Pd3463 are annotated as a FAD-dependent pyridine nucleotide-disulphide oxidoreductase. All three show high sequence identity to dihydrolipoamide dehydrogenase which is part of the pyruvate dehydrogenase complex and is responsible for converting pyruvate to acetyl-CoA and CO₂ (Jolley *et al.*, 1996). Pd0551, Pd4760 and Pd0611. Pd3669 shows high sequence identity to NADPH-glutathione reductase which reduces glutathione disulphide (GSSG) to the sulfhydryl form GSH, which is a cellular antioxidant (Meister, 1988; Mannervik, 1987).

The result from bioinformatic analysis revealed a novel flavohemoglobin (*fhb*) Pd1689 in the genome of *P. denitrificans* as gene Pd1689. PD1689 protein sequence aligns to the Hmp family, which suggests a similar function. Its role as an active gene under nitrite stress conditions was explored by RNA extraction from cells grown with nitrite and consequent transcriptional investigation. To further elucidate the role of the *fhb* identified, *P. denitrificans* cells were grown up under both no nitrite and nitrite stressed conditions and analysed for the expression of *fhb*.

4.4.3 Transcription of the flavohemoglobin in *P. denitrificans* during batch growth in the presence of nitrite

Transcriptional analysis was carried out using quantitative reverse transcriptase polymerase chain reaction (qRT-PCR) using RNA extracted from cells grown using the shaking flask technique as detailed in the methods. No DNA contamination was observed by DNA gel electrophoresis, and RNA quality was examined for degradation using the BIORAD Experion virtual shown in figure 4.5. The bands are distinct and clear, indicating that the RNA is not degraded.

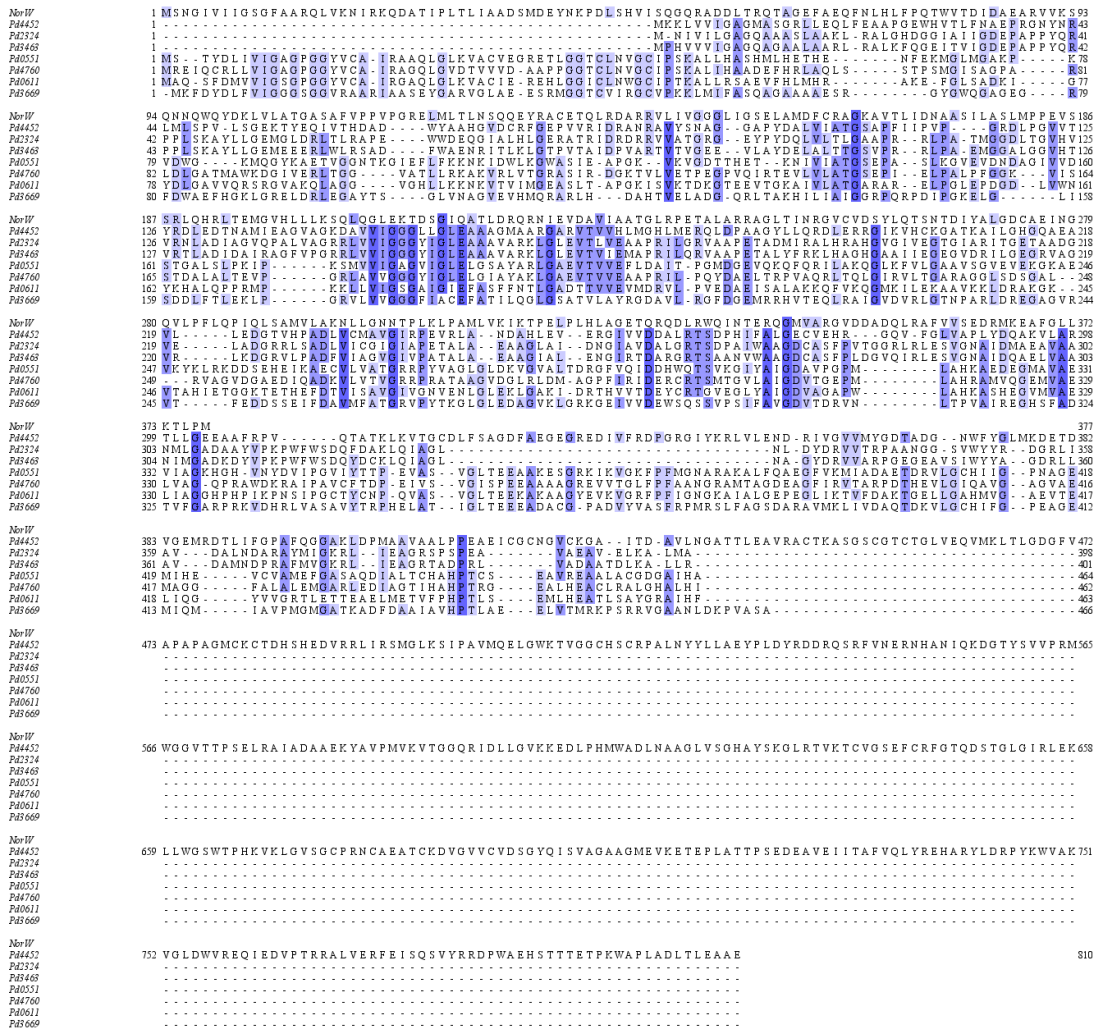


Figure 4.4: Alignment of the *E. coli* NorW to *P. denitrificans* genome using NCBI:BLAST analysis. NorW is aligned to the top five candidates. Multiple protein alignment using EMBL-EBI:Clustal Omega is presented in JalView, colouring by percentage identity.

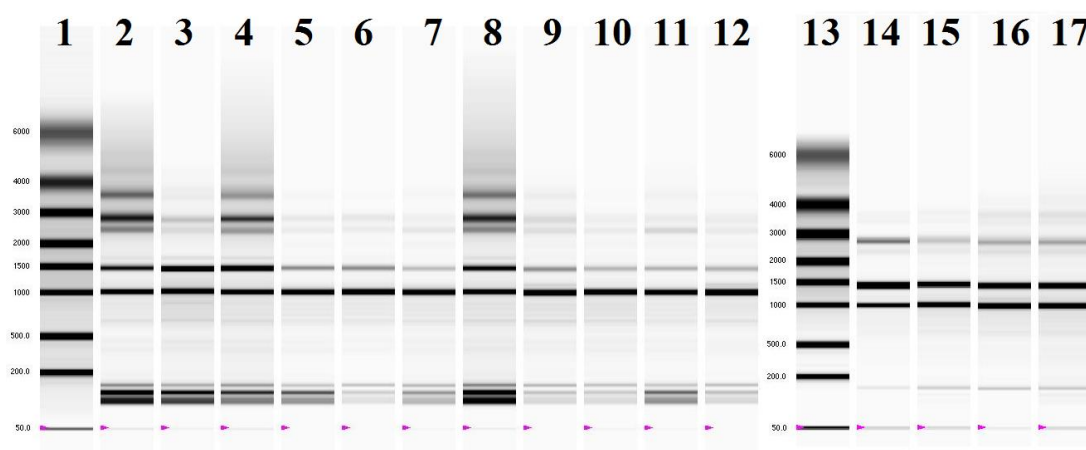


Figure 4.5: Experion virtual RNA gel showing samples of RNA from the growth of *P. denitrificans* using the shaking flask technique in minimal salts media, pH 7.5. Media supplemented with ammonium chloride, 10 mM, sodium succinate, 30 mM and Vishniac trace element solution, with sodium nitrite additions as stated. Ladder (bp): 1, 13; standard (no nitrite) 2 (563.3 ng. μl^{-1}), 3 (193.6ng. μl^{-1}) 14 (277.4ng. μl^{-1}); 10 mM nitrite: 15 (307.0 ng. μl^{-1}), 16 (310.0 ng. μl^{-1}), 17 (304.9ng. μl^{-1}); 12.5 mM nitrite 4 (541.6 ng. μl^{-1}), 5 (212.6 ng. μl^{-1}), 6 (186.5 ng. μl^{-1}); 15 mM nitrite: 7 (164.1 ng. μl^{-1}), 8 (578.2 ng. μl^{-1}), 9 (249.4 ng. μl^{-1}); 17.5 mM nitrite 10 (275.5 ng. μl^{-1}), 11 (278.5ng. μl^{-1}), 12 (286.7 ng. μl^{-1}).

Expression of *fhb* is measured with RNA extracted from cells grown in the presence of nitrite. This is normalised to the expression in cells in the absence of nitrite. These expression values were additionally normalised to glyceraldehyde 3-phosphate dehydrogenase gene (GAPDH) Pden_4465 which was the internal standard housekeeping gene, which is used in qRT-PCR studies of *P. denitrificans* (Bouchal *et al.*, 2010). The range of nitrite concentrations tested for expression of *fhb* was 10, 12.5, 15 and 17.5 mM and the normalised expression levels are shown in figure 4.6. It is apparent that expression of *fhb* increases with the addition of nitrite. The expression increases initially at 10 mM nitrite to a $\Delta\Delta C(t)$ value of 2.6 ± 0.6 . Expression is then stable between the nitrite addition of 12.5 – 17.5 mM levels, showing expression $\Delta\Delta C(t)$ values of between 3.3 ± 0.9 and 3.9 ± 1.8 . The flavohemoglobin investigated in this chapter was selected for mutational studies based on the *fhb* expression levels observed at varying nitrite concentrations, its predicted *Hmp* similarity and its potential detoxification function. The *fhb* was deleted by allelic exchange to study the phenotype of *P. denitrificans* in the presence of nitrite without the presence of *fhb*. This was in order to determine its role within nitrite tolerance and to determine if the expression of *fhb* is necessary for *P. denitrificans* to grow in the presence of nitrite.

4.4.4 Flavohemoglobin mutation study in *P. denitrificans* using SacB-mediated allelic exchange

As described previously, the flavohemoglobin gene (*fhb*) is transcribed in *P. denitrificans* when nitrite is present in aerobic conditions. The following section describes the mutational analyses carried out to characterise the function of *fhb* and whether *fhb* is part of a defence mechanism and provides a contribution to the growth of *P. denitrificans*. A deletion mutant was created and its phenotype was characterised using the plate reader batch growth technique. This mutant was subsequently complemented to restore the wild-type phenotype. The mutant and complementation techniques were used to determine whether the *fhb* gene is necessary in conveying nitrite resistance to nitrite in *P. denitrificans*.

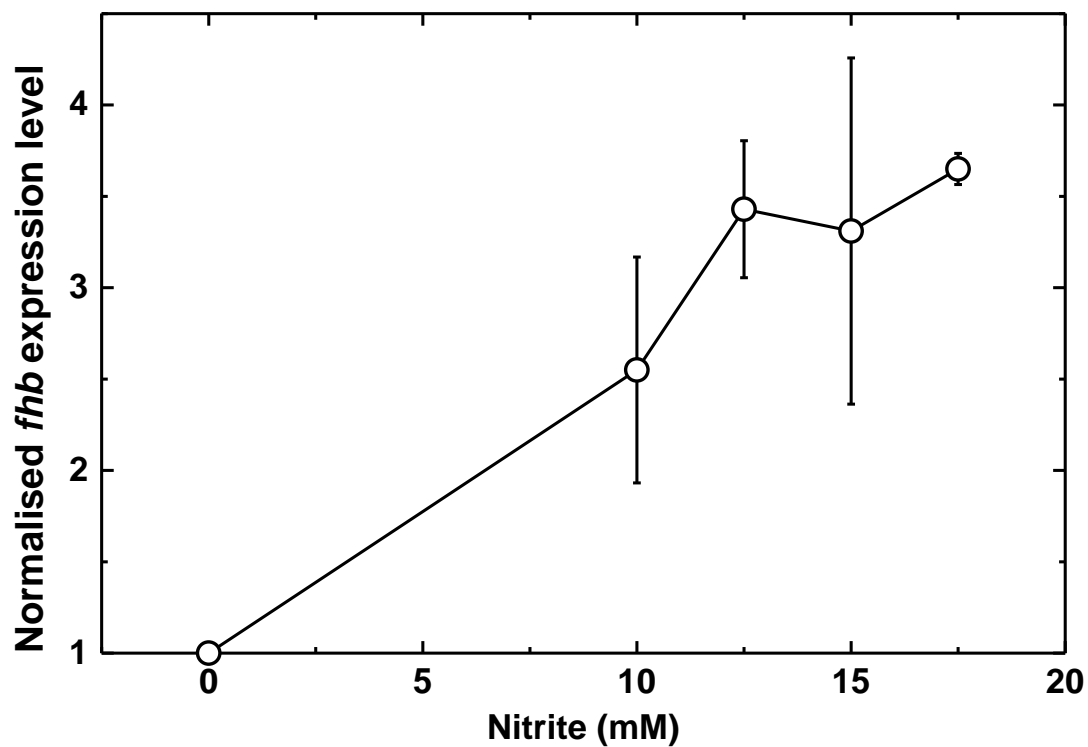


Figure 4.6: Normalised expression of the flavohemoglobin (*fhb*) (Pd1689) in *P. denitrificans* in the presence of nitrite. Expression normalised to the glyceraldehyde 3-phosphate dehydrogenase (GAPDH) housekeeping gene. Error bars denote standard error $n = 3$.

The flavohemoglobin gene was deleted using SacB-mediated allelic exchange (first described by Ried (1987)) using the plasmid pK18*mobsacB* (Schäfer *et al.*, 1994) which lacks the necessary elements for replication outside of *E. coli* (narrow host-range) and is thus termed a suicide plasmid, since it will only be replicated in another bacterium if it is recombined into chromosomal DNA. The pK18*mobsacB* plasmid also contains levansucrase (*sacB*), whose product in gram positive bacteria is involved in cell-wall synthesis. Expression of *sacB* from pK18*mobsacB* is inducible by the substrate for SacB (Levansucrase; EC 2.4.1.10) sucrose, which is polymerised and forms a levan-polysaccharide product that is toxic to gram negative bacteria. Thus, *sacB* and sucrose can be used as a counter-selective marker in gram-negative bacteria like *P. denitrificans*. Therefore, *P. denitrificans* containing the plasmid within its genome will metabolise sucrose and generate inhibition of growth. However if the plasmid has been removed from the genome of *P. denitrificans*, the cells will have removed *sacB* from the *P. denitrificans* genome. They will not metabolise the sucrose to the lethal metabolite and will be able to grow on LB containing sucrose.

In order to delete *fhb*, two 5' and 3' regions, one upstream and one downstream of *fhb* were selected in such a way that excision and deletion of the *fhb* gene would occur when the 5' and 3' regions were exchanged with their chromosomal counterparts. Restriction sites were added to these primers to enable restriction digestion and insertion into the plasmid pK18*mobsacB*. The restriction site on end position of the flanking region is shown diagrammatically in figure 4.7.

These regions were checked and found to be devoid of *Pst*I, *Xba*I and *Xma*I sites which would interfere with the subsequent cloning reactions. A stop codon was not added, and it was ensured that the TAG within the TCTAGA *Xba*I site was in-frame so there would be a premature stop codon as well as deleting the rest of the gene. Genomic DNA isolated from *P. denitrificans* was used as a template for PCR reactions and the 5' and 3' regions of *fhb* were amplified to produce DNA products 771 and 868 bp in size for the 5' and 3' regions, respectively. For the generation of the suicide plasmid, the two flanking regions were inserted into the pK18*mobsacB* plasmid as shown diagrammatically in figure 4.8 to produce plasmid pKH002 for conjugation into *P. denitrificans*.

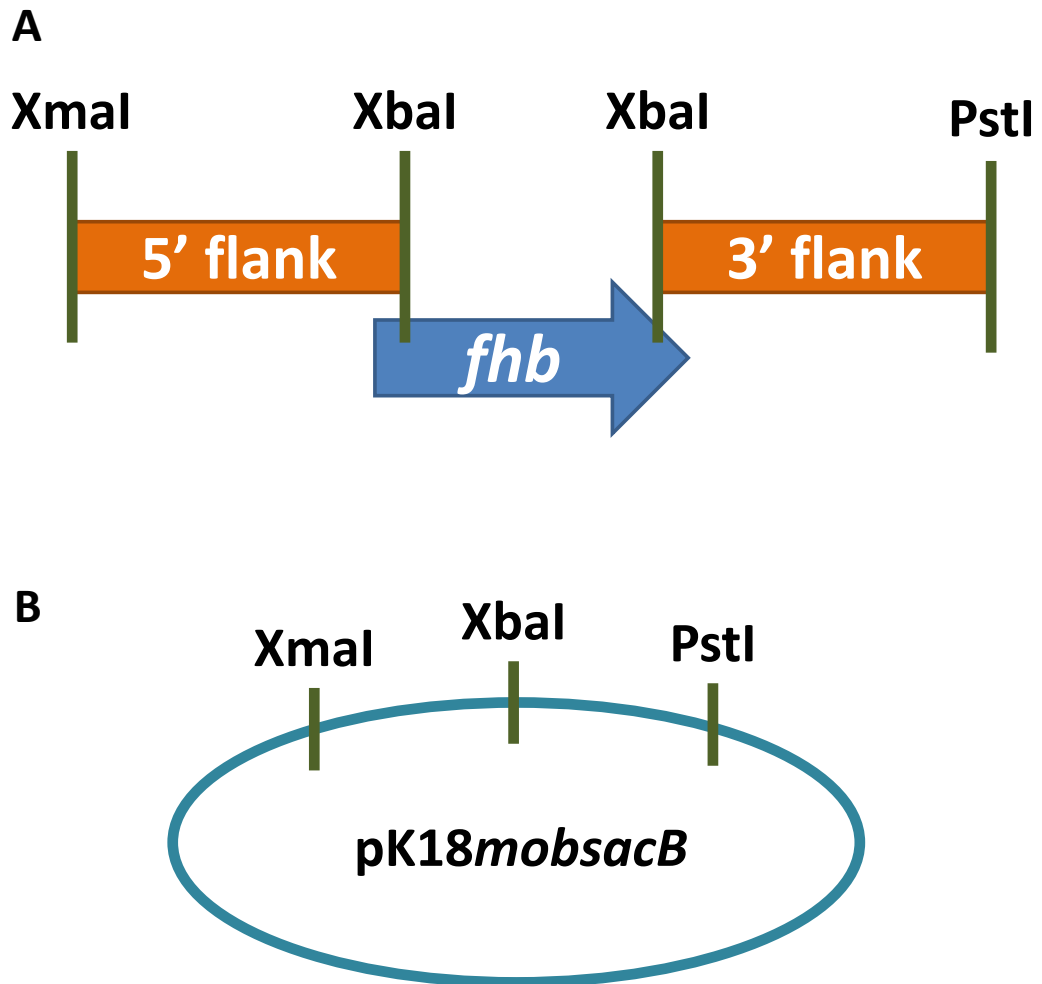


Figure 4.7: The 3' and 5' flanking regions with restriction sites (A) either site of the flavohemoglobin gene from *P. denitrificans*. The flanking regions are amplified with corresponding sticky ends by addition of restriction sites to primers. These restriction sites are used for insertion into the pK18mobsacB plasmid (B).

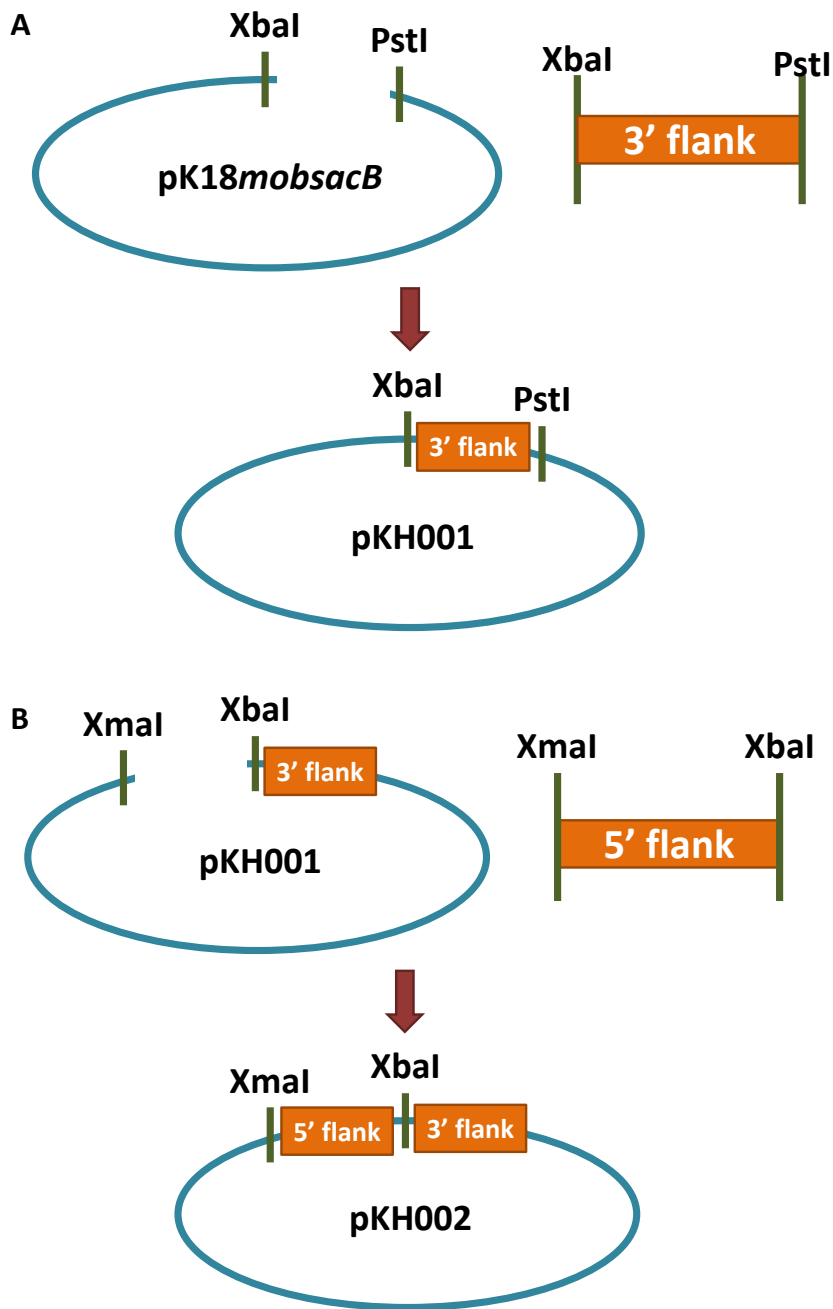


Figure 4.8: Insertion of the 3' and 5' flanking regions into the *pK18mobsacB* plasmid. A: insertion of 3' flanking region into *pK18mobsacB* plasmid. B: insertion of 5' flanking region to plasmid containing ligated 3' flanking region. PCR amplification of flanking regions. This is followed by restriction digestion with complementary restriction enzymes of both the plasmid and insert and ligation of insert to plasmid.

Ligation was undertaken using a 1:3 molar ratio of pK18*obsacB* vector to 3' fragment insert with the T4 DNA ligase method as detailed in the methods chapter. This was carried out initially with the 3' flanking fragment, and additionally with water as a ligation control to demonstrate the efficiency of the dephosphorylation for preventing re-ligation of the plasmid. Later, each ligation reaction transformed into competent *E. coli* JM101 cells. Two additional controls were used for the transformation; uncut plasmid, which demonstrates quality of competent cells, and digested plasmid, which ensured the plasmid was cut. The transformations were selected by plating on solid LB agar containing kanamycin (Kan). The plasmid pK18*obsacB* contains a multi-cloning site situated within the *lacZ α* gene encoding α -subunit of β -galactosidase. When expressed in a *lacZ α* deficient strain (e.g. *E. coli* JM101, which only contains the ω -subunit of LacZ), this provides functional LacZ. This can be used for cloning purposes, when DNA is inserted into the multi-cloning site of pK18*obsacB*, *lacZ α* is interrupted and β -galactosidase activity is lost. Therefore, the LB^{Kan} agar plates were additionally supplemented with both isopropylthio- β -galactoside (IPTG) and 5-bromo-4-chloro-3-indolyl- β -D-galactopyranoside (X-gal). IPTG serves as an inducer for LacZ expression, and X-gal is a galactose analogue that produces a chromogenic (blue) product when cleaved by LacZ. This results in cells transformed with plasmid containing recombinant DNA producing white colonies and cells transformed with non-recombinant plasmids will grow into blue colonies.

Single-colony transformants that grew were a mixture of white and blue colonies, indicating that the ligations and transformations had worked. For example, the plate containing transformants with the un-digested plasmid had > 1000 colonies, indicating that the *E. coli* JM101 cells were competent to take up plasmid DNA. Both the plate with cells transformed with *XbaI-PstI* digested pK18*obsacB* and the plate with the digested and alkaline phosphatase-treated plasmid DNA had 36 blue colonies, indicating that the digestion and dephosphorylation reactions were successful. The plate containing transformants from the insert:plasmid ligation showed approximately 27 blue colonies and 46 white colonies. Eight white colonies were selected for further analysis and inoculated and grown overnight in LBK^{an} liquid media. The corresponding recombinant plasmids were isolated by mini preparation (see the methods chapter) and their inserts were checked by restriction digest using *XbaI* and *PstI* followed by DNA gel electrophoresis. This yielded one plasmid which contained a fragment the same size as the 3' fragment and was termed pKH001.

This process was repeated for the insertion of the 5' flanking insert. For the 5' flank insertion a Kan resistance screen was used. The transformation screen used the same controls and yielded several colonies as potential candidates showing Kan resistance. Kan resistance is transferred to the *P. denitrificans* while the plasmid is in the genome. The master plate was used to transfer 14 candidates which underwent colony PCR. Two colonies were selected for a plasmid mini preparation and restriction digestion using *Xba*I and *Xma*I to confirm the 5' flanking insert and *Xba*I and *Pst*I to confirm the 3' flanking insert were in place. This generated the plasmid was termed pKH002; it is a pK18*mobsacB*-derivative with inserted 3' and 5' flanking regions of the *fhb* gene. A virtual representation of the pKH002 plasmid is shown in figure 4.9, showing the position of the PCR inserts and corresponding restriction digestion sites.

4.4.5 Conjugal transfer of pKH002 to *P. denitrificans* and deletion of the flavohemoglobin gene

The pKH002 plasmid was inserted into *P. denitrificans* using triparental mating as described in the methods using *E. coli* containing the conjugal transfer plasmid pRK2013. These Kan^R transconjugants were then picked and purified by re-streaking on to new plates of the same LB Rif Kan plates. This single cross over event is shown in figure 4.10 To select for a double cross over event and induce the deletion of the chromosomal *fhb* gene by allelic exchange, a second selection was carried out. Briefly, the Kan^R transconjugants were grown in the absence of antibiotics in LB medium until stationary phase. These stationary phase cells were serially diluted and 100 µl of the 10⁰ – 10⁻⁶ dilutions were plated on to LB media containing 20% sucrose (w/v). In addition, the 10⁻⁶ dilutions were also plated on to media without sucrose as an extra control, and all plates were incubated for 4 days at 30°C. The control plates without sucrose had approximately 1000 colonies, which equated to 1.0 x 10¹⁰ CFU/ml. The effect of sucrose on the number of colonies was striking. On the 10⁻⁴ plate only 2 colonies appeared, and 26 were on the 10⁻³ plate, indicating a CFU/ml on sucrose of approximately 2.6 x 10⁵, indicating a frequency of double recombination of approximately 1 in every 38,500 colonies.

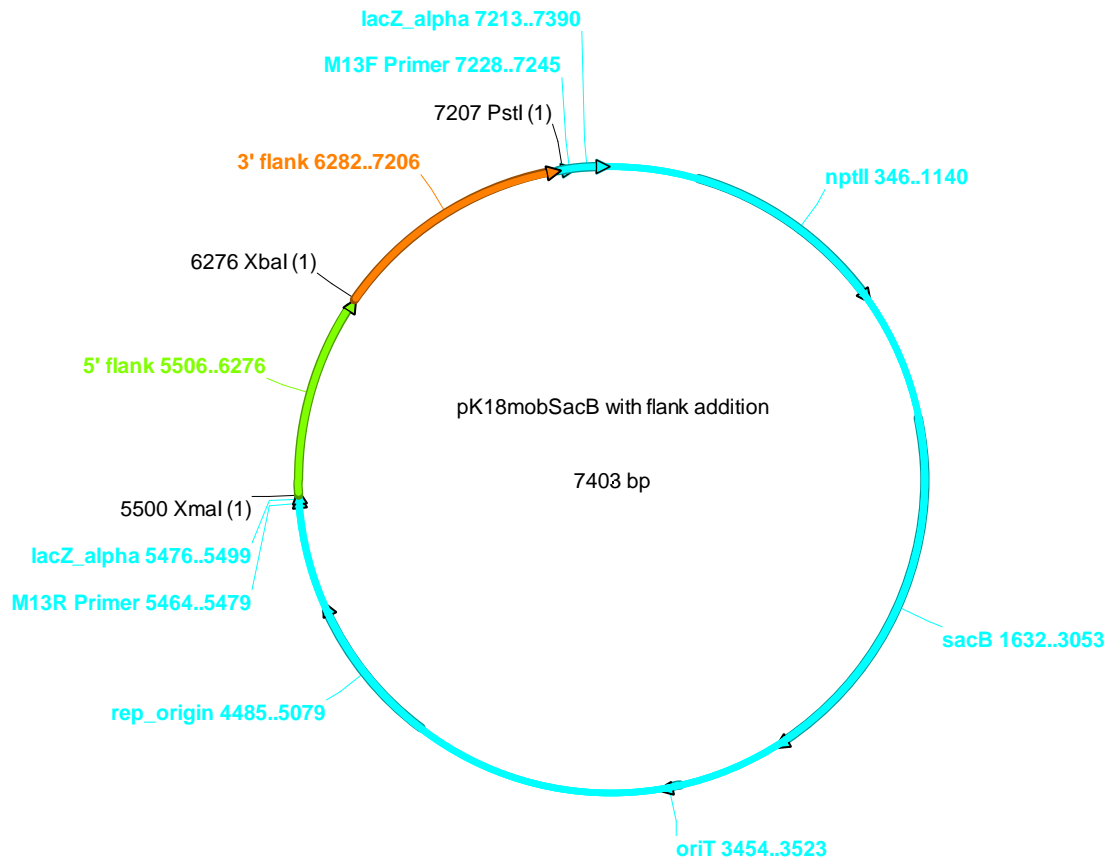


Figure 4.9: The pK18*mobsacB* plasmid showing the inserted 3' and 5' flanking fragments and restriction cut sites: *Xma*I, *Xba*I and *Pst*I. Also shown is the levan sucrose sacB (1421 bp) and neomycin phosphotransferase gene conveying kanamycin resistance NPT II (794 bp) and disruption of the lacZ- α .

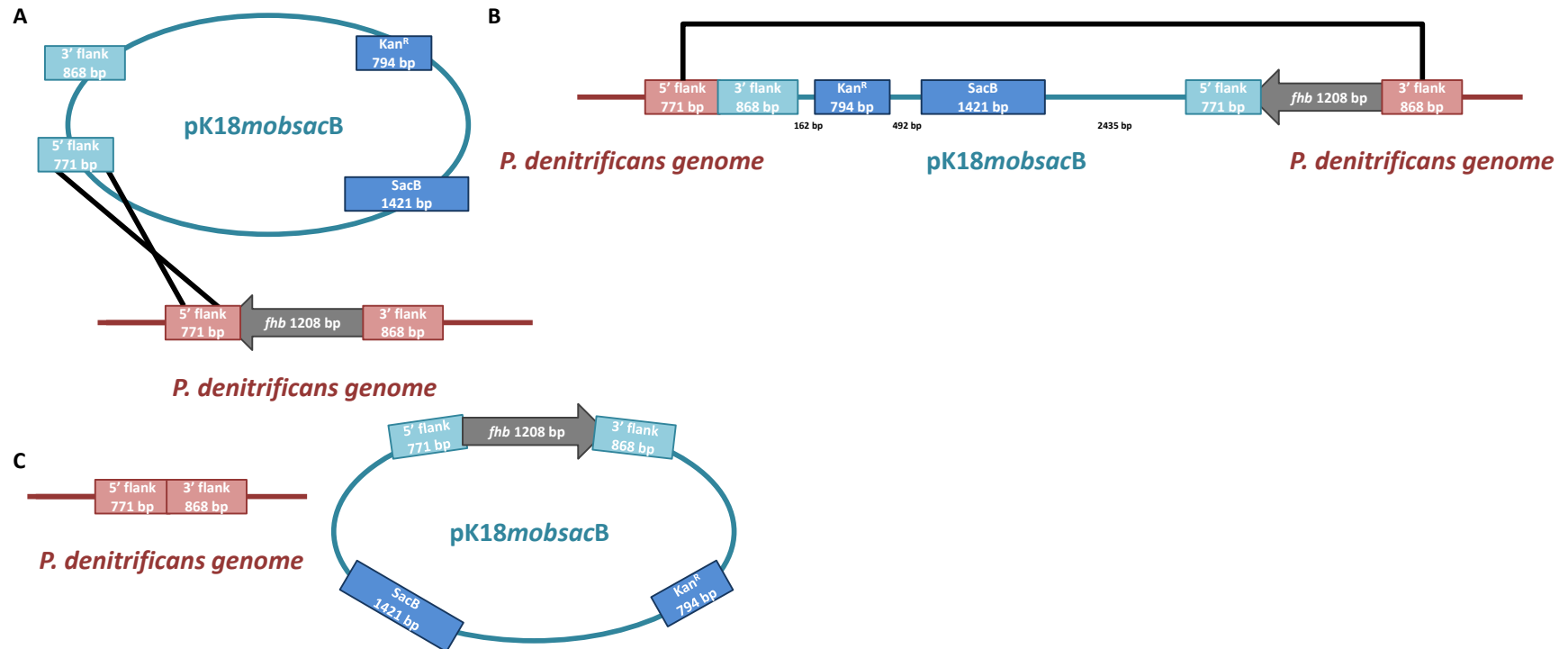


Figure 4.10: Single and double cross over of the pKH002 plasmid in *P. denitrificans*, yielding two colonies devoid of the kanamycin resistance and sucrose induced levan toxin. A: primary cross over inserting plasmid into the *P. denitrificans* genome and conveying kanamycin resistance to the organism. B: Plasmid in *P. denitrificans* genome. The secondary cross over removes plasmid and flavohemoglobin gene from the *P. denitrificans* genome. C: Cross overs complete, levan sucrose *sacB* and neomycin phosphotransferase gene NPT II are removed from the *P. denitrificans* genome, losing kanamycin resistance. The subsequent *P. denitrificans* genome lacking *fhb* is termed PDKH001.

To screen the resultant, sucrose-resistant colonies for the loss of the pKH002-derived DNA, encoding the Kan^R marker, colonies were picked using sterile toothpicks and transferred to LB plates containing Rif, and then subsequently to plates containing Rif and Kan. Those that had lost the Kan^R marker were then screened by PCR to further characterise the deletion. Of 12 colonies picked to Rif and Rif Kan LB plates, two were selected for further analysis. These were inoculated into LB media and grown to stationary phase prior to extraction of genomic DNA. These DNA isolations were then used as templates to amplify the region surrounding *fhb*,

The action of the double cross over event is shown in figure 4.10. Consistent with a successful deletion, bands of ~600 bp were seen in the mutant, whereas the WT yielded a band of ~1.1 kb, consistent with the 1154 bp expected. This shows loss of ~500 bp the mutant *P. denitrificans* genome. The PCR products from the *fhb* mutant were also sequenced to confirm the mutation, and this new *fhb* strain was labelled *P. denitrificans* PDKH01. The deletion of *fhb* gene was confirmed using a genomic DNA preparation and the flanking PCR primers and sequencing. The sequence data was aligned to the genome sequence of *P. denitrificans* at the region of interest to confirm the loss of *fhb*. This sequence data showed a confirmed loss of 534 bp in mutant *P. denitrificans* genome. This determines the band seen from mutant *P. denitrificans* gDNA in figure 4.11 lanes 2 and 3, at 620 bp in size and confirms the removal of 534 bp of gDNA. Alignment of the sequenced DNA to that of the *P. denitrificans* genome shows a missing portion which covers a large portion of the *fhb* shown in figure 4.12. The missing portion of 534 bp in the 1671981 – 1672515 bp range removes the globin, haem containing portion of the gene. This leaves 592 bp of the FAD / NAD binding domain in the 1671389 - 1671981 bp range of the *fhb* remaining in the genome of *P. denitrificans*.

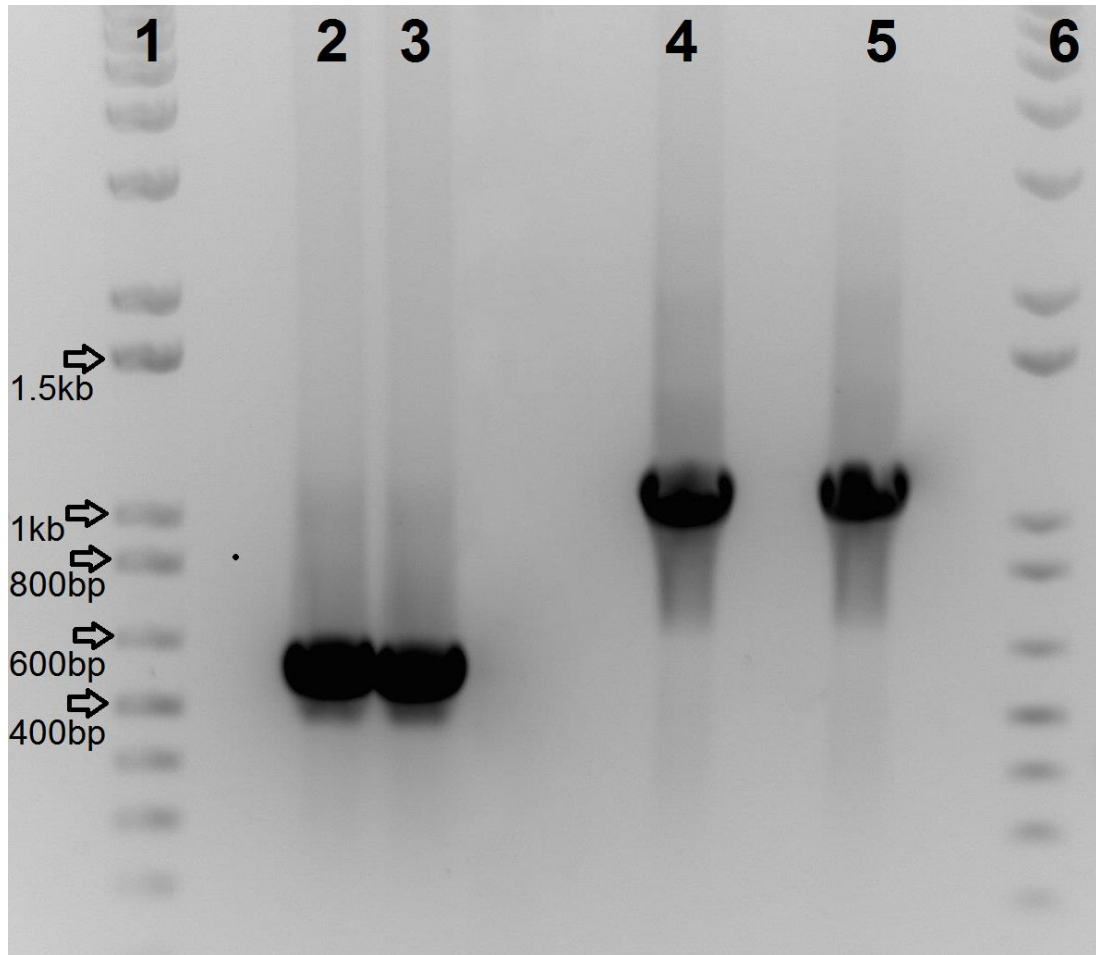
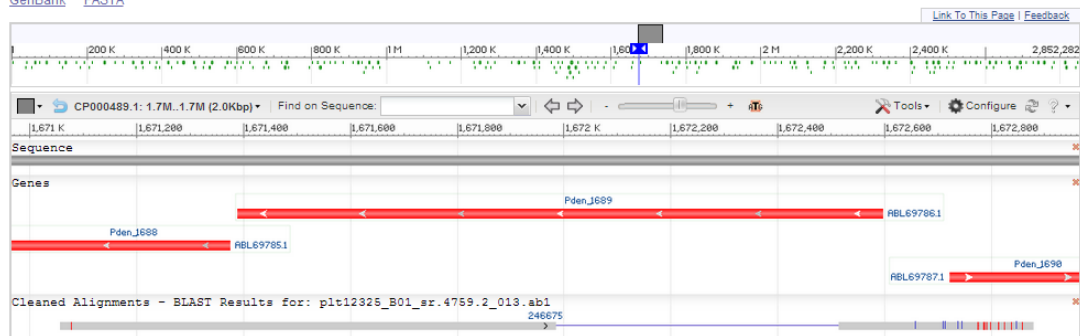


Figure 4.11: Genomic DNA extracted from wild type (WT) *P. denitrificans* and mutant *P. denitrificans* showing deletion of ~500 bp region at the site of the flavohemoglobin gene (*fhb*). 1: DNA ladder, 2 and 3 two colonies of *P. denitrificans* genomic DNA (gDNA) of approximately 600 bp, 4 and 5 WT *P. denitrificans* gDNA of approximately 1.1 kb. There is a ~500 bp loss of DNA in the mutant *P. denitrificans* genome.

Paracoccus denitrificans PD1222 chromosome 1, complete sequence

GenBank: CP000489.1
[GenBank](#) [FASTA](#)

A



Paracoccus denitrificans PD1222 chromosome 1, complete sequence

GenBank: CP000489.1
[GenBank](#) [FASTA](#)

B

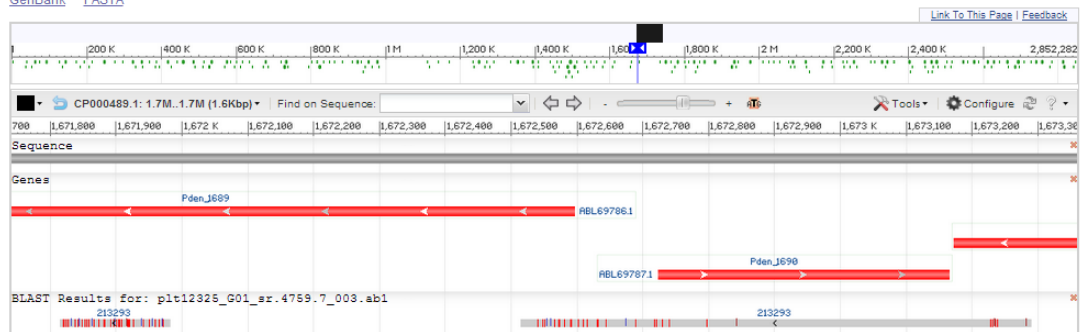


Figure 4.12: Sequencing of the flavohemoglobin mutation. Sequencing data is grey against the *P. denitrificans* genome (red). A: 5' to 3' sequence read and B: 3' to 5' sequence read of genomic DNA from *P. denitrificans* using *fhb* primers showing missing portion of the *fhb* gene.

4.4.6 Growth phenotype of the *P. denitrificans* flavohemoglobin deletion mutant

The role of the flavohemoglobin (*fhb*) was investigated by mutational study which removed the functional *fhb* (Pden_1689). Growth of the mutant was carried out using plate reader batch culture for growth phenotype comparison to the wild type (WT) strain of *P. denitrificans* in minimal salts media at pH 7.5. Growth was measured over 30 hours by optical density at 600 nm that was adjusted to a pathlength of 1 cm with the addition of filter sterilised sodium nitrite concentrations and is shown in figure 4.13. Addition of nitrite to the Δfhb strain of *P. denitrificans* shows an inhibitory effect on growth. Increased nitrite concentration leads to an increased lag phase of growth and a reduction in final optical density. Growth continues to a nitrite concentration of 50 mM nitrite before growth is inhibited.

The kinetic parameters of apparent growth constant (μ_{app} h⁻¹) and maximum biomass produced (Y_{max} AU) were taken from these growth curves and are summarised in the appendix. The μ_{app} was taken from the linear gradient of the growth curve semi log plot of the as detailed in the methods. The kinetic parameters for the Δfhb were compared to the WT strain of *P. denitrificans* growth in batch culture on plates at pH 7.5 and are shown figure 4.14. Without nitrite the Δfhb has a lower μ_{app} of 0.31 ± 0.01 h⁻¹ than that of the WT, which has a μ_{app} of 0.44 ± 0.01 h⁻¹ (figure 4.14 A).

The Δfhb μ_{app} is fairly irregular at concentrations below 40 mM nitrite. This is a greater variation than the WT type which shows an unfluctuating μ_{app} decrease as nitrite concentration increases to 40 mM nitrite. The Δfhb shows growth inhibition at a nitrite concentration of 50 mM. The WT strain is able to grow at 50 mM nitrite and has a value of 0.33 ± 0.01 h⁻¹. Final WT growth inhibition occurs at 55mM nitrite, which is 5 mM higher than the deletion mutant. The μ_{app} of the WT increases between 50 – 55 mM over the highest 5 mM of nitrite tolerance. This is not seen in the Δfhb over the 45 – 50 mM final tolerance of the Δfhb .

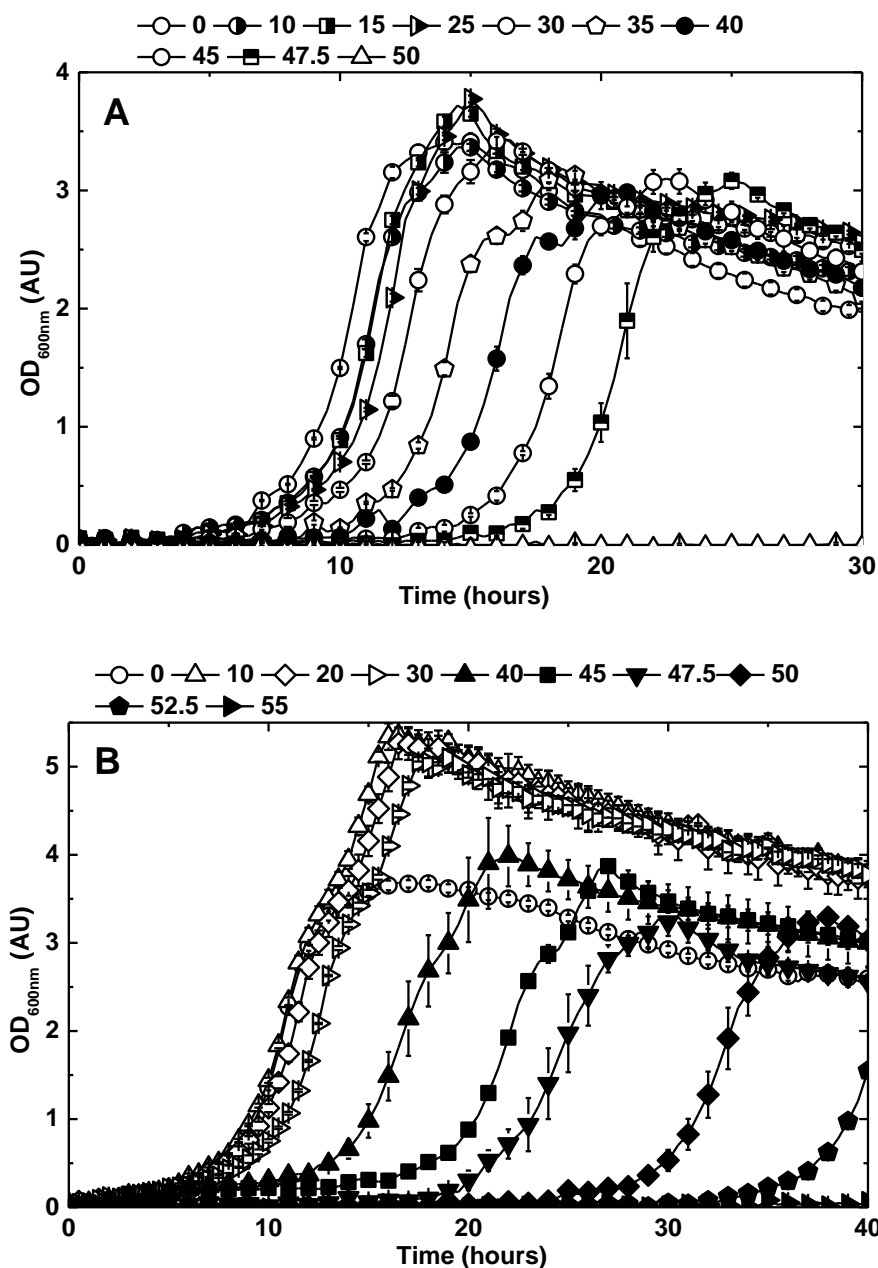


Figure 4.13: A: Growth of FHB deletion mutant, error bars denote standard error $n = 3$ and B: Growth of WT *P. denitrificans*, error bars denote standard error $n = \geq 3$. Minimal salts media, pH 7.5, supplemented with ammonium chloride, 10 mM, sodium succinate, 30 mM and Vishniac trace element solution, with various sodium nitrite concentrations (mM) as shown in the key above the figure. Measured by optical density at 600 nm (OD_{600nm}) adjusted to a pathlength of 1 cm against time (h). Cells were grown in 100 μ l total volume with shaking at 400 rpm. OD_{600nm} was measured every 0.5 h, 1 h values shown.

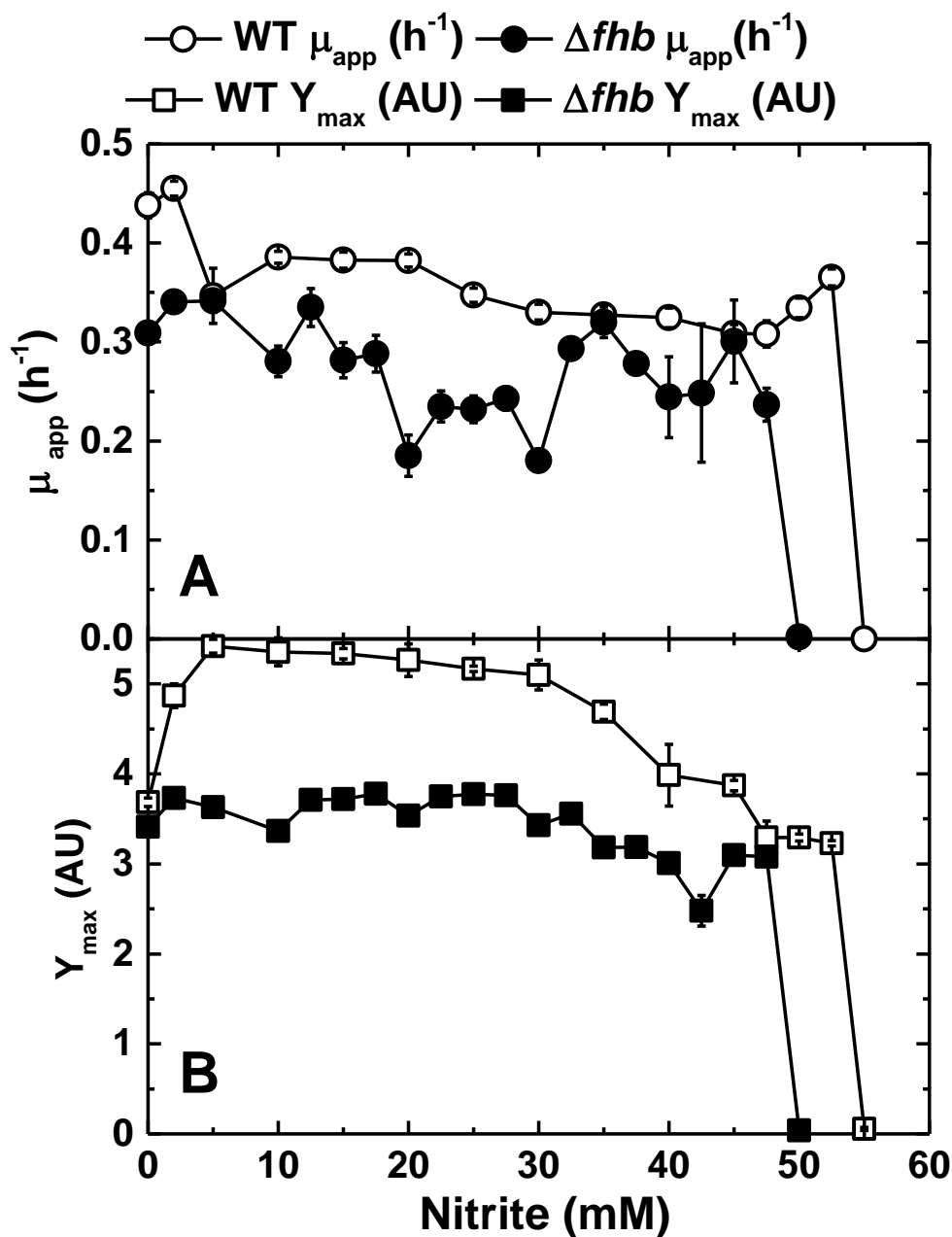


Figure 4.14: Summarised apparent growth constant (μ_{app}) and maximum biomass produced (Y_{max} AU) at various calculated nitrite (mM) concentrations for the growth of *P. denitrificans* and the Δfhb mutant. Growth in minimal salts media, pH 7.5, supplemented with ammonium chloride, 10 mM, sodium succinate, 30 mM and Vishniac trace element solution. Measured by optical density at 600 nm (OD_{600nm}) adjusted to a pathlength of 1 cm against time (h). Error bars denote standard error $n = \geq 3$.

Significantly, the increased growth as shown by Y_{\max} AU that is stimulated by nitrite addition in the WT strain is not observed in the deletion mutant (figure 4.14 B). Maximum biomass production for the Δfhb remains similar to that of growth without nitrite until inhibition occurs at 50 mM nitrite. The Δfhb has an Y_{\max} of 3.4 ± 0.1 AU with 0 mM nitrite, which increases to 3.8 ± 0.03 at 25 mM nitrite which decreases to 3.1 ± 0.1 at 45 mM nitrite addition. The WT shows an increase in Y_{\max} from 3.7 ± 0.05 AU at 0 mM nitrite to a highest Y_{\max} of 5.4 ± 0.1 AU at 5 mM nitrite. A >4.0 AU Y_{\max} , is maintained between at concentrations >45 mM nitrite. Y_{\max} , then reduces to 3.2 ± 0.03 AU at 52.5 mM nitrite addition.

4.4.7 The flavohemoglobin complementation using vector reinsertion into *P. denitrificans*

The mutant phenotype was complemented *in trans* by reinsertion of the *fhb* into *P. denitrificans* using the wide host-range pOT2 vector (Spaink *et al.*, 1987). Primers were designed to amplify *fhb* plus 264 bp of DNA upstream to include any native *cis*-acting elements. *Xba*I restriction sites were added to these oligonucleotides to enable restriction digestion of the plasmid pOT2 at the *Xba*I site and insertion of the amplified PCR product

No additional *Xba*I sites were located in the region, which would interfere with the insertion reaction. Genomic DNA isolated from *P. denitrificans* was used as a template for PCR reactions and the complementary fragment containing *fhb* was amplified to produce the DNA product of 1499 bp. The resulting *fhb* cleaned PCR product (18.5 ng.ml^{-1}) and dephosphorylated plasmid (22.5 ng.ml^{-1}) were ligated using a 1:3 molar ratio of pOT2 to fragment insert with the T4 DNA ligase method as previously described and detailed in the methods. This was carried out initially with the insert fragment and a water ligation control to demonstrate the efficiency of the dephosphorylation for preventing relegation of the plasmid. Later, each ligation reaction transformed into competent *E. coli* JM101 cells. As above, two additional controls were used for the transformation; uncut pOT2 and digested plasmid. The transformations were selected by plating on solid LB agar containing gentamicin (Gent).

A broad number of colonies were produced and colony PCR used to identify candidates containing the *fhb* fragment. Of these 13 were selected for plasmid mini preparation. The resulting plasmid was entered into the *P. denitrificans* genome using the triparental mating method. Colonies were screened with gentamicin confirming the presence of the pOT2 plasmid. Midi preparation of the plasmid and restriction digest, using *Xba*I, confirmed the insertion of the *fhb* into *P. denitrificans* (figure 4.15). This plasmid was labelled pKH003. The *fhb* was expressed from its own promoter by incorporating the 200 bp of DNA upstream of the *fhb* gene, rather than an inducible, ectopic promoter. Conjugation of the pKH003 into *P. denitrificans* used triparental mating as described in the methods chapter and transconjugants section. Colonies were selected with Gent^R and then selected on LB^{Rif} Gent to confirm growth of *P. denitrificans*. A plate reader growth experiment was under-taken examining the growth of the *fhb* complement *P. denitrificans* under nitrite stress. The pH 7.5 experiment was repeated as carried out for WT and mutant Δfhb *P. denitrificans* using minimal salt media and addition of nitrite. The phenotype of growth at high nitrite was restored as can be seen in figure 4.16, which shows growth of the WT, mutant Δfhb and *fhb* complemented *P. denitrificans* grown at 50 mM sodium nitrite. Growth is seen in the WT and *fhb* complement *P. denitrificans*, but the mutant Δfhb *P. denitrificans* is devoid of growth.

4.5 Discussion

4.5.1 Comparison of the batch culture growth in 250 ml flasks and 0.1 μ l plate well

The use of batch growth by shaking flask technique has been validated by comparative studies within this chapter. The apparent growth constant (μ_{app}) is identical across both the shaking flask (SF) and plate reader (PR) batch growth techniques. There is also a similarity across the highest cellular density achieved (Y_{max}) for both SF and PR techniques. This 0.51 AU difference between the Y_{max} of the SF and PR batch culture may be due to a difference in the stimulatory effect seen in the previous chapter when nitrite is at a concentration which stimulates growth rather than inhibits it. It has been suggested in the previous chapter that growth stimulation may be due to assimilation of nitrite or denitrification at low oxygen tolerance. The use of a shake flask may be causing a higher level of nitrite consumption, as it could have a higher tendency to reach anaerobicity at high cellular density. This is an

additional reason for the extraction of RNA at mid exponential growth for transcriptional analysis. In this way, anaerobic or assimilatory effects will not be observed at mid exponential growth phase. This suggests the growth method does not affect the rate of cellular division or consumption of nutrients in *P. denitrificans*. This allows both methods of batch culture to be used and compared through this study and validates the SF technique as a reproducible, scaled up method of growing cells under nitrite stress conditions. There is an observable increase in lag phase in the PR technique when compared directly to the SF technique. This is due to the method of inoculation. Both batch growth techniques were inoculated using a 1% volume of 1 OD unit of cells growth previously overnight. The PR flasks were inoculated into 10 ml vials, from which aliquots of 100 μ l were removed for the 96 well plates. Comparatively, the shaking flask was inoculated directly in to the 50 ml flask using aseptic technique. More cells are transferred to the shake flask due to the use of a larger pipette tip.

4.5.2 The role of *P. denitrificans* flavohemoglobin in nitrite tolerance

Bioinformatic analysis of the *P. denitrificans* genome has produced a candidate with homology to a known nitric oxide (NO) detoxification protein Hmp. This gene was Pd1689 encoding a flavohemoglobin (*fhb*). The *fhb* was the only gene showing sequence similarity to the *Salmonella Typhimurium* Hmp and so was explored using mutation manipulation. Successful completion of *fhb* mutant allowed phenotype characterisation of the Δ *fhb* strain. Growth of this mutant occurs at very high nitrite concentrations up to 50 mM (figure 4.13). This suggests that *fhb* would act at high nitrite concentrations to provide an additional level of tolerance at the very end of nitrite tolerance, where it would be able to complement additional stress response systems. Although apparent growth follows a similar pattern to that of the wild type (WT) (figure 4.14), it is more variable and shows fluctuation. There is also a lack of the characteristic increase in exponential growth between 50 to 55 mM nitrite. This increase in μ_{app} at 50 mM nitrite before sudden growth inhibition at 55 mM seen in the WT is not seen in the mutant. The additional feature of mutant growth inhibition at 50 mM nitrite suggests that the growth increase seen between 50 – 55 mM may be representative of *fhb* utilisation. This would explain its absence in the Δ *fhb* deletion mutant.

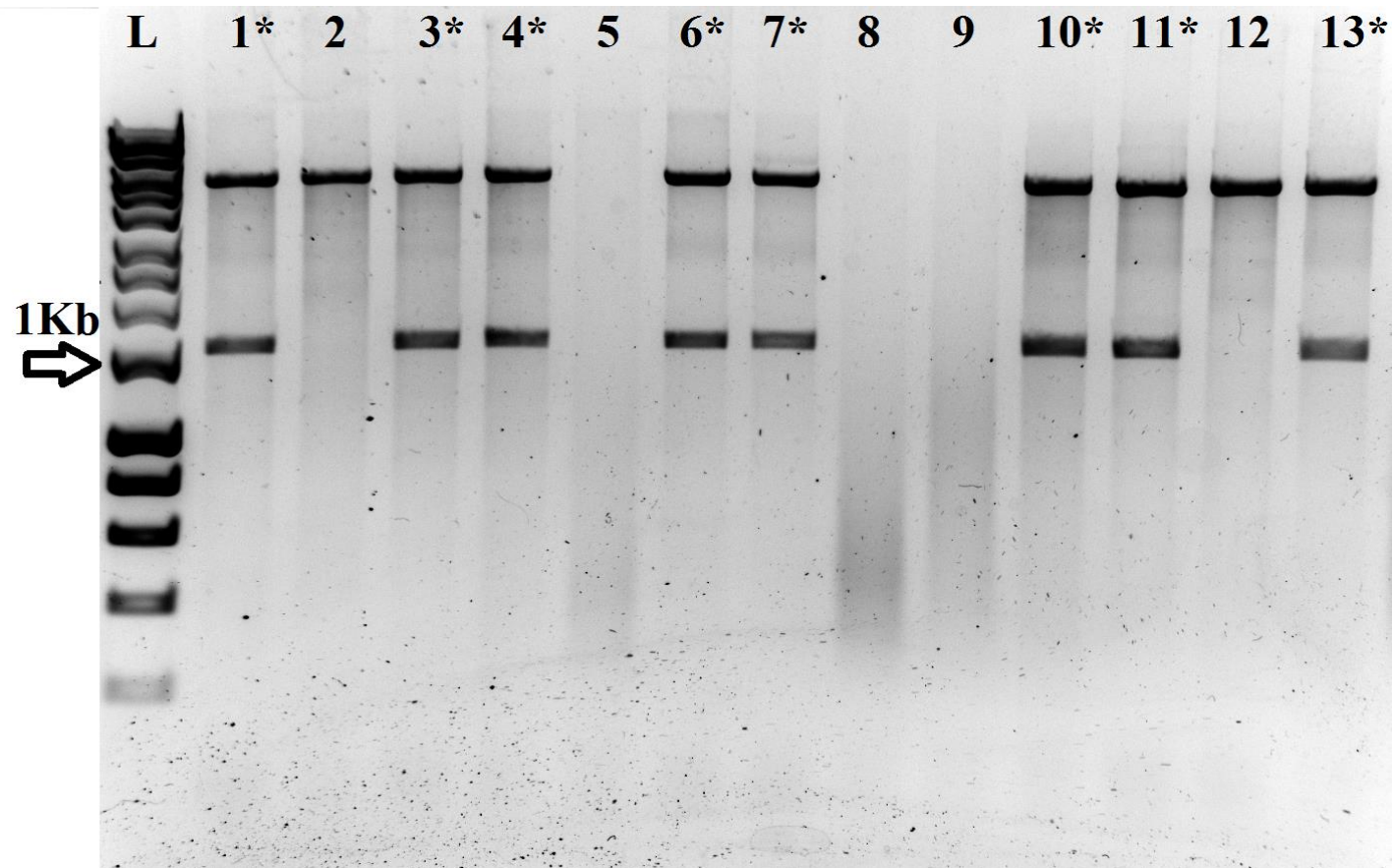


Figure 4.15: Restriction digests of screened colonies containing pOT2 with the flavohemoglobin insert. L: 1 kb ladder, 1 – 13: colonies selected from gentamicin screening plates after transformation of the flavohemoglobin fragment and pOT2 plasmid, analysed by plasmid mini preparation and digestion with *Xba*I.

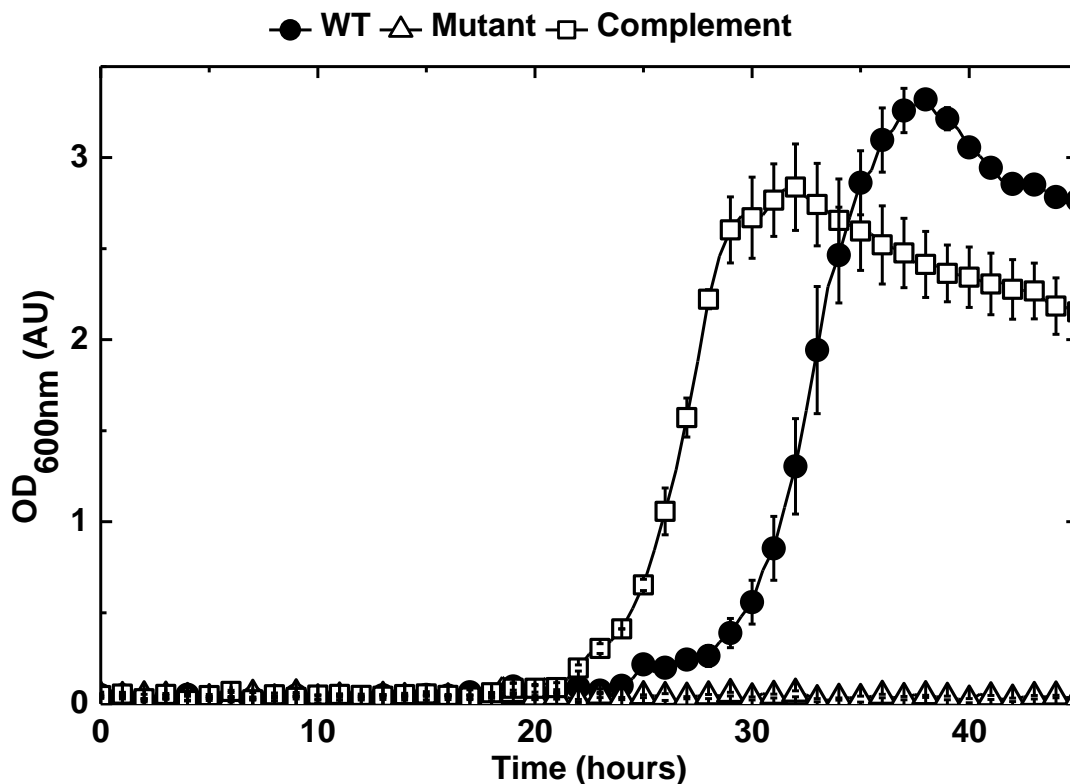


Figure 4.16: Growth of *P. denitrificans* wild type (WT), FHB deletion mutant and FHB complement strain (as shown in key at the top of the figure). Grown in minimal salts media at pH 7.5 and supplemented with ammonium chloride, 10 mM, sodium succinate, 30 mM and Vishniac trace element solution, with 50 mM sodium nitrite. Measured by optical density at 600 nm (OD_{600nm}) adjusted to a pathlength of 1 cm against time (h). Cells were grown in 100 μ l total volume with shaking at 400 rpm. OD_{600nm} was measured every 0.5 h, 1 h values shown. Error bars denote standard error $n = 3$.

The generation of biomass differs greatly between the Δfhb and WT strains. In the WT there is a characteristic stimulation of biomass production which is seen to occur from 2 mM nitrite to 50 mM nitrite. This is distinctly not the case for Δfhb . For the Δfhb biomass production remains relatively constant and similar to that of Δfhb without nitrite. Biomass stimulation is a unique characteristic of the WT strain of *P. denitrificans*. These observations suggest that *fhb* provides an additional 5 mM tolerance to nitrite above 50 mM. In that additional 5 mM growth rate increases and generating a surge of growth before inhibition of growth occurs. At lower nitrite concentrations, *fhb* provides additional tolerance in a so far unknown cooperative capacity stabilising and providing consistency in exponential growth which becomes erratic in Δfhb . Finally *fhb* provides a stimulation of biomass production at >50 mM levels of nitrite. This may be due to its action as a nitric oxide dioxygenase, catalyzing the production of nitrate for assimilation into biomass. The action of Hmp is as a nitric oxide dioxygenase to catalyse the conversion of NO to NO₃⁻: $2\text{NO} + 2\text{O}_2 + \text{NAD(P)H} \rightarrow 2\text{NO}_3^- + \text{NAD(P)}^+ + \text{H}^+$ in the presence of oxygen (Forrester and Foster, 2012). The *fhb* homology to *Hmp* suggests it can function to catalyse the same reaction. It is apparent that a novel flavohemoglobin resides in the genome of *P. denitrificans* showing homology to that of the *Salmonella Typhimurium Hmp*. Based on the evidence presented in the phenotyping of an *fhb* deletion mutant, *fhb* is suggested to play a role in high level nitrite tolerance. At the lower nitrite levels explored, exponential growth of the mutant is comparable to that of the wild type (WT).

4.5.3 Bioinformatic characterisation of a transcriptional regulator in association with the flavohemoglobin in *P. denitrificans*

Further bioinformatic characterisation of *fhb* shows a transcriptional regulator up stream of the *fhb* Pden_1689. This gene is Pden_1690 and is annotated in the NCBI database as encoding for a protein of a transcriptional regulator of the BadM/Rrf2 family. The regulator Pd1690 is annotated in the National Centre for Biotechnology Information (NCBI) database with reference sequence: YP_915483 and of 147 amino acids (aa) in length. NCBI annotation shows a helix-turn-helix domain region at aa 1 to 136, which is described more specifically within the EMBL-EBI database as a winged helix-turn-helix transcription repressor; the winged nature of the helix-turn-helix coming from two small beta-sheet loops; these two wings (W1, W2), three alpha helices (H1, H2, H3) and three beta-sheets (S1, S2,

S3) arranged as H1-S1-H2-H3-S2-W1-S3-W2 (Gajiwala and Burley, 2000). Additional features are DNA-binding and homology to the Rrf2 superfamily in the 1 to 127 region. Rrf2 proteins belong to a family of transcriptional regulator typically found upstream as an initial gene for the sulphur assimilation (SUF) operon. The SUF operon acts as an alternative iron-sulphur cluster (ISC) system pathway under conditions of iron limitation and in the presence of oxidative stress. A feature classification as carried out in *Bacillus subtilis* in the European Bioinformatics Institute (EMBL-EBI) database InterPro of significance was the association with the transcriptional repressor HTH-type NsrR (Nakano *et al.*, 2006). NsrR is characterised as a protective mechanism for bacterial cells against nitrosative stress. It features nitric oxide-sensitivity which induces release of NsrR from DNA and transcription of nitric oxide detoxification enzymes including *Hmp* (Bodenmiller and Spiro, 2006). Exploration of HTH-type NsrR (HAMAP accession MF_01177) found 751 hits within the UniProt and UniProtKB database, 335 of which are from *Escherichia coli* and 151 from *Salmonella choleraesuis*. Multiple candidates have been found with potential capability to detoxify nitric oxide (NO) and sequence similarity to the *fhb* and *norW* flavorubredoxin. Transcriptional analysis of these genes by type II microarray will be able to establish the levels of gene transcription in the presence of nitrite for the multiple genes of interest, and develop a postulated model for the effect of nitrite-induced stress and NO detoxification at a transcriptional level.

4.6 References

- ANDREWS, S. C., SHIPLEY, D., KEEN, J. N., FINDLAY, J. B., HARRISON, P. M. & GUEST, J. R. 1992. The haemoglobin-like protein (HMP) of *Escherichia coli* has ferrisiderophore reductase activity and its C-terminal domain shares homology with ferredoxin NADP⁺ reductases. *FEBS Letters*, 302, 247-52.
- BELL, L. C., RICHARDSON, D. J. & FERGUSON, S. J. 1992. Identification of nitric oxide reductase activity in *Rhodobacter capsulatus*: the electron transport pathway can either use or bypass both cytochrome *c*₂ and the cytochrome *bc*₁ complex. *Journal of General Microbiology*, 138, 437-43.
- BODENMILLER, D. M. & SPIRO, S. 2006. The *yjeB* (*nsrR*) gene of *Escherichia coli* encodes a nitric oxide-sensitive transcriptional regulator. *Journal of Bacteriology*, 188, 874-881.
- BOUCHAL, P., STRUHÁROVÁ, I., BUDINSKÁ, E., ŠEDO, O., VYHLÍDALOVÁ, T., ZDRÁHAL, Z., VAN SPANNING, R. & KUČERA, I. 2010. Unraveling an FNR based regulatory circuit in *Paracoccus denitrificans* using a proteomics-based approach. *Biochimica et Biophysica Acta - Proteins and Proteomics*, 1804, 1350-1358.

- BOYSEN, A., MOLLER-JENSEN, J., KALLIPOLITIS, B., VALENTIN-HANSEN, P. & OVERGAARD, M. 2010. Translational regulation of gene expression by an anaerobically induced small non-coding RNA in *Escherichia coli*. *Journal of Biological Chemistry*, 285, 10690-702.
- BROWNING, D. F., BEATTY, C. M., WOLFE, A. J., COLE, J. A. & BUSBY, S. J. 2002. Independent regulation of the divergent *Escherichia coli* *nrfA* and *acsPI* promoters by a nucleoprotein assembly at a shared regulatory region. *Molecular Microbiology*, 43, 687-701.
- BROWNING, D. F., LEE, D. J., SPIRO, S. & BUSBY, S. J. 2010. Down-regulation of the *Escherichia coli* K-12 *nrf* promoter by binding of the NsrR nitric oxide-sensing transcription repressor to an upstream site. *Journal of Bacteriology*, 192, 3824-8.
- BUSCH, A., FRIEDRICH, B. & CRAMM, R. 2002. Characterization of the *norB* gene, encoding nitric oxide reductase, in the nondenitrifying cyanobacterium *Synechocystis* sp. strain PCC6803. *Applied and Environmental Microbiology*, 68, 668-72.
- DAIBER, A., DAUB, S., BACHSCHMID, M., SCHILDKNECHT, S., OELZE, M., STEVEN, S., SCHMIDT, P., MEGNER, A., WADA, M., TANABE, T., MUNZEL, T., BOTTARI, S. & ULLRICH, V. 2013. Protein tyrosine nitration and thiol oxidation by peroxynitrite-strategies to prevent these oxidative modifications. *International Journal of Molecular Sciences*, 14, 7542-70.
- DARWIN, A., HUSSAIN, H., GRIFFITHS, L., GROVE, J., SAMBONGI, Y., BUSBY, S. & COLE, J. 1993. Regulation and sequence of the structural gene for cytochrome *c₅₅₂* from *Escherichia coli*: not a hexahaem but a 50 kDa tetrahaem nitrite reductase. *Molecular Microbiology*, 9, 1255-65.
- DE BOER, A. P. N., VAN DER OOST, J., REIJNDERS, W. N. M., WESTERHOFF, H. V., STOUTHAMER, A. H. & VAN SPANNING, R. J. M. 1996. Mutational analysis of the *nor* gene cluster which encodes nitric-oxide reductase from *Paracoccus denitrificans*. *European Journal of Biochemistry*, 242, 592-600.
- ERMLER, U., SIDDIQUI, R. A., CRAMM, R. & FRIEDRICH, B. 1995. Crystal structure of the flavohemoglobin from *Alcaligenes eutrophus* at 1.75 Å resolution. *EMBO Journal*, 14, 6067-77.
- FIELD, S. J., THORNDYCROFT, F. H., MATORIN, A. D., RICHARDSON, D. J. & WATMOUGH, N. J. 2008. The respiratory nitric oxide reductase (NorBC) from *Paracoccus denitrificans*. *Methods in Enzymology*, 437, 79-101.
- FORRESTER, M. T. & FOSTER, M. W. 2012. Protection from nitrosative stress: A central role for microbial flavohemoglobin. *Free Radical Biology and Medicine*, 52, 1620-1633.
- GAJIWALA, K. S. & BURLEY, S. K. 2000. Winged helix proteins. *Current Opinion in Structural Biology*, 10, 110-116.
- GARDNER, A. M., HELMICK, R. A. & GARDNER, P. R. 2002. Flavorubredoxin, an inducible catalyst for nitric oxide reduction and detoxification in *Escherichia coli*. *Journal of Biological Chemistry*, 277, 8172-8177.
- GARDNER, P. R., GARDNER, A. M., MARTIN, L. A., DOU, Y., LI, T., OLSON, J. S., ZHU, H. & RIGGS, A. F. 2000. Nitric-oxide dioxygenase activity and function of flavohemoglobins. sensitivity to nitric oxide and carbon monoxide inhibition. *Journal of Biological Chemistry*, 275, 31581-7.
- GARDNER, P. R., GARDNER, A. M., MARTIN, L. A. & SALZMAN, A. L. 1998. Nitric oxide dioxygenase: an enzymic function for flavohemoglobin. *Proceedings of the National Academy of Sciences*, 95, 10378-83.
- GILL, S. R., FOUTS, D. E., ARCHER, G. L., MONGODIN, E. F., DEBOY, R. T., RAVEL, J., PAULSEN, I. T., KOLONAY, J. F., BRINKAC, L., BEANAN, M., DODSON,

- R. J., DAUGHERTY, S. C., MADUPU, R., ANGIUOLI, S. V., DURKIN, A. S., HAFT, D. H., VAMATHEVAN, J., KHOURI, H., UTTERBACK, T., LEE, C., DIMITROV, G., JIANG, L., QIN, H., WEIDMAN, J., TRAN, K., KANG, K., HANCE, I. R., NELSON, K. E. & FRASER, C. M. 2005. Insights on evolution of virulence and resistance from the complete genome analysis of an early methicillin-resistant *Staphylococcus aureus* strain and a biofilm-producing methicillin-resistant *Staphylococcus epidermidis* strain. *Journal of Bacteriology*, 187, 2426-38.
- HAUSLADEN, A., GOW, A. J. & STAMLER, J. S. 1998. Nitrosative stress: metabolic pathway involving the flavohemoglobin. *Proceedings of the National Academy of Sciences*, 95, 14100-5.
- HENZLER, H. J. & SCHEDEL, M. 1991. Suitability of the shaking flask for oxygen supply to microbiological cultures. *Bioprocess Engineering*, 7, 123-131.
- HOUSEHOLDER, T. C., FOZO, E. M., CARDINALE, J. A. & CLARK, V. L. 2000. *Gonococcal* nitric oxide reductase is encoded by a single gene, *norB*, which is required for anaerobic growth and is induced by nitric oxide. *Infection and Immunity*, 68, 5241-6.
- HUTCHINGS, M. I., MANDHANA, N. & SPIRO, S. 2002. The *norR* protein of *Escherichia coli* activates expression of the flavorubredoxin gene *norV* in response to reactive nitrogen species. *Journal of Bacteriology*, 184, 4640-4643.
- JOLLEY, K. A., RAPAPORT, E., HOUGH, D. W., DANSON, M. J., WOODS, W. G. & DYALL-SMITH, M. L. 1996. Dihyrolipoamide dehydrogenase from the halophilic archaeon *Haloferax volcanii*: homologous overexpression of the cloned gene. *Journal of Bacteriology*, 178, 3044-8.
- KIM, S. O., ORII, Y., LLOYD, D., HUGHES, M. N. & POOLE, R. K. 1999. Anoxic function for the *Escherichia coli* flavohaemoglobin (Hmp): reversible binding of nitric oxide and reduction to nitrous oxide. *FEBS Letters*, 445, 389-394.
- KWIATKOWSKI, A. V., LARATTA, W. P., TOFFANIN, A. & SHAPLEIGH, J. P. 1997. Analysis of the role of the *nnrR* gene product in the response of *Rhodobacter sphaeroides* 2.4.1 to exogenous nitric oxide. *Journal of Bacteriology*, 179, 5618-5620.
- LACELLE, M., KUMANO, M., KURITA, K., YAMANE, K., ZUBER, P. & NAKANO, M. M. 1996. Oxygen-controlled regulation of the flavohemoglobin gene in *Bacillus subtilis*. *Journal of Bacteriology*, 178, 3803-3808.
- LAVER, J. R., STEVANIN, T. M., MESSENGER, S. L., LUNN, A. D., LEE, M. E., MOIR, J. W. B., POOLE, R. K. & READ, R. C. 2010. Bacterial nitric oxide detoxification prevents host cell S-nitrosothiol formation: A novel mechanism of bacterial pathogenesis. *FASEB Journal*, 24, 286-295.
- MANNERVIK, B. 1987. The enzymes of glutathione metabolism: An overview. *Biochemical Society Transactions*, 15, 717-8.
- MARCHLER-BAUER, A., LU, S., ANDERSON, J. B., CHITSAZ, F., DERBYSHIRE, M. K., DEWEESE-SCOTT, C., FONG, J. H., GEER, L. Y., GEER, R. C., GONZALES, N. R., GWADZ, M., HURWITZ, D. I., JACKSON, J. D., KE, Z., LANCZYCKI, C. J., LU, F., MARCHLER, G. H., MULLOKANDOV, M., OMELCHENKO, M. V., ROBERTSON, C. L., SONG, J. S., THANKI, N., YAMASHITA, R. A., ZHANG, D., ZHANG, N., ZHENG, C. & BRYANT, S. H. 2011. CDD: a Conserved Domain Database for the functional annotation of proteins. *Nucleic acids research*, 39, D225-D229.
- MASON, M. G., SHEPHERD, M., NICHOLLS, P., DOBBIN, P. S., DODSWORTH, K. S., POOLE, R. K. & COOPER, C. E. 2009. Cytochrome *bd* confers nitric oxide resistance to *Escherichia coli*. *Nature Chemical Biology*, 5, 94-96.

- MEISTER, A. 1988. Glutathione metabolism and its selective modification. *Journal of Biological Chemistry*, 263, 17205-8.
- MILLS, P. C., RICHARDSON, D. J., HINTON, J. C. D. & SPIRO, S. 2005. Detoxification of nitric oxide by the flavorubredoxin of *Salmonella enterica serovar Typhimurium*. *Biochemical Society Transactions*, 33, 198-199.
- MILLS, P. C., ROWLEY, G., SPIRO, S., HINTON, J. C. & RICHARDSON, D. J. 2008. A combination of cytochrome c nitrite reductase (NrfA) and flavorubredoxin (NorV) protects *Salmonella enterica serovar Typhimurium* against killing by NO in anoxic environments. *Microbiology*, 154, 1218-28.
- NAKANO, M. M., GENG, H., NAKANO, S. & KOBAYASHI, K. 2006. The nitric oxide-responsive regulator NsrR controls ResDE-dependent gene expression. *Journal of Bacteriology*, 188, 5878-5887.
- PACHER, P., BECKMAN, J. S. & LIAUDET, L. 2007. Nitric oxide and peroxynitrite in health and disease. *Physiological Reviews*, 87, 315-424.
- PESCE, A., COUTURE, M., DEWILDE, S., GUERTIN, M., YAMAUCHI, K., ASCENZI, P., MOENS, L. & BOLOGNESI, M. 2000. A novel two-over-two alpha-helical sandwich fold is characteristic of the truncated hemoglobin family. *EMBO Journal*, 19, 2424-34.
- POOCK, S. R., LEACH, E. R., MOIR, J. W., COLE, J. A. & RICHARDSON, D. J. 2002. Respiratory detoxification of nitric oxide by the cytochrome c nitrite reductase of *Escherichia coli*. *Journal of Biological Chemistry*, 277, 23664-9.
- POOLE, R. K. & HUGHES, M. N. 2000. New functions for the ancient globin family: bacterial responses to nitric oxide and nitrosative stress. *Molecular Microbiology*, 36, 775-83.
- RIED, J. L. & COLLMER, A. 1987. An *nptI-sacB-sacR* cartridge for constructing directed, unmarked mutations in gram-negative bacteria by marker exchange-ejection mutagenesis. *Gene*, 57, 239-46.
- SCHÄFER, A., TAUCH, A., JÄGER, W., KALINOWSKI, J., THIERBACH, G. & PÜHLER, A. 1994. Small mobilizable multi-purpose cloning vectors derived from the *Escherichia coli* plasmids pK18 and pK19: selection of defined deletions in the chromosome of *Corynebacterium glutamicum*. *Gene*, 145, 69-73.
- SPAINK, H. P., OKKER, R. J. H., WIJFFELMAN, C. A., PEES, E. & LUGTENBERG, B. J. J. 1987. Promoters in the nodulation region of the *Rhizobium leguminosarum* Sym plasmid pRL1JI. *Plant Molecular Biology*, 9, 27-39.
- STEVANIN, T. M., POOLE, R. K., DEMONCHEAUX, E. A. & READ, R. C. 2002. Flavohemoglobin Hmp protects *Salmonella enterica serovar typhimurium* from nitric oxide-related killing by human macrophages. *Infection and Immunity*, 70, 4399-405.
- TARRICONE, C., GALIZZI, A., CODA, A., ASCENZI, P. & BOLOGNESI, M. 1997. Unusual structure of the oxygen-binding site in the dimeric bacterial hemoglobin from *Vitreoscilla* sp. *Structure*, 5, 497-507.
- THORNDYCROFT, F. H., BUTLAND, G., RICHARDSON, D. J. & WATMOUGH, N. J. 2007. A new assay for nitric oxide reductase reveals two conserved glutamate residues form the entrance to a proton-conducting channel in the bacterial enzyme. *Biochemical Journal*, 401, 111-119.
- TUCKER, N. P., LE BRUN, N. E., DIXON, R. & HUTCHINGS, M. I. 2010. There's NO stopping NsrR, a global regulator of the bacterial NO stress response. *Trends in Microbiology*, 18, 149-156.
- TUNBRIDGE, A. J., STEVANIN, T. M., LEE, M., MARRIOTT, H. M., MOIR, J. W., READ, R. C. & DOCKRELL, D. H. 2006. Inhibition of macrophage apoptosis by

- Neisseria meningitidis* requires nitric oxide detoxification mechanisms. *Infection and Immunity*, 74, 729-33.
- VAN DYKE, K. 1997. The possible role of peroxynitrite in Alzheimer's disease: a simple hypothesis that could be tested more thoroughly. *Medical Hypotheses*, 48, 375-80.
- VASUDEVAN, S. G., ARMAREGO, W. L. F., SHAW, D. C., LILLEY, P. E., DIXON, N. E. & POOLE, R. K. 1991. Isolation and nucleotide sequence of the *hmp* gene that encodes a haemoglobin-like protein in *Escherichia coli* K-12. *Molecular and General Genetics*, 226, 49-58.
- WAKABAYASHI, S., MATSUBARA, H. & WEBSTER, D. A. 1986. Primary sequence of a dimeric bacterial haemoglobin from *Vitreoscilla*. *Nature*, 322, 481-3.

5 Analysis of transcriptional regulation of *P. denitrificans* under nitrite stress by type II microarray

Contents

5	Analysis of transcriptional regulation of <i>P. denitrificans</i> under nitrite stress by type II microarray.....	176
5.1	List of figures	177
5.2	List of tables	179
5.3	Introduction and experimental approach	179
5.3.1	Transcriptional analysis by type II microarray.....	180
5.3.2	Whole genome analysis in <i>Escherichia coli</i> and <i>Pseudomonas aeruginosa</i>	181
5.3.3	Design of a <i>P. denitrificans</i> specific microarray	184
5.3.4	Quality control procedures and confirming qRT-PCR.....	186
5.4	Results and discussion	187
5.4.1	RNA extraction and microarray transcriptional analysis	187
5.4.2	Verification of microarray using qRT-PCR.....	196
5.4.3	Flavo-hemoglobin and flavo-rubredoxin genes found in the <i>P. denitrificans</i> genome	199
5.4.4	Microarray results for genes encoding ‘stress responsive’ proteins	202
5.4.5	Transcription regulatory gene changes in microarray data set.....	203
5.4.6	Genes encoding repair mechanisms in <i>P. denitrificans</i>	207
5.4.7	Genes encoding oxidases.....	213
5.5	Conclusions	217
5.6	References.....	220

5.1 List of figures

Figure 5.1: Schematic representation of steps carried out during the microarray analysis procedure. Illustrated here are preparatory steps, both for the formation and printing of slides (probe preparation), as well as the preparation of cell culture for harvesting of RNA, cDNA generation and fluorescent probe labelling (target preparation). These are followed by the steps involved in array hybridisation, image overlay and normalisation before subsequent statistical analysis (analysis).182

Figure 5.2: *P. denitrificans* growth measured in optical density ($\ln OD_{600nm}$) over a 24 hour (h) time frame. grown in standard minimal media at pH 7.5 with 10 mM ammonium chloride (NH_4Cl); open circles, with a growth rate μ_{app} 0.44 ± 0.01 . Comparatively, *P. denitrificans* was also grown in nitrosative stress conditions of minimal media at pH 7.5 with 10 mM NH_4Cl and 12.5 mM nitrite (NO_2^-); open triangles, with a growth rate μ_{app} 0.35 ± 0.01 . Both growth conditions were sampled at early exponential growth phase for RNA extraction and subsequent transcriptional microarray analysis; horizontal dotted line.188

Figure 5.3: Gene cluster for Pd1689 and 1690 shown in red. Genes of similar function are shown as blue arrows showing the phenylacetic acid degradation protein Pd4800, phenylacetate-CoA ligase Pd4801 and transcriptional regulator Pd4802. Gene information: gene number, fold change, base pair size (bp) and amino acid size (aa) are shown in gene arrows. Separating base pairs between genes are shown at the bottom.201

Figure 5.4: Pd0944 BLAST analysis showing similarity in protein sequence to TetrR regulatory proteins in *Rhodobacter sphaeroides*, *Agrobacterium tumefaciens*, *Novosphingobium nitrogenifigens*, *Halomonas anticariensis* and *Rhizobium grahamii*.205

Figure 5.5: Pd3069 BLAST analysis showing similarity in protein sequence to LysR family transcriptional regulator in organisms *Rhizobium leguminosarum*, *Pseudomonas fluorescens*, *Pelobacter carbinolicus*, *Streptomyces coelicoflavus* and *Xanthobacter autotrophicus*.206

Figure 5.6: BLAST comparison of Pd4589 and 4586 Chaperonin protein sequences against model organisms.209

Figure 5.7: Gene arrangement of Pd4586 and 4589, red arrows. Genes of similar function are shown as blue arrows. Protein annotations: unknown Pd4583, dehydrogenase reductase Pd4584, Pd4585 chaperonin groEL (cpn60), chaperonin groES (cpn10) Pd4586, unknown Pd4587, chaperonin heat shock protein HSP20 Pd4588 and Pd4589. Gene information: gene number, fold change, base pair size (bp) and amino acid size (aa) are shown in gene arrows. Yellow star denotes signal peptide. Separating base pairs between genes are shown at the bottom.210

Figure 5.8: Pd4799 alignment to the model organisms: *Rhodobacter sphaeroides*, *Drosophila melanogaster*, *Caenorhabditis elegans*, *Bacillus subtilis*, *Arabidopsis thaliana*, showing a high level of conservation across a wide range of organisms.211

Figure 5.9: Gene cluster for Pd4799 shown in red. Genes of similar function are shown as blue arrows showing the phenylacetic acid degradation protein Pd4800, phenylacetate-CoA ligase Pd4801 and transcriptional regulator Pd4802. Gene information: gene number, fold change, base pair size (bp) and amino acid size (aa) are shown in gene arrows. Separating base pairs between genes are shown at the bottom.212

Figure 5.10: Alignment of Pd5108 to model organisms: *Bacillus subtilis* subsp. *subtilis* str. 168, *Saccharomyces cerevisiae* YJM789, *Drosophila melanogaster*, *Homo sapiens*, *Caviaporcellus*. The C- and also N-terminus alignment for *P. denitrificans*, *B. subtilis* and *S. cerevisiae* show additional residues. Loop regions appear at residues 80-90 and 124-139 *P. denitrificans*, *B. subtilis*.....215

Figure 5.11: Gene cluster for Pd5108 (cytochrome *ba*₃ oxidase) shown in red. Genes of similar function are shown as blue arrows showing the Pd5107, Pd5106 and Pd5105 cytochrome-*c* oxidase, cytochrome-*c* oxidase subunit III and cytochrome-*c* oxidase subunit IV respectively. Gene information: gene number, fold change, base pair size (bp) and amino acid size (aa) are shown in gene arrows. Separating base pairs between genes are shown at the bottom. Yellow star indicates a signalling peptide.216

Figure 5.12: Proposed model for the aerobic stress response of *P. denitrificans* in the presence of 12.5 mM nitrite grown in batch culture at pH 7.5. This model displays the input of nitrite additions, subsequent protonation of nitrite forming free nitrous acid (FNA) (HNO₂) and movement of FNA across the membrane into the cytoplasm, chemical decomposition and disproportionation yield reactive nitrogen species (RNS) including nitric oxide (NO). Detoxification of NO by the flavohemoglobin (Fhb) forming either nitrous oxide in the absence of oxygen or nitrate in the presence of oxygen. Uncoupling effect of proton movement across the membrane by FNA is counter balanced by cytochrome *bas*₃ oxidase leading to the export of protons and the generation of ATP by the F₁ F₀ ATP synthase.219

5.2 List of tables

Table 5.1: Gene regulation in <i>P. denitrificans</i> under nitrosative stress conditions normalised to standard growth conditions. Growth conditions are minimal media at pH 7.5 with 10 mM NH ₄ Cl and 30 mM sodium succinate, plus nitrite: 12.5 mM sodium nitrite addition. Showing 84 genes A: highly transcribed in the presence of nitrite and B: highly down-regulated in the presence of nitrite. A: with 95% significance. B: 90% significance. Those highlighted in orange have been used for further bioinformatic analysis. Annotations are based on bioinformatic BLAST analysis for <i>P. denitrificans</i> or alternative organism bracketed.* Putative protein with uncharacterised function.	190
Table 5.2: The qRT-PCR and microarray transcriptional values for selected genes of interest.	198
Table 5.3: Transcription levels for genes showing similarity to the flavohemoglobin protein sequence (Fhb) from <i>P. denitrificans</i> and the flavorubedoxin of <i>Escherichia coli</i> (NorW).	200

5.3 Introduction and experimental approach

The bioinformatic analysis of chapter 3 undertook an exploration of the *P. denitrificans* genome to locate possible detoxification genes, capable of the conversion of nitric oxide (NO) to the less toxic nitrous oxides: nitrous oxide (N₂O) or nitrate (NO₃⁻). This resulted in the finding of a flavohemoglobin (*fhb*) with gene identifier Pd1689. This gene encodes a protein sequence with high homology to the Hmp flavohemoglobin found in *Salmonella typhimurium*. Further exploration of *fhb* showed consistent higher transcription levels of ≥ 2 fold with nitrite present in the growth medium at 10, 12.5, 15, and 17.5 mM concentrations. Exploration of the *fhb* using mutational studies showed that the *fhb* is required for growth at the high end tolerance of nitrite and contributes to production of biomass at all nitrite concentrations. However growth of *P. denitrificans fhb* mutant (Δfhb) in the presence of nitrite was possible and maintained which has suggested that *fhb* contributes to a larger metabolic response produced by *P. denitrificans*.

A protein BLAST analysis of *fhb* showed a further five genes with homology to Fhb within the *P. denitrificans* genome. These genes are of interest as they may provide additional tolerance and may be providing a contributing factor for resistance of *P. denitrificans* to nitrite. To elucidate the role these five homologous *fhb*-like genes have in the tolerance of *P.*

denitrificans to nitrite and in order to further analyse the transcriptional changes being undertaken by *P. denitrificans* in response to nitrite, a type II microarray was carried out on the genome of *P. denitrificans*. The microarray technique employed in this chapter provides a method of analysing transcriptional changes across the whole genome of *P. denitrificans*. The type II microarray used explores the global transcriptional changes occurring in *P. denitrificans* when 12.5 mM nitrite is present. This will elucidate the role of the additional five *fhb* and explore new genes of interest which are shown in the microarray results.

5.3.1 Transcriptional analysis by type II microarray

The study of bacterial gene expression profiling has become a major tool for discovery in bacterial genetics (Cook *et al.*, 2002). Microarray experiments have been used previously to provide a description of genome-wide expression changes under nitrosative stress (Constantinidou *et al.*, 2006; Filenko *et al.*, 2007). Microarrays have been designed for a multitude of specific analytic methods, to detect and measure gene expression at mRNA or protein level: they can be used for the detection of mutations and as a tool for genotyping and to sequence or re-sequence DNA and locate chromosomal changes by comparative genomic hybridisation (CGH) (Baumbusch *et al.*, 2008). The process for this analytical technique involves five steps of processing: firstly the coupling of biomolecules to a platform; preparing samples for detection; hybridisation; scanning; and analysis of the data generated (Knudsen, 2004; Lorkowski and Cullen, 2006; Tarca *et al.*, 2006). Microarray analysis relies on DNA hybridisation. This hybridisation occurs between two complementary DNA strands by Watson-Crick's base interaction principle (Crick and Watson, 1954). This process has been developed from foundation methods of southern blot analysis DNA-DNA and northern blot analysis DNA-mRNA hybridisations (Tarca *et al.*, 2006) and integral in the production of a fluorescence image (figure 5.1).

Bacterial cells were cultured and harvested at an early to mid-exponential phase growth point in the growth conditions to be compared in the microarray analysis. Cells harvested at this point are used for the extraction of mRNA. Quality and purity checks are undertaken to ensure the mRNA extracted is suitable for generation of cDNA. Expression level is determined via quantification of 532 nm (green) and 635 nm (red) emission values measuring the amount of fluorescence measured at each sequence specific location. This value is directly proportional to the relative amount of mRNA and gDNA on the

experimental slide. Although this method cannot quantify the absolute expression level of a gene by quantifying true concentrations of RNA, it can compare expression levels in known conditions, and therefore highlight potential candidate for further exploration (Tarca *et al.*, 2006).

5.3.2 Whole genome analysis in *Escherichia coli* and *Pseudomonas aeruginosa*

The microarray technique has been employed for global gene study of *Escherichia coli* and *Pseudomonas aeruginosa* for the study of nitrite metabolism and associated regulation. Whole genome arrays have been carried out successfully to explore large numbers of transcription changes under one test condition to explore nitrosative stress. In 2004, Firoved *et al.* (2004) set out the transcriptional analysis of *Pseudomonas aeruginosa* to explore the effect of nitric oxide (NO) on the pathogenic potency of *P. aeruginosa* in cystic fibrosis (Firoved *et al.*, 2004).

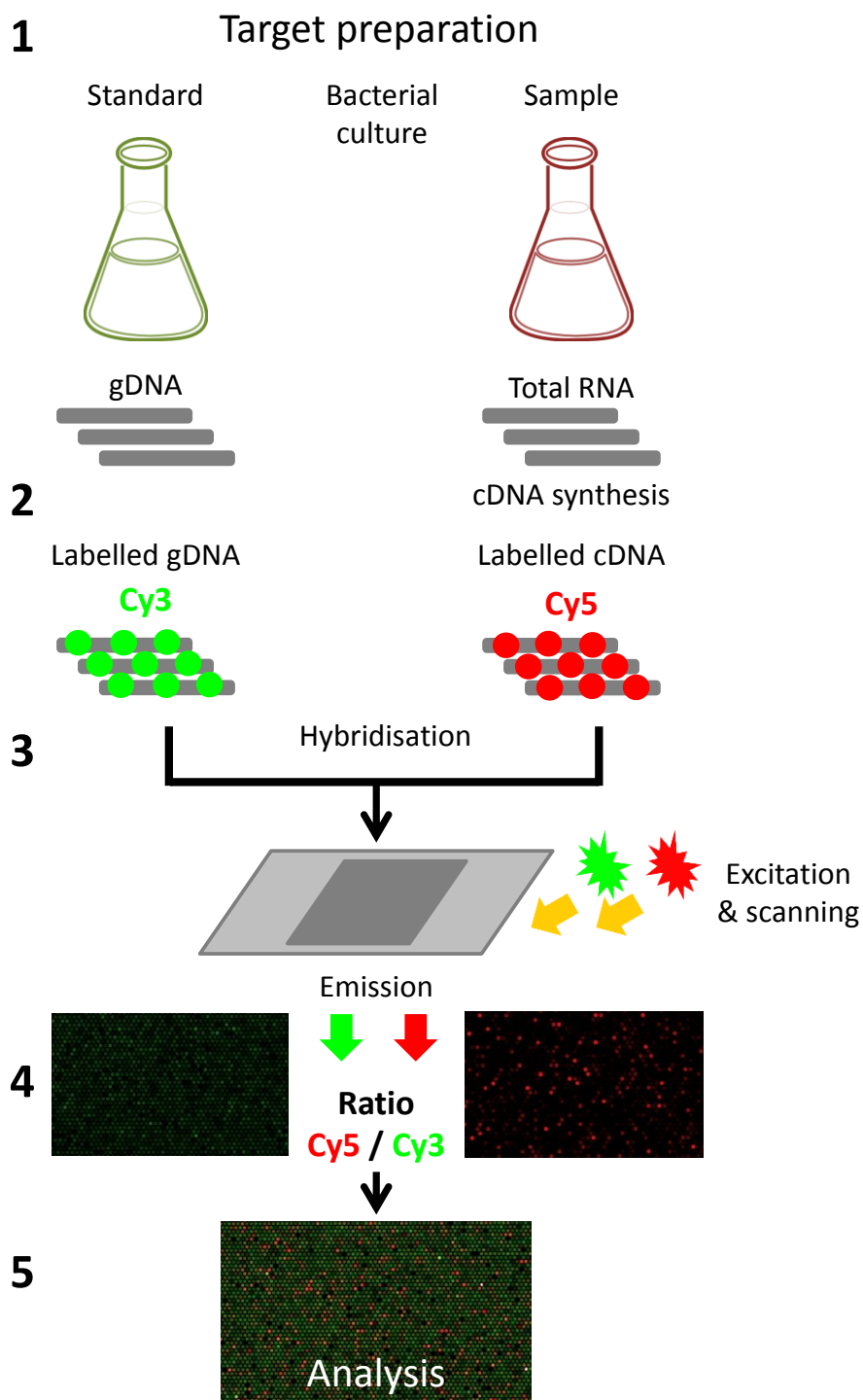


Figure 5.1: Schematic representation of steps carried out during the microarray analysis procedure. 1: preparatory steps of cell culture for harvesting of RNA and gDNA; 2: cDNA generation and fluorescent probe labelling (target preparation); 3: array hybridisation; 4: image overlay and normalisation; 5: statistical analysis.

Constantinidou *et al.* (2006) set up a reproducible technique for the exploration of the FNR regulon in *E. coli*. In this work the characterisation of FNR as a regulator allowed the author to summarise that FNR has a role in at least 103 operons and were able to cross reference this with the regulator NarXL which was also responsible for the co regulation of 24 of these operons. In this study it was clearly identified that microarray results can present a vast array of genes changing under what is thought to be a single condition. However it was identified that changes between the growth conditions can interfere with these results. This is why in this work close attention was paid to comparing growth conditions which were comparable in their growth phenotype. This decreased the overall number of transcriptional changes. In this way, changes unique to the presence of nitrite can then be more readily distinguished from that of growth related transcriptional interference.

In the work of Constantinidou *et al.* (2006), the growth of an *fnr* mutant (Δfnr) was not comparable to that of a wild type strain (WT). They therefore reduced the difference between growth conditions and paid particular attention to finding growth conditions which ensured both WT and Δfnr anaerobic growth rates were similar. This in turn resulted in less genes changing overall. Therefore identification of those associated with the mutations studied was achieved and a more defined role for Fnr elucidated.

Fileiko *et al.* (2007) presented the microarray exploration of the NsrR regulon in *Escherichia coli*, building on the method set out by Constantinidou (2006). Here it was confirmed that NsrR regulates the expression of *hmpA*, the homologous gene to that of the *fhb* explored in the previous chapter, along with a further three genes involved in stress response to nitrite and reactive nitrogen species (RNS) such as nitric oxide (NO). Additionally the Nap and Nrf periplasmic nitrate and nitrite reductases were part of the large NsrR regulon, which separated the regulatory process of periplasmic and cytoplasmic nitrate/nitrite reduction (Fileiko *et al.*, 2007).

Fileiko *et al.* (2007) used the Agilent GeneSpring GX software was used for analysis of the transcriptional data. In present work this software will also be used. GenSpring is a statistical tool which allows the ranking of genes by the change between the two test conditions: 12.5 mM nitrite and no nitrite. Additionally the reliability of the change can be ranked to ensure observed changes are significant between the three biological replicates used for each of the test conditions. Subsequent identification of gene function is obtained by bioinformatic techniques (Constantinidou *et al.*, 2006). Sequence alignments were achieved using the basic local alignment search tool (BLAST) a computer algorithm

accessed online at the National Center for Biotechnology Information (NCBI) website which rapidly aligns and compares a query DNA or protein sequence with a database of sequences (Mount, 2007; Altschul *et al.*, 1990; Collins and Coulson, 1984).

5.3.3 Design of a *P. denitrificans* specific microarray

The microarray technique employed in this work has been successfully used in the study of copper control in nitrous oxide emission in *P. denitrificans* by Sullivan *et al* (2013). The methodology used by Sullivan *et al*, has made it possible to transcriptionally analyse the entire *P. denitrificans* genome and this has been applied to the condition of nitrite stress.

The microarray uses the common reference of genomic DNA (gDNA) which undertakes the same preparatory techniques and is scanned and analysed from the same experimental slide as the RNA samples taken from growth with and without 12.5 mM nitrite. The use of gDNA as a reference value has been verified in work by Gadgil *et al.* (2005) and is widely used for the 'reference design' microarray technique, whereby all cDNA (created from the sampled RNA) samples are hybridized to a common reference. Genomic DNA has been suggested to be used as a universal reference for bacterial systems due to the low percentage of non-coding sequences. The analysis by Gadgil (2005) for the use of gDNA was consistent as a universal reference. Assay performance was also not significantly affected by variation in initial gDNA concentration or hybridization time.

The gDNA is extracted from the aerobic growth of *P. denitrificans* in Luria Broth as described in the methods. Direct labelling of gDNA for microarray hybridization was carried out using the Klenow fragment of *E. coli* DNA polymerase I and Cy3 dCTP fluorescent dye. Incorporation of Cy5-dCTP Blue dye to the cDNA occurs during the reverse transcription of the RNA samples. This gDNA is situated in one channel of each array slide. This technique of using standard gDNA in each slide provides a slide based control for each slide examined. It also allows normalisation of the fluorescence expressed on the slides using a sample and is needed for the data to be directly compared across more than one slide.

For this microarray, three biologically independent RNA samples were extracted for each of the two growth conditions; 1: without nitrite, 2: with 12.5 mM nitrite. This made a total of six biologically independent RNA samples. Each sample was applied to a microarray slide. From each biologically separate sample, 10 µg of RNA was isolated for analysis. These

samples of RNA were reverse transcribed to cDNA using the Agilent Technologies AffinityScript™ multiple temperature reverse transcriptase and labelled with fluorescent Cy5-dCTP using random primers. Similarly the gDNA was also fluorescently labelled with Cy3-dCTP. This label was applied to 10 µg of gDNA using a Bioprime DNA labelling system from Invitrogen.

The labelled gDNA and cDNA was then mixed in the proportion of a 1:5 respectively into hybridisation buffer for hybridisation onto the experimental slide. The microarray slides are custom made 4 x 44 K oligonucleotide array slides designed specifically for the genome of *P. denitrificans* by Agilent. The complete sample containing Cy labelled gDNA and cDNA and buffer was loaded directly to the gasket slide and the microarray lid brought to contact with the gasket slide and sample contents. The two slides sandwiched the hybridisation mix and are sealed within a chamber. This was then continually rotated inside an oven at 55°C and in the dark to allow hybridisation to the array slide to occur over a period of ~60 h.

Once hybridised, the array slides were washed twice with a 6 x SSPE solution containing 0.2 M phosphate buffer, 2.98 M NaCl, 20 mmol.L⁻¹ EDTA at pH 7.4 for 5 min and a 0.6 x SSPE solution containing 0.18% polyethylene glycol 200 also for 5 min. The slides were centrifugally dried before being placed into a GenePix 4000B scanner from Axon Instruments and excited at 532 and 635 nm to visualise the fluorescence levels for each array dot. GenePix Pro software (Axon Instruments) was used to quantify the fluorescence levels and standardise the scanning process for multiple slide comparison. The quantification method using GenePix Pro software standardised the processing of the experimental slides to allow direct comparison across multiple slides. Fluorescence was detected for each dot and background intensities. Each dot was filtered to omit those with a reference signal which deviated lower than two standard deviations from the background intensity. Highly deviant dots were then omitted from the subsequent analysis steps.

Each array slide fluorescence intensity level varies depending on the level of Cy-dye incorporation. Therefore signal intensity was also corrected to allow comparison of multiple slides. This correction was carried out by subtracting the background fluorescence values. After these standardisation procedures, the ratio of Cy5-dCTP Blue (cDNA):Cy3-dCTP Red (gDNA) was calculated. Normalisation of the fluorescence level was carried out with Batch Anti-Banana Algorithm in R (BABAR). The normalisation is a cyclic loss normalisation across the entire dataset (Alston *et al.*, 2010). The unprocessed GenePix microarray files are directly imported to BABAR. Normalisation within the heterogeneous dataset produces

values which can then be directly compared between different microarrays after validation and confirmation of result using qRT-PCR. Genes were filtered using GeneSpring 7.3 (Agilent). The criteria for the filter were to output genes showing ± 2 fold change (relative normalised ratio) in transcription in 12.5 mM nitrite when compared to growth without nitrite and to have significance of $\geq 95\%$ significance $p = 0.05$ across the three biological replicates.

5.3.4 Quality control procedures and confirming qRT-PCR

Confirmation of transcriptional changes in the presence of nitrosative stress postulated by microarray analysis was carried out using qRT-PCR. Primers were identified for the selected genes and checked for functionality using genomic DNA extracted from *P. denitrificans* prior to use on cDNA generated by RT-PCR from the same RNA triplicate pool as that used in the microarray. This technique quantified transcription levels using the addition of a fluorophore and by measure of fluorescence to confirm transcriptional observations made using microarray analysis. The use of qRT-PCR presents a real-time amplification and quantification of RNA species by photospectrometric measurement of cDNA with intercalated fluorescent dye. The housekeeping gene Glyceraldehyde 3-phosphate dehydrogenase (*gapdh*) (Barber *et al.*, 2005; Reid *et al.*, 2006) was used in all qRT-PCR. The *gapdh* (Pden_4465) housekeeping gene was verified using a secondary housekeeping gene DNA polymerase III subunit β (*polB*) (Pden_0342) to confirm no change in *gapdh* levels in the +nitrite and –nitrite conditions compared.

The relative expression ratio is calculated using the qRT-PCR change in threshold cycle denoted by $C(t)$ and measured as fluorescence increase above background between the control standard conditions and that of nitrosative stress. The qRT-PCR expression values are generated using the $\Delta\Delta C(t)$ mathematical model (Livak and Schmittgen, 2001) with efficiencies of between 90 - 100%. This method defines the fold change ($\Delta\Delta C(t)$) in the samples as:

$$\text{Relative normalised ratio} = 2^{\Delta(\Delta C T)}$$

where $\Delta C(t) = C(t)_{\text{target}} - C(t)_{\text{gapdh}}$ and $\Delta\Delta C(t) = \Delta C(t)_{+\text{nitrite}} - \Delta C(t)_{-\text{nitrite}}$ with efficiency assumed to be 100%. Efficiency is calculated from the calibration curve of serially diluted *P. denitrificans* gDNA $E = 10^{(-1/\text{slope})}$.

5.4 Results and discussion

5.4.1 RNA extraction and microarray transcriptional analysis

The two growth conditions compared by microarray analysis are 12.5 mM nitrite (+nitrite) and compared to growth without nitrite (-nitrite). *P. denitrificans* cells were prepared for transcriptional characterisation by type II microarray by growth in shaking flasks (SF) from RNA extracted in the growth conditions described in chapter 4. Figure 5.2 shows a semi log plot of the growth of *P. denitrificans* +nitrite and -nitrite growth in SF conditions. Cells were grown to an OD of approximately 0.45 AU at which point cell activity is ceased for RNA extraction. This is shown by a vertical line in figure 5.2.

Selection of 12.5 mM nitrite provides sufficient nitrite induced stressed for observational changes in transcript in +nitrite growth conditions as was seen in in the increased transcription of the flavohemoglobin (*fhb*) gene in chapter 3. Growth at 12.5 mM is similar to that reduces growth differences which may interfere with the transcriptional data.

The gradient of exponential growth well as final OD of stationary phase are also similar between the growth of *P. denitrificans* +nitrite and -nitrite which will reduce the interference of growth related transcriptional changes in the microarray transcriptional analysis.

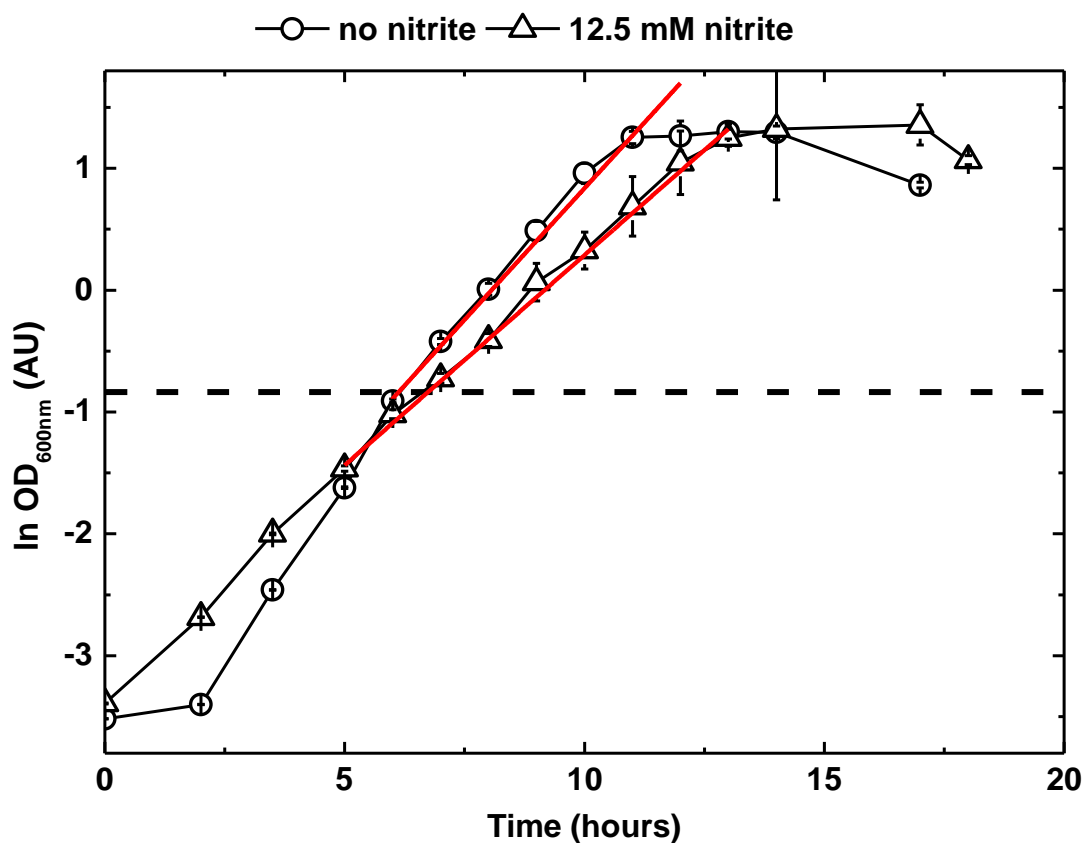


Figure 5.2: *P. denitrificans* growth measured in optical density ($\ln OD_{600\text{nm}}$) over a 24 hour (h) time frame. Grown in standard minimal media at pH 7.5 with 10 mM ammonium chloride (NH_4Cl); open circles, with a growth rate $\mu_{\text{app}} 0.44 \pm 0.01$. Comparatively, *P. denitrificans* was also grown in nitrosative stress conditions of minimal media at pH 7.5 with 10 mM NH_4Cl and 12.5 mM nitrite (NO_2^-); open triangles, with a growth rate $\mu_{\text{app}} 0.35 \pm 0.01$. Both growth conditions were sampled at early exponential growth phase for RNA extraction and subsequent transcriptional microarray analysis; horizontal dotted line.

The experimental conditions covered six blocks. Each experimental array slide contains four blocks, therefore the experimental procedure required the use of two array slides; four blocks from one, and two from the second slide. Analysis carried out by rank product analysis summarised genes of $\geq 95\%$ significance ($p = 0.05$) across the three biological replicates used and with a ± 2 fold change in transcription. The genes which fit these criteria are summarised in table 5.1.

This ± 2 fold change in transcription shows genes which are transcribed two-fold higher or two-fold lower in +nitrite when compared with -nitrite. The value of 1 represents no change between the two experimental conditions. Additional contributions of numerically grouped genes which present potential gene clusters and are of 90% significance across the three biological replicates are also explored in the case where a gene cluster is suggested.

Microarray analysis yielded >5k genes and their associated expressions levels in nitrosative stress conditions. Of these only 84 genes matched the analytical criteria used and showed a ± 2 fold change in transcription across the three replicates used. Expansion of the significance criteria to 90% ($p = 0.1$) yielded only 146 genes showing a transcriptional change of $\geq 95\%$ significance ($p = 0.05$) and with a ± 2 fold change in transcription.

Additionally, examining the data set also shows little indication of growth related changes in transcription; the large portion of genes changing group into shock and repair categories. This verifies the growth phenotypes of the conditions compared are similar across all six replicates and indicates a high level of accuracy in maintaining duplicated growth conditions for the growth of *P. denitrificans* both +nitrite and -nitrite as well as accurate harvesting of the RNA when the growth conditions matched between both treatments.

Many of the genes of interest are postulated as having a protein of uncharacterised function, or are incorrectly annotated. Bioinformatic analysis of these genes has generated potential protein identity and functionality. This was carried out using the NCBI BLAST analysis software which generated a list of top hits showing similar alignment to the protein of interest. Both contribute to a suggested protein function and associated annotation of the gene. This technique was used to isolate the conserved domains and therefore distinct functional and structural components of the protein, linking a unique folding attribute of the polypeptide to specific function (Marchler-Bauer *et al.*, 2009; Marchler-Bauer and Bryant, 2004; Marchler-Bauer *et al.*, 2011)

Table 5.1: Gene regulation in *P. denitrificans* under nitrosative stress conditions normalised to standard growth conditions. Growth conditions are minimal media at pH 7.5 with 10 mM NH₄Cl and 30 mM sodium succinate, plus nitrite: 12.5 mM sodium nitrite addition. Showing 84 genes A: highly transcribed in the presence of nitrite and B: highly down-regulated in the presence of nitrite. A: with 95% significance. B: 90% significance. Those highlighted in orange have been used for further bioinformatic analysis. Annotations are based on bioinformatic BLAST analysis for *P. denitrificans* or alternative organism bracketed.* Putative protein with uncharacterised function.

A	Mean normalised transcription ^a				Fold change ^b	Gene annotation
	Minus		Plus			
Gene	nitrite	±SD	nitrite	±SD		
Pd3605	0.13	0.03	0.38	0.08	3.00	hypothetical protein possible YvrJ protein family
Pd3764	0.12	0.03	0.35	0.13	2.89	hypothetical protein
Pd2988	0.52	0.15	1.44	0.29	2.74	hypothetical protein
Pd5108	0.98	0.23	2.40	0.42	2.45	cytochrome ba3 quinol oxidase subunit 2
Pd3750	0.22	0.04	0.53	0.11	2.43	hypothetical protein
Pd4586	16.33	1.44	38.20	0.81	2.34	chaperonin Cpn10
Pd4576	0.25	0.05	0.58	0.04	2.31	conserved hypothetical protein
Pd1690	0.59	0.19	1.27	0.17	2.16	transcriptional regulator, BadM/Rrf2 family
Pd0744	37.08	6.85	81.66	7.63	2.20	LSU ribosomal protein L1P
Pd1689	0.45	0.11	0.97	0.07	2.17	globin FHB

Pd4799	0.48	0.11	1.04	0.06	2.17	Enoyl-CoA hydratase / short chain enoyl-CoA hydratase
Pd2112	0.08	0.01	0.19	0.04	2.21	flagellar hook-basal body complex protein FliE
Pd3460	0.76	0.21	1.60	0.15	2.12	ABC polyamine/opine transporter, periplasmic substrate-binding
Pd3211	0.52	0.11	1.12	0.18	2.14	aldehyde dehydrogenase
Pd3118	1.34	0.14	2.89	0.32	2.15	methionine aminopeptidase, type I
Pd4895	0.21	0.00	0.45	0.06	2.12	BFD domain protein (2Fe-2S)-binding domain protein
Pd2787	3.98	1.13	8.16	0.25	2.05	Smr protein/MutS2
Pd4589	0.50	0.04	1.08	0.27	2.15	hypothetical protein
Pd4577	0.30	0.08	0.62	0.13	2.08	short-chain dehydrogenase/reductase SDR
Pd2409	1.15	0.13	2.39	0.15	2.07	hypothetical protein
Pd3216	2.52	0.69	5.06	0.26	2.01	tartronate semialdehyde reductase
Pd4930	0.56	0.13	1.13	0.08	2.02	2-keto-3-deoxy-phosphogalactonate aldolase

B	Mean normalised transcription ^a				Fold change ^b	Gene annotation
	Minus		Plus			
Gene	nitrite	±SD	nitrite	±SD		
Pd1707	2.86	1.66	0.47	0.33	0.16	conserved hypothetical protein
Pd1483	0.93	0.49	0.16	0.02	0.17	Conjugal transfer protein TrbC
Pd2366	7.87	1.09	1.36	0.07	0.17	Aldehyde dehydrogenase (NAD(+))
Pd1725	4.66	3.01	0.88	0.60	0.19	hypothetical protein
Pd1129	1.69	0.48	0.35	0.12	0.20	von Willebrand factor, type A
Pd2368	7.78	3.11	1.65	0.10	0.21	protein of unknown function DUF779
Pd3408	0.28	0.13	0.07	0.03	0.24	hypothetical protein
Pd2367	5.02	1.28	1.24	0.16	0.25	Alcohol dehydrogenase GroES domain protein
Pd1566	17.52	9.10	4.82	1.43	0.28	cobalamin-5'-phosphate synthase
Pd0944	1.55	0.44	0.49	0.10	0.32	transcriptional regulator, TetR family
Pd0996	0.32	0.15	0.10	0.03	0.32	gene transfer agent
Pd0020	1.05	0.19	0.34	0.03	0.32	Pyrrolo-quinoline quinone
Pd1097	0.57	0.19	0.19	0.08	0.33	conserved hypothetical protein
Pd0263	0.87	0.40	0.29	0.05	0.34	DNA-cytosine methyltransferase
Pd2445	0.73	0.22	0.26	0.04	0.35	protein of unknown function DUF796

Pd0260	0.54	0.18	0.19	0.07	0.36	hypothetical protein
Pd4290	1.85	0.62	0.68	0.14	0.37	conserved hypothetical protein
Pd1225	0.62	0.20	0.23	0.04	0.37	hypothetical protein
Pd1461	0.45	0.15	0.17	0.07	0.38	GCN5-related N-acetyltransferase
Pd0366	0.31	0.10	0.12	0.02	0.39	phage head-tail adaptor, putative
Pd1486	0.21	0.08	0.08	0.03	0.39	TonB-dependent receptor
Pd3263	0.48	0.18	0.19	0.06	0.39	hypothetical protein
Pd1703	0.80	0.15	0.32	0.10	0.40	quinohemoprotein amine dehydrogenase, 60 kDa subunit
Pd1537	0.23	0.07	0.09	0.03	0.41	hypothetical protein
Pd2701	0.45	0.09	0.19	0.04	0.41	hypothetical protein
Pd2118	0.73	0.07	0.31	0.09	0.42	conserved hypothetical protein
Pd1210	0.64	0.18	0.27	0.05	0.42	HupE/UreJ protein
Pd2205	18.03	5.68	7.64	1.09	0.42	heat shock protein Hsp20
Pd3010	1.92	0.72	0.81	0.32	0.42	periplasmic binding protein
Pd1477	0.49	0.18	0.21	0.07	0.43	Conjugal transfer protein
Pd2467	0.71	0.22	0.30	0.07	0.43	response regulator receiver protein
Pd3069	0.53	0.09	0.23	0.01	0.43	transcriptional regulator, LysR family
Pd0025	1.08	0.40	0.47	0.13	0.43	hypothetical protein

Pd0159	1.11	0.28	0.48	0.10	0.44	hypothetical protein
Pd0390	0.74	0.16	0.32	0.03	0.44	protein of unknown function DUF983
Pd3429	0.43	0.13	0.19	0.02	0.44	TRAP dicarboxylate transporter, DctM subunit
Pd1629	1.91	0.53	0.85	0.03	0.45	RNA polymerase, sigma-24 subunit, ECF subfamily
Pd0219	0.31	0.10	0.14	0.03	0.45	hypothetical protein
Pd3530	1.06	0.21	0.48	0.07	0.45	Siderophore-interacting protein
Pd2652	1.90	0.52	0.85	0.05	0.45	flagellar biosynthetic protein FliP
Pd0021	1.40	0.22	0.63	0.09	0.45	hypothetical protein
Pd0276	0.57	0.15	0.26	0.04	0.45	conserved hypothetical sugar-binding protein
Pd1606	0.26	0.06	0.12	0.01	0.46	Methyltransferase type 12
Pd3748	0.57	0.20	0.26	0.07	0.46	hypothetical protein
Pd3521	0.51	0.17	0.24	0.03	0.46	TonB-dependent siderophore receptor
Pd1911	9.32	2.59	4.36	0.48	0.47	hypothetical protein
Pd1446	0.37	0.06	0.17	0.01	0.47	major facilitator superfamily MFS_1
Pd1126	0.95	0.24	0.45	0.13	0.47	conserved hypothetical protein
Pd0102	0.21	0.07	0.10	0.02	0.47	phage transcriptional regulator, AlpA
Pd4193	0.46	0.11	0.22	0.05	0.47	hypothetical protein
Pd3983	2.50	0.56	1.19	0.05	0.48	conserved hypothetical protein

Pd2634	0.43	0.09	0.21	0.01	0.48	HNH endonuclease
Pd3464	1.32	0.11	0.63	0.08	0.48	ferredoxin
Pd0252	1.42	0.37	0.68	0.12	0.48	transposase (class I)
Pd1125	0.92	0.24	0.45	0.06	0.48	ATPase associated with various cellular activities
Pd4243	2.82	0.76	1.36	0.19	0.48	GntR domain protein
Pd3531	0.57	0.00	0.28	0.05	0.49	periplasmic binding protein
Pd2886	1.15	0.33	0.56	0.08	0.49	conserved hypothetical protein
Pd1521	0.59	0.10	0.29	0.08	0.49	hypothetical protein
Pd3827	1.52	0.45	0.74	0.19	0.49	hypothetical protein
Pd3021	0.77	0.19	0.38	0.09	0.49	succinate dehydrogenase subunit C
Pd2648	0.54	0.03	0.27	0.03	0.50	flagellar basal body-associated protein FliL

^a Normalised to internal gDNA fluorescence, mean value of three biologically independent experiments, \pm SD = standard deviation of biological replicates

^o Fold change derived by plus / minus nitrite mean transcription values

5.4.2 Verification of microarray using qRT-PCR

Confirmation of the microarray was carried out by qRT-PCR using primers designed for the gene of interest listed in the methods. This additional transcriptional analysis technique has been used to validate the reproducibility of the microarray results by means of a complementary transcriptional analysis technique. The qRT-PCR and associated microarray transcriptional values are listed in table 5.2. Initial qRT-PCR analysis examined the known denitrification genes for transcription to confirm that denitrification and nitrite assimilation was not being carried out by *P. denitrificans* under the experimental conditions. NapA is the catalytic subunit of the periplasmic nitrate reductase whereby NapAB receives electrons from NapC. NAP is induced by aerobic growth of *P. denitrificans* on a reduced carbon source (Sears *et al.*, 2000). In this experiment, succinate was used as the carbon source and therefore NapA activity was not expected. NapA activity was not seen in the microarray and this was also confirmed by the qRT-PCR.

NarG is the catalytic subunit of the cytoplasmic nitrate reductase which is upregulated in anaerobic growth conditions in the presence of nitrate (Richardson *et al.*, 2001). NarG was also not shown to change in the experimental conditions both in the qRT-PCR and microarray data. NirS and NorB are the catalytic subunits of the nitrite reductase and nitric oxide reductase enzymes form the denitrification pathways of *P. denitrificans*. All contain FNR binding sequences and are suggested to be only upregulated in anaerobic growth (Van Spanning *et al.*, 1995).

NasB is the catalytic subunit of the nitrite assimilation. The presence of 10 mM ammonium chloride in the growth media provides a direct nitrogen source and has been shown to suppress the assimilatory pathways which are regulated to provide a nitrogen source from available nitrite when ammonia is not present (Gates *et al.*, 2011). As was expected, NasS transcription was not seen in +nitrite growth conditions. Therefore nitrite present in the media is not being assimilated into biomass.

An additional confirmation performed on the microarray data was the replication of results observed. The following eight genes were selected for the purpose of corroborating the microarray results which met the statistical filter of >95% and ± 2 fold change in transcription with additional qRT-PCR: Pden_3605, 1690, 1129, 5108, 1629 and 3429. The

levels of transcription are summarised in table 5.2 and confirm similar levels of transcription between the two methods.

This provides additional validity for the microarray data and confirms the GenePix standardisation processes and BABAR normalisation step provides values which are comparable to that of qRT-PCR.

Table 5.2: The qRT-PCR and microarray transcriptional values for selected genes of interest.

Gene identifier (Pden_)		Fold change +nitrite / -nitrate		
		Microarray transcription*	qRT-PCR transcription*	±SD
3605	Acid stress ¹	3.00	2.06	1.27
1690	<i>fhb</i> BadM reg.	2.16	3.61	1.88
1129	Von Willebrand	0.21	0.43	0.25
5108	<i>ba</i> ₃	2.45	2.68	0.89
1629	sigma-24	0.45	0.39	0.13
3429	DctM subunit	0.44	0.47	0.10
1689	<i>fhb</i>	2.17	3.43	0.37
4721	<i>napA</i>	0.89	0.38	0.10
4236	<i>narG</i>	1.72	0.84	0.15
2487	<i>nirS</i>	0.59	1.12	0.13
2483	<i>norB</i>	0.54	0.65	0.05
4452	<i>nasB</i>	0.93	1.18	0.14
4465	<i>gapdh</i> *	1.18	0.98	0.04
0342	<i>polB</i>	1.12	1.03	0.04

*all qRT-PCR results use *gapdh* as housekeeping gene for normalisation, with the exception of *gapdh* itself whose transcription was verified with *polB* as housekeeping gene ±SD standard deviation n = 3 biologically independent replicates (additional 3 technical replicates)

¹ highest fold change in microarray dataset

5.4.3 Flavohemoglobin and flavorubedoxin genes found in the *P. denitrificans* genome

Chapter 4 carried out BLAST analysis of the flavohemoglobin (Fhb) and found homology in 5 additional genes sharing 24 - 33% identity to Fhb: Pd1179, Pd1188, Pd2831, Pd4896 and Pd4806. BLAST analysis was also carried out of the flavorubedoxin NorW and identified the following homologous genes: Pd4452, Pd2324, Pd3463, Pd0551, Pd4760, Pd0611, Pd3669. The levels of transcription and significance between the three biological replicates were analysed using the >2 fold change in transcription and 95% significance statistical cut off. None of the genes passed the statistical cut off.

The relative normalised ratio of transcription levels from the microarray data is presented in table 5.3 for each of the Fhb and NorW homologs. Each value is near to 1.0. The value near to 1.0 shows that the quantified value for the target gene is the same in both +nitrite and -nitrite conditions. Therefore there is no suggestion that 12.5 mM nitrite induces the transcription of these genes.

The *fhb* itself shows consistent increased transcription in +nitrite conditions. Its transcription is 2.17 fold in the microarray data set, which means that 12.5 mM nitrite induces transcription of *fhb* and confirms previous qRT-PCR data with the same level of transcription seen in chapter 3. It is also over the 95% significance cut off, showing that the *fhb* is consistently upregulated across the three biological replicates used in this microarray.

Examination of the genes either side of the *fhb* brought to light Pd1690 with 2.16 -fold increased transcription with +nitrite at 95% significance which is shown in figure 5.3. This matches the *fhb* level of increased transcription and neighbours the *fhb*. Pd1690 is a regulatory protein of the NsrR family Pd1690 and was explored in the previous chapter. Its close proximity to the *fhb* and similar level of increased transcription in the presence of nitrite suggests a gene cluster. The NsrR homolog may be acting to affect the transcription of the *fhb*. There are no other neighbouring genes showing any transcriptional change that meets the analytical criteria.

Table 5.3: Transcription levels for genes showing similarity to the flavohemoglobin protein sequence (Fhb) from *P. denitrificans* and the flavorubedoxin of *Escherichia coli* (NorW).

Gene ID (Pden)	Mean normalised transcription ^a				Fold change ^b	Gene annotation
	-nitrite	±SD	+nitrite	±SD		
1179	0.10	0.01	0.16	0.04	1.55	oxidoreductase
1188	0.32	0.03	0.33	0.02	1.05	ferredoxin
2831	0.52	0.11	0.53	0.09	1.03	ferredoxin
4896	0.23	0.05	0.26	0.01	1.10	oxidoreductase
4806	0.39	0.07	0.54	0.01	1.39	phenylacetate-CoA oxygenase/reductase
4452	0.31	0.03	0.29	0.02	0.93	assimilatory nitrite reductase (NAD(P)H) large subunit prec.
2324	3.29	0.67	3.88	0.45	1.18	FAD-dependent pyridine nucleotide-disulphide oxidoreductase
3463	0.83	0.35	0.90	0.09	1.09	FAD-dependent pyridine nucleotide-disulphide oxidoreductase
0551	13.06	2.15	10.22	0.56	0.78	dihydrolipoamide dehydrogenase
4760	1.37	0.27	1.05	0.19	0.76	dihydrolipoamide dehydrogenase
0611	11.09	0.71	14.64	0.78	1.32	dihydrolipoamide dehydrogenase
n	6.49	0.53	7.64	0.98	1.18	NADPH-glutathione reductase

^a Normalised to internal gDNA fluorescence, mean n = 3, ±SD = standard deviation ^o Fold change = +nitrite / -nitrite (mean transcription values)

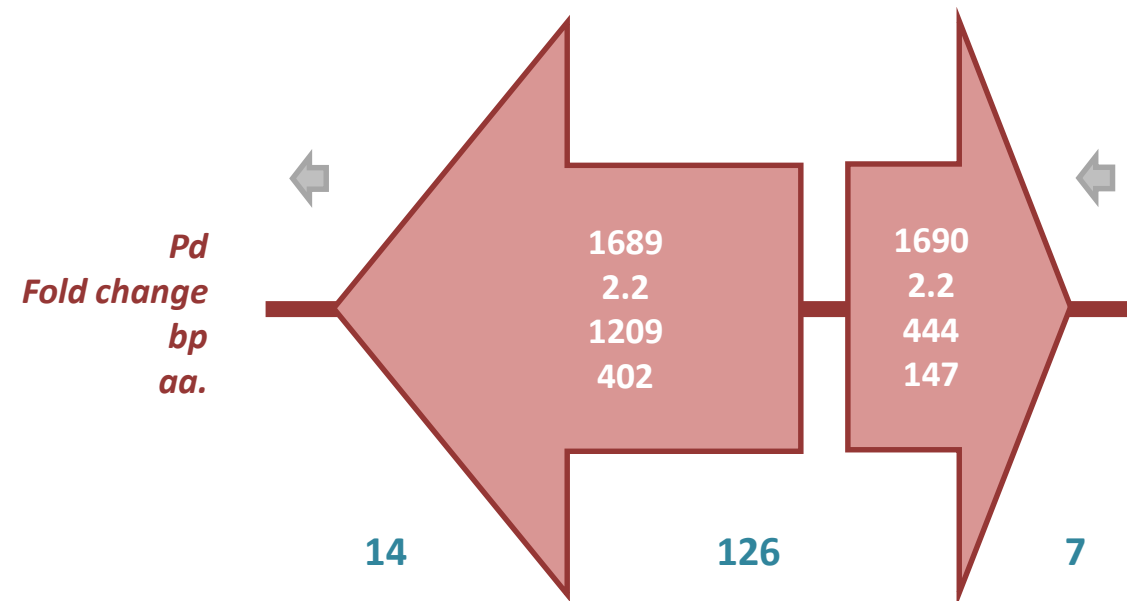


Figure 5.3: Gene cluster for Pd1689 and 1690 shown in red. Genes of similar function are shown as blue arrows showing the phenylacetic acid degradation protein Pd4800, phenylacetate-CoA ligase Pd4801 and transcriptional regulator Pd4802. Gene information: gene number, fold change, base pair size (bp) and amino acid size (aa) are shown in gene arrows. Separating base pairs between genes are shown at the bottom.

NsrR acts as a protective mechanism against nitrosative stress. NsrR binds to the DNA upstream of gene and prevents its transcription. It features an iron sulphur cluster which conveys nitric oxide-sensitivity and releases NsrR from DNA allowing transcription to occur (Bodenmiller and Spiro, 2006). Pd1690 is 2.16 transcribed +nitrite, which may suggest it acts to prevent the transcription of an additional gene.

The role of the *fhb* described in the previous chapter as a potential protection mechanism used by *P. denitrificans* in response to reactive nitrogen species is confirmed by the transcriptional data generated in this microarray. The microarray data examined here does not include any additional genes which share the *fhb* role. Therefore Pden_1689 is the only gene seen in these conditions capable of detoxifying nitric oxide. It is likely that this *fhb* encodes a protein which is solely responsible for the detoxification of nitric oxide generated from nitrite (Forrester and Foster, 2012).

5.4.4 Microarray results for genes encoding ‘stress responsive’ proteins

Pd3605 (NCBI Reference Sequence: YP_917368) codes for a postulated 93 aa protein which is found on chromosome 2 of *P. denitrificans* and shows highest regulation at 3 fold increase in transcription in the presence of nitrite (table 5.1). Pd3605 is not annotated. A Sequence Similarity DataBase (SSDB) motif search using the KEGG SSDB Database (Kanehisa, 2002) shows similarity of Pd3605 with the YvrJ protein family recently identified in 2008, between residues 9-27. This family of characteristically short proteins are postulated to be induced in acid stress. YvrJ is controlled by the YvrI-YvrHa sigma factor in *Bacillus subtilis* (MacLellan *et al.*, 2008; MacLellan *et al.*, 2009) which is essential for expression of oxalate decarboxylase under acid pH stress conditions. Oxalate decarboxylase acts under acidic conditions to rebalance excess protons by catalysing the conversion of oxalate into formate and carbon dioxide with the consumption of a proton.

BLAST analysis of the protein shows very limited alignment to several also uncharacterised, hypothetical proteins within several organisms including: the freshwater cyanobacterium *Synechocystis* sp. PCC 680; the unicellular ciliate protozoa *Paramecium tetraurelia* strain d4-2; and *Erysipelotrichaceae* bacterium 2_2_44A. The sixth and twelfth hit suggest homology to proteins postulated to be part of the amidohydrolase family in *Clostridium* sp. HGF2 and be a sensor with HAMP domain from *Paenibacillus dendritiformis* C454, a

pattern-forming bacterium originally classified as *Bacillus* until 1993 (Ash *et al.*, 1993), respectively.

Pd3601 has a signalling peptide, but investigation of the genes between 3601 and 3606 does not show significant alteration in transcription between the two conditions examined and none show function similarity or protein function similarity to Pd3605. These results offer little to suggest a specific function of Pd3605, but may postulate use in acid-induced stress conditions or as a response mechanism to stress.

5.4.5 Transcription regulatory gene changes in microarray data set

In addition to the Pd1690 NsrR-like regulator, two further regulatory genes were shown to be down regulated +nitrite. These are Pd0944, a TetR family transcriptional regulator showing 0.32 fold transcription +nitrite and Pd3069 LysR family transcriptional regulator with 0.43 fold transcription +nitrite (table 5.1). BLAST analysis of the TetR regulator Pd0944 showed all hits to TetR regulators in a diverse array of organisms, confirming its annotation to be correct shown in figure 5.4.

TetR regulators are Tetracycline transcriptional regulators which act to inhibit bacterial protein synthesis by binding to the 30S ribosomal subunit, and preventing association of the aminoacyl-tRNA to the ribosomal acceptor A site in response to tetracycline. The action is reversible with removal of tetracycline. TetR proteins are a common regulatory protein which are expressed in >115 genera of bacteria and archaea. TetR shares the helix-turn-helix (HTH) structure DNA-binding domain of NsrR and can bind a target directly. TetR can bind directly to *tetA* and repress its function when tetracycline is not present. TetA then exports tetracycline out of the cell before it can attach to the ribosomes and inhibit protein synthesis (Kisker *et al.*, 1995). Additionally they have been found contribute to more complicated regulatory sequences and can be both acted upon by an additional regulator or act upon another regulator (Ramos *et al.*, 2005). Although TetR regulators are associated with pathways for the biosynthesis of antibiotics and differentiation processes, the likely reason under nitrosative stress for its down regulation is in the response to stress and toxic chemicals (Ramos *et al.*, 2005).

The second regulator of the LysR family which is a member of the type 2 periplasmic binding fold protein superfamily it shares the DNA binding helix-turn-helix (HTH) motif (Sung and Fuchs, 1992) (figure 5.5). The LysR family functions to modulate the frequency, rate or amount of transcription and acting directly with DNA. The LysR regulators are implicated in many broad functions and comprise the largest family of prokaryotic transcription factors (Zaim and Kierzek, 2003). Of note is the role of LysR family regulator *hrg* found in *Salmonella enterica serovar Typhimurium*. Lahiri *et al* (2008) performed mutational studies which showed *hrg*, conveyed resistance to sodium nitrite at pH 5.0 as well as oxidative stress such as hydrogen peroxide (H₂O₂). Over expression the *hrg* increased survival rates over wild type (WT) *S. typhimurium*. A deficient strain showed a decreased in growth over WT (Lahiri *et al.*, 2008). Additionally, OxyR transcriptional regulators which regulate the stress response to H₂O₂, are from the LysR family (Zaim and Kierzek, 2003).

Observations made by qRT-PCR regarding the upregulation of the flavohemoglobin (*fhb*) and an associated Rrf2 regulatory gene at position Pd1690 on chromosome 1 is confirmed by microarray analysis and found to be with homology to NsrR. This regulatory gene shows an upregulation in response to nitrosative stress. The proximity of the regulatory Pd1690 gene to the *fhb* on chromosome 1 of the *P. denitrificans* genome suggests Pd1690 may function to operate a regulatory role on the function of the *fhb* in response to nitrosative stresses presented to the bacterial cell. The two additional TetR and LysR regulatory genes which show downregulation may be associated with this in a larger and more complicated regulatory sequence two or more regulators are acting together.

Induced transcription in +nitrite conditions of the *fhb* may come from one or both of the TetR and LysR transcription regulators. Their down regulation in response to +nitrite growth conditions would lead to a reduction in the regulator DNA binding capabilities and allow the expression of *fhb*. This regulation may also be part of a large cascade featuring the NsrR family Pd1690, which is upregulated in +nitrite conditions. It is possible that the NO sensitive NsrR-like regulator is transcribed in direct response to the presence of NO and binds to prevent transcription of TetR and/or LysR, preventing their binding to DNA upstream of *fhb* and allowing its transcription to occur.

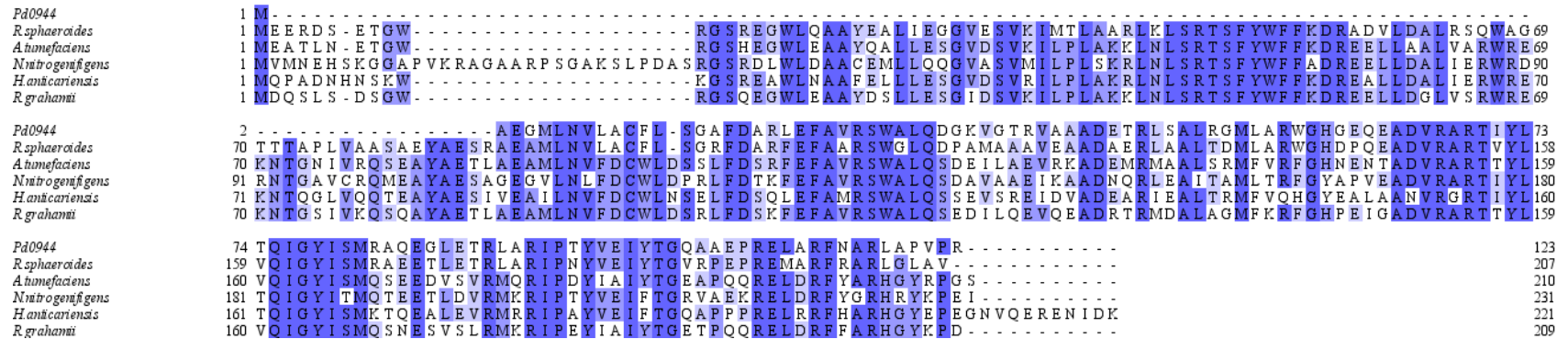


Figure 5.4: Pd0944 BLAST analysis showing similarity in protein sequence to TetR regulatory proteins in *Rhodobacter sphaeroides*, *Agrobacterium tumefaciens*, *Novosphingobium nitrogenifigens*, *Halomonas anticariensis* and *Rhizobium grahamii*.

```

Pd3069                1 M-----DWNDLK YFLAVAESRSLSAASRRRLGVSTSTVSRRITALEOALGVSLFRHHFDGYELTEAGMNLQMPAEQAESSLKAFERSAKDR85
g|489675100|ref|WP_003579342.1| 1 M-----NWDDLK VFI FVAKSNNVTEAGNSLKVSASTVSRKIAALEESLSTVLFLKKTNGYFLTEAGKAMPLALETQERFKLMERQMSQP85
g|489331783|ref|WP_003239040.1| 1 M-----DQNWND I RFFLALSRTT SFVSAATQLKVTHSTVSRRISALETALQTKL FVRTEKGCRLTSAGEQLPLAELEKAALKFQEHVPDR87
g|404492696|ref|YP_006716802.1| 1 M-----DQNWND I RFFLALSRTT SFVSAATQLKVTHSTVSRRISALETALQTKL FVRTEKGCRLTSAGEQLPLAELEKAALKFQEHVPDR87
g|494706717|ref|WP_007442619.1| 1 M-----DQNWND I RFFLALSRTT SFVSAATQLKVTHSTVSRRISALETALQTKL FVRTEKGCRLTSAGEQLPLAELEKAALKFQEHVPDR87
g|154246137|ref|YP_001417095.1| 1 MRAGDFD WSDLTF FLAVARAGRLLTAAARLKVHEHSTVSRRIGALEEALGAKLFDRRPHGYGLTAAGERLMAAAEGMETLALAAQGEIGGA90

Pd3069                2
g|489675100|ref|WP_003579342.1| 86 SDTLSG I VRLDAP FELLGQQILLPSLAGFMQDYPGIQLDIRSSVRPVQLATQQSDIVLRIVPPERGSYRMSVGKVAFGLYAHRNYLEALG175
g|489331783|ref|WP_003239040.1| 86 NDRMAGPVRIDCFELMGTHLIIPGLADFHDRYPEISFDFINTAVSSKLTQSHSDIIRLRRPENGFTMRRVGTLMQGLFCSDGYATANR175
g|404492696|ref|YP_006716802.1| 88 DNQLSGTIRIATPDGLGHCFLASRINALQSKNPLLEIELIAVPMYYSLSKREVDILITVKKPTVDRIARRITNYRFGFLFASREYLEGFP177
g|494706717|ref|WP_007442619.1| 2
g|154246137|ref|YP_001417095.1| 91 DLGVA GTVRIGAFDGGFTFFLAPRISALADLHPELD IQLLAMPRLFSLSKREADIAISLSRPK EGR LHARKLTDYRLGLYASRA YLERHG180

Pd3069                18 YPDVPE DLHRHQVIGWTEDLTYLAMANWLA SHCPGVRPSLRLTSFAAQAEAVRQAGAGWAVLPDFIAV-----PAGFAPGMPDLFRSE-S100
g|489675100|ref|WP_003579342.1| 176 QPSNDRDLRSHRIIGWSEELR YLSMSVWLDELDPLOPAMRLSSFTAQLTAVESSLGIAVLPCEFAA-----HRTGLVPVLEDLPRLT-L258
g|489331783|ref|WP_003239040.1| 176 LPDTPDDLQHHHLIGWTEEMS YMPLAQWLNEVSGEQK PVMRVSNLNAQLKAVEAHLGIAALPTVVAH-----QSGLRQVLAD-SPLRS S258
g|404492696|ref|YP_006716802.1| 178 PIQKFGDLAEHRFVGYIDDLLYDOKLRFLEEYSPALKTSFRSSTIIACMNA LKAGAGIGVIPYFMAH-----TERDLVPVLPFE-NYLE-R360
g|494706717|ref|WP_007442619.1| 37 P QDAYDLTGHDIVGYVEDLIYAPELRYLDEVSPGLKPVLSSSSIRAQREI IAGNGGIGVLP CFMAT-----GLQRVLPDLW-IE-R116
g|154246137|ref|YP_001417095.1| 181 P I E S R A G L Q R H P F I G Y V D D L I Y A P E L D Y V P L V A K D I R V R L K S S S L V A O L T A T Q A G A G V C V L P C F M A D L F A G D R P N A L V P I L P G D V G L T - R 269

Pd3069                101 ELWLLTHAQSRA LQRVNLVRDRVIVAIREELNQLQPQHS A-----140
g|489675100|ref|WP_003579342.1| 259 DLWLLVHDQAGRTPRVQIVKEHLVKILAENAEQLEG-----294
g|489331783|ref|WP_003239040.1| 259 DIWLLRNQA TQGVGRVDQVVDYLT E L F H S K T A E M Q-----293
g|404492696|ref|YP_006716802.1| 261 EFWLQVNPDSKKLARVRE AIDFIVEQMLSQSHLFLSLPEG-----300
g|494706717|ref|WP_007442619.1| 117 RFWLS THREVHGSAR IKA VHAWIKD ICDMHRTRLS PHERRGSDQDRPARQGSKRR-----171
g|154246137|ref|YP_001417095.1| 270 TFWLLTH TDTRDLAR I R V A A D F I A G V V Q A A R G Q F L S P R-----307

```

Figure 5.5: Pd3069 BLAST analysis showing similarity in protein sequence to LysR family transcriptional regulator in organisms *Rhizobium leguminosarum*, *Pseudomonas fluorescens*, *Pelobacter carbinolicus*, *Streptomyces coelicoflavus* and *Xanthobacter autotrophicus*.

5.4.6 Genes encoding repair mechanisms in *P. denitrificans*

The bioinformatic analysis of the microarray data presented in table 5.1 has shown many genes, which display functions associated with repair and maintenance mechanisms, changing their regulation in response to nitrite. Gene Pd2988 (YP_916767.1) shows a 2.7 fold increase in transcription under nitrosative stress conditions and is an unannotated gene on the NCBI database of 60 aa in length. Pd2988 is listed with residue region 19 to 53 showing homology to anaerobic ribonucleotide-triphosphate reductase. This is an enzyme which generates deoxyribonucleotides from ribonucleotides, necessary to maintain DNA during cell division and DNA repair (Torrents *et al.*, 2002). Its high upregulation in +nitrite suggests a requirement for *P. denitrificans* to repair DNA. An SSDB motif search for Pd2988, shows a region spanning 20-53 bp with homology to a NrdD motif associated with the FNR mediated control of nucleotide reductases during a shift to anaerobiosis (Boston and Atlung, 2003). This is a highly conserved domain across all classes of proteobacteria.

A pseudoazurin electron transfer protein sits at Pd2983 and the surrounding genes Pd2987 and Pd2989 are of the same anaerobic ribonucleotide-triphosphate reductase family. Pd2989 contains a cobalamin riboswitch and Pd2992 a signal peptide. However Pd2983, 2987, 2989 and 2992 show no change in transcription. This suggests a potential gene grouping. It is known the reactive nitrogen species such as nitric oxide (NO), cause damage to DNA (Drabløs *et al.*, 2004; Setlow, 2013; Yaduvanshi *et al.*, 2012). So it is likely that nitrite is generating nitrogen oxide species which are in turn damaging DNA.

The chaperonin cpn10 (groES) Pd4586 (YP_918345) and chaperone hsp20 Pd4589 (YP_918348) show an increased transcription fold change of 2.3 and 2.1 respectively under nitrosative stress. The function of Pd4589 and 4586 as chaperonin proteins has been confirmed by BLAST analysis, which showed many chaperonin scores at >95% from a range of organisms. The alignment of the chaperonin genes Pd4589 and 4586 is shown in figure 5.6 against model organisms containing the hsp20 and cpn10 genes respectively. This figure confirms the likely function of Pd4589 and 4586 and additionally shows the high conservation of chaperonin proteins across a range of organisms. These genes are situated amongst additional chaperonin genes in the genome of *P. denitrificans* which additionally show increased transcription in the presence of nitrite (figure 5.7).

Cpn10 has conserved domains within groES (Marchler-Bauer *et al.*, 2011). GroES is required for folding and assembly of some proteins and are induced under stress conditions for stabilisation protection of disassembled proteins. Protein damage is likely to occur under nitrite stress and chaperonin proteins aid the folding of proteins with energy from ATP. (Sigler *et al.*, 1998; Hartl and Hayer-Hartl, 2002; Luke and Wittung-Stafshede, 2006).

Pd4799 is annotated as a 262 aa enoyl-CoA hydratase which is confirmed by BLAST analysis, showing 100% similarity to protein annotated with the same function. The annotated conserved domains for Pd4799 (YP_918556) reveal acrotonase-like region at 11-188 and 214-260 aa which is part of the crotonase/enoyl-coenzyme A (CoA) hydratase superfamily. This superfamily contains high diversity including enoyl-CoA hydratase, naphthoate synthase, methylmalonyl-CoA decarboxylase, 3-hydroxybutyryl-CoA dehydratase, and dienoyl-CoA isomerase enzymes. The BLAST analysis shows high alignment scores for a variety of proteobacteria for enoyl-CoA hydratase or, more specifically, phenylacetate degradation probable enoyl-CoA hydratase (Agnihotri and Liu, 2003; Holden *et al.*, 2001).

BLAST alignment against model organisms *Rhodobacter sphaeroides*, *Drosophila melanogaster*, *Caenorhabditis elegans*, *Bacillus subtilis*, *Arabidopsis thaliana* in figure 5.8 shows high conservation over a diverse range of organisms, indicating a likely enoyl-CoA hydratase function for Pd4799.

Exploration of the gene surrounding Pd4799, presents two additional candidates showing similar function and increased expression under nitrite stress, which is shown in figure 5.9 BLAST analysis of Pd4800 and 4801 shows possible respective phenylacetic acid degradation phenylacetate-CoA ligase. This suggests possible catabolism of aromatic compounds (Abe-Yoshizumi *et al.*, 2004).

In this microarray, genes associated with DNA repair, protein repair and fatty acid synthesis are seen to be upregulated in +nitrite when compared with -nitrite. It is therefore suggested that these genes are part of a generalised stress response triggered by the presence of 12.5 mM sodium nitrite. It is likely that nitrite is resulting in the formation of reactive nitrogen species (RNS) which are in turn causing damage to the cellular structure of *P. denitrificans*. This damage is affecting the DNA of *P. denitrificans* These stress response genes encode likely functions as repair of DNA or protein as well as those involved in fatty acid synthesis is likely due to a generalised, metabolic repair and stress response system in *P. denitrificans*.

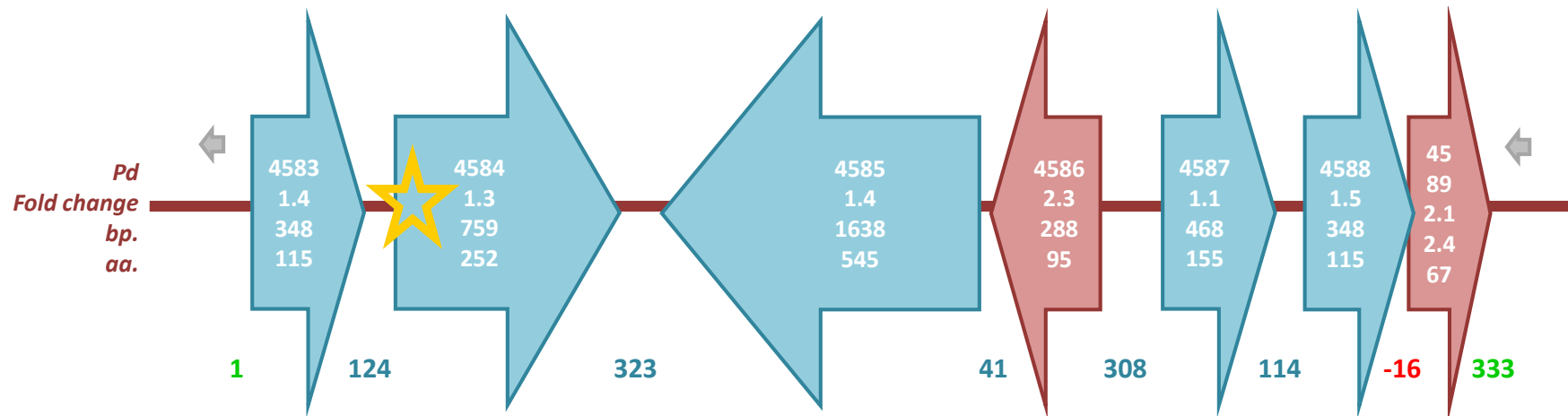


Figure 5.7: Gene arrangement of Pd4586 and 4589, red arrows. Genes of similar function are shown as blue arrows. Protein annotations: unknown Pd4583, dehydrogenase reductase Pd4584, Pd4585 chaperonin groEL (cpn60), chaperonin groES (cpn10) Pd4586, unknown Pd4587, chaperonin heat shock protein HSP20 Pd4588 and Pd4589. Gene information: gene number, fold change, base pair size (bp) and amino acid size (aa) are shown in gene arrows. Yellow star denotes signal peptide. Separating base pairs between genes are shown at the bottom.

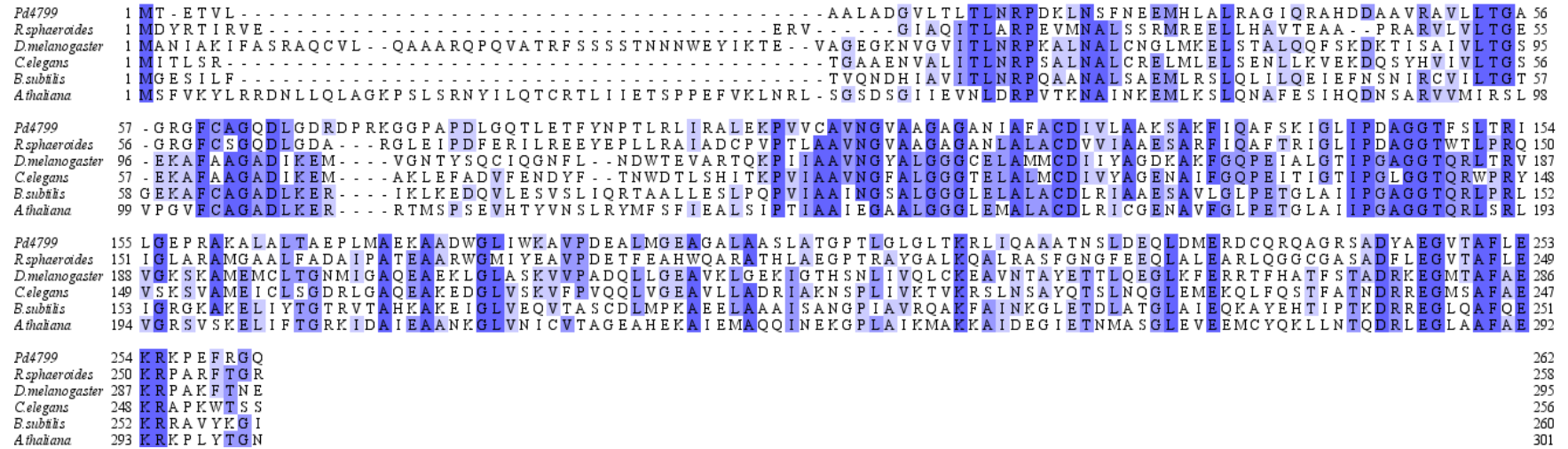


Figure 5.8: Pd4799 alignment to the model organisms: *Rhodobacter sphaeroides*, *Drosophila melanogaster*, *Caenorhabditis elegans*, *Bacillus subtilis*, *Arabidopsis thaliana*, showing a high level of conservation across a wide range of organisms.

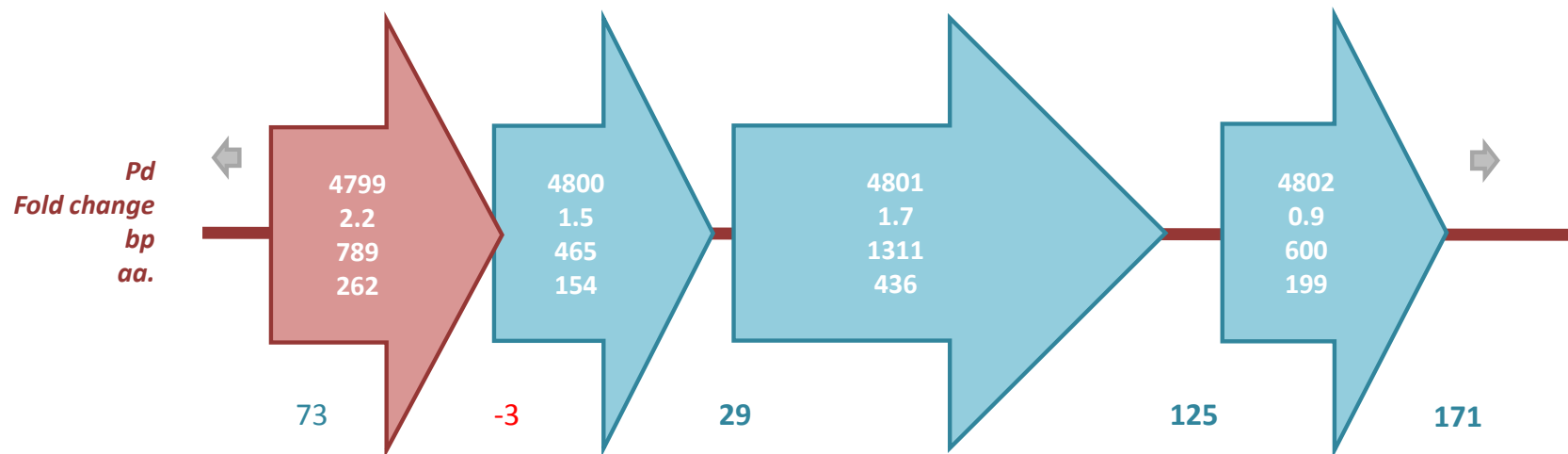


Figure 5.9: Gene cluster for Pd4799 shown in red. Genes of similar function are shown as blue arrows showing the phenylacetic acid degradation protein Pd4800, phenylacetate-CoA ligase Pd4801 and transcriptional regulator Pd4802. Gene information: gene number, fold change, base pair size (bp) and amino acid size (aa) are shown in gene arrows. Separating base pairs between genes are shown at the bottom.

5.4.7 Genes encoding oxidases

Pd5108 is a gene coding for the well-known and characterised cytochrome ba_3 quinol oxidase subunit II (accession: ABL73168.1). Cytochrome ba_3 quinol oxidase shows a consistent increased fold change of 2.5 in the microarray (table 5.1) and 2.7 in the qRT-PCR (table 5.2). Cytochrome ba_3 mediates electron transfer between quinol to the catalytic subunit I binuclear centre (Chang *et al.*, 2012). Cytochrome ba_3 forms part of the *b*-type subfamily of the haem or copper oxidases (HCO) representing a superfamily of enzymes including cytochrome *c* and quinol oxidases (García-Horsman *et al.*, 1994), which are found in the aerobic respiratory chain of both mitochondria and bacteria and have unusually high divergence in amino acid sequence while maintaining similarity in structural formation. A-type include cytochromes aa_3 and C-type oxidases (cbb_3) (Tiefenbrunn *et al.*, 2011). Cytochrome ba_3 is a large periplasmic domain of 400 residues in size, containing a signal peptide region predicted by SignalP 2.0 HMM (signal peptide with probability 0.95) with cleavage site probability 0.48 between residues 23 and 24 (Nielsen and Krogh, 1998).

There are three types of terminal oxidase; cytochrome aa_3 , cbb_3 and ba_3 that are found in *P. denitrificans*. Environmental pressures have generated a variety of oxidisable substrates and terminal electron acceptors that bacteria and archaea can use for survival. The aa_3 complex is expressed in normal atmospheric conditions, the cbb_3 has a relatively high affinity for oxygen so can be expressed under conditions of low oxygen, for example micro-aerobic soils, ba_3 has a low affinity for oxygen and is expressed under high oxygen conditions. Additionally cytochrome *c* peroxidase is expressed in low oxygen conditions to detoxify oxygen species such as hydrogen peroxide, protecting protein function (Pettigrew *et al.*, 2003). By expressing the appropriate terminal oxidase, respiration can occur under differing oxygen levels in aerobic growth whether allowing respiration to continue despite anoxia or in near pure oxygen atmosphere (Ellington *et al.*, 2003). These terminal electron acceptors generate less energy per molecule metabolised, but allow bacteria to colonise areas which are entirely anaerobic by adaption of respiration and control of electron flux (Arnoux *et al.*, 2003; Baker *et al.*, 1998; Richardson, 2000).

P. denitrificans employs the use of the TCA cycle for both aerobic and anaerobic growth with denitrification. The NADH dehydrogenase (complex I), succinate dehydrogenase (complex II), quinone/quinol (Q) pool, cytochrome bc_1 complex (complex III), cytochrome *c*

and aa_3 type cytochrome c oxidase (complex IV) have all been found in the genome of *P. denitrificans* and shown to be the electron transport chain for this bacterium.

BLAST analysis of cytochrome ba_3 shows closest homology to ubiquinol oxidase subunit II found in *Agrobacterium albertimagni* AOL15 and *Bradyrhizobium sp.*. Initial BLAST analysis shows high alignment scores to many proteobacteria showing high conservation of the cytochrome c oxidase subunit II, periplasmic domain (COX2) superfamily and COX Aromatic Rich Motif (pfam06481) (Marchler-Bauer *et al.*, 2011; Tsukihara *et al.*, 1996). Alignment to model organisms in figure 5.10 shows high conservation across a wide variety of organisms. Additionally the neighboring genes Pd5107, 5106 and 5105 are also annotated as cytochrome c oxidase shown in figure 5.11. And have fold changes of 1.9, 1.4 and 1.1 respectively which do not pass the statistical cut off of >2 fold change and >95% significance. It has been shown (van Rijn *et al.*, 1996) that electron flow to cytochrome c can be altered in the nitrite reducing organism *Pseudomonas sutzeri*, and this shows similarity to that of the transcription levels seen in *P. denitrificans* when exposed to nitrite.

The ba_3 cytochrome is membrane bound and a proton pump that contributes to the generation of proton motive force. It therefore would be able to remove intracellular protons and maintain a membrane potential which is suitable for ATP synthesis. One reason for the activation of ba_3 in +nitrite may be due to the uncoupling effect of free nitrous acid (FNA) as a protonated and uncharged molecule, FNA may diffuse across the membrane and enter the *P. denitrificans* cell. Once inside the cell, that FNA may dissociate to leave an intracellular proton. This movement would be continual; each FNA which passes across the membrane and enters the cell would lead to additional nitrite molecule protonation to form FNA to maintain equilibrium between FNA and nitrite. It has been suggested that FNA is capable of generating an influx of protons into bacterial cytoplasm leading to an uncoupling effect of the protonmotive force needed for ATP generation. This has been suggested to be a cause of growth inhibition associated with nitrite. The observed ba_3 contributes to this theory by introducing a redox balancing gene associated with nitrite stress in *P. denitrificans*. FNA can uncouple the protonmotive force of oxidative phosphorylation by acting as a protonophore; shutting protons across the membrane and into the cytosol. This would act to change the membrane polarity and disrupt the influx of protons associated with ATP synthesis by ATP synthase (Rake and Eagon, 1980; Rowe *et al.*, 1979; Williams *et al.*, 1978).

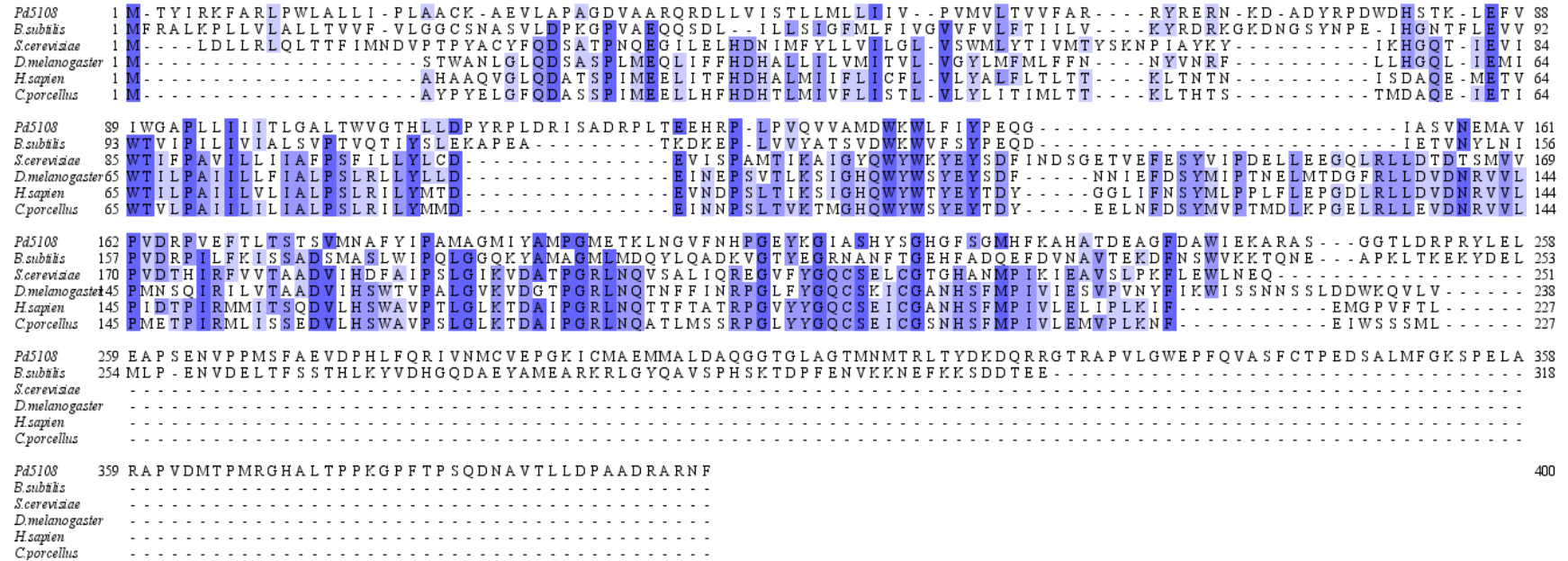


Figure 5.10: Alignment of Pd5108 to model organisms: *Bacillus subtilis* subsp. *subtilis* str. 168, *Saccharomyces cerevisiae* YJM789, *Drosophila melanogaster*, *Homo sapiens*, *Caviaporcellus*. The C- and also N-terminus alignment for *P. denitrificans*, *B. subtilis* and *S. cerevisiae* show additional residues. Loop regions appear at residues 80-90 and 124-139 *P. denitrificans*, *B. subtilis*.

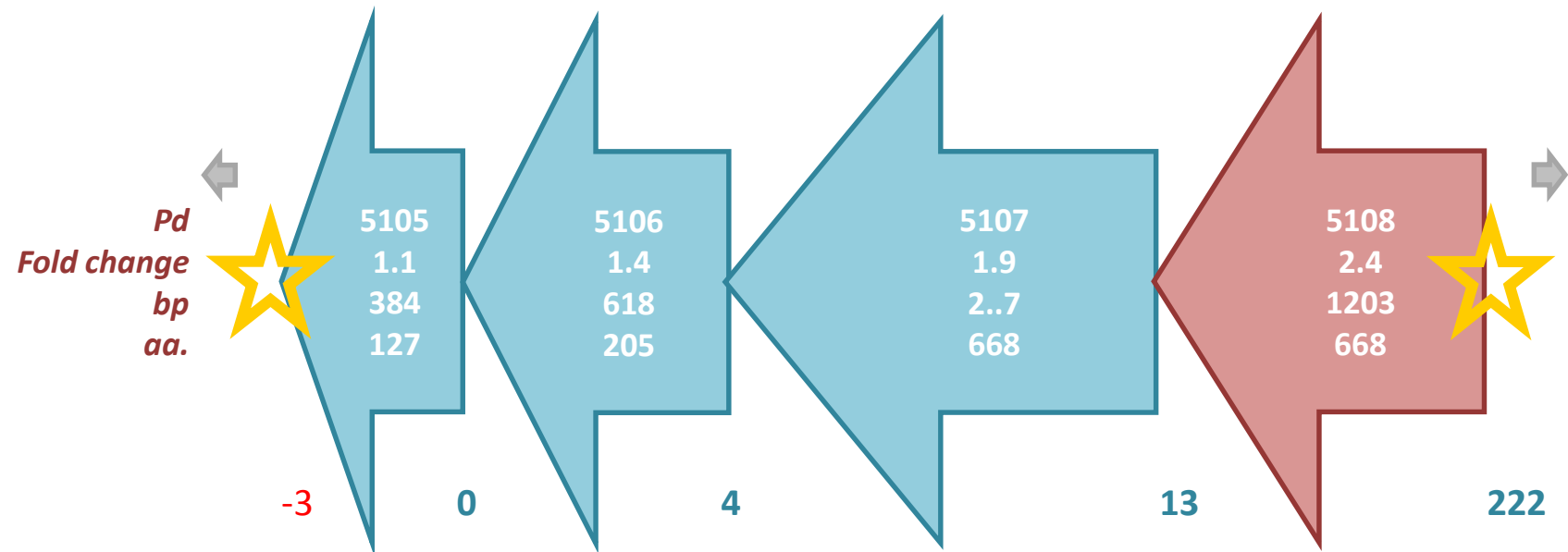


Figure 5.11: Gene cluster for Pd5108 (cytochrome ba_3 oxidase) shown in red. Genes of similar function are shown as blue arrows showing the Pd5107, Pd5106 and Pd5105 cytochrome-*c* oxidase , cytochrome-*c* oxidase subunit III and cytochrome-*c* oxidase subunit IV respectively. Gene information: gene number, fold change, base pair size (bp) and amino acid size (aa) are shown in gene arrows. Separating base pairs between genes are shown at the bottom. Yellow star indicates a signalling peptide.

5.5 Conclusions

This work carried out across three chapters has begun to put in a place a postulated model of nitrite response in *P. denitrificans* under nitrosative stress induced by 12.5 mM nitrite addition to minimal media growth conditions that is shown in figure 5.12. It has been observed that nitrite has a pH specific, inhibitory effect on the growth phenotype of *P. denitrificans* grown in minimal salts media. The addition of nitrite has the additional effect of stimulating higher levels cellular growth (Y_{\max}) when compared to growth of *P. denitrificans* without nitrite present. It has been seen that the flavohemoglobin (*fhb*) Pd1689 is constitutively expressed in the presence of nitrite over a range of nitrite concentrations between 10 – 17.5 mM during aerobic batch growth of *P. denitrificans* at pH 7.5. The microarray data suggests that this is the only Hmp or NorW homologue expressed in the presence of 12.5 mM nitrite in aerobic batch growth at pH 7.5. The other proteins known to be associated with catalysis of nitrite and nitric oxide such as the nitrite reductase (*nirS*), nitric oxide reductase (*norB*) and nitrite assimilatory pathway (*nasB*) are also suggested to not be involved in these conditions of *P. denitrificans* growth.

Mutational study of *fhb* has explored the role further with a Δfhb strain of *P. denitrificans* which is able to tolerate 5 mM higher nitrite concentrations and does not show the increased cellular growth seen in the WT strain during aerobic batch growth at pH 7.5. This implicates *fhb* in a role of both high nitrite tolerance and cellular growth at lower nitrite concentrations. The microarray data has also linked an NsrR-like regulatory protein as well as TetR and LysR regulatory proteins to the presence of nitrite. The NsrR family of regulatory proteins is NO sensitive, which suggests a possible association with the function of the *fhb*.

The microarray results seen here in chapter 5 have revealed a further significant finding of the cytochrome *ba*₃ oxidase that is transcribed in the aerobic batch culture of *P. denitrificans* in the presence of nitrite. Cytochrome *ba*₃ oxidase acts to catalyse the conversion of oxygen to water and removal of protons from the cytoplasm across the membrane. This suggests a counter effect to the presence of FNA and its association with uncoupling of the protonmotive force. The observed toxicity of nitrite and nitrite associated expression of *fhb* suggests the movement of nitrite across the membrane of *P. denitrificans* is likely. FNA is a route of transport for nitrite and in moving across the membrane would be able to dissociate and generate an internal movement of protons across the membrane. A mechanism of proton removal which provides a counter balance to the movement of protons would be a suitable

defence mechanism and ensure the continued proton gradient necessary for ATP synthesis and respiration to continue.

This has brought together a suggested model for the interaction of these genes in a defence mechanism that is postulated to provide nitrite tolerance in the aerobic batch growth of *P. denitrificans*. This postulated model is detailed in figure 5.12. This model shows the movement of nitrite into the cell via the changeless molecule FNA which dissociates and produces a proton and NO. The *fnb* is transcribed to detoxify NO in the presence of oxygen that will likely lead to the production of nitrate, but has the capability to produce nitrous oxide. The cytochrome *ba₃* oxidase is also transcribed for the removal of protons for the continued respiration and ATP synthesis in *P. denitrificans*.

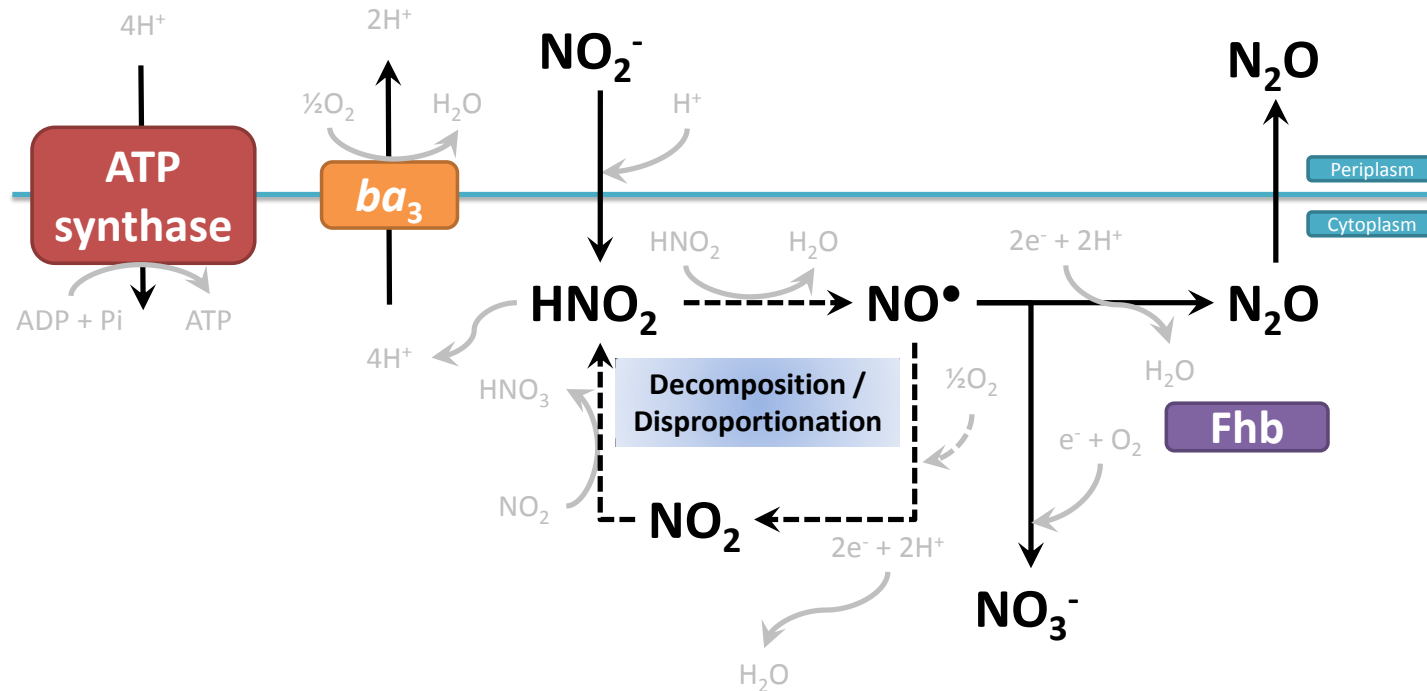


Figure 5.12: Proposed model for the aerobic stress response of *P. denitrificans* in the presence of 12.5 mM nitrite grown in batch culture at pH 7.5. This model displays the input of nitrite additions, subsequent protonation of nitrite forming free nitrous acid (FNA) (HNO_2) and movement of FNA across the membrane into the cytoplasm, chemical decomposition and disproportionation yield reactive nitrogen species (RNS) including nitric oxide (NO). Detoxification of NO by the flavohemoglobin (Fhb) forming either nitrous oxide in the absence of oxygen or nitrate in the presence of oxygen. Uncoupling effect of proton movement across the membrane by FNA is counter balanced by cytochrome ba_3 oxidase leading to the export of protons and the generation of ATP by the $F_1 F_0$ ATP synthase.

5.6 References

- ABE-YOSHIZUMI, R., KAMEI, U., YAMADA, A., KIMURA, M. & ICHIHARA, S. 2004. The evolution of the phenylacetic acid degradation pathway in bacteria. *Bioscience, Biotechnology, and Biochemistry*, 68, 746-8.
- AGNIHOTRI, G. & LIU, H.-W. 2003. Enoyl-CoA hydratase: Reaction, mechanism, and inhibition. *Bioorganic & Medicinal Chemistry*, 11, 9-20.
- ALSTON, M. J., SEERS, J., HINTON, J. C. D. & LUCCHINI, S. 2010. BABAR: An R package to simplify the normalisation of common reference design microarray-based transcriptomic datasets. *BMC Bioinformatics*, 11.
- ALTSCHUL, S. F., GISH, W., MILLER, W., MYERS, E. W. & LIPMAN, D. J. 1990. Basic local alignment search tool. *Journal of Molecular Biology* 215, 403-10.
- ARNOUX, P., SABATY, M., ALRIC, J., FRANGIONI, B., GUIGLIARELLI, B., ADRIANO, J. M. & PIGNOL, D. 2003. Structural and redox plasticity in the heterodimeric periplasmic nitrate reductase. *Nature Structural Biology*, 10, 928-934.
- ASH, C., PRIEST, F. G. & COLLINS, M. D. 1993. Molecular identification of rRNA group 3 bacilli (Ash, Farrow, Wallbanks and Collins) using a PCR probe test. *Antonie van Leeuwenhoek, International Journal of General and Molecular Microbiology*, 64, 253-260.
- BAKER, S. C., FERGUSON, S. J., LUDWIG, B., PAGE, M. D., RICHTER, O. M. & VAN SPANNING, R. J. 1998. Molecular genetics of the genus *Paracoccus*: metabolically versatile bacteria with bioenergetic flexibility. *Microbiology and Molecular Biology Reviews*, 62, 1046-78.
- BARBER, R. D., HARMER, D. W., COLEMAN, R. A. & CLARK, B. J. 2005. GAPDH as a housekeeping gene: Analysis of GAPDH mRNA expression in a panel of 72 human tissues. *Physiological Genomics*, 21, 389-395.
- BAUMBUSCH, L. O., AARØE, J., JOHANSEN, F. E., HICKS, J., SUN, H., BRUHN, L., GUNDERSON, K., NAUME, B., KRISTENSEN, V. N., LIESTØL, K., BØRRESEN-DALE, A. L. & LINGJÆRDE, O. C. 2008. Comparison of the Agilent, ROMA/NimbleGen and Illumina platforms for classification of copy number alterations in human breast tumors. *BMC Genomics*, 9, 1-16.
- BODENMILLER, D. M. & SPIRO, S. 2006. The *yjeB* (*nsrR*) gene of *Escherichia coli* encodes a nitric oxide-sensitive transcriptional regulator. *Journal of Bacteriology*, 188, 874-881.

- BOSTON, T. & ATLUNG, T. 2003. FNR-mediated oxygen-responsive regulation of the *nrdDG* operon of *Escherichia coli*. *Journal of Bacteriology*, 185, 5310-3.
- CHANG, H.-Y., CHOI, S. K., VAKKASOGLU, A. S., CHEN, Y., HEMP, J., FEE, J. A. & GENNIS, R. B. 2012. Exploring the proton pump and exit pathway for pumped protons in cytochrome *ba₃* from *Thermus thermophilus*. *Proceedings of the National Academy of Sciences*, 109, 5259-5264.
- COLLINS, J. F. & COULSON, A. F. W. 1984. Applications of parallel processing algorithms for DNA sequence analysis. *Nucleic Acids Research*, 12, 181-192.
- CONSTANTINIDOU, C., HOBMAN, J. L., GRIFFITHS, L., PATEL, M. D., PENN, C. W., COLE, J. A. & OVERTON, T. W. 2006. A reassessment of the FNR regulon and transcriptomic analysis of the effects of nitrate, nitrite, NarXL, and NarQP as *Escherichia coli* K12 adapts from aerobic to anaerobic growth. *Journal of Biological Chemistry*, 281, 4802-15.
- COOK, S. A., ROSENZWEIG, A. & TOMASELLI, G. F. 2002. DNA microarrays: Implications for cardiovascular medicine. *Circulation Research*, 91, 559-564.
- CRICK, F. H. C. & WATSON, J. D. 1954. The complementary structure of deoxyribonucleic acid. *Proceedings of the Royal Society of London. Series A. Mathematical and Physical Sciences*, 223, 80-96.
- DRABLØS, F., FEYZI, E., AAS, P. A., VAAGBØ, C. B., KAVLI, B., BRATLIE, M. S., PEÑA-DIAZ, J., OTTERLEI, M., SLUPPHAUG, G. & KROKAN, H. E. 2004. Alkylation damage in DNA and RNA - Repair mechanisms and medical significance. *DNA Repair*, 3, 1389-1407.
- ELLINGTON, M. J. K., SAWERS, G., SEARS, H. J., SPIRO, S., RICHARDSON, D. J. & FERGUSON, S. J. 2003. Characterization of the expression and activity of the periplasmic nitrate reductase of *Paracoccus pantotrophus* in chemostat cultures. *Microbiology*, 149, 1533-1540.
- FILENKO, N., SPIRO, S., BROWNING, D. F., SQUIRE, D., OVERTON, T. W., COLE, J. & CONSTANTINIDOU, C. 2007. The NsrR regulon of *Escherichia coli* K-12 includes genes encoding the hybrid cluster protein and the periplasmic, respiratory nitrite reductase. *Journal of Bacteriology*, 189, 4410-7.
- FIROVED, A. M., WOOD, S. R., ORNATOWSKI, W., DERETIC, V. & TIMMINS, G. S. 2004. Microarray analysis and functional characterization of the nitrosative stress response in nonmucoid and mucoid *Pseudomonas aeruginosa*. *Journal of Bacteriology*, 186, 4046-50.

- FORRESTER, M. T. & FOSTER, M. W. 2012. Protection from nitrosative stress: A central role for microbial flavohemoglobin. *Free Radical Biology and Medicine*, 52, 1620-1633.
- GADGIL, M., LIAN, W., GADGIL, C., KAPUR, V. & HU, W. S. 2005. An analysis of the use of genomic DNA as a universal reference in two channel DNA microarrays. *BMC Genomics*, 6.
- GARCÍA-HORSMAN, J. A., BARQUERA, B., RUMBLEY, J., MA, J. & GENNIS, R. B. 1994. The superfamily of heme-copper respiratory oxidases. *Journal of Bacteriology*, 176, 5587-5600.
- GATES, A. J., LUQUE-ALMAGRO, V. M., GODDARD, A. D., FERGUSON, S. J., ROLDÁN, M. D. & RICHARDSON, D. J. 2011. A composite biochemical system for bacterial nitrate and nitrite assimilation as exemplified by *Paracoccus denitrificans*. *Biochemical Journal*, 435, 743-753.
- HARTL, F. U. & HAYER-HARTL, M. 2002. Molecular chaperones in the cytosol: from nascent chain to folded protein. *Science*, 295, 1852-1858.
- HOLDEN, H. M., BENNING, M. M., HALLER, T. & GERLT, J. A. 2001. The crotonase superfamily: divergently related enzymes that catalyze different reactions involving acyl coenzyme a thioesters. *Accounts of Chemical Research*, 34, 145-57.
- KANEHISA, M. 2002. The KEGG database. *Novartis Foundation Symposium*, 247, 91-101; discussion 101-3, 119-28, 244-52.
- KISKER, C., HINRICHS, W., TOVAR, K., HILLEN, W. & SAENGER, W. 1995. The complex formed between Tet repressor and tetracycline-Mg₂⁺ reveals mechanism of antibiotic resistance. *Journal of molecular biology*, 247, 260-280.
- KNUDSEN, S. 2004. *Guide to analysis of DNA microarray data*, John Wiley & Sons.
- LAHIRI, A., DAS, P. & CHAKRAVORTTY, D. 2008. The LysR-type transcriptional regulator Hrg counteracts phagocyte oxidative burst and imparts survival advantage to *Salmonella enterica serovar Typhimurium*. *Microbiology*, 154, 2837-46.
- LIVAK, K. J. & SCHMITTGEN, T. D. 2001. Analysis of relative gene expression eata using real-time quantitative PCR and the 2^{ΔΔCT} method. *Methods*, 25, 402-408.
- LORKOWSKI, S. & CULLEN, P. M. 2006. *Analysing Gene Expression, A Handbook of Methods: Possibilities and Pitfalls*, John Wiley & Sons.
- LUKE, K. & WITTUNG-STAFSHED, P. 2006. Folding and assembly pathways of co-chaperonin proteins 10: Origin of bacterial thermostability. *Archives of Biochemistry and Biophysics*, 456, 8-18.

- MACLELLAN, S. R., HELMANN, J. D. & ANTELMANN, H. 2009. The YvrI alternative sigma factor is essential for acid stress induction of oxalate decarboxylase in *Bacillus subtilis*. *Journal of Bacteriology*, 191, 931-9.
- MACLELLAN, S. R., WECKE, T. & HELMANN, J. D. 2008. A previously unidentified sigma factor and two accessory proteins regulate oxalate decarboxylase expression in *Bacillus subtilis*. *Molecular Microbiology*, 69, 954-67.
- MARCHLER-BAUER, A., ANDERSON, J. B., CHITSAZ, F., DERBYSHIRE, M. K., DEWEESE-SCOTT, C., FONG, J. H., GEER, L. Y., GEER, R. C., GONZALES, N. R., GWADZ, M., HE, S., HURWITZ, D. I., JACKSON, J. D., KE, Z., LANCZYCKI, C. J., LIEBERT, C. A., LIU, C., LU, F., LU, S., MARCHLER, G. H., MULLOKANDOV, M., SONG, J. S., TASNEEM, A., THANKI, N., YAMASHITA, R. A., ZHANG, D., ZHANG, N. & BRYANT, S. H. 2009. CDD: Specific functional annotation with the Conserved Domain Database. *Nucleic acids research*, 37, D205-D210.
- MARCHLER-BAUER, A. & BRYANT, S. H. 2004. CD-Search: protein domain annotations on the fly. *Nucleic Acids Research*, 32, W327-31.
- MARCHLER-BAUER, A., LU, S., ANDERSON, J. B., CHITSAZ, F., DERBYSHIRE, M. K., DEWEESE-SCOTT, C., FONG, J. H., GEER, L. Y., GEER, R. C., GONZALES, N. R., GWADZ, M., HURWITZ, D. I., JACKSON, J. D., KE, Z., LANCZYCKI, C. J., LU, F., MARCHLER, G. H., MULLOKANDOV, M., OMELCHENKO, M. V., ROBERTSON, C. L., SONG, J. S., THANKI, N., YAMASHITA, R. A., ZHANG, D., ZHANG, N., ZHENG, C. & BRYANT, S. H. 2011. CDD: a Conserved Domain Database for the functional annotation of proteins. *Nucleic acids research*, 39, D225-D229.
- MOUNT, D. W. 2007. Using the Basic Local Alignment Search Tool (BLAST). *Cold Spring Harbor Protocols*, 2007, pdb.top17.
- NIELSEN, H. & KROGH, A. 1998. Prediction of signal peptides and signal anchors by a hidden Markov model. *Proceedings of the National Academy of Sciences*, 6, 122-30.
- PETTIGREW, G. W., GOODHEW, C. F., COOPER, A., NUTLEY, M., JUMEL, K. & HARDING, S. E. 2003. The electron transfer complexes of cytochrome c peroxidase from *Paracoccus denitrificans*. *Biochemistry*, 42, 2046-55.
- RAKE, J. B. & EAGON, R. G. 1980. Inhibition, but not uncoupling, of respiratory energy coupling of three bacterial species by nitrite. *Journal of Bacteriology*, 144, 975-982.

- RAMOS, J. L., MARTINEZ-BUENO, M., MOLINA-HENARES, A. J., TERAN, W., WATANABE, K., ZHANG, X., GALLEGOS, M. T., BRENNAN, R. & TOBES, R. 2005. The TetR family of transcriptional repressors. *Microbiology and Molecular Biology Reviews*, 69, 326-56.
- REID, K. E., OLSSON, N., SCHLOSSER, J., PENG, F. & LUND, S. T. 2006. An optimized grapevine RNA isolation procedure and statistical determination of reference genes for real-time RT-PCR during berry development. *BMC Plant Biology*, 6.
- RICHARDSON, D. J. 2000. Bacterial respiration: A flexible process for a changing environment. *Microbiology*, 146, 551-571.
- RICHARDSON, D. J., BERKS, B. C., RUSSELL, D. A., SPIRO, S. & TAYLOR, C. J. 2001. Functional, biochemical and genetic diversity of prokaryotic nitrate reductases. *Cellular and Molecular Life Sciences*, 58, 165-178.
- ROWE, J. J., YARBROUGH, J. M., RAKE, J. B. & EAGON, R. G. 1979. Nitrite inhibition of aerobic bacteria. *Current Microbiology*, 2, 51-54.
- SEARS, H. J., SAWERS, G., BERKS, B. C., FERGUSON, S. J. & RICHARDSON, D. J. 2000. Control of periplasmic nitrate reductase gene expression (*napEDABC*) from *Paracoccus pantotrophus* in response to oxygen and carbon substrates. *Microbiology*, 146 (Pt 11), 2977-85.
- SETLOW, P. 2013. Resistance of Bacterial Spores to Chemical Agents. *Russell, Hugo & Ayliffe's*. Wiley-Blackwell.
- SIGLER, P. B., XU, Z. H., RYE, H. S., BURSTON, S. G., FENTON, W. A. & HORWICH, A. L. 1998. Structure and function in GroEL-mediated protein folding. *Annual Review of Biochemistry*, 67, 581-608.
- SULLIVAN, M. J., GATES, A. J., APPIA-AYME, C., ROWLEY, G. & RICHARDSON, D. J. 2013. Copper control of bacterial nitrous oxide emission and its impact on vitamin B12-dependent metabolism. *Proceedings of the National Academy of Sciences*.
- SUNG, Y. C. & FUCHS, J. A. 1992. The *Escherichia coli* K-12 *cyn* operon is positively regulated by a member of the *lysR* family. *Journal of bacteriology*, 174, 3645-3650.
- TARCA, A. L., ROMERO, R. & DRAGHICI, S. 2006. Analysis of microarray experiments of gene expression profiling. *American Journal of Obstetrics and Gynecology*, 195, 373-388.
- TIEFENBRUNN, T., LIU, W., CHEN, Y., KATRITCH, V., STOUT, C. D., FEE, J. A. & CHEREZOV, V. 2011. High resolution structure of the *ba₃* cytochrome *c* oxidase from *Thermus thermophilus* in a lipidic environment. *PLoS ONE*, 6, e22348.

- TORRENTS, E., ALOY, P., GIBERT, I. & RODRIGUEZ-TRELLES, F. 2002. Ribonucleotide reductases: divergent evolution of an ancient enzyme. *Journal of Molecular Evolution*, 55, 138-52.
- TSUKIHARA, T., AOYAMA, H., YAMASHITA, E., TOMIZAKI, T., YAMAGUCHI, H., SHINZAWA-ITOH, K., NAKASHIMA, R., YAONO, R. & YOSHIKAWA, S. 1996. The whole structure of the 13-subunit oxidized cytochrome *c* oxidase at 2.8 Å. *Science*, 272, 1136-44.
- VAN RIJN, J., TAL, Y. & BARAK, Y. 1996. Influence of volatile fatty acids on nitrite accumulation by a *Pseudomonas stutzeri* strain isolated from a denitrifying fluidized bed reactor. *Applied and Environmental Microbiology*, 62, 2615-20.
- VAN SPANING, R. J. M., DE BOER, A. P. N., REIJNDERS, W. N. M., DE GIER, J. W. L., DELORME, C. O., STOUTHAMER, A. H., WESTERHOFF, H. V., HARMS, N. & VAN DER OOST, J. 1995. Regulation of oxidative phosphorylation: The flexible respiratory network of *Paracoccus denitrificans*. *Journal of Bioenergetics and Biomembranes*, 27, 499-512.
- WILLIAMS, D. R., ROWE, J. J., ROMERO, P. & EAGON, R. G. 1978. Denitrifying *Pseudomonas aeruginosa*: Some parameters of growth and active transport. *Applied and Environmental Microbiology*, 36, 257-263.
- YADUVANSHI, S. K., SRIVASTAVA, N., PRASAD, G. B., YADAV, M., JAIN, S. & YADAV, H. 2012. Genotoxic potential of reactive oxygen species (Ros), lipid peroxidation and DNA repair enzymes (Fpg and Endo III) in alloxan injected diabetic rats. *Endocrine, metabolic and immune disorders drug targets*.
- ZAIM, J. & KIERZEK, A. M. 2003. The structure of full-length LysR-type transcriptional regulators. Modeling of the full-length OxyR transcription factor dimer. *Nucleic Acids Research*, 31, 1444-54.

6 Metabolic analysis of nitrosative stress in batch and continuous culture of *P. denitrificans* in a continuous culture system

Contents

6	Metabolic analysis of nitrosative stress in batch and continuous culture of <i>P. denitrificans</i> in a continuous culture system.....	226
	Contents.....	226
6.1	List of figures	227
6.2	List of tables	229
6.3	Introduction and experimental approaches	229
6.3.1	Metabolic pathways of <i>P. denitrificans</i> for nitrogenous oxides and carbon metabolism.....	230
6.3.2	Comparative batch and continuous culture of <i>P. denitrificans</i>	232
6.4	Results	233
6.4.1	Growth of <i>P. denitrificans</i> at varying succinate concentrations.....	233
6.4.2	Growth of <i>P. denitrificans</i> on the reduced carbon substrate butyrate.....	236
6.4.3	Metabolite analysis in batch culture of <i>P. denitrificans</i> under 12.5 mM nitrite stress	239
6.4.4	Development of continuous culture methodology.....	241
6.4.5	Transcription under continuous culture growth of <i>P. denitrificans</i>	250
6.5	Discussion	251
6.5.1	Increased transcription of the flavohemoglobin	252
6.5.2	Nitrogenous oxide production from <i>P. denitrificans</i> in the presence of nitrite	253

6.5.3	Carbon metabolism of <i>P. denitrificans</i>	253
6.6	References.....	256

6.1 List of figures

Figure 6.1:	Growth of <i>P. denitrificans</i> on minimal salts media with 10 mM ammonia chloride at pH 7.5 with varying levels of sodium succinate carbon source. Succinate levels are shown above in mM. Error bars denote standard error n = 3.	235
Figure 6.2:	Growth of <i>P. denitrificans</i> with 10 mM sodium butyrate as sole carbon source in minimal salts media and 10 mM ammonia chloride at pH 7.5. Various media pH values have been examined and are listed in the legend. Growth measured using optical density (OD) (AU). Error bar denote standard error (n = 3).	237
Figure 6.3:	The apparent growth rate (μ_{app}) (h^{-1}) for the growth of <i>P. denitrificans</i> on 30 mM succinate (circles) and 10 mM butyrate (triangles), without nitrate (open) and with nitrate (closed). Growth is in minimal salts media with 10 mM ammonia chloride at pH 7.0, 7.5, 8.0 and 8.5. Error bars denote standard error (n = ≥ 3).	238
Figure 6.4:	Levels of the metabolites nitrate, nitrite and nitrous oxide for growth of <i>P. denitrificans</i> in minimal salts media with 10 mM ammonia chloride and 30 mM succinate carbon source at pH 7.5 A: without nitrite, B: with 11.7 \pm 0.2 mM nitrite present. Nitrous oxide levels are show above that of background atmospheric levels. Error bars denote standard error (n = 3).....	240
Figure 6.5:	Diagram of chemostat kinetics F is the volumetric flow rate of nutrient solution (0.08 L.h ⁻¹); X is the cell biomass (g.L ⁻¹); S and P denote the substrate and product consumption and production respectively (mM). Subscript 0 denotes the parameters at the feed medium. At steady state, X ₀ = 0 g.L ⁻¹ . Dilution rate (D) can be determined by D = F / vessel volume, the reciprocal of residence time: 0.08 L.h ⁻¹ / 1.5 L D = 0.053 h ⁻¹	243
Figure 6.6:	Schematic of a continuous culture chemostat. Computer controlled elements: peristaltic pumps leading to media feed, acid and base, monitoring of pH by electrode probe, adjustment of pH through automatic activation of acid and base peristaltic pumps, monitoring dissolved oxygen (DO) by electrode probe, maintenance of constant agitation (Agit.), maintenance of constant gas flow, monitoring of temperature and adjustment of temperature by automatic adjustment of water temperature through water jacket.....	244
Figure 6.7:	Continuous culture of <i>P. denitrificans</i> under nitrosative stress with nitrite addition to minimal salts media at pH 7.5 and 10 mM ammonium chloride (n = 3). At 28	

hours feed was applied at a dilution rate of 0.053 h^{-1} (black line at 28 hours) Feed was replenished at 78 hours (black line at 78 hours), Maintaining steady state for 123 hours after inoculation. Feed batch indicated by vertical line. A: average dissolved oxygen (DO), optical density (OD) and biomass. Growth was measured spectrophotometrically at 600 nm (open circles) and converted to biomass (open diamond) showing exponential growth over 28 hours. B: average concentration of nitrate, nitrite and nitrous oxide throughout the incubation period. Nitrous oxide is shown as nitrous oxide above atmospheric background levels $\mu\text{M}\cdot\text{hour}^{-1}$. (Error bars denote standard deviation; $n = 3$)......246

Figure 6.8: Continuous culture of *P. denitrificans* under standard growth conditions minimal salts media at pH 7.5 and 10 mM ammonium chloride. Growth was measured spectrophotometrically at 600 nm (open up pointing triangle) and converted to biomass (open diamond) showing exponential growth over 19 hours. At 28 hours feed was applied at a dilution rate of 0.053 h^{-1} (black line at 28 hours) Feed was replenished at 78 hours (black line at 78 hours), Maintaining steady state for 123 hours after inoculation. Nitrous oxide production (open squares) with biomass production (open diamonds). Nitrous oxide is shown as nitrous oxide above atmospheric background levels $\mu\text{M}\cdot\text{hour}^{-1}$. Feed batch indicated by vertical line (Giannopoulos *et al.*, data unpublished)......248

Figure 6.9: Continuous culture of *P. denitrificans* under nitrosative stress with nitrite and nitrate addition to minimal salts media at pH 7.5 and 10 mM ammonium chloride ($n = 3$). At 28 hours feed was applied at a dilution rate of 0.053 h^{-1} (black line at 28 hours) Feed was replenished at 78 hours (black line at 78 hours), Maintaining steady state for 123 hours after inoculation. Feed batch indicated by vertical line. A: average dissolved oxygen (DO), optical density (OD) at 600 nm and biomass. Growth was measured spectrophotometrically at 600 nm (open circles) and converted to biomass (open diamond) showing exponential growth over 28 hours. B: average concentration of nitrate, nitrite and nitrous oxide throughout the incubation period. Nitrous oxide is shown as nitrous oxide above atmospheric background levels $\mu\text{M}\cdot\text{hour}^{-1}$. (Error bars denote standard deviation; $n = 3$)......249

Figure 6.10: Transport across cellular membrane of *P. denitrificans* by protonation. Butyric acid ($\text{CH}_3\text{CH}_2\text{COOH}$) in the protonated form and deprotonated in the ion form ($\text{CH}_3\text{CH}_2\text{COO}^-$). Free nitrous acid (FNA) (HNO_2) in the protonated form and ion form (NO_2^-).255

6.2 List of tables

Table 6.1: The calculation of yield (Y) from biomass (ΔX) ($\text{g}\cdot\text{L}^{-1}$) and substrate available (ΔS) ($\text{g}\cdot\text{L}^{-1}$).....	234
Table 6.2: The 0.5 hourly monitored parameters with associated variance and error for continuous culture within a chemostat containing <i>P. denitrificans</i> grown in the following conditions: +nitrate -nitrite ¹ = 21 mM sodium nitrate, -nitrate +nitrite = 36 mM sodium nitrite, and +nitrate +nitrite = 25 mM nitrite with 8 mM nitrate. DO = dissolved oxygen. SE = standard error (n=3).	245
Table 6.3: The transcriptional data for continuous culture growth of <i>P. denitrificans</i> in minimal salts media at pH 7.5. Growth conditions were as follows: +nitrate -nitrite ¹ = 21 mM sodium nitrate, -nitrate +nitrite = 36 mM sodium nitrite, and +nitrate +nitrite = 25 mM nitrite with 8 mM nitrate. SE = standard error (n=3).	251

6.3 Introduction and experimental approaches

It has been identified that *P. denitrificans* undergoes a pH dependent inhibition of growth in the presence of sodium nitrite additions to minimal salts growth media. It was established that the optimal pH range for growth of *P. denitrificans* is pH 7.5 – 8.0. This pH specific growth was further investigated. The likely route of this effect was attributed to the internalisation and disproportionation of free nitrous acid FNA to form RNS such as NO and peroxy nitrite, which are capable of producing the growth inhibition observed by acting detrimentally on the protein metal centres and DNA of *P. denitrificans* to inhibit the growth of *P. denitrificans*. Bioinformatic analysis of the *P. denitrificans* genome identified a number of genes which had homology to the key known NO detoxification proteins Hmp and NorVW. These as well as the well-studied denitrification and assimilatory genes known to be expressed in *P. denitrificans* such as the nitrite reductase (*nirS*), nitric oxide reductase (*norB*) and assimilatory nitrite reductase (*nasB*), were transcriptionally explored to determine what genes were upregulated in the nitrite stress conditions. A novel flavohemoglobin (*fhb*) gene was identified as expressed in the presence of nitrite. Also found to be associated with nitrite was an *fhb* associated transcriptional regulator, a series of protein, DNA and lipid repair mechanisms as well as the *ba₃* oxidase. The role of *ba₃* oxidase in nitrite tolerance may be to counter the uncoupling effects of FNA.

A deletion mutant of the *fhb* (Δfhb) was created. The growth of this mutant in the presence of nitrite was possible, which has suggested that *fhb* contributes to a larger metabolic response produced by *P. denitrificans*. The metabolic by-products of the growth of *P. denitrificans* with nitrite present will be investigated in this chapter. Additionally the dependency of nitrite stress on carbon source will be investigated. This thesis has focused on the growth of *P. denitrificans* on succinate, a relatively oxidised carbon source. It is possible the sensitivity to nitrite / FNA will be dependent on carbon substrate. Therefore to close the thesis some preliminary investigation of growth on a more reduced carbon source in place of succinate - the short chain fatty acid butyrate - was undertaken.

6.3.1 Metabolic pathways of *P. denitrificans* for nitrogenous oxides and carbon metabolism

P. denitrificans is a well-known model denitrifier capable of carrying out the sequential reduction of nitrate (NO_3^-) to nitrite (NO_2^-), nitric oxide (NO), nitrous oxide (N_2O) and atmospheric nitrogen (N_2) to provide a flow of electrons as the terminal oxidase in respiration. During full denitrification, accumulation of nitrogenous oxide intermediates is not seen and the production of di nitrogen as a final production of denitrification can be quantified with the use of N^{15} (Richardson, 2001). *P. denitrificans* is able to metabolise nitrate using NAR, NAP and NAS. NAR is the cytoplasmic nitrate reductase associated with expression in anaerobic growth conditions in the presence of nitrate used for respiration without oxygen present. The catalytic component of NAR, NarG, is self-regulated by NarX as well as by the Fumarate and Nitrate Regulatory protein (FNR). This causes positive regulation of NarG in the presence of nitrate and negative regulation of NarG in the presence of oxygen (Richardson, 2001). The second respiratory nitrate reductase is found in a periplasm (NAP) and is not associated with the generation of protonmotive force and the regulation of NAP has not been associated with levels of nitrate or oxygen, but instead has been seen to respond to levels of reductants in the ubiquinol / quinone pool (Q-pool) when growth of *P. denitrificans* is on a relatively reduced carbon source such as butyrate. The β -oxidation pathway acts to convert 4 carbon butyrate into 2 carbon acetyl-CoA for entry into the citric acid cycle 10 NADH and FADH_2 molecules for each butyrate molecule consumed. These feed directly into the Q-pool in the Q-Cycle and disrupt membrane potential by creating a disproportionately larger amount of ubiquinol (Watmough and Frerman, 2010)

and disrupt the catalytic action of the cytochrome bc_1 complex (Kurihara *et al.*, 1992; Müller *et al.*, 2010; Kunau *et al.*, 1995). NapC oxidises ubiquinol to ubiquinone and removes electrons from the Q-Pool for the reduction of nitrate to nitrite by NapAB. The assimilatory nitrate reductase NAS is induced by an absence of ammonium and can be expressed both aerobically and anaerobically. *P. denitrificans* expresses the NAS to produce ammonium from nitrate and/or nitrite for incorporation into biomass (Richardson, 2000). In *P. denitrificans* nitrite and nitric oxide reduction is carried out by the iron based cytochrome cd_1 nitrite reductase (cd_1 NIR) and nitric oxide reductase (NOR) which are expressed during low oxygen conditions when nitrite and nitric oxide are present. The expression of cd_1 NIR and NOR is tightly coupled to the levels of nitrite and nitric oxide by the Nitrite and Nitric oxide Regulatory protein (NNR). This is thought to be due to the relative nature of these nitrogenous oxides and prevents them from accumulating to levels which are detrimental to growth during anaerobic respiration (Kwiatkowski *et al.*, 1997; Bergaust *et al.*, 2012).

The characterisation of the *fhb* gene as a homologue of Hmp suggests that there is a likelihood of it functioning as a nitric oxide detoxifying flavohemoglobin. It would therefore be a route for the production of nitrate or nitrous oxide. Fhb are capable of acting as a nitric oxide dioxygenase for the conversion of nitric oxide to nitrate at high oxygen levels or nitrous oxide at low oxygen levels: $2\text{NO} + 2\text{O}_2 + \text{NAD(P)H} \rightarrow 2\text{NO}_3^- + \text{NAD(P)}^+ + \text{H}^+$ and $2\text{NO} + 2\text{H}^+ \rightarrow 2\text{N}_2\text{O} + \text{H}_2\text{O}$ (Forrester and Foster, 2012). The Hmp was first identified in *E. coli* and has been extensively studied for its function and structural characteristics. Knock out mutants have been constructed both in *E. coli* and *S. typhimurium* which significantly reduced survival rates of the bacteria in the presence of nitric oxide. Levels of nitric oxide however are not likely to accumulate to levels exceeding μM amounts, making observation of nitrate and nitrous oxide unlikely.

The carbon substrate used in microbiological experiments can have a large effect on the growth of the organism. Growth of *P. denitrificans* on succinate provides a relatively oxide carbon source which feeds directly into the citric acid (TCA) cycle and generates 1 FADH_2 and 3 NADH per TCA cycle.. Altering the carbon substrate for a relatively reduced carbon source such as butyrate causes an alteration in the metabolism of *P. denitrificans*. In butyrate metabolism, the fatty acid must first be converted the acetyl-CoA in order to be fed into TCA cycle. The β -oxidation converts butyrate (4C) into acetyl-CoA (2C) and generates of 1 NADH and 1 FADH_2 . The two acetyl-CoA molecules enter the citric acid cycle and generate a further 1 FADH_2 and 3 NADH per TCA cycle, resulting in 10 NADH and FADH_2 in total

in comparison the 4 NADH and FADH₂ from the metabolism of succinate. These NADH and FADH₂ feed directly into the ubiquinol / quinone pool in the Q-Cycle causing a disruption of the membrane potential and generating ubiquinol which limits the catalytic action of the cytochrome *bc*₁ complex. The mechanism of restoration of the Q-pool comes in the form of the periplasmic nitrate reductase (NAP). NAP uses the reduction of nitrate to remove the excess electrons in the Q-pool and restoring catalytic action of the cytochrome *bc*₁ complex. Additionally the concentration of carbon source can be a limiting factor in the growth of microorganisms. This feature is utilised by chemostatic culture to prevent over-population of the culture vessel during continuous culture. Growth studies were undertaken with *P. denitrificans* to determine the concentration at which carbon limitation with succinate would be effective in chemostatic culture and to explore the combined effects of nitrite and reduced carbon metabolism.

6.3.2 Comparative batch and continuous culture of *P. denitrificans*

Both batch and continuous culture techniques have been employed for investigation of nitrosative stress response of *P. denitrificans* to nitrite in this work. The batch culture replicates a phenomenon in which a compound is introduced once over a relative short time. During that time cell density increases to cause changes in the oxic environment and diffusion of oxygen with production of metabolites altering pH and causing cell interaction with compounds both beneficial and toxic. Cell growth is limited by nutrient levels or by accumulation of waste products, as fresh media is not added and waste products are not removed. In this mode, a higher cell concentration is achieved allowing the observation of complete growth and the total biomass achievable. During batch culture the phases of growth and growth phenotype unique to *P. denitrificans* under nitrosative stress can be observed; the length of lag phase indicating cellular adaption to growth conditions, the gradient and length of exponential growth, the biomass concentration at which stationary phase is achieved.

Continuous culture by comparison, allows maintenance of a constant growth environment, in which all parameters which affect growth can be constantly maintained within set parameters in the design of the experiment. For this experiment, steady levels of bacterial biomass in the reaction vessel by the addition of fresh media and removal of by-products and cells at a set rate. Subsequently the bacteria in the vessel will consume the nutrients required

for growth, but the growth rate is controlled by the dilution rate of the chemostat. Another additional way of controlling the growth rate is to supply the media with a limited nutrient compound. The above technique in continuously stirred tank reactors (CSTR) is widely known as chemostat because the chemical parameters that are essential are maintained at steady rates. In these experiments it was possible to control bacterial growth in the chemostat by controlling the dilution rate and by using sodium succinate as a limiting nutrient. Cells are maintained by addition of fresh media and removal of waste products preventing accumulation of by-products whilst maintaining required nutrients at the optimum levels needed for cell growth and metabolism. The set parameters and dilution rate of fresh media addition maintain a constant cell density at mid exponential state of growth. This system of cell culture permits direct observation of sodium nitrite effect without change in growth conditions on cells maintained at a constant state of growth providing a unique comparison to that of batch culture. RNA extracted during continuous culture can also be used to ascertain transcription differences unique to the addition of sodium nitrite in isolation from other growth induced changes in growth found in batch culture.

6.4 Results

6.4.1 Growth of *P. denitrificans* at varying succinate concentrations

For the growth experiments a large volume of *P. denitrificans* cells is needed for the metabolic analysis of nitrogenous oxides. The shaking flask technique was employed to batch culture *P. denitrificans* aerobically at a volume of 50 ml as described in the methods and used in the previous chapter for RNA extraction. Succinate concentration has a distinct effect on the growth of *P. denitrificans* shown in figure 6.1, which is defined here by the maximum optical density (Y_{\max} AU) achieved in the growth conditions examined and listed in table 6.1. At 0 mM sodium succinate, growth was not observed. The addition of 2.5 mM shows growth which reaches Y_{\max} 0.61 \pm 0.01 AU. An Y_{\max} of 3.1 \pm 0.1 AU is achieved with both 20 and 30 mM succinate. Provision of 20 mM provides sufficient carbon for maximal growth in minimal salts media at pH 7.5 and Y_{\max} does not increase with 30 mM succinate provided. This was examined further using the apparent growth yield (Y_{app}) calculated for biomass (g.l^{-1}) produced as a function of succinate substrate (g.l^{-1}): $Y_{\text{app}} = \Delta X / \Delta S$. The Y_{app} was calculated using the conversion of Y_{\max} to approximate A: biomass in dry weight (g) per

litre using the dry weight of *P. denitrificans* cells in (g.L^{-1}) (ΔX), B: the conversion of succinate (M) to succinate g.L^{-1} (ΔS):

$$\text{A: Biomass } \text{g.L}^{-1} (\Delta X) = Y_{\text{max}} (\text{AU}) \times 0.52 \text{ g.L}^{-1}$$

$$\text{B: Succinate } \text{g.L}^{-1} (\Delta S) = \text{succinate (M)} \times 118.1 \text{ g.mol}^{-1}$$

Table 6.1: The calculation of yield (Y) from biomass (ΔX) (g.L^{-1}) and substrate available (ΔS) (g.L^{-1}).

Sodium succinate (mM)	Y_{max} (AU)	$\pm\text{SE}$	ΔX (g.L^{-1})	ΔS (g.L^{-1})	Y_{app}
0	0.176	0.022	0.091	0	
2.5	0.612	0.005	0.317	0.295	1.074
5	0.928	0.063	0.481	0.590	0.814
10	1.885	0.026	0.977	1.181	0.827
20	3.110	0.072	1.612	2.362	0.682
30	3.114	0.140	1.614	3.543	0.455

ΔX = Biomass (g.L^{-1}), ΔS = Succinate carbon substrate (g.L^{-1}), Y_{max} = maximum optical density at 600 nm (AU), $\pm\text{SE}$ = standard error (n = 3)

The apparent growth yield (Y_{app}) calculated for each concentration of succinate provides an estimate of biomass generation per available mol of succinate to *P. denitrificans*. As concentrations increases, Y_{app} decreases. This may be due to a saturation of carbon metabolism and not all succinate being consumed during growth. Carbon consumption may cease due to accumulation of toxic compounds in the batch culture or limitation of another nutrient in the minimal salts media. The Y_{app} and Y_{max} were both used to suggest that 5 mM is a carbon limiting substrate for the growth of *P. denitrificans* in minimal salts media and at pH 7.5. This concentration of succinate was used in the chemostat culture, to ensure carbon limitation in the chemostat culture of *P. denitrificans*.

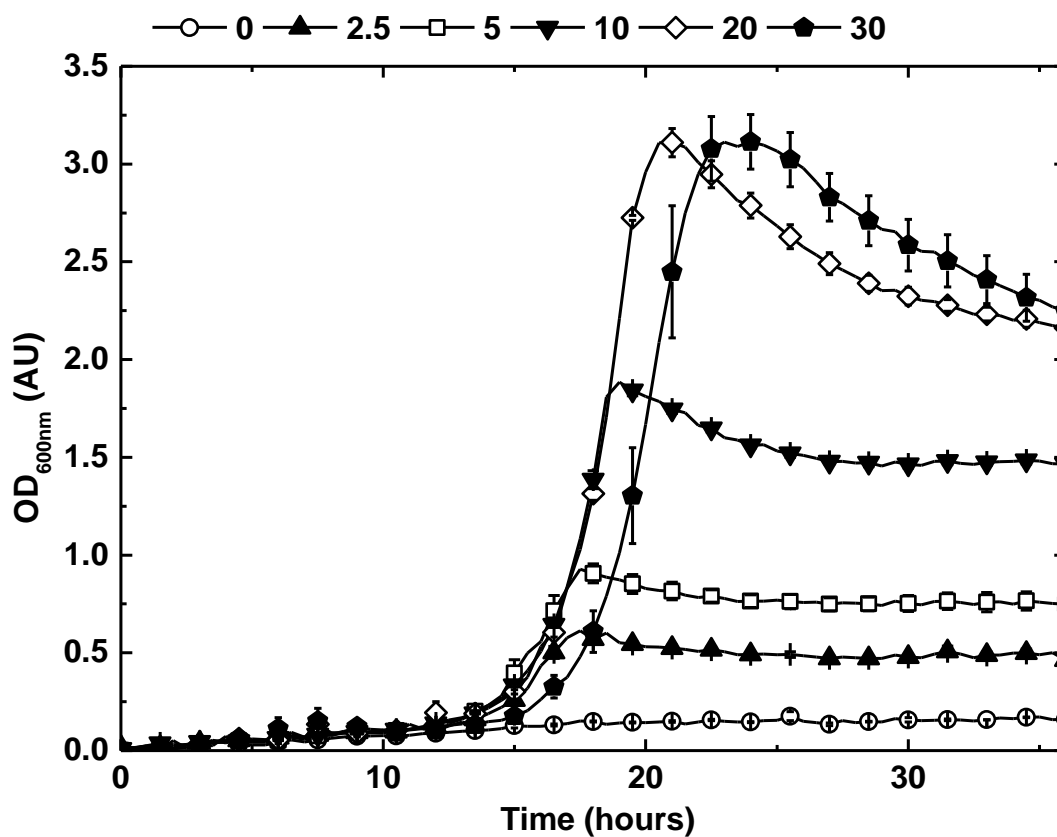


Figure 6.1: Growth of *P. denitrificans* on minimal salts media with 10 mM ammonia chloride at pH 7.5 with varying levels of sodium succinate carbon source. Succinate levels are shown above in mM. Error bars denote standard error n = 3.

6.4.2 Growth of *P. denitrificans* on the reduced carbon substrate butyrate

The growth of *P. denitrificans* on a reduced carbon source was investigated with the shaking flask method of growth phenotyping to characterise the effect of the relatively reduced, butyrate carbon source on the growth of *P. denitrificans* at a range of pH values. *P. denitrificans* was grown on butyrate as the sole carbon source at a concentration of 10 mM over a pH range of 6.5, 7.0, 7.5, 8.0 and 8.5 which is shown in figure 6.2. *P. denitrificans* is unable to growth at pH 6.5. At pH 7.0, the growth of *P. denitrificans* generates a maximum optical density (Y_{\max}) of 0.59 ± 0.20 AU. The Y_{\max} increases with pH value to 0.87 ± 0.06 and 1.50 ± 0.12 AU during growth at pH 7.5 and pH 8.0 respectively. Growth at pH 8.5 shows a similar profile to that of pH 8.0; however it shows a lower Y_{\max} of 1.16 ± 0.018 AU at pH 8.5. Growth of *P. denitrificans* is most proficient at pH 8.0.

Growth with 10 mM butyrate was then examined both with 20 mM nitrate present and at the pH values of pH 7.0, 7.5, 8.0 and 8.5 shown in figure 6.3. These comparisons were made using the apparent growth rate ($\mu_{\max} \text{ h}^{-1}$). The apparent growth rate ($\mu_{\text{app}} \text{ h}^{-1}$) was taken using a semi log plot of the growth curve and taking the gradient of the linear portion from the growth curve as detailed in the methods. It is observed that the presence of nitrate does not cause a noticeable change in the growth of *P. denitrificans* on butyrate. This can be seen at all pH values investigated. When compared to the growth of *P. denitrificans* on succinate with nitrate present a phenotype is observed. Nitrate is observed to reduce the $\mu_{\max} \text{ h}^{-1}$ of growth on succinate. Both carbon sources do not suggest a link between the pH value and the concentration of nitrate present in the media.

Also shown in figure 6.3 is the growth of *P. denitrificans* on succinate and butyrate over a range of nitrite concentrations for direct comparison. Addition of nitrite has a detrimental effect on the growth of *P. denitrificans* with butyrate as is seen with succinate. However growth inhibition is seen at a lower concentration of nitrite than that in growth with succinate. At pH 7.0 growth on butyrate is inhibited a 5 mM nitrite addition. At pH 7.5 this inhibition is seen at 20 mM. At pH 8.0 this inhibition increases further to 90 mM and the highest tolerance to nitrite is observed at pH 8.5 120 mM. It is apparent that growth on butyrate mirrors that of succinate as it increases its tolerance of nitrite with the increase in pH value. The combination of more acidic pH at pH 7.0 and butyrate carbon source is the most detrimental for the exponential growth of *P. denitrificans*.

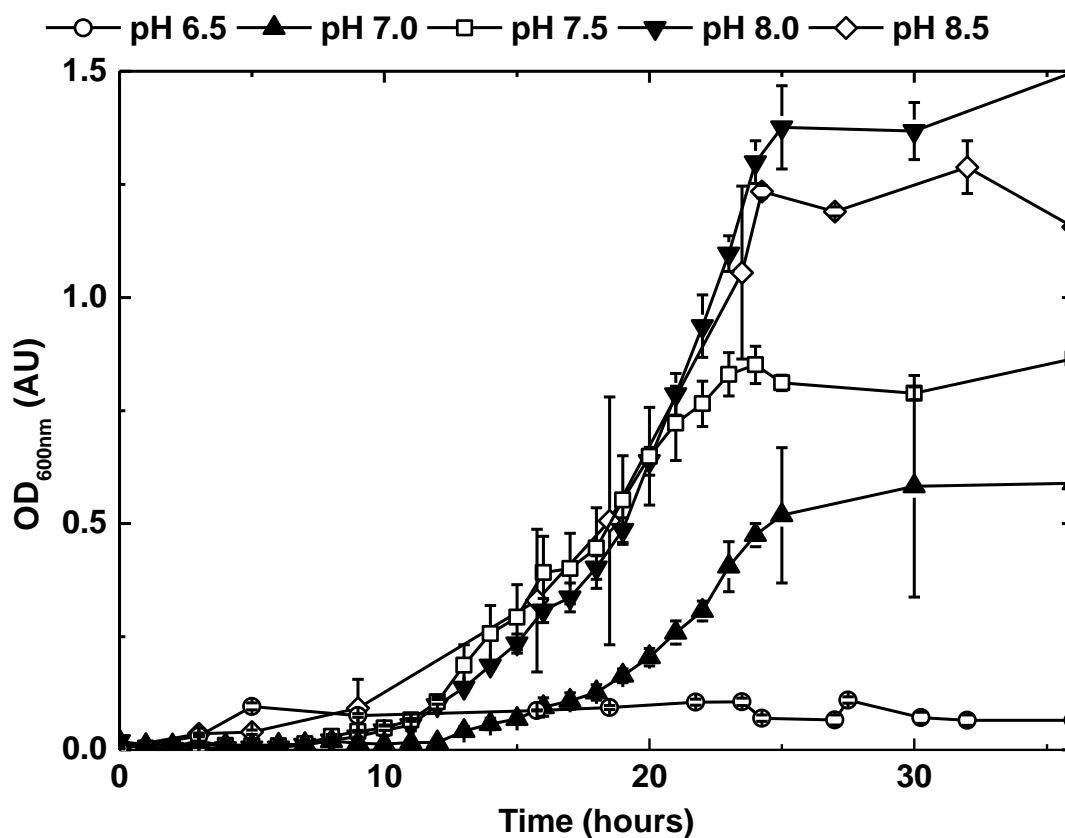


Figure 6.2: Growth of *P. denitrificans* with 10 mM sodium butyrate as sole carbon source in minimal salts media and 10 mM ammonia chloride at pH 7.5. Various media pH values have been examined and are listed in the legend. Growth measured using optical density (OD) (AU). Error bar denote standard error (n = 3).

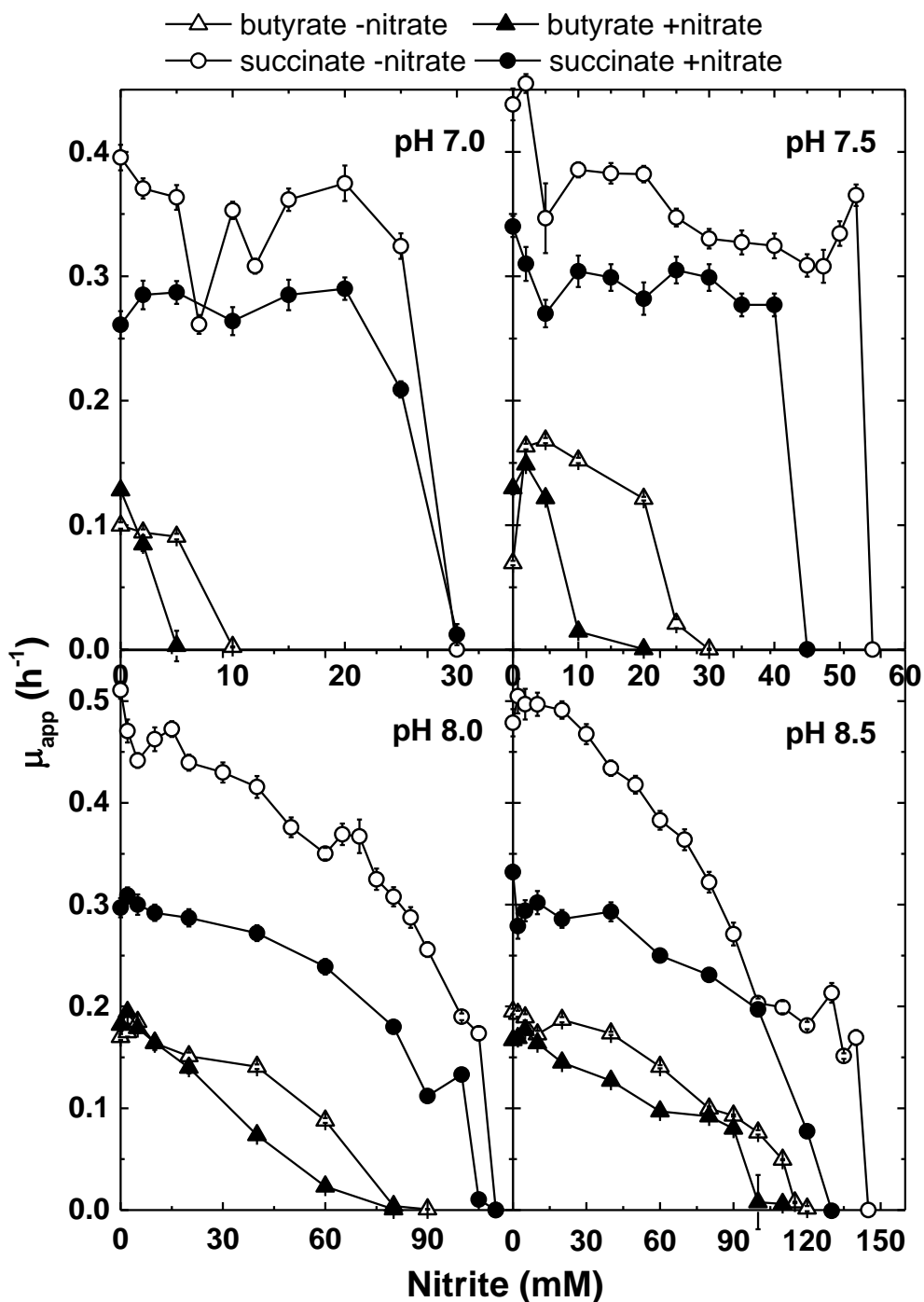


Figure 6.3: The apparent growth rate (μ_{app}) (h⁻¹) for the growth of *P. denitrificans* on 30 mM succinate (circles) and 10 mM butyrate (triangles), without nitrate (open) and with nitrate (closed). Growth is in minimal salts media with 10 mM ammonia chloride at pH 7.0, 7.5, 8.0 and 8.5. Error bars denote standard error (n = ≥3).

6.4.3 Metabolite analysis in batch culture of *P. denitrificans* under 12.5 mM nitrite stress

Phenotypic characterisation of *P. denitrificans* was carried out using minimal salts media at pH 7.5 as stated in methods, with additional Vishniac's trace elements solution 2 mL L⁻¹ (Vishniac and Santer, 1957) and the nitrogen source was added in the form of NH₄Cl 10 mM. Disodium succinate was provided as the carbon source at 30 mM. Media pH was adjusted to 7.5 using sodium hydroxide 10 M. The standard growth conditions were aerobic with a total volume 50 mL and 200 rpm orbital shaking on a shaking incubator in a controlled temperature room at 30°C. By measuring rate of growth, using optical density (OD) at 600nm, a growth profile carried out in the growth conditions without nitrite (-nitrite) was compared with a growth profile with 12.5 mM nitrite (+nitrite). This is shown in figure 6.4 using three biological replicates for each of the two growth conditions. These two conditions compared were the same as those examined by qRT-PCR and microarray transcriptional analysis in chapters 4 and 5. This provides concentrations of nitrate, nitrite and nitrous oxide present at the time of RNA extraction.

In both the -nitrite and +nitrite experimental growth conditions, the lag phase of growth continued for ~2 h before exponential growth phase was reached. In the -nitrite growth conditions the exponential growth continued for 9 h until stationary phase was reached at 11 h after inoculation (T₀). This is shown in panel A of figure 6.4. In the +nitrite growth conditions, the exponential growth phase continued 11 h and reached stationary phase of growth 13 h after inoculation which is shown in panel B of figure 6.4. The addition of 12.5 mL nitrite has extended the length of exponential growth without showing noticeable change in the lag phase. This difference in exponential growth can be seen in the kinetic parameters. Growth -nitrite has an apparent growth rate of μ_{app} 0.44 ±0.01. Comparatively, growth +nitrite has a lower apparent growth rate of μ_{app} 0.35 ±0.01.

Metabolic analysis of nitrite and nitrate was carried out by High Pressure Liquid Chromatography (HPLC) and nitrous oxide emissions detected using Gas Chromatography (GC) analysis. Sampling and Analytical techniques are detailed in the methods. No nitrite was present in the -nitrite growth media. Additionally, no nitrous oxide or nitrate was detected during growth -nitrite (figure 6.4 A).

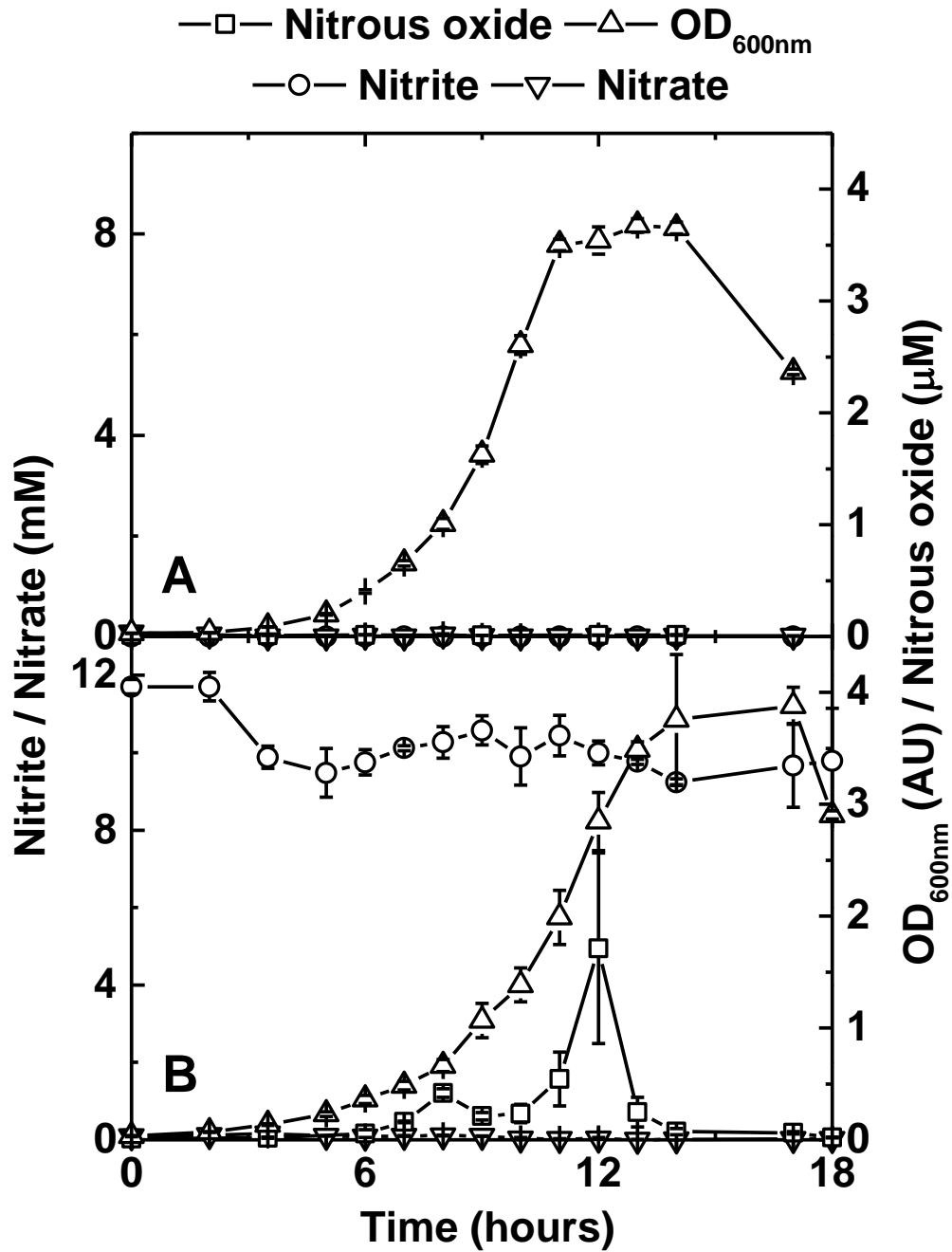


Figure 6.4: Levels of the metabolites nitrate, nitrite and nitrous oxide for growth of *P. denitrificans* in minimal salts media with 10 mM ammonia chloride and 30 mM succinate carbon source at pH 7.5 A: without nitrite, B: with 11.7 ± 0.2 mM nitrite present. Nitrous oxide levels are shown above that of background atmospheric levels. Error bars denote standard error (n = 3).

With the addition of nitrite there is a noticeable change in the nitrogen oxides observed. Nitrite is present at a concentration of 11.7 ± 0.2 mM in the minimal media at T_0 . It is observed that this concentration of nitrite decreases by 2.5 mM and reaches a lowest concentration of 9.2 ± 0.1 within 5 h of growth during the early exponential phase of growth. Nitrous oxide is seen to be produced in +nitrite growth conditions. A peak of 1.7 ± 0.9 μM N_2O is formed after 12 h of growth, which reduces to atmospheric levels during late exponential growth phase.

6.4.4 Development of continuous culture methodology

To maintain continuous culture, 2.5 L bio-reactors (BioFlo 310, New Brunswick Scientific) (Heijnen and Romein, 1995; Kovárová-Kovar and Egli, 1998) were set up (figure 6.6). Each experiment was replicated with three biologically independent replicates. Assay conditions for metabolites were replicated technically ≥ 2 times. Each chemostat was inoculated from a separate cell line isolated from three separate colonies grown in LB^{Rif} and adapted to minimal media ensuring three biologically independent experiments. Each BioFlo® 310 chemostat contains a total volume capacity of 2.5 L and holds 1.5 L minimal media, providing a headspace of 1.0 L. Cells are initially maintained as a temporary batch system, in which the amount of media remained at 1.5 L without any addition or removal of media for the generation of biomass. Once growth of *P. denitrificans* had established overnight to reach stationary phase, the media feed was initiated and continually supplied to the well-stirred culture from which liquid and gas samples were collected at intervals while simultaneously media is displaced through to waste. This initiated the start of continuous growth. After the initiation of continuous growth in the vessel and approximately two vessel volumes have passed through the system, we observed that the biomass and the measured metabolites remained unchanged. This phase of growth during the incubation indicates that steady rates are achieved. At steady state, microorganisms are maintained at the exponential phase of growth in an unsealed vessel. The concentrations of cells, products, substrates and pH are constant, which is a vastly differing growth arrangement to that of batch growth conditions. In batch growth conditions, the vessel is closed and nothing is added or removed. The culture environment changes continually; metabolite formation and excretion and substrate utilisation determine growth, which passes through distinct growth phases. Growth terminates after a certain time interval determined by the level of nutrients available and

their exhaustion rate or by the level of by-products generated from growth and whether these are able to reach a toxic level.

The maintenance of continuous culture requires maintaining cell concentration, products and substrates using the control elements: pH, dissolved oxygen (DO) and temperature (T) as described in the methods. The pH value of the chemostat is maintained at a set value by connection to pumps, one supplying sulphuric acid and a second supplying sodium hydroxide base to make minor pH adjustments to the chemostat. DO is adjusted manually via controller by increase of air flow and agitation for dispersal of airflow through media environment. Fresh sterile medium is fed to the completely mixed and aerated reactor with suspension removed at the same rate maintaining a constant liquid volume in the reaction vessel. By maintaining steady state, the system remains in equilibrium and it is possible to derive a material balance on the cell and substrate concentration around the chemostat yield. The continuous culture contains media with 5 mM succinate (carbon limitation) compared to the 30 mM succinate available in the plate reader and shaking flask batch culture experimental set up (carbon sufficiency). Carbon limitation was used in the media to calculate and control the growth rates for the chemostat experiments.

Continuous culture was used to explore the effect of nitrogen oxides on the growth of *P. denitrificans* in continuous culture and at higher levels than have been explored in the previous chapters of this work. Each experimental condition used three biologically independent replicates and are shown as average values. The parameters of DO, pH, agitation, gas flow, and temperature were monitored during continuous culture of *P. denitrificans* in continuous culture at a 0.5 h rate as described in the methods. The DO and pH parameters, were maintained at the levels shown in table 6.2. The pH of the system was maintained at an average of 7.5 for the duration of the experiment with variance and standard deviation tending to zero. Temperature was maintained at an average of 30°C with a variance and standard deviation also tending to zero. Aeration and agitation of the chemostat system remained at 3 L.min⁻¹ and 400 rpm respectively. Gas flow was shut off during gas sampling time for 20 min for the accumulation of gases in the vessel headspace for sampling and nitrous oxide analysis. Samples were taken regularly at a time interval of approximately 3 per 24 hours. These samples were analysed immediately for optical density and stored at -20°C for later metabolic analysis by high pressure liquid chromatography (HPLC) for nitrite and nitrate assay.

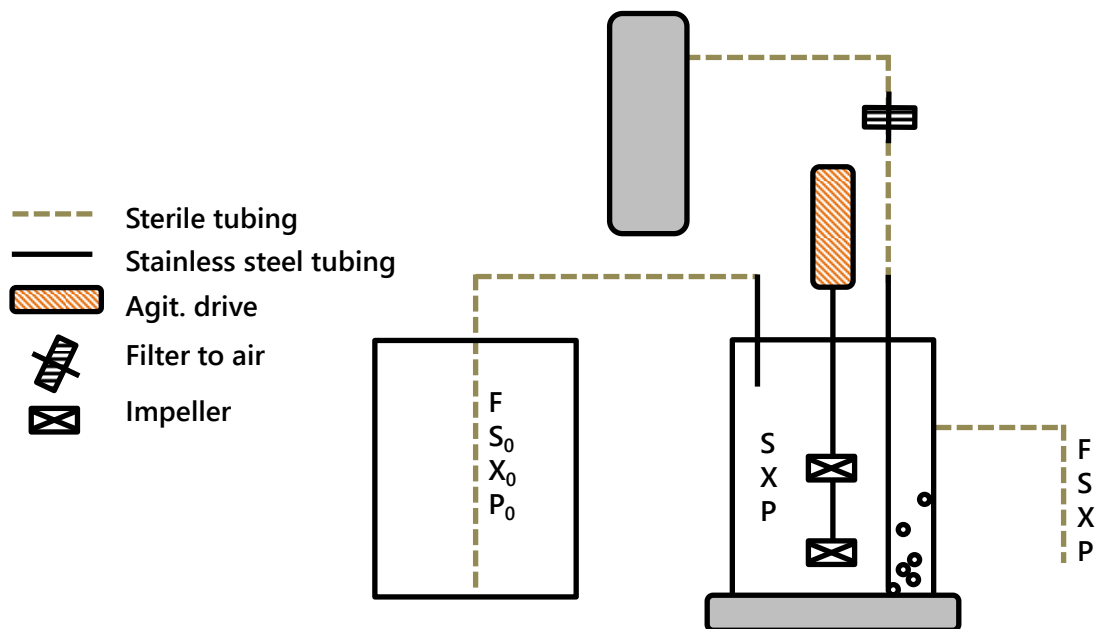


Figure 6.5: Diagram of chemostat kinetics F is the volumetric flow rate of nutrient solution (0.08 L.h^{-1}); X is the cell biomass (g.L^{-1}); S and P denote the substrate and product consumption and production respectively (mM). Subscript 0 denotes the parameters at the feed medium. At steady state, $X_0 = 0 \text{ g.L}^{-1}$. Dilution rate (D) can be determined by $D = F / \text{vessel volume}$, the reciprocal of residence time: $0.08 \text{ L.h}^{-1} / 1.5 \text{ L}$
 $D = 0.053 \text{ h}^{-1}$.

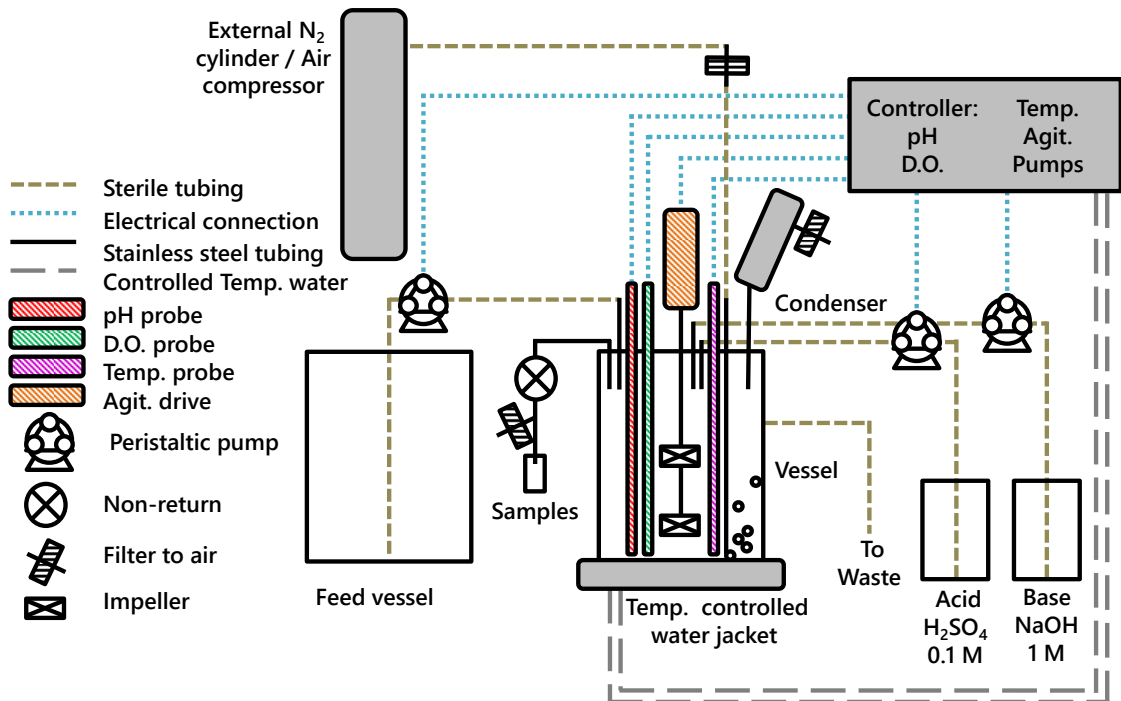


Figure 6.6: Schematic of a continuous culture chemostat. Computer controlled elements: peristaltic pumps leading to media feed, acid and base, monitoring of pH by electrode probe, adjustment of pH through automatic activation of acid and base peristaltic pumps, monitoring dissolved oxygen (DO) by electrode probe, maintenance of constant agitation (Agit.), maintenance of constant gas flow, monitoring of temperature and adjustment of temperature by automatic adjustment of water temperature through water jacket.

Table 6.2: The 0.5 hourly monitored parameters with associated variance and error for continuous culture within a chemostat containing *P. denitrificans* grown in the following conditions: +nitrate -nitrite¹ = 21 mM sodium nitrate, -nitrate +nitrite = 36 mM sodium nitrite, and +nitrate +nitrite = 25 mM nitrite with 8 mM nitrate. DO = dissolved oxygen. SE = standard error (n=3).

Growth condition	Mean DO (mM)	±SE	Mean pH	±SE
+nitrite / -nitrate	0.246	0.009	7.507	0.008
+nitrite / +nitrate	0.244	0.011	7.520	0.021

P. denitrificans was grown in the presence of nitrogenous oxides sodium nitrite and sodium nitrate under continuous culture growth conditions. The effect of nitrite (+nitrite / -nitrate) in isolation was evaluated using sodium nitrite addition to the growth conditions. After initial inoculation of the chemostat vessel with culture at 0 h, *P. denitrificans* biomass increases following an exponential growth during a temporary batch growth condition of 27 hours. At that point, *P. denitrificans* the culture has reached a biomass of $0.25 \pm 0.03 \text{ g.L}^{-1}$ ($\text{OD}_{600\text{nm}}$ $0.49 \pm 0.06 \text{ AU}$) and the dilution rate is switched on at a rate of 0.53 L.h^{-1} . The medium in the vessel and the medium in the feed reservoir contained identical media with sodium nitrite addition. At 28 h media feed was applied and at 77 h media feed was replenished to replace diminishing feed stock and feed rate remained unchanged. Both feed attachments are shown in figure 6.7 indicated by black lines. After initial biomass accumulation, biomass reduced and entered a steady state. This level of growth continued at steady state maintaining a continuous biomass of $0.20 \pm 0.01 \text{ g.L}^{-1}$ ($\text{OD}_{600\text{nm}}$ of $0.38 \pm 0.01 \text{ AU}$). Nitrite concentration was assayed using High Pressure Liquid Chromatography (HPLC). Nitrite levels were $35.7 \pm 1.3 \text{ mM}$ at the time of inoculation and averaged $28.6 \pm 0.7 \text{ mM}$ of nitrite through steady state growth. Throughout the incubation period no significant increase or decrease in the levels of both nitrite and nitrate was observed with minimal fluctuation in measured nitrate and nitrite levels with each media feed change (figure 6.7 B). Nitrate levels maintained at $2.6 \pm 0.2 \text{ mM}$ which were identical to that of media without inoculum: $2.2 \pm 0.9 \text{ mM}$ suggesting no increase or decreased linked to the inoculation or growth of *P. denitrificans*.

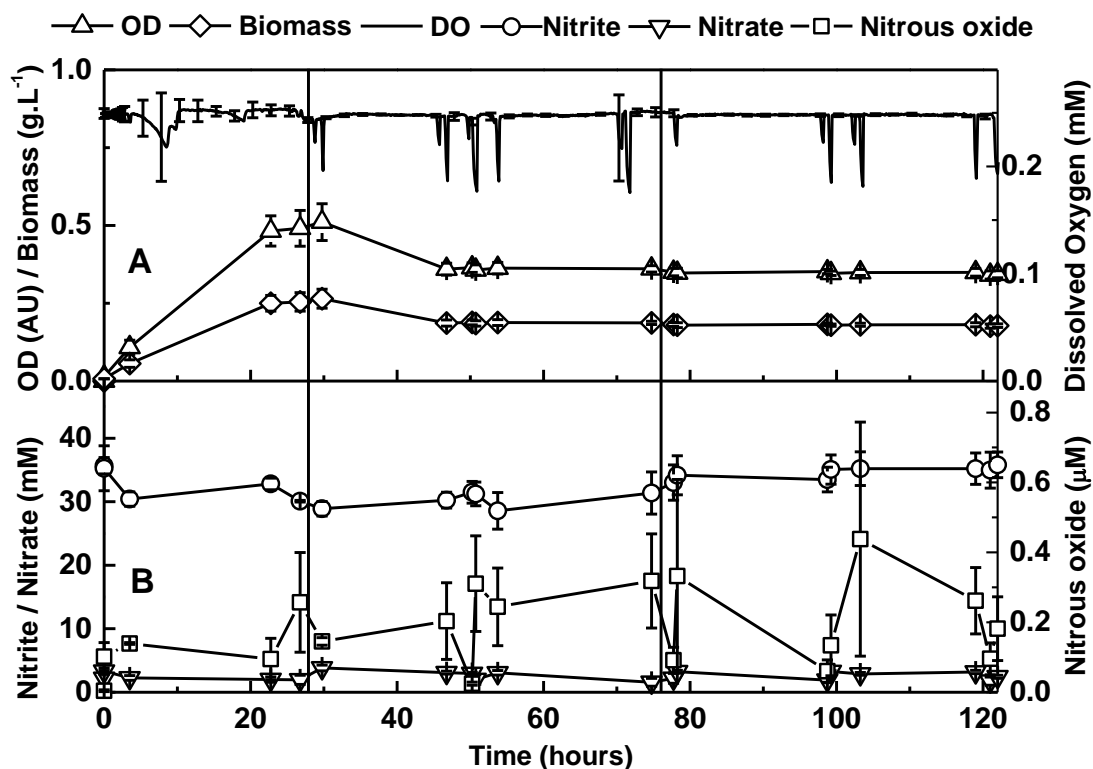


Figure 6.7: Continuous culture of *P. denitrificans* under nitrosative stress with nitrite addition to minimal salts media at pH 7.5 and 10 mM ammonium chloride (n = 3). At 28 hours feed was applied at a dilution rate of 0.053 h^{-1} (black line at 28 hours). Feed was replenished at 78 hours (black line at 78 hours), Maintaining steady state for 123 hours after inoculation. Feed batch indicated by vertical line. A: average dissolved oxygen (DO), optical density (OD) and biomass. Growth was measured spectrophotometrically at 600 nm (open circles) and converted to biomass (open diamond) showing exponential growth over 28 hours. B: average concentration of nitrate, nitrite and nitrous oxide throughout the incubation period. Nitrous oxide is shown as nitrous oxide above atmospheric background levels $\mu\text{M}\cdot\text{hour}^{-1}$. (Error bars denote standard deviation; n = 3.)

Nitrous oxide was detected at levels above atmospheric. All values shown in figure 6.7 are values minus that of background atmospheric samples taken during the 122 h experiment from the compressed air supply feeding directly to the chemostat vessel. Levels shown in figure 6.7 B are those which accumulated over the 20 min air shut down within the vessel headspace. Nitrous oxide levels fluctuated, showing reduction linked to sampling and media change over. Average nitrous oxide levels were $0.20 \pm 0.03 \mu\text{M}$ for the duration of the steady state growth between 46 to 122 h of the continuous culture experiment.

Continuous culture of *P. denitrificans* was carried out in the presence of nitrate (-nitrite / +nitrate) in minimal salts media containing 10 mM ammonia chloride and at pH 7.5. This was carried out in collaboration with George Giannopoulos for the experiments investigating a comparison of aerobic and anaerobic continuous culture of *P. denitrificans* (Giannopoulos *et al.*, data unpublished) and is shown in figure 6.8. Biomass of *P. denitrificans* was accumulated after a 0 h initial inoculation over 22 h before feed was applied reaching a biomass of $0.36 \pm 0.01 \text{ g.L}^{-1}$ ($\text{OD}_{600\text{nm}} 0.69 \pm 0.01 \text{ AU}$) (figure 6.8 A). Feed was applied at a dilution rate 0.53 L.h^{-1} with renewal of feed occurring at 66 h, shown in figure 6.8 by vertical black lines. The medium applied also contained nitrate. Biomass maintained a steady state between 22 and 120 h and *P. denitrificans* accumulated biomass of $0.33 \pm 0.01 \text{ g.L}^{-1}$ ($\text{OD}_{600\text{nm}}$ of $0.63 \pm 0.01 \text{ AU}$). Nitrogenous oxide levels are shown in figure 6.8 B. The levels of nitrite observed began at 0 mM at the time of inoculation and remained at 0 mM for the duration of the experiment. Nitrate also showed no change starting at 0 h at $21.4 \pm 0.5 \text{ mM}$ and remaining at $20.8 \pm 0.2 \text{ mM}$ over steady state growth. Little variation or fluctuation was seen in these levels. Similarly to that of growth with nitrite present, nitrous oxide was seen in micro molar levels above that of atmospheric. Nitrous oxide averaged $0.11 \pm 0.03 \mu\text{M}$ during steady state of growth.

Continuous culture of *P. denitrificans* was carried out in the presence of both nitrite and nitrate (+nitrite / +nitrate) simultaneously in minimal salts media at pH 7.5 with 10 mM ammonium chloride. In the presence of both nitrate and nitrite biomass accumulated higher than that of +nitrite / -nitrate and less than -nitrite / +nitrate conditions (figure 6.9 A). Biomass reached a maximum of $0.28 \pm 0.01 \text{ g.L}^{-1}$ ($\text{OD}_{600\text{nm}} 0.54 \pm 0.01 \text{ AU}$) over 23 h of growth before feed and the establishment of a steady state of growth. During steady state growth of *P. denitrificans* the biomass reduced to $0.19 \pm 0.01 \text{ g.L}^{-1}$ ($\text{OD}_{600\text{nm}} 0.69 \pm 0.01 \text{ AU}$). This growth is similar to that of growth with nitrite only.

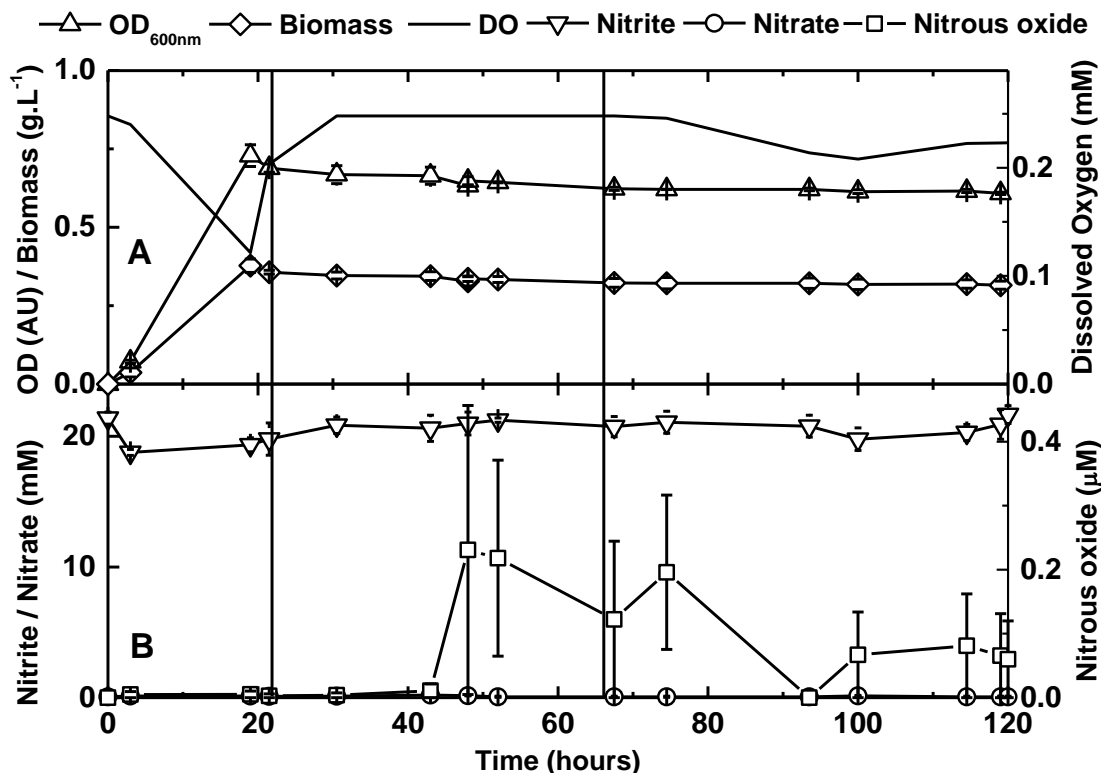


Figure 6.8: Continuous culture of *P. denitrificans* under standard growth conditions minimal salts media at pH 7.5 and 10 mM ammonium chloride. Growth was measured spectrophotometrically at 600 nm (open up pointing triangle) and converted to biomass (open diamond) showing exponential growth over 19 hours. At 28 hours feed was applied at a dilution rate of 0.053 h^{-1} (black line at 28 hours). Feed was replenished at 78 hours (black line at 78 hours), maintaining steady state for 123 hours after inoculation. Nitrous oxide production (open squares) with biomass production (open diamonds). Nitrous oxide is shown as nitrous oxide above atmospheric background levels $\mu\text{M}\cdot\text{hour}^{-1}$. Feed batch indicated by vertical line (Giannopoulos *et al.*, data unpublished).

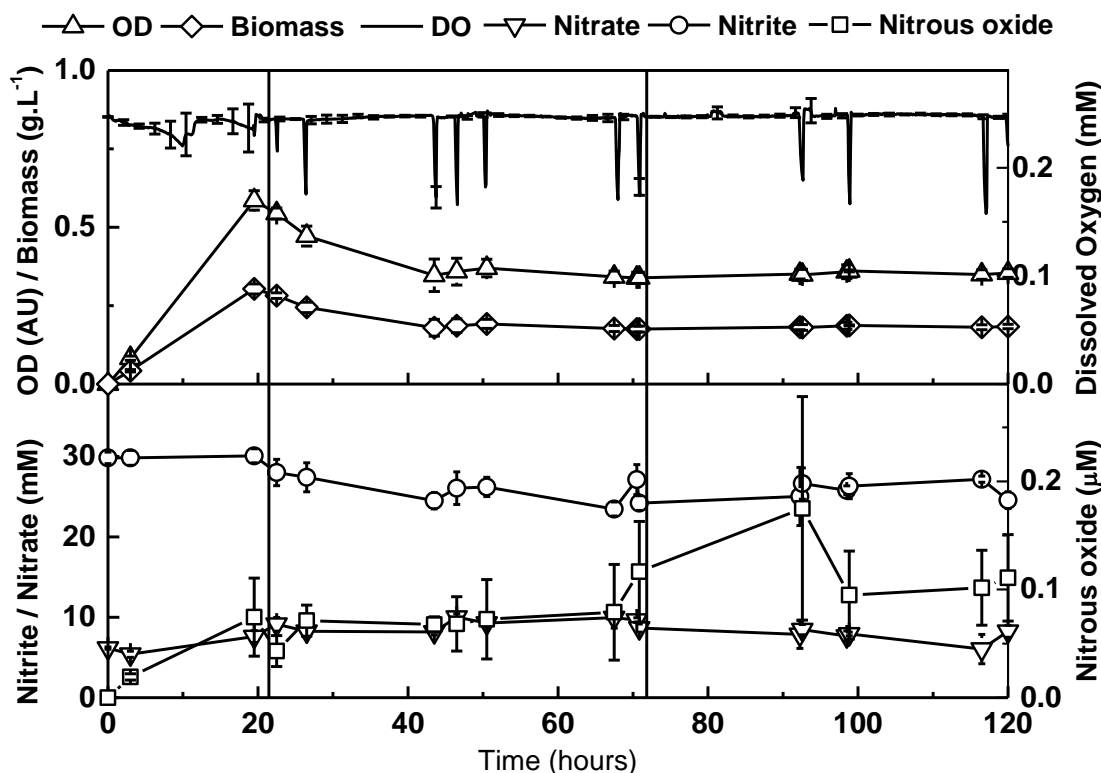


Figure 6.9: Continuous culture of *P. denitrificans* under nitrosative stress with nitrite and nitrate addition to minimal salts media at pH 7.5 and 10 mM ammonium chloride ($n = 3$). At 28 hours feed was applied at a dilution rate of 0.053 h^{-1} (black line at 28 hours). Feed was replenished at 78 hours (black line at 78 hours), maintaining steady state for 123 hours after inoculation. Feed batch indicated by vertical line. A: average dissolved oxygen (DO), optical density (OD) at 600 nm and biomass. Growth was measured spectrophotometrically at 600 nm (open circles) and converted to biomass (open diamond) showing exponential growth over 28 hours. B: average concentration of nitrate, nitrite and nitrous oxide throughout the incubation period. Nitrous oxide is shown as nitrous oxide above atmospheric background levels $\mu\text{M}\cdot\text{hour}^{-1}$. (Error bars denote standard deviation; $n = 3$.)

Nitrite and nitrate both remain at an unfluctuating concentration from the point of inoculation and over steady state growth. At inoculation (0 h), nitrite is 28.0 ± 1.64 mM and remains at 25.7 ± 0.35 mM between 23 and 120 h. Nitrate is at 9.13 ± 0.85 mM and remains at 8.48 ± 0.3 mM between 23 and 120 h of steady state growth. Nitrous oxide is observed at a level similar to growth with nitrate alone at 0.10 ± 0.01 μ M above that of the atmospheric levels.

6.4.5 Transcription under continuous culture growth of *P. denitrificans*

RNA extractions were carried out on *P. denitrificans* cells on all three chemostat conditions after 120 h of continuous culture. The level of *fhb* transcription is examined in RNA extracted from growth +nitrite / -nitrate and +nitrite / +nitrate with qualitative RT-PCR. These two conditions are compared to that of -nitrite / +nitrate, which was provided by G. Giannopoulos. Fold change expression values are shown for two sets of primers used for the identification of the *fhb* gene. These two primers are selected to provide coverage of both the flavin containing and haem containing domains of the *fhb*. The fold change shows consistently high expression of the *fhb* in +nitrite / -nitrate and +nitrite / +nitrate with *fhb1* showing expression of 34.7 ± 1.6 and 23.5 ± 5.7 respectively and *fhb2* 34.3 ± 4.2 25.2 ± 10.5 respectively and are shown in table 6.3. The genes associated with the denitrification pathway were also investigated using qRT-PCR to compare the conditions of +nitrite / -nitrate to that of -nitrite / +nitrate. The cytoplasmic nitrate reductase (*narG*), the nitrite reductase (*nirS*), the nitric oxide reductase (*norB*) and the nitrous oxide reductase (*nosZ*) show no change in transcription between the two conditions. Additionally the periplasmic nitrate reductase (*napA*) and the nitrite assimilatory pathway (*nasB*) show an increase in transcription of 6.86 ± 0.14 and 6.09 ± 1.17 fold in +nitrite / -nitrate. Cytochrome *ba*₃ oxidase is also shown to be upregulated 3.16 ± 0.14 fold in the +nitrite / -nitrate. This is consistent with the levels of expression *ba*₃ oxidase in chapter 5.

Table 6.3: The transcriptional data for continuous culture growth of *P. denitrificans* in minimal salts media at pH 7.5. Growth conditions were as follows: +nitrate -nitrite¹ = 21 mM sodium nitrate, -nitrate +nitrite = 36 mM sodium nitrite, and +nitrate +nitrite = 25 mM nitrite with 8 mM nitrate. SE = standard error (n=3).

Gene					
identifier	Gene name	+nitrite		+nitrite	
(Pden_)		-nitrate*	±SE*	+nitrate*	±SE*
1689	<i>fhb1</i>	34.67	1.62	23.54	5.70
1689	<i>fhb2</i>	34.25	4.20	25.22	10.46
4721	<i>napA</i>	6.86	0.14		
4236	<i>narG</i>	1.44	0.37		
2487	<i>nirS</i>	1.05	0.26		
2483	<i>norB</i>	0.88	0.12		
4452	<i>nasB</i>	6.09	1.17		
4465	<i>gapdh</i>	1.76	0.28		
5108	<i>ba₃</i>	3.16	0.14		
4219	<i>nosZ</i>	0.93	0.04		

*all qRT-PCR results use *gapdh* as housekeeping gene for normalisation, ±SD standard deviation n = 3 biologically independent replicates (additional 3 technical replicates)

6.5 Discussion

This exploration of the continuous culture of *P. denitrificans* under aerobic and nitrogenous oxide stress conditions has sought to finalise the experimental procedure needed for accurate culture aeration within a continuous culture system. The methodology of monitoring the aerobicity and determining its effectiveness was explored by monitoring of experimental parameters and with conformational transcriptomics. Additional exploration of maintenance of pH was explored, both with comparison to that of batch culture and shown in the appendix. Both techniques have been compared with both offering distinct insights for the investigation of aerobic and nitrosative stress culturing of our culture systems.

The use of 35.8 ± 2.0 mM sodium nitrite as a suitable concentration for induction of nitrosative stress was suitable. It was sufficient to produce observable nitrous oxide gas in level which were double that seen with nitrate and nitrite and nitrate in combination. The transcription of *fhb* has been seen at levels which exceed that previously seen. The nitrite level was not in excess to cause inhibition of growth, or reduce the effective cell growth at steady state under continuous culture conditions within the chemostat (figure 6.7).

6.5.1 Increased transcription of the flavohemoglobin

It has been observed that a flavohemoglobin of gene designation Pd1689 has been highly induced in these conditions. This hereby unknown gene of interest has presented itself both within batch and continuous cultured conditions of growth in the mRNA isolated from *P. denitrificans*. It has appeared as a ~2 fold increased expression in batch culture at 12.5, 15, and 17.5 mM sodium nitrite addition. The *fhb* gene has now been observed in continuous culture at 24.6 ± 1.1 mM sodium nitrite with 8.3 ± 0.7 mM sodium nitrate at 20 and 35 fold increase and at 10 and 15 fold increase when under the highest nitrosative stress level which has been transcriptionally analysed of 35.8 ± 2.0 mM sodium nitrite as shown in table 6.3. Significant upregulation of the *fhb* under nitrosative stress conditions with positive correlation to media nitrite levels are observed. Additionally nitrous oxide was detected in the chemostat vessel headspace, observable above that of surrounding atmospheric samples. This is indicative of a nitrogenous compound having an effect on the intracellular metabolism of *P. denitrificans* and of the possible need for *fhb* for growth under sustained stress conditions.

It is also seen in the transcriptional data set from chemostatic growth that *nasB* is upregulated 6 fold under nitrite stress. This is indicative of nitrite, and/or nitrate assimilation by *P. denitrificans* under conditions of high nitrite and/or nitrate concentration. NAS is suppressed by the presence of ammonium, however in these experiments a concentration of 10 mM ammonium chloride has been used for the suppression of the NAS system. In these growth conditions of high nitrite and nitrate concentrations, it is likely that the NAS pathway is active and consuming nitrite and/or nitrite.

6.5.2 Nitrogenous oxide production from *P. denitrificans* in the presence of nitrite

Nitrous oxide accumulation is seen in all growth conditions investigated. This was seen as a sharp peak of nitrous oxide in batch culture and as a fluctuating accumulation on continuous culture. The concentration of nitrous oxide accumulated remained consistently in the micro molar range for both batch and continuous culture. It was observed during batch growth that nitrite levels decreased by approximately 3 mM. This suggests a possible consumption of nitrite. This is unlikely to be due to denitrification as has been seen in the previous qRT-PCR and microarray transcriptional data which have shown no change in the transcription of nitrite reductase (NIR), the nitric oxide reductase (NOR) and the nitrite assimilatory pathway (NAS). During the growth of *P. denitrificans* in an anaerobic culture with nitrite it would be expected that nitrite concentration would reduce due to action by the nitrite reductase (NIR) with the subsequent formation of nitric oxide (NO). NOR would carry out the conversion NO to nitrous oxide (N₂O) ensuring toxic levels of NO are not accumulated, which would in turn be reduced to atmospheric nitrogen (N₂). No accumulation of N₂O would be observed in a fully anoxic system. The media used in this experimentation contains sufficient trace element of iron, molybdenum and copper to enable full enzymological capability of the *P. denitrificans*. The observed levels of N₂O may be due to the direct action of NO detoxification by *fhb*. Its consistent, low-levels however suggest it may be due to the reactive nature of nitrite in well oxygenated systems and could be the product of chemical nitrite breakdown (Takahama *et al.*, 2009; Squadrito and Pryor, 1998).

6.5.3 Carbon metabolism of *P. denitrificans*

The growth of *P. denitrificans* on the reduced carbon substrate of butyrate shows the same pH dependent characteristic seen in the growth of *P. denitrificans* on succinate. Y_{\max} was highest at pH 8.0, favouring a slightly alkaline environment. To investigate the addition of nitrate the apparent growth constant ($\mu_{\text{app}} \text{ h}^{-1}$) was derived and compared. Nitrate had no effect on growth of *P. denitrificans* with butyrate as the carbon source for growth. However, the addition of nitrate showed a significant decrease in $\mu_{\text{app}} \text{ h}^{-1}$ when growth of *P. denitrificans* was on succinate. The $\mu_{\text{max}} \text{ h}^{-1}$ decrease with the presence of nitrate suggests nitrate alters the metabolism of *P. denitrificans* when succinate is the carbon source which

reduces the exponential rate of growth. This is contrary to the stimulatory effect observed with nitrite addition which indicates nitrate is not metabolised in the same manner. The likely route of nitrate metabolism is uptake by the assimilatory pathway. Nitrate is actively internalised and converted to ammonia for incorporation into cellular material such as protein and DNA (NAS) (Sears *et al.*, 1997). The transcriptional data taken from the chemostatic growth conditions of this work suggest *nasB* is expressed with high nitrite concentrations. This suggests that 10 mM ammonium chloride may not be sufficient in suppressing the NAS pathway, when nitrite or nitrate is present at higher concentrations. Nitrate has a pK_a value of -1.3 (Moir and Wood, 2001), therefore it is unlikely that nitrate is protonated and able to pass across the phospholipid bilayer. This is also confirmed by the lack of any connection seen by pH and nitrate concentration.

In aerobic growth, reduced carbon is metabolised by the β -oxidation pathway which can increase electron flow into the Q-pool causes an uncoupling of ATP synthesis. To restore the Q-pool, the *P. denitrificans* can use the periplasmic nitrate reductase to remove excess electron from the Q-pool and rebalance ATP synthesis. The reduction of nitrate generates nitrite and this may contribute to the reduction in nitrite tolerance observed in figure 6.3. Nitrate reduction by *P. denitrificans* may be causing an increase in the extracellular nitrite concentration, and thus increase the cytotoxic effect. The decreased tolerance seen in growth on succinate may also be indicative of background levels of nitrate reduction occurring via either the cytoplasmic nitrate reductase (NAR) from background levels of NAR to partial anoxia at high optical densities towards the stationary phase of growths. Butyric acid ($pK_a = 4.8$) is also itself an uncoupler of protonmotive force, like FNA. It can pass across membrane in the protonate form and deprotonate on entering the cell. Thus the combination of butyrate and FNA may be more toxic than succinate and FNA (figure 6.10).

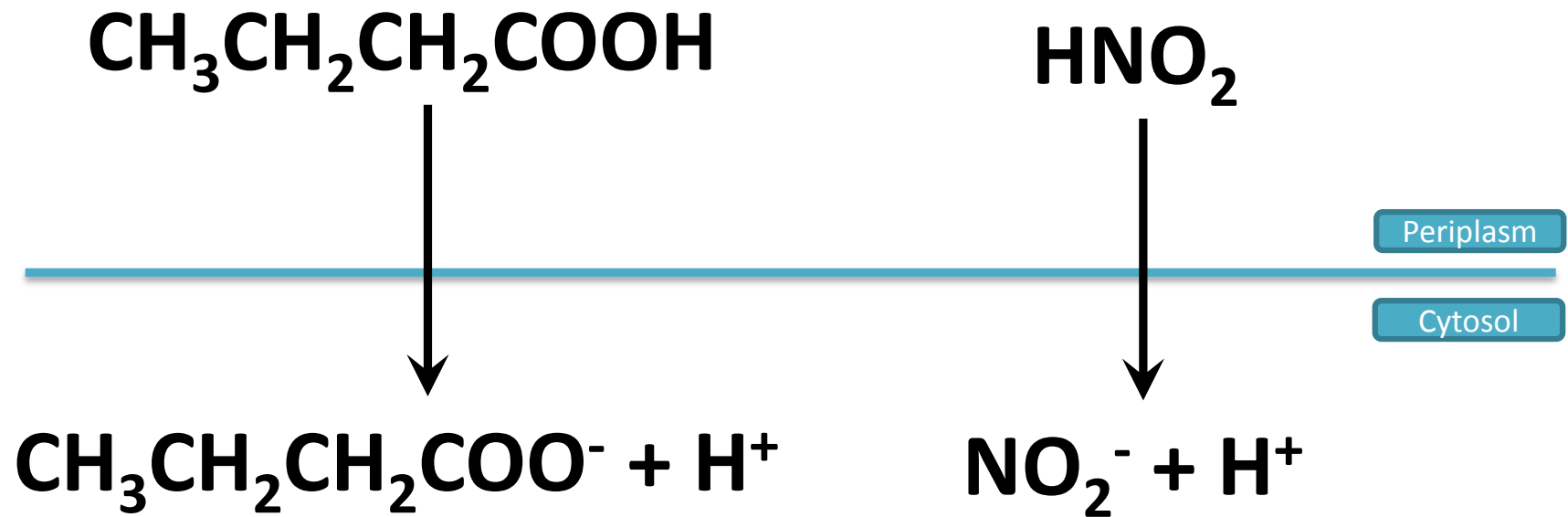


Figure 6.10: Transport across cellular membrane of *P. denitrificans* by protonation. Butyric acid ($\text{CH}_3\text{CH}_2\text{COOH}$) in the protonated form and deprotonated in the ion form ($\text{CH}_3\text{CH}_2\text{COO}^-$). Free nitrous acid (FNA) (HNO_2) in the protonated form and ion form (NO_2^-).

6.6 References

- BERGAUST, L., VAN SPANING, R. J., FROSTEGARD, A. & BAKKEN, L. R. 2012. Expression of nitrous oxide reductase in *Paracoccus denitrificans* is regulated by oxygen and nitric oxide through FnrP and NNR. *Microbiology*, 158, 826-34.
- FORRESTER, M. T. & FOSTER, M. W. 2012. Protection from nitrosative stress: A central role for microbial flavohemoglobin. *Free Radical Biology and Medicine*, 52, 1620-1633.
- HEIJNEN, J. J. & ROMEIN, B. 1995. Derivation of kinetic equations for growth on single substrates based on general properties of a simple metabolic network. *Biotechnology Progress*, 11, 712-716.
- KOVÁROVÁ-KOVAR, K. & EGLI, T. 1998. Growth kinetics of suspended microbial cells: From single-substrate- controlled growth to mixed-substrate kinetics. *Microbiology and Molecular Biology Reviews*, 62, 646-666.
- KUNAU, W. H., DOMMES, V. & SCHULZ, H. 1995. β -oxidation of fatty acids in mitochondria, peroxisomes, and bacteria: A century of continued progress. *Progress in Lipid Research*, 34, 267-342.
- KURIHARA, T., UEDA, M., OKADA, H., KAMASAWA, N., NAITO, N., OSUMI, M. & TANAKA, A. 1992. Beta-oxidation of butyrate, the short-chain-length fatty acid, occurs in peroxisomes in the yeast *Candida tropicalis*. *Journal of Biochemistry*, 111, 783-787.
- KWIATKOWSKI, A. V., LARATTA, W. P., TOFFANIN, A. & SHAPLEIGH, J. P. 1997. Analysis of the role of the *nnrR* gene product in the response of *Rhodobacter sphaeroides* 2.4.1 to exogenous nitric oxide. *Journal of Bacteriology*, 179, 5618-5620.
- MOIR, J. W. B. & WOOD, N. J. 2001. Nitrate and nitrite transport in bacteria. *Cellular and Molecular Life Sciences*, 58, 215-224.
- MÜLLER, N., WORM, P., SCHINK, B., STAMS, A. J. M. & PLUGGE, C. M. 2010. Syntrophic butyrate and propionate oxidation processes: From genomes to reaction mechanisms. *Environmental Microbiology*, 2, 489-499.
- RICHARDSON, D. J. 2000. Bacterial respiration: A flexible process for a changing environment. *Microbiology*, 146, 551-571.
- RICHARDSON, D. J. 2001. Introduction: Nitrate reduction and the nitrogen cycle. *Cellular and Molecular Life Sciences*, 58, 163-164.

- SEARS, H. J., LITTLE, P. J., RICHARDSON, D. J., BERKS, B. C., SPIRO, S. & FERGUSON, S. J. 1997. Identification of an assimilatory nitrate reductase in mutants of *Paracoccus denitrificans* GB17 deficient in nitrate respiration. *Archives of Microbiology*, 167, 61-66.
- SQUADRITO, G. L. & PRYOR, W. A. 1998. Oxidative chemistry of nitric oxide: The roles of superoxide, peroxynitrite, and carbon dioxide. *Free Radical Biology and Medicine*, 25, 392-403.
- TAKAHAMA, U., HIROTA, S. & KAWAGISHI, S. 2009. Effects of pH on nitrite-induced formation of reactive nitrogen oxide species and their scavenging by phenolic antioxidants in human oral cavity. *Free Radical Research*, 43, 250-61.
- VISHNIAC, W. & SANTER, M. 1957. The *Thiobacilli*. *Bacteriological reviews*, 21, 195-213.
- WATMOUGH, N. J. & FRERMAN, F. E. 2010. The electron transfer flavoprotein: Ubiquinone oxidoreductases. *Biochimica et Biophysica Acta - Bioenergetics*, 1797, 1910-1916.

7 General discussion and future work

Contents

7	General discussion	258
7.1	List of figures	258
7.2	The effect of nitrite and associated reactive nitrogen species on the aerobic growth of <i>Paracoccus denitrificans</i> PD1222	259
7.3	Further investigation of nitrogenous oxides	259
7.4	Effect of nitrite on oxidases	260
7.5	Regulatory response of <i>Paracoccus denitrificans</i> PD1222 to nitrite	262
7.6	Further metabolic investigation	262
7.7	Reduced carbon sources	263
7.8	Comparison of a model nitrifying bacterium	263
7.9	Concluding remarks	264
7.10	References.....	264

7.1 List of figures

Figure 7.1: The oxygen consumption rates of *Paracoccus denitrificans* PD1222 measured in oxygen mM.OD unit⁻¹.min⁻¹ as a function of nitrite dosage using a Clarke electrode. Cells were inoculated to minimal salts media with 10 mM ammonium chloride at pH 7.5.261

7.2 The effect of nitrite and associated reactive nitrogen species on the aerobic growth of *Paracoccus denitrificans* PD1222

In this study, the effect of nitrite on the aerobic growth of *Paracoccus denitrificans* PD122 has been investigated. This work has identified and postulated the function of an unknown flavohemoglobin (*fhb*) which shows association with nitrosative stress tolerance. The successful deletion and complementation of this gene in *P.denitrificans*, has shown *fhb* to convey both a stimulation in biomass generation and an increased tolerance of 5 mM nitrite additionally. Transcriptional analysis has revealed an NsrR-like, TetR and LysR regulatory group, introducing a possible regulatory response induced by nitrite and specific to aerobically. The growth of *P. denitrificans* was explored in batch and continuous culture. Both conditions of growth show the *fhb*, associated NsrR-like regulator and *ba₃* to be transcribed in the presence of nitrite.

This work investigates nitrosative stress in an aerobic environment which provides a unique perspective to the area of aerobic nitrite tolerance and nitrous oxide emission in wastewater and soil environments. Such in depth investigation of a denitrifying organism in pure culture could provide an insight into the mixed culture systems found in wastewater treatment, where the bactericidal property of FNA is being harnessed in the water-industry, for example in the prevention of pipe spoilage (Jiang et al., 2011, Wang et al., 2013).

7.3 Further investigation of nitrogenous oxides

The generation of reactive nitrogen species is an ‘occupational hazard’ for denitrifying bacteria. Both nitrite and nitric oxide are cytotoxins independently. Nitrite toxicity is notably pH dependent which pertains to a role for free nitrous acid (FNA) as the molecule conveying toxicity at a concentration of $2.8 \pm 0.4 \mu\text{M}$. It is suggested that nitrite toxicity is associated with its protonated form of FNA which can cross the cytoplasmic membrane as the freely diffusing uncharged lipophilic species and disproportionate to form nitric oxide and, if oxygen is present, peroxy nitrite. Observation of increased cytochrome *ba₃* oxidase expression in association with high nitrite dosage has corroborated work carried out on the uncoupling effect seen in association with nitrite / FNA (Sijbesma et al., 1996, Rake and Eagon, 1980).

The use of liposomes as a method of reproducing a specific cellular environment where intracellular pH and components can be generated and maintained within a lipophilic, membrane-bound vesicle has been well reproduced in recent studies (White et al., 2013) and their use in the containment of superoxide and peroxynitrite previously confirmed (White et al., 1994). Further work in the area of FNA intracellular movement area will elucidate the chemical action of nitrite / FNA when in contact with a bacterial cell membrane, by generating liposomes containing a neutral cytoplasmic pH and suspended in contact with an acidic external environment. The liposome's internal pH change can be measured colorimetrically to determine if protons can be shuttled across a membrane. Additionally, the generation of nitric oxide can be examined colourmetrically or by use of fluorescent diaminofluoresceins (Kojima et al., 1998). Liposomes can be collected and the contents extracted to examine further the end product of nitrogen oxides enclosed within a cellular membrane environment. In this way a biologically relevant context is applied to the chemical alteration of nitrogen oxides which has been well studied (Squadrito and Pryor, 1998).

7.4 Effect of nitrite on oxidases

Nitrite and nitric oxide have been found to act directly with, and reduce the activity of, oxidases (Kucera et al., 1986, Cooper and Brown, 2008). Inhibition of oxidase by NO is complex and has split opinion as to whether it acts competitively to oxygen (Antunes et al., 2004) and/or uncompetitively (Pearce et al., 2003), via the nitrosylation of cytochrome or through a direct interaction of an oxidised binuclear centre nitric oxide resulting in the formation of a nitrite bound cytochrome (Sarti et al., 2000).

The use of a Clarke oxygen electrode can further clarify the extent nitrite inhibits growth of *P. denitrificans* by measuring the oxygen consumption of cells exposed to nitrite. Preliminary data has been collected using whole cell assay construction containing minimal salts media at pH 7.5 and *P. denitrificans* cells which are stirred and oxygenated. Additions of nitrite showed an overall decrease in oxygen consumption with increased nitrite addition which is shown figure 7.1.

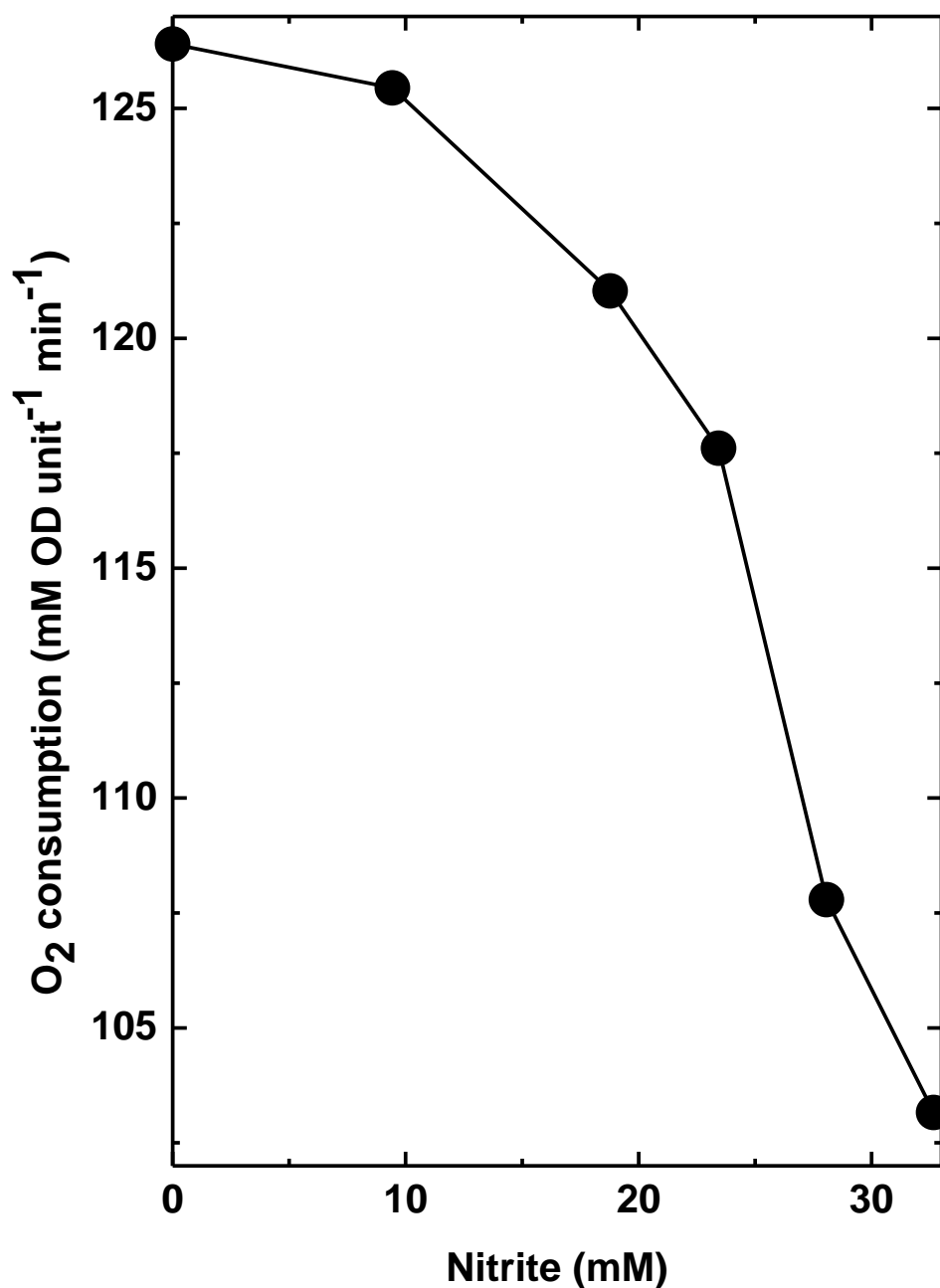


Figure 7.1: The oxygen consumption rates of *Paracoccus denitrificans* PD1222 measured in oxygen mM.OD unit⁻¹.min⁻¹ as a function of nitrite dosage using a Clarke electrode. Cells were inoculated to minimal salts media with 10 mM ammonium chloride at pH 7.5.

7.5 Regulatory response of *Paracoccus denitrificans* PD1222 to nitrite

The participation of an NsrR-like gene in response to nitrite suggests a nitric oxide sensitive regulator is present in *P. denitrificans* and neighbours the *fhb* which has been confirmed to be associated with nitrite resistance. The transcription of an NsrR-like regulator in response to nitrosative stress agrees with previous work (Tucker et al., 2008, Filenko et al., 2007) confirming a link between nitric oxide and NsrR regulatory proteins. Additional regulators show downregulation under nitrosative stress and suggest the NsrR-like regulator may act in association with additional regulators to bring about the transcription of cellular protection mechanisms in response to nitrite. Identification of the NsrR-like gene acting to repress *fhb* could be carried out using a mutational study. Deletion of the NsrR-like regulator would remove its function within the cell. This mutant can then be tested under nitrous oxide stresses for *fhb* expression and tolerance to nitrite. Nakano et al., carried out the deletion of an NsrR gene using a null mutant (Nakano et al., 2006) in which lacZ fusion was created to identify the gene the regulator acted on to suppress. The generation of a *fhb*-lacZ would be a useful tool for the identification of *fhb* and NsrR-like regulator association.

7.6 Further metabolic investigation

The identification of *fhb* has presented the need to for further elucidation of the role the *fhb* plays in *P. denitrificans*. Further work on the *fhb* would require the analysis of its functionality. Flavohemoglobins are capable of the production of nitrate and nitrous oxide. Nitrate was not observed in the conditions at levels which detectable, however identification of the route by which nitrous oxide is generated may be found through the use of stable isotopes, namely N^{15} , embedded into nitrite. In this way nitrous oxide containing N^{15} could be confirmed as a product of nitrite. FNA concentration is widely estimated by calculation from nitrite. Although this approach is well documented and provides a precise indication of the total FNA concentration in the medium, it limits our understanding of the biological levels of FNA within the cell. Further progress in the field of FNA detection as suggested above (liposome sensors) could enhance our understanding of relevant FNA concentrations and track its biological pathways of degradation.

7.7 Reduced carbon sources

Chapter 6 set up the examination of nitrite stress on butyrate, which is a reduced carbon source. Initial investigation has shown that the exponential rate of growth on butyrate is reduced when compared to that of succinate. The metabolism of butyrate is known to cause an uncoupling effect of the Quinone-pool and so provides an addition to the potential uncoupling effects of FNA. It was observed that oxidation of a reduced carbon source induces a similar nitrite tolerance despite a reduction in exponential growth. To our knowledge this unique observation could elucidate a new mechanism involving quinone related e^- flow. This leads to the requirement of validation through additional reduced carbon source investigations. A comparative study of oxidised carbon sources such as malate and fumarate in addition to succinate would provide a broader analysis of the effect an oxidised carbon source has on the growth of *P. denitrificans* in the presence of nitrite. Further short-chain fatty acids (SCFA) such as acetate, propionate, and butyrate, with extension to longer chain pentanoate (valerate) hexanoate (caproate), heptanoate (enanthic) octanoate (caprylate), would offer further insight into the effect of nitrite sensitivity.

7.8 Comparison of a model nitrifying bacterium

The work carried out has been focused on the effect of nitrite on a denitrifying bacterium which can be used to inform the broader bacteria responses to nitrite. Pathogenic enteric bacteria have been the focus of recent work to investigate the effects and tolerance mechanisms to nitric oxide (Stevanin et al., 2002, Bodenmiller and Spiro, 2006, Mills et al., 2005, Rowley et al., 2012). It would be of great interest to compare a bacterium found in soil and water environments such as the ammonia oxidising *Nitrosomonas europaea*. Study in the area of ammonia and nitrite oxidation is largely studied in enriched mixed culture systems (Vadivelu et al., 2006). This work can be easily applied to other organisms of significance to the nitrogen cycle. Nitrite reductase (NOR) capability has been explored in *Nitrosomonas europaea* (Poth and Focht, 1985). *N. europaea* is ammonia oxidising lithoautotrophic bacterium which contributes to nitrification, but has also been suggested to carry out a truncated denitrification path, reducing nitrite to nitrous oxide (Beaumont et al., 2004). Current research is focused on nitrous oxide producing functions of *N. europaea*, which opens an opportunity for investigation of the effect of nitrite on *N. europaea*. *N.*

europaea is a candidate which therefore presents itself as of interest to the area of nitrosative stress and is a useful candidate for the techniques used in this work.

7.9 Concluding remarks

Denitrifying bacteria will frequently be exposed to nitrite in oxic environments, leading to FNA formation and the generation of cytoplasmic reactive nitrogen species as a consequence. This work has explored the effect of nitrite on aerobic *P. denitrificans* metabolism with the identification of a cytoplasmic system that is contributing to the survival of *P. denitrificans* at high nitrite concentrations. The research provides metabolic and transcriptional information of a model denitrifying organism, suggesting a novel gene involved and the respective metabolic pathway of the response to nitrite. These findings have potentially numerous practical implications in the water industry to those developing and applying nitrite / FNA biocidal treatment applications. This research has contributed to the understanding of the little-known and complex interactions between microorganisms and nitrogenous compounds. This elucidates further the understanding of the mechanisms of nitrosative stress response at a transcriptional level and of the metabolic features and characteristics of the response currently unknown in *P. denitrificans*.

7.10 References

- ANTUNES, F., BOVERIS, A. & CADENAS, E. 2004. On the mechanism and biology of cytochrome oxidase inhibition by nitric oxide. *Proceedings of the National Academy of Sciences of the United States of America*, 101, 16774-16779.
- BEAUMONT, H. J. E., LENS, S. I., REIJNDERS, W. N. M., WESTERHOFF, H. V. & VAN SPANNING, R. J. M. 2004. Expression of nitrite reductase in *Nitrosomonas europaea* involves NsrR, a novel nitrite-sensitive transcription repressor. *Molecular Microbiology*, 54, 148-158.
- BODENMILLER, D. M. & SPIRO, S. 2006. The *yjeB* (*nsrR*) gene of *Escherichia coli* encodes a nitric oxide-sensitive transcriptional regulator. *Journal of Bacteriology*, 188, 874-881.
- COOPER, C. E. & BROWN, G. C. 2008. The inhibition of mitochondrial cytochrome oxidase by the gases carbon monoxide, nitric oxide, hydrogen cyanide and hydrogen

- sulfide: Chemical mechanism and physiological significance. *Journal of Bioenergetics and Biomembranes*, 40, 533-539.
- FILENKO, N., SPIRO, S., BROWNING, D. F., SQUIRE, D., OVERTON, T. W., COLE, J. & CONSTANTINIDOU, C. 2007. The NsrR regulon of *Escherichia coli* K-12 includes genes encoding the hybrid cluster protein and the periplasmic, respiratory nitrite reductase. *Journal of Bacteriology*, 189, 4410-7.
- JIANG, G., GUTIERREZ, O. & YUAN, Z. 2011. The strong biocidal effect of free nitrous acid on anaerobic sewer biofilms. *Water Research*, 45, 3735-3743.
- KOJIMA, H., NAKATSUBO, N., KIKUCHI, K., KAWAHARA, S., KIRINO, Y., NAGOSHI, H., HIRATA, Y. & NAGANO, T. 1998. Detection and imaging of nitric oxide with novel fluorescent indicators: Diaminofluoresceins. *Analytical Chemistry*, 70, 2446-2453.
- KUCERA, I., KOZÁK, L. & DADÁK, V. 1986. The inhibitory effect of nitrite on the oxidase activity of cells of *Paracoccus denitrificans*. *FEBS Letters*, 205, 333-336.
- MILLS, P. C., RICHARDSON, D. J., HINTON, J. C. D. & SPIRO, S. 2005. Detoxification of nitric oxide by the flavorubredoxin of *Salmonella enterica* serovar *Typhimurium*. *Biochemical Society Transactions*, 33, 198-199.
- NAKANO, M. M., GENG, H., NAKANO, S. & KOBAYASHI, K. 2006. The nitric oxide-responsive regulator NsrR controls ResDE-dependent gene expression. *Journal of Bacteriology*, 188, 5878-5887.
- PEARCE, L. L., BOMINAAR, E. L., HILL, B. C. & PETERSON, J. 2003. Reversal of cyanide inhibition of cytochrome *c* oxidase by the auxiliary substrate nitric oxide: an endogenous antidote to cyanide poisoning? *Journal of Biological Chemistry*, 278, 52139-45.
- POTH, M. & FOCHT, D. D. 1985. N kinetic analysis of N₂O production by *Nitrosomonas europaea*: An examination of nitrifier denitrification. *Applied and Environmental Microbiology*, 49, 1134-41.
- RAKE, J. B. & EAGON, R. G. 1980. Inhibition, but not uncoupling, of respiratory energy coupling of three bacterial species by nitrite. *Journal of Bacteriology*, 144, 975-982.
- ROWLEY, G., HENSEN, D., FELGATE, H., ARKENBERG, A., APPIA-AYME, C., PRIOR, K., HARRINGTON, C., FIELD, S. J., BUTT, J. N., BAGGS, E. & RICHARDSON, D. J. 2012. Resolving the contributions of the membrane-bound and periplasmic nitrate reductase systems to nitric oxide and nitrous oxide

- production in *Salmonella enterica serovar Typhimurium*. *Biochemical Journal*, 441, 755-62.
- SARTI, P., GIUFFRÉ, A., FORTE, E., MASTRONICOLA, D., BARONE, M. C. & BRUNORI, M. 2000. Nitric oxide and cytochrome *c* oxidase: Mechanisms of inhibition and NO degradation. *Biochemical and Biophysical Research Communications*, 274, 183-7.
- SIJBESMA, W. F., ALMEIDA, J. S., REIS, M. A. & SANTOS, H. 1996. Uncoupling effect of nitrite during denitrification by *Pseudomonas fluorescens*: An in vivo (31)P-NMR study. *Biotechnology and Bioengineering*, 52, 176-82.
- SQUADRITO, G. L. & PRYOR, W. A. 1998. Oxidative chemistry of nitric oxide: The roles of superoxide, peroxyxynitrite, and carbon dioxide. *Free Radical Biology and Medicine*, 25, 392-403.
- STEVANIN, T. M., POOLE, R. K., DEMONCHEAUX, E. A. & READ, R. C. 2002. Flavohemoglobin Hmp protects *Salmonella enterica serovar typhimurium* from nitric oxide-related killing by human macrophages. *Infection and Immunity*, 70, 4399-405.
- TUCKER, N. P., HICKS, M. G., CLARKE, T. A., CRACK, J. C., CHANDRA, G., LE BRUN, N. E., DIXON, R. & HUTCHINGS, M. I. 2008. The transcriptional repressor protein NsrR senses nitric oxide directly via a [2Fe-2S] cluster. *PLoS ONE*, 3, e3623.
- VADIVELU, V. M., KELLER, J. & YUAN, Z. 2006. Effect of free ammonia and free nitrous acid concentration on the anabolic and catabolic processes of an enriched *Nitrosomonas* culture. *Biotechnology and Bioengineering*, 95, 830-839.
- WANG, Q., YE, L., JIANG, G. & YUAN, Z. 2013. A free nitrous acid (FNA)-based technology for reducing sludge production. *Water Research*, 47, 3663-3672.
- WHITE, C. R., BROCK, T. A., CHANG, L. Y., CRAPO, J., BRISCOE, P., KU, D., BRADLEY, W. A., GIANTURCO, S. H., GORE, J. & FREEMAN, B. A. 1994. Superoxide and peroxyxynitrite in atherosclerosis. *Proceedings of the National Academy of Sciences*, 91, 1044-1048.
- WHITE, G. F., SHI, Z., SHI, L., WANG, Z., DOHNALKOVA, A. C., MARSHALL, M. J., FREDRICKSON, J. K., ZACHARA, J. M., BUTT, J. N., RICHARDSON, D. J. & CLARKE, T. A. 2013. Rapid electron exchange between surface-exposed bacterial cytochromes and Fe(III) minerals. *Proceedings of the National Academy of Sciences*, 110, 6346-6351.

8 Appendices

Contents

8	Appendices	267
8.1	List of figures	267
8.2	3 The effect of extracellular pH and nitrite on batch culture growth kinetics of <i>Paracoccus denitrificans</i>	270
8.3	4 The role of flavohemoglobin in <i>P. denitrificans</i> under nitrite induced stress...277	
8.4	5 Metabolic analysis of nitrosative stress in batch and continuous culture of <i>P. denitrificans</i> in a continuous culture system.....	285

8.1 List of figures

Figure 8.1:	PCR amplified 3' and 5' flanking region of the flavohemoglobin gene (<i>fhb</i>) in <i>P. denitrificans</i> . A, 1: DNA ladder, 2: 3' flanking region (868 bp) PCR product, and B, 3: DNA ladder, 4: 5' flanking region (771 bp) PCR product. PCR products were gel extracted.	277
Figure 8.2:	Restriction digests of 3' and 5' flanking region of the flavohemoglobin gene (<i>fhb</i>) in <i>P. denitrificans</i> . 1: 1kb DNA ladder, 2: 3' flanking region cut with <i>Xba</i> I and <i>Pst</i> I, 3: pk18 <i>mobsacB</i> plasmid cut with <i>Xba</i> I and <i>Pst</i> I, 4: DNA ladder, 5: pKH001 plasmid cut with <i>Xba</i> I and <i>Xma</i> I, 6: 5' flanking region cut with <i>Xba</i> I and <i>Xma</i> I.....	278
Figure 8.3:	Restriction digests of screened colonies. A: 8 colonies selected from IPTG/X-gal/kanamycin screening plates after transformation of the 3' flanking fragment and pk18 <i>mobSacB</i> plasmid, analysed by plasmid mini preparation and digestion with <i>Xba</i> I and <i>Pst</i> I. B: 14 colonies selected by kanamycin resistance after transformation of the 5' flanking fragment and pk18 <i>mobSacB</i> plasmid+3' flank, analysed by colony PCR followed by digestion with <i>Xba</i> I and <i>Xma</i> I.....	279
Figure 8.4:	DNA electrophoresis gel displaying the two colonies successfully containing the pKH002 plasmid with a 3' and 5' flanking region inserts. 1: ladder, 2: cut pK18 <i>mobsacB</i> (5.7 Kb), 3: cut pKH002 , linearized plasmid 7.4 Kb, 4: 3' flanking region PCR product (868	

bp), 5: cut pKH002 cut with *PstI* and *XbaI* showing a 868 bp insert and 6.5 Kb plasmid, 6: 5' flanking region PCR product (771 bp), 7: cut pKH002 with 3' and 5' flanking region insert cut with *XmaI* and *XbaI* showing a 771 bp insert and 6.6 Kb plasmid, 8: cut pKH002 with 3' and 5' flanking region insert cut with *XmaI* and *PstI* showing a 1.6 Kb 3' and 5' flanking region insert.280

Figure 8.5: PCR amplified 1542 bp flavohemoglobin region from *P. denitrificans*.281

Figure 8.6: Detailed dissolved oxygen (DO) values (closed circle) taken at 0.5 h intervals, with points shown every 25 values for clarity of figure, using Biocommand. Maintained oxygenation shown by horizontally linear values and 20 min airflow shutoff for gas sampling can be seen as points of fast reduction followed by return of DO. Detailed pH values (open forward triangle) taken at 0.5 h intervals. Points are shown every 25 values for clarity of figure, using Biocommand. Growth conditions of minimal salts media, pH 7.5 with nitrite addition. Three biologically and technically separate chemostat experiments are shown (A, B, C).285

Figure 8.7: Parameters monitored by Biocommand program for continuous culture of *P. denitrificans* under nitrosative stress with nitrite addition to minimal salts media at pH 7.5 and 10 mM ammonium chloride (n = 3). A: Dissolved oxygen (DO), pH and temperature were measured at 0.5 h time intervals for the duration of the experiment. B: Agitation and air flow. Plotted are every 25 points for all parameters with error bars for clarity of figure.286

Figure 8.8: Average fluctuations on dissolved oxygen levels (DO) (blue dotted line) shown in correlation to that of airflow shut down (red dashed line) and gas sampling time points for nitrous oxide analysis. Air flow was turned off for 20 min prior to gas sampling for accumulation of nitrous oxide gas to reach levels for detection. Growth conditions of minimal salts media, pH 7.5 with nitrite addition (Error bars denote standard deviation; n = 3.)287

Figure 8.9: Parameters monitored by Biocommand program for continuous culture of *P. denitrificans* under nitrosative stress of 24.6 ± 1.1 mM nitrite with 8.3 ± 0.7 mM nitrate addition to minimal salts media at pH 7.5 and 10 mM ammonium chloride (n = 3). A, dissolved oxygen (DO), pH and temperature were measured at 0.5 h time intervals for the duration of the experiment. B, agitation and air flow. Plotted are every 25 points for all parameters with error bars for clarity of figure.288

Figure 8.10: RNA quality check using Experion for growth conditions nitrosative stress 35.804 ± 2.024 mM sodium nitrite addition to minimal salts media at pH 7.5 and 10 mM ammonium chloride.289

Figure 8.11: Fluctuations on dissolved oxygen levels (DO) (blue dotted line) shown in correlation to that of airflow shut down (red dashed line) and gas sampling time points for nitrous oxide analysis. Air flow was turned off for 20 min prior to gas sampling for accumulation of nitrous oxide gas to reach levels for detection.....290

8.2 3 The effect of extracellular pH and nitrite on batch culture growth kinetics of *Paracoccus denitrificans*

Table 8.1: The Y_{max} and $\mu_{app} h^{-1}$ values for growth of *Paracoccus denitrificans* under standard growth conditions at various media pH values: minimal salts media, supplemented with ammonium chloride, 10 mM; sodium succinate, 30 mM; Vishniac trace element solution. Measured by optical density at 600 nm (OD_{600nm}) adjusted to a pathlength of 1 cm against time (h).

pH	$\mu_{app} h^{-1}$			Y_{max}^*		
	Average	$\pm SE$	%	Average	$\pm SE$	%
6.0	0.009	0.042	2.05	0.053	0.250	1.43
6.5	0.286	0.018	65.30	0.039	0.004	1.05
7.0	0.395	0.010	90.18	3.364	0.118	90.67
7.5	0.438	0.013	-	3.710	0.047	-
8.0	0.511	0.008	116.67	3.027	0.060	81.59
8.5	0.479	0.013	109.36	3.234	0.002	87.17
9.0	0.272	0.015	62.10	2.157	0.059	58.14
μ_{app}	(h^{-1})	=	apparent	growth	constant	

Y_{max} (AU) maximum optical density produced * Y_{max} stated as OD_{600nm} corrected to 1 cm pathlength

Table 8.2: The Y_{\max} (AU) values for growth of *Paracoccus denitrificans* under standard growth conditions at pH 7.0, 7.5, 8.0 and 8.5: minimal salts media, supplemented with ammonium chloride, 10 mM; sodium succinate, 30 mM; Vishniac trace element solution. Various additions of sodium nitrite as stated. Measured by optical density at 600 nm ($OD_{600\text{nm}}$) adjusted to a pathlength of 1 cm against time (h). Maximum optical density (Y_{\max})* \pm SE

pH 7.0			pH 7.5			pH 8.0			pH 8.5		
Nitrite (mM)	Y_{\max} (AU)	\pm SE									
0	3.364	0.118	0	3.683	0.047	0	3.027	0.060	0	3.234	0.002
2	3.655	0.078	2	4.870	0.133	2	3.859	0.058	2	3.689	0.013
5	3.819	0.174	5	5.418	0.077	5	4.269	0.254	5	3.689	0.140
7	4.123	0.112	10	5.357	0.155	10	4.361	0.137	10	3.559	0.116
10	3.992	0.205	15	5.337	0.057	15	4.769	0.103	20	3.635	0.101
12	4.480	0.003	20	5.265	0.181	20	4.920	0.104	30	3.651	0.047
15	3.644	0.106	25	5.168	0.031	30	4.573	0.114	40	3.720	0.082
20	3.991	0.014	30	5.098	0.166	40	4.302	0.204	50	3.234	0.113
25	2.661	0.038	35	4.690	0.084	50	4.496	0.093	60	3.401	0.113
30	0.037	0.007	40	3.986	0.344	55	4.041	0.145	70	3.418	0.056
			45	3.871	0.058	60	4.037	0.255	80	3.107	0.118
			47.5	3.295	0.182	65	4.063	0.127	90	2.576	0.168
			50	3.293	0.039	70	4.071	0.068	100	2.515	0.029

52.5	3.230	0.028	75	2.353	0.031	110	1.652	0.031
55	0.057	0.018	80	2.357	0.112	120	1.431	0.163
			85	2.565	0.075	130	1.805	0.092
			90	2.342	0.089	135	1.437	0.321
			100	0.837	0.226	140	0.357	0.105
			105	0.094	0.092	145	0.057	0.035

Maximum optical density (Y_{\max} AU) * \pm se. Y_{\max} stated as OD600nm corrected to 1 cm pathlength. (SE denote standard error; $n > 3$.)

Table 8.3: The $\mu_{app} h^{-1}$ values for growth of *Paracoccus denitrificans* under standard growth conditions at pH 7.0, 7.5, 8.0 and 8.5: minimal salts media, supplemented with ammonium chloride, 10 mM; sodium succinate, 30 mM; Vishniac trace element solution. Various additions of sodium nitrite as stated. Measured by optical density at 600 nm (OD_{600nm}) adjusted to a pathlength of 1 cm against time (h).

pH 7.0			pH 7.5			pH 8.0			pH 8.5		
Nitrite			Nitrite			Nitrite			Nitrite		
(mM)	$\mu_{app} h^{-1}$	$\pm SE$									
0	0.395	0.010	0	0.438	0.013	0	0.511	0.008	0	0.479	0.013
2	0.371	0.620	2	0.455	0.008	2	0.471	0.011	2	0.505	0.017
5	0.363	0.648	5	0.347	0.028	5	0.442	0.007	5	0.497	0.015
7	0.261	0.698	10	0.386	0.006	10	0.462	0.012	10	0.497	0.011
10	0.353	0.674	15	0.383	0.008	15	0.472	0.008	20	0.491	0.009
12	0.308	0.763	20	0.382	0.007	20	0.440	0.008	30	0.467	0.010
15	0.362	0.684	25	0.347	0.007	30	0.430	0.010	40	0.434	0.008
20	0.375	0.676	30	0.330	0.008	40	0.416	0.011	50	0.418	0.009
25	0.324	0.454	35	0.327	0.010	50	0.376	0.010	60	0.383	0.009
30	0.000	0.018	40	0.324	0.010	55	0.350	0.006	70	0.364	0.010
			45	0.309	0.009	60	0.369	0.010	80	0.322	0.010
			47.5	0.308	0.013	65	0.367	0.016	90	0.271	0.011
			50	0.334	0.010	70	0.325	0.010	100	0.203	0.005
			52.5	0.365	0.009	75	0.308	0.009	110	0.199	0.006

55	0.000	0.000	80	0.287	0.010	120	0.181	0.004
			85	0.256	0.007	130	0.213	0.010
			90	0.190	0.003	135	0.151	0.003
			100	0.174	0.007	140	0.169	0.007
			105	0.000	0.000	145	0.000	0.000

Apparent growth constant ($\mu_{app} h^{-1}$). (SE denote standard error; $n>3$.)

Table 8.4: Conversion table of nitrite (mM) and free nitrous acid (FNA)

pH 7.0		pH 7.5		pH 8.0		pH 8.5	
Nitrite	FNA	Nitrite	FNA	Nitrite	FNA	Nitrite	FNA
(mM)	(μM)	(mM)	(μM)	(mM)	(μM)	(mM)	(μM)
0	0.00	0	0.00	0	0.00	0	0.00
2	0.36	2	0.11	2	0.04	2	0.01
5	0.89	5	0.28	5	0.09	5	0.03
7	1.24	10	0.56	10	0.18	10	0.06
10	1.78	15	0.84	15	0.27	20	0.11
12	2.13	20	1.12	20	0.36	30	0.17
15	2.67	25	1.41	30	0.53	40	0.22
20	3.56	30	1.69	40	0.71	50	0.28
25	4.45	35	1.97	50	0.89	60	0.34
30	5.33	40	2.25	60	1.07	70	0.39
35	6.22	45	2.53	65	1.16	80	0.45
		48	2.67	70	1.24	90	0.51
		50	2.81	75	1.33	100	0.56
		53	2.95	80	1.42	110	0.62
		55	3.09	85	1.51	120	0.67
				90	1.60	130	0.73

100	1.78	135	0.76
105	1.87	140	0.79
110	1.96	145	0.82

8.3 4 The role of flavohemoglobin in *P. denitrificans* under nitrite induced stress

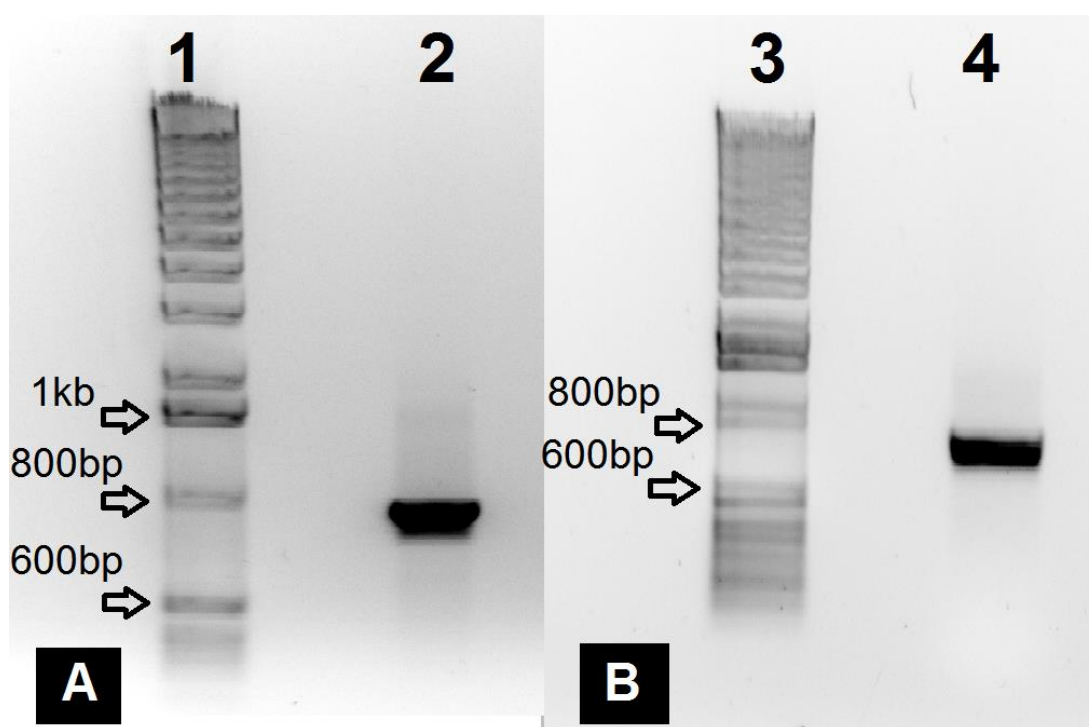


Figure 8.1: PCR amplified 3' and 5' flanking region of the flavohemoglobin gene (*fhb*) in *P. denitrificans*. A, 1: DNA ladder, 2: 3' flanking region (868 bp) PCR product, and B, 3: DNA ladder, 4: 5' flanking region (771 bp) PCR product. PCR products were gel extracted.

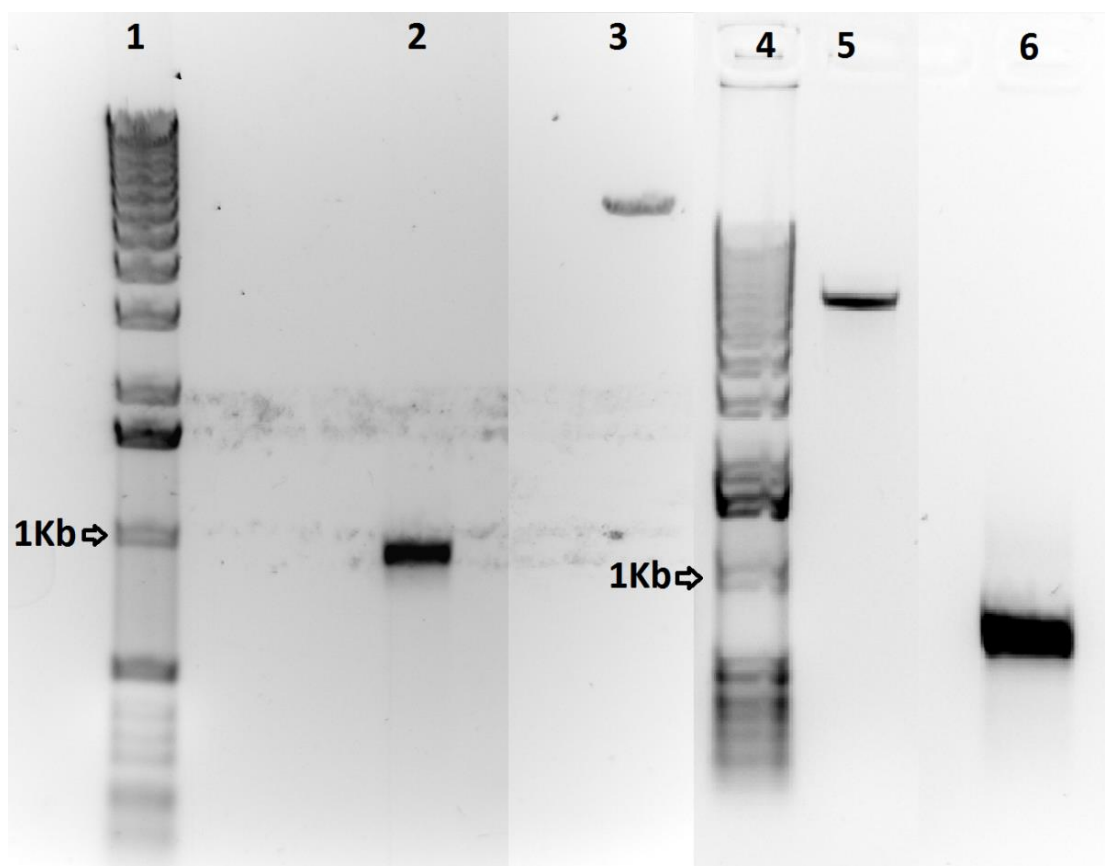


Figure 8.2: Restriction digests of 3' and 5' flanking region of the flavohemoglobin gene (*fhb*) in *P. denitrificans*. 1: 1kb DNA ladder, 2: 3' flanking region cut with *Xba*I and *Pst*I, 3: *pk18mobsacB* plasmid cut with *Xba*I and *Pst*I, 4: DNA ladder, 5: *pKH001* plasmid cut with *Xba*I and *Xma*I, 6: 5' flanking region cut with *Xba*I and *Xma*I.

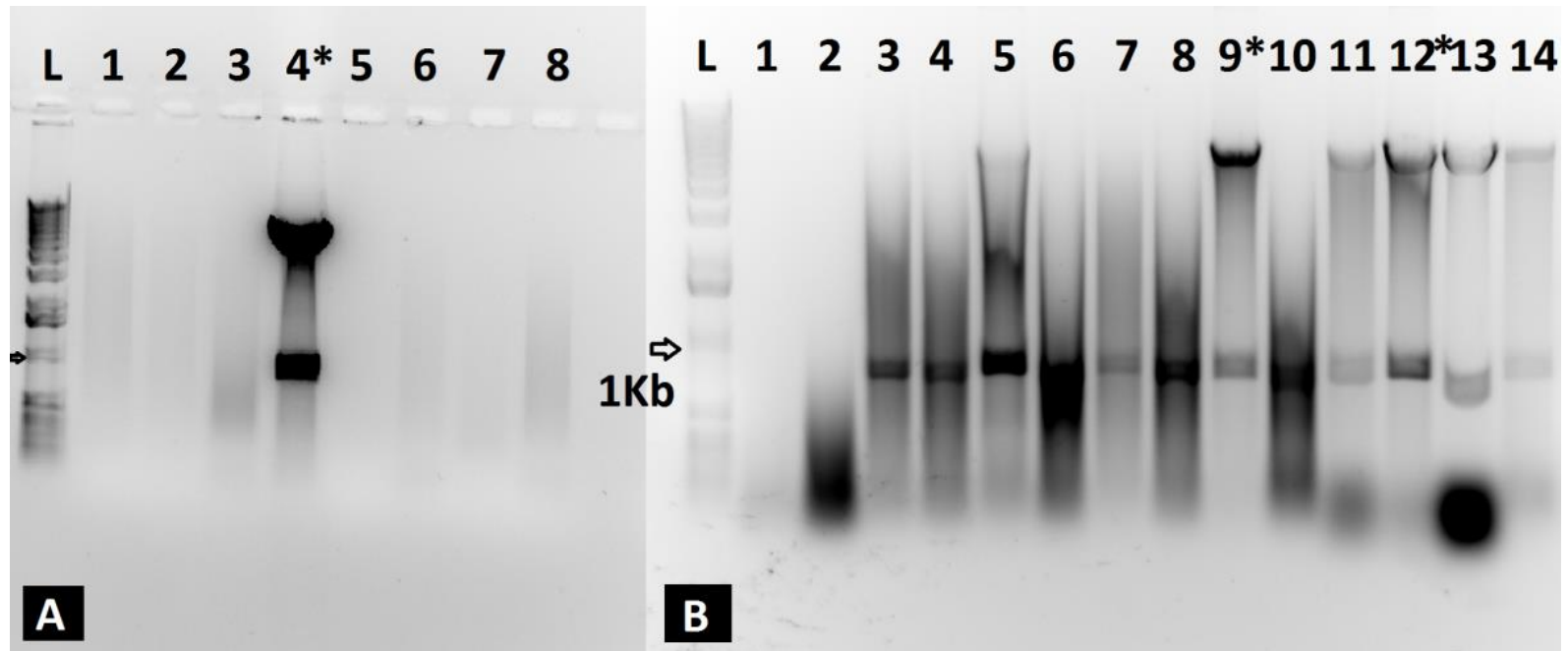


Figure 8.3: Restriction digests of screened colonies. A: 8 colonies selected from IPTG/X-gal/kanamycin screening plates after transformation of the 3' flanking fragment and pk18mobSacB plasmid, analysed by plasmid mini preparation and digestion with *Xba*I and *Pst*I. B: 14 colonies selected by kanamycin resistance after transformation of the 5' flanking fragment and pk18mobSacB plasmid+3' flank, analysed by colony PCR followed by digestion with *Xba*I and *Xma*I.

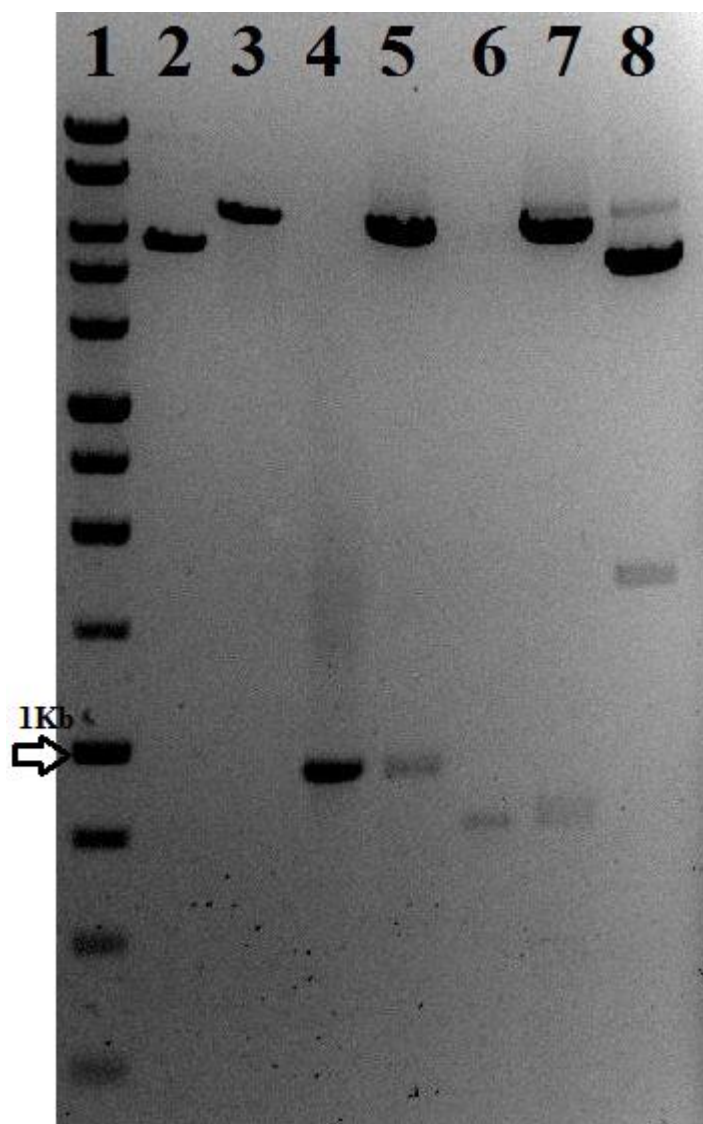


Figure 8.4: DNA electrophoresis gel displaying the two colonies successfully containing the pKH002 plasmid with a 3' and 5' flanking region inserts. 1: ladder, 2: cut pK18*mobsacB* (5.7 Kb), 3: cut pKH002 , linearized plasmid 7.4 Kb, 4: 3' flanking region PCR product (868 bp), 5: cut pKH002 cut with *PstI* and *XbaI* showing a 868 bp insert and 6.5 Kb plasmid, 6: 5' flanking region PCR product (771 bp), 7: cut pKH002 with 3' and 5' flanking region insert cut with *XmaI* and *XbaI* showing a 771 bp insert and 6.6 Kb plasmid, 8: cut pKH002 with 3' and 5' flanking region insert cut with *XmaI* and *PstI* showing a 1.6 Kb 3' and 5' flanking region insert.

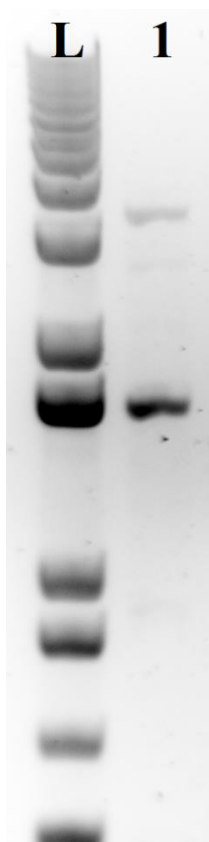


Figure 8.5: PCR amplified 1542 bp flavohemoglobin region from *P. denitrificans*.

Table 8.5: Apparent growth rate ($\mu_{app} h^{-1}$) and maximum optical density (Y_{max} AU) for the growth of *P. denitrificans* without nitrite and with 12.5 mM nitrite addition to minimal salts media, pH 7.5 with 10 mM ammonium chloride addition in plate reader batch culture and shaking flask batch culture growth conditions.

Nitrite (mM)	Plate reader				Shaking flask			
	$\mu_{app} (h^{-1})$		$Y_{max} (AU)$		$\mu_{app} (h^{-1})$		$Y_{max} (AU)$	
	Average	$\pm SE$	Average	$\pm SE$	Average	$\pm SE$	Average	$\pm SE$
0	0.44	0.01	3.68	0.05	0.44	0.01	3.68	0.06
12.5	0.35	0.01	3.37	0.02	0.35	0.01	3.88	0.17

μ_{app} (h⁻¹) = apparent growth constant

Y_{max} (AU) maximum biomass produced * Y_{max} stated as OD_{600nm} corrected to 1 cm pathlength

pH 7.5

Table 8.6: Summarised apparent growth constant ($\mu_{app} h^{-1}$) and maximum biomass produced (Y_{max} AU) at various calculated nitrite (mM) for the growth of *P. denitrificans* and the Δfhb mutant. Measured by optical density at 600 nm (OD_{600nm}) adjusted to a pathlength of 1 cm.

Nitrite (mM)	WT				Nitrite (mM)	Δfhb			
	$\mu_{app} (h^{-1})$	$\pm SE$	Y_{max} (AU)	$\pm SE$		$\mu_{app} (h^{-1})$	$\pm SE$	Y_{max} (AU)	$\pm SE$
0	0.438	0.013	3.683	0.047	0	0.309	0.011	3.411	0.074
2	0.455	0.008	4.870	0.133	2	0.340	0.005	3.731	0.021
5	0.347	0.028	5.418	0.077	5	0.342	0.011	3.632	0.022
10	0.386	0.006	5.357	0.155	10	0.280	0.016	3.365	0.087
15	0.383	0.008	5.337	0.057	12.5	0.335	0.019	3.709	0.056
20	0.382	0.007	5.265	0.181	15	0.281	0.018	3.719	0.032
25	0.347	0.007	5.168	0.031	17.5	0.288	0.019	3.778	0.026
30	0.330	0.008	5.098	0.166	20	0.185	0.021	3.537	0.067
35	0.327	0.010	4.690	0.084	22.5	0.235	0.016	3.747	0.088
40	0.324	0.010	3.986	0.344	25	0.232	0.013	3.775	0.029
45	0.309	0.009	3.871	0.058	27.5	0.243	0.012	3.764	0.041
47.5	0.308	0.013	3.295	0.182	30	0.180	0.009	3.429	0.034
50	0.334	0.010	3.293	0.039	32.5	0.293	0.007	3.559	0.072
52.5	0.365	0.009	3.230	0.028	35	0.320	0.015	3.184	0.045
55	0.000	0.000	0.057	0.018	37.5	0.278	0.011	3.185	0.036

40	0.244	0.041	3.008	0.074
42.5	0.248	0.070	2.479	0.170
45	0.301	0.042	3.099	0.103
47.5	0.237	0.017	3.081	0.068
50	0.029	0.008	0.096	0.042

8.4 5 Metabolic analysis of nitrosative stress in batch and continuous culture of *P. denitrificans* in a continuous culture system

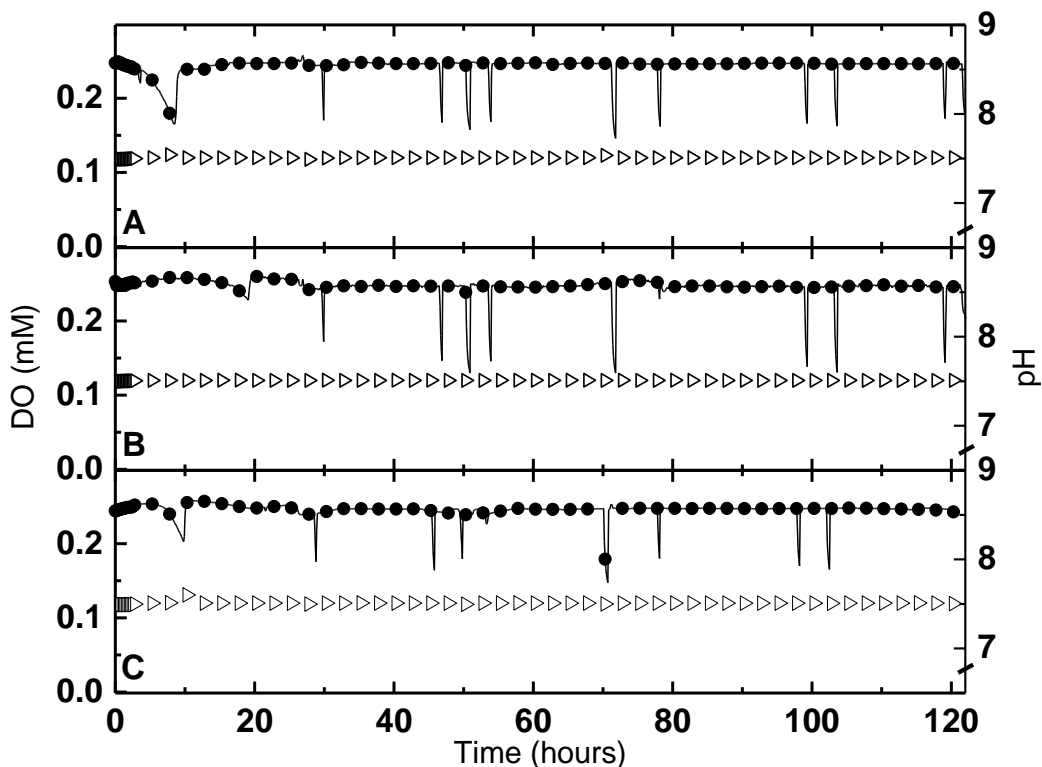


Figure 8.6: Detailed dissolved oxygen (DO) values (closed circle) taken at 0.5 h intervals, with points shown every 25 values for clarity of figure, using Biocommand. Maintained oxygenation shown by horizontally linear values and 20 min airflow shutoff for gas sampling can be seen as points of fast reduction followed by return of DO. Detailed pH values (open forward triangle) taken at 0.5 h intervals. Points are shown every 25 values for clarity of figure, using Biocommand. Growth conditions of minimal salts media, pH 7.5 with nitrite addition. Three biologically and technically separate chemostat experiments are shown (A, B, C).

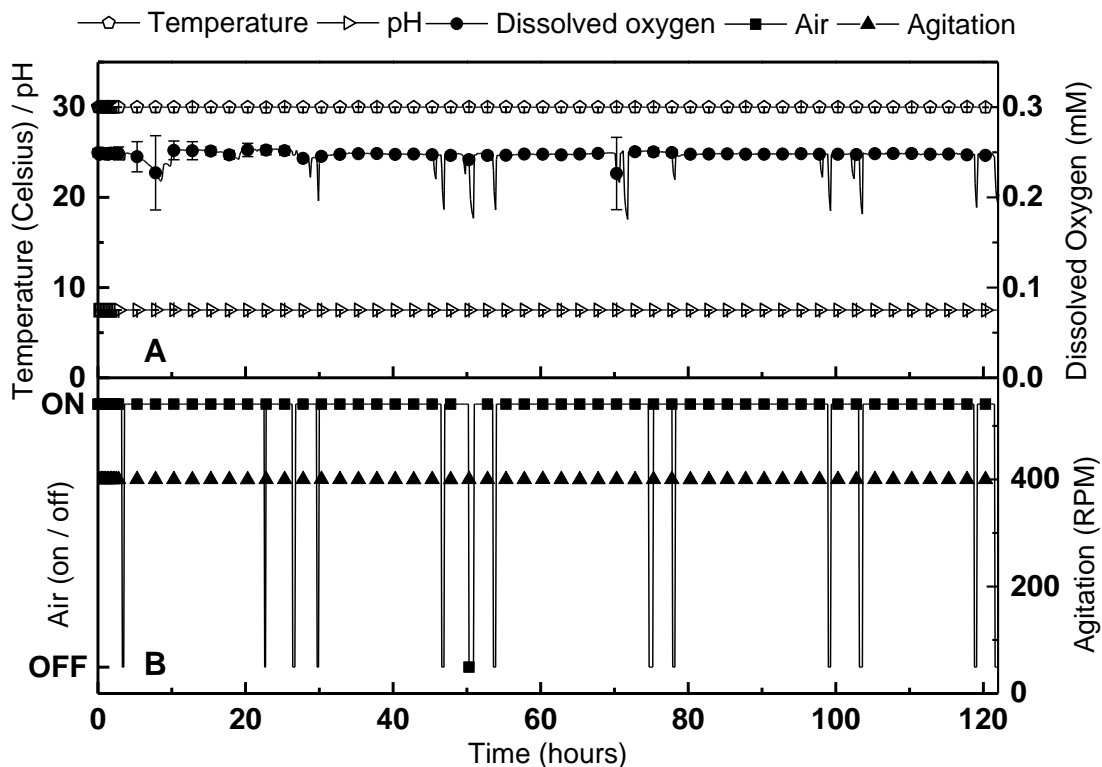


Figure 8.7: Parameters monitored by Biocommand program for continuous culture of *P. denitrificans* under nitrosative stress with nitrite addition to minimal salts media at pH 7.5 and 10 mM ammonium chloride (n = 3). A: Dissolved oxygen (DO), pH and temperature were measured at 0.5 h time intervals for the duration of the experiment. B: Agitation and air flow. Plotted are every 25 points for all parameters with error bars for clarity of figure.

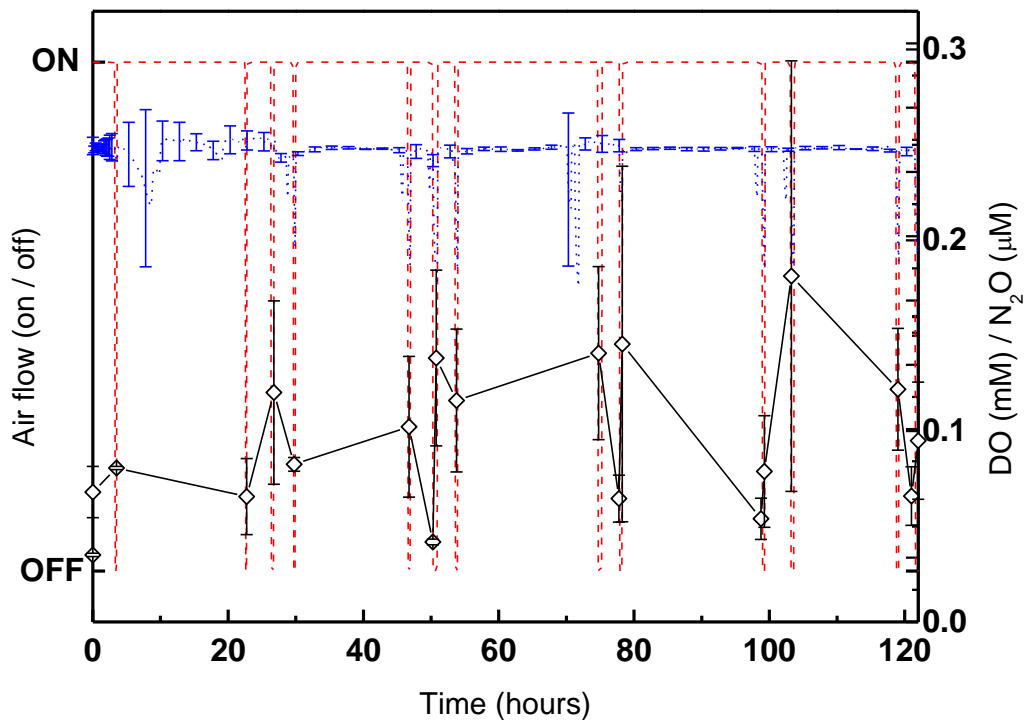


Figure 8.8: Average fluctuations on dissolved oxygen levels (DO) (blue dotted line) shown in correlation to that of airflow shut down (red dashed line) and gas sampling time points for nitrous oxide analysis. Air flow was turned off for 20 min prior to gas sampling for accumulation of nitrous oxide gas to reach levels for detection. Growth conditions of minimal salts media, pH 7.5 with nitrite addition (Error bars denote standard deviation; n = 3.)

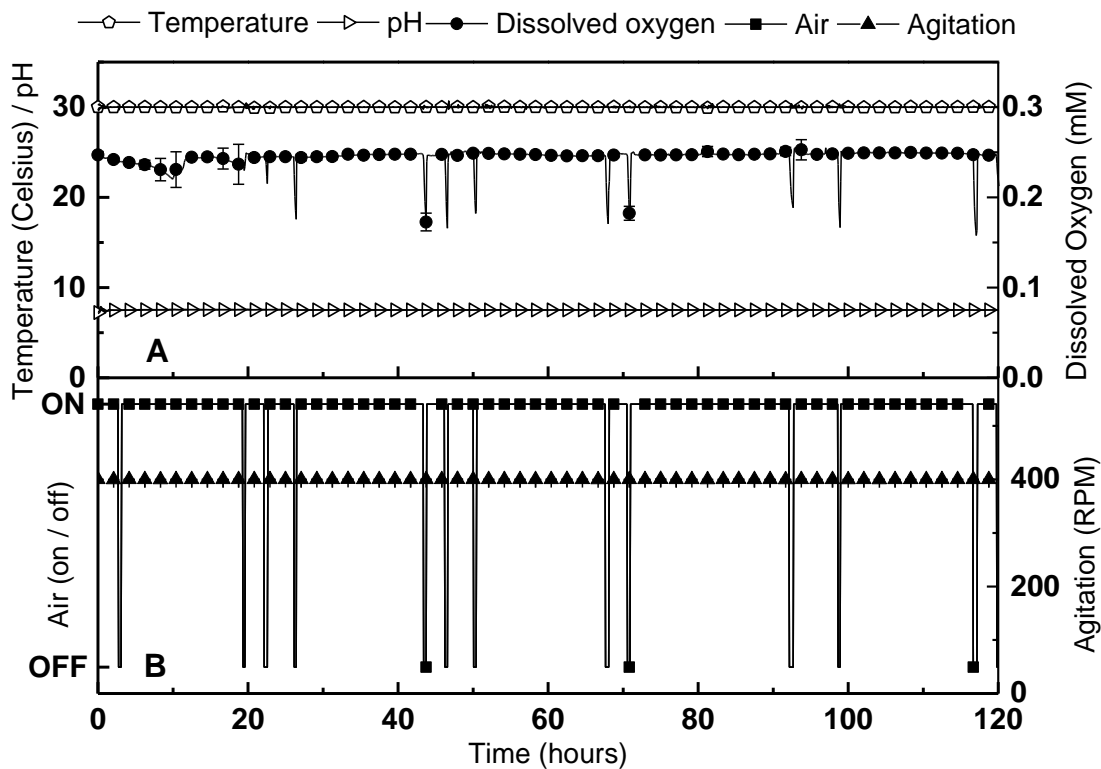


Figure 8.9: Parameters monitored by Biocommand program for continuous culture of *P. denitrificans* under nitrosative stress of 24.6 ± 1.1 mM nitrite with 8.3 ± 0.7 mM nitrate addition to minimal salts media at pH 7.5 and 10 mM ammonium chloride ($n = 3$). A, dissolved oxygen (DO), pH and temperature were measured at 0.5 h time intervals for the duration of the experiment. B, agitation and air flow. Plotted are every 25 points for all parameters with error bars for clarity of figure.

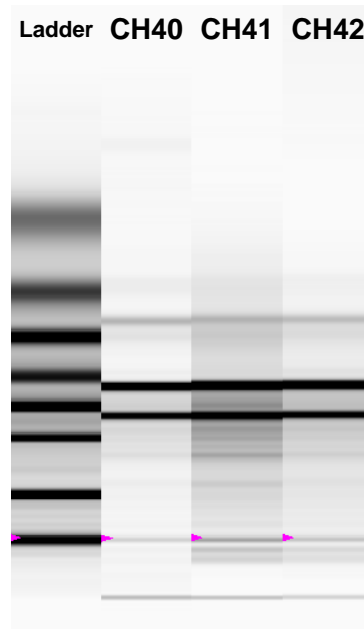


Figure 8.10: RNA quality check using Experion for growth conditions nitrosative stress 35.804 ± 2.024 mM sodium nitrite addition to minimal salts media at pH 7.5 and 10 mM ammonium chloride.

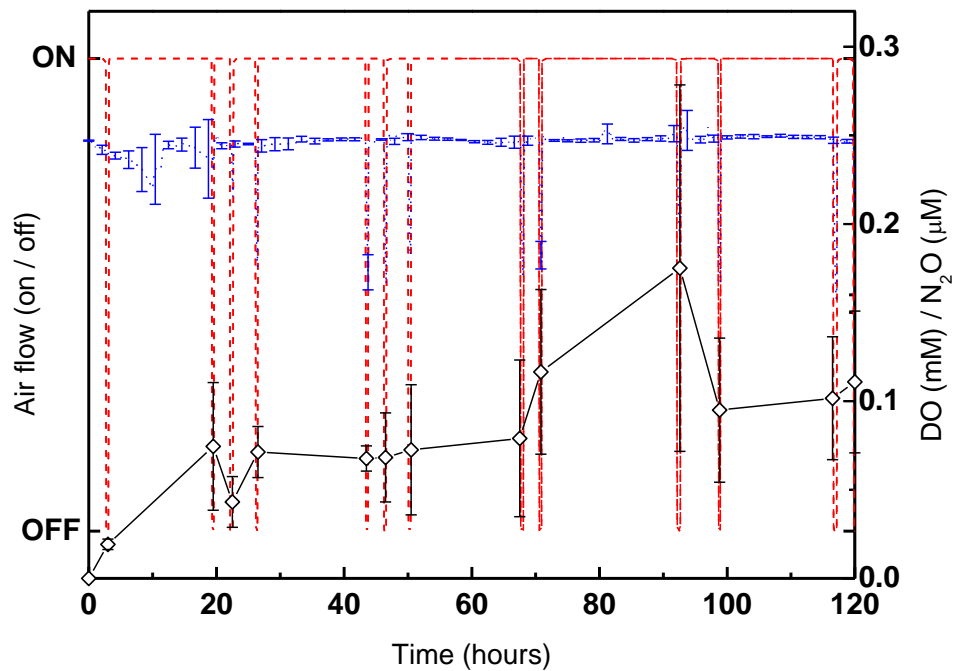


Figure 8.11: Fluctuations on dissolved oxygen levels (DO) (blue dotted line) shown in correlation to that of airflow shut down (red dashed line) and gas sampling time points for nitrous oxide analysis. Air flow was turned off for 20 min prior to gas sampling for accumulation of nitrous oxide gas to reach levels for detection.

Table 8.7: Summary of dissolved oxygen (DO) for all continuous culture experiments, details of aerobic chemostat oxygenation and fluctuation.

Chemostat sample name	DO (mM)				
	Mean	Variance	Standard Deviation	Low value	High Value
CH40	0.245	0.054	0.012	0.162	0.254
CH41	0.244	0.079	0.014	0.143	0.270
CH42	0.244	0.049	0.011	0.145	0.256
CH43	0.244	0.075	0.014	0.147	0.259
CH44	0.248	0.078	0.014	0.131	0.261
CH45	0.247	0.036	0.009	0.149	0.259